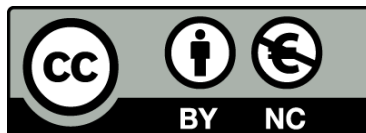




UNIVERSITAT_{DE}
BARCELONA

An epigenetic approach to fatty acid metabolism in haematological malignancies

Michael Maher



Aquesta tesi doctoral està subjecta a la llicència **Reconeixement- NoComercial 4.0. Espanya de Creative Commons.**

Esta tesis doctoral está sujeta a la licencia **Reconocimiento - NoComercial 4.0. España de Creative Commons.**

This doctoral thesis is licensed under the **Creative Commons Attribution-NonCommercial 4.0. Spain License.**

Universitat de Barcelona

Facultat de Biologia

Programa de Doctorat en Biomedicina

**An epigenetic approach to fatty acid metabolism in
haematological malignancies**

Memòria presentada per

Michael Maher

per optar al grau de doctor per la Universitat de Barcelona

Tesi realitzada a

l'Institut de Recerca contra la Leucèmia Josep Carreras

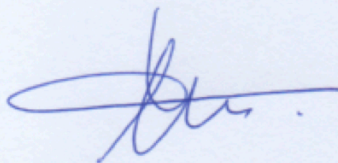
Director

BUSCHBECK
K MARCUS
-
X5649408X

Digitally signed
by BUSCHBECK
MARCUS -
X5649408X
Date: 2020.12.21
12:06:08 +01'00'

Marcus
Buschbeck

Tutor



Francesc
Villarroya Gombau

Doctorand



Michael
Maher



UNIVERSITAT DE
BARCELONA



Institut de Recerca
CONTRA LA LEUCÈMIA
Josep Carreras

*Anois teacht an Earraigh
beidh an lá dul chun shíneadh,
Is tar éis na Féil' Bríde
ardóidh mé mo sheol.
Antaine Ó Raifteirí*

Acknowledgements

The PhD is an expedition that is by no means a solo effort; it takes a supportive team of individuals who contribute their time and expertise throughout the four years. My journey was no exception; I had the pleasure to work with people who were more than generous to lend me their experience and know-how. From the dark corners of Western blot development rooms to the bright lights of cell culture hoods and scientific conferences, I have been blessed with the help and advice of numerous fellow PhD students, post-docs and PIs.

First and foremost, I would like to thank Marcus; as my tutor, mentor and guide, you gave me a unique opportunity to learn the ropes of biological investigation in what was a vibrant environment, both in the lab and among our wider circles. I am coming away from the lab having learned what it takes to be scientist, and with that, a few revelations about myself too.

Many personalities have come and gone throughout the Buschbeck lab family history. I am forever grateful to my lab mates who have been there during the dark and the light, from dawn till dusk. Iva, like scared little rabbits in headlights, we began our adventure together on a bright December morning. We grew during these years; we conquered our own hills and we changed for the better. Thank you for sharing the trip with me. Raquel, our humble leukaemia team sprouted and grew legs when you arrived! I am grateful for your advice and suggestions as my project progressed and regressed and everything in-between. Jeannine, as my guide into the world of screens, thank you for giving me a leg-up into my first real foray into independent lab work. David, sparing any Star Wars tropes, your Job-like patience and sage words were guiding lights any time I needed them. And were in no way reminiscent of Yoda, I swear 😊. Vane, muchísimas gracias por estar siempre a nuestro lado. Tu espíritu calmante fue un regalo todos los días en el laboratorio! Gracias por tus consejos y ayuda. Marguerite-Marie, we may share space on the Enneagram, but stories come full circles and we're never stuck in the same rhythm. Onwards and upwards! Roberto, thank you for all the bioinfo assistance. While I will never make a risotto in the oven again, to put it in a *nutshell*, I will make a note of always delineating a 'stone' from a 'grunge'. Ollie, René and Laura, the newest arrivals to the lab, have brought fresh energy to those tip-ex coloured benches and I hope there'll be many more evenings of Rick Astley,

Galician wine and complaints about leg day to come. Sarah, I am continually impressed with your style of work and way with words. The bumps I came across were most definitely smoothed with your help. Much inspiration came from Anna's PhD thesis, for which I must be on the all-time top reader list at this point. And Julien, who, even though we shared lab space for only a brief time, provided ample colour and noise that was a soundtrack for my starting period in the lab.

It must be the mountain air, because across the great expanse of the Can Ruti campus I crossed paths with a bunch of friendly, positive folk. Muchas gracias a Marco y Gerard en IGTP, que me han ayudado y avisado durante mis varias visitas al servicio de FACS. Además, a Óscar y su equipo en el UPF por las horas de 'sorting' que pasaron conmigo. Thank you to Sonia and the Christinas for their feedback and input during many of our shared lab meetings. Thank you to Fumi, Myako and Emili for being such great neighbours all these years, both at the IMPPC and IJC. Our newer neighbours at the Risueño lab, in particular Pepe and Antonia, provided me with valuable reagents and cell lines and were always willing to lend their skills and expertise where I had none. Ha sido un gran placer conocer y colaborar con Marc Sorigué y Sara Vegara del Departamento de Hematología en los últimos dos años. Muchas gracias por vuestro gran trabajo! Isabel, muchas gracias a por tu ayuda en los últimos meses y por dar tu tiempo a nuestros experimentos. Further afield, I thank the members of the Johannes Zuber and his team in Vienna who provided us with the tools and the know-how to carry out our knockdown screens.

A big *moltes gràcies* goes to Carles Cantó, who provided me a warm welcome (and return!) to the Nestlé Institute of Health Sciences in Lausanne during my secondment. It was an pleasure and honour to be able to spend time in such a renowned lab group and learn from experts in cellular metabolism. A special mention to my fellow ChroMe, Miriam, who graciously gave her time to show me the world and ways of Western blots; to Angelique, who provided friendly company evenings and weekends; and to Magali, for showing me around the highways and byways of their impressive Oroboros instrument. Overall, my stay at NIHS was a special time to revisit old friends and make new ones in the process.

Being part of the ChroMe family has been a special experience I will always treasure. Iva, Miriam, Salva, Joan, Paula, Haris, Raian, Tia, Magdalini, Kelly, Yang, Silvia, Berta and Laura, thank you for the happy memories. We shared fun times on obscure islands of golden sands and snow-covered forests and in halls of not-so obscure institutes, over countless exotic dishes that were always 'local' to at least one of us and on boat trips on a lavish yacht and a questionable 'punt'. I'm looking forward to seeing you all again along whatever paths these roads are taking us.

To all the PIs of the ChroMe network, thank you for your support, your guidance and your insight during our many retreats together. It was a pleasure to get know you over scientific discussions and various local beverages. Thank you, Catherine, for kindly giving your time and advice during our annual review meetings. It was always great to receive fresh perspectives. To CJ, for opening our minds and eyes to other ways of being and seeing. To Anna and Salva, for encouraging us to brave the heady waters of bioinformatics. To Anton, Jules and Jonathan, thank you for keeping the ship on course! I would like to thank my monitoring committee at the UB, Neus Agell and Virginia Amador, for their constructive and helpful feedback during our annual review meetings.

All roads lead to paradise, and I have met many inspiring characters and friends along the way who have helped and pushed me at various stages by opening doors or simple words of wisdom: From my first taste of bench work at the microbiology labs of University College Cork; to being part of an idea that bloomed from small beginnings in a former floppy disk factory in Limerick; to life in rural Bavaria with some nutritional science thrown in; an MSc project beside Lake Geneva; all culminating in life and times in Barcelona during the last five years. A big thank you to you all.

I would like to give the final word to the constants, the rocks in my life who have stayed on regardless of the score line.

To my friends, for the Skypes, the bike trips, the runs in the woods, the impromptu day pints, and for bringing me back to Earth.

To my family, my parents, my brothers, my aunt and uncles and my special grandmother, for the hugs, the home-cooked dinners, the open doors, and the belief.

To Luísa, my one and only, for sticking by during all kinds of stormy weather. *Você é sim, E nunca meu não.* Obrigado, Milu.

The role of fatty acids to overcome stress and contribute to disease progression is becoming increasingly evident in haematological diseases. Further, epigenetic factors play an important role in the aetiology of myelodysplastic syndromes (MDS) and the transformation to secondary acute myeloid leukaemia (sAML). To investigate this in the MDS/sAML cell line, SKK-1, we employed a shRNA knockdown screen to target 912 epigenetic regulators. We then coupled this loss-of-function approach to a fatty acid metabolism-based assay with which we were able to cell-sort the SKK-1 cells based on the fatty acid uptake. Here I describe the methodology of this epigenetics-metabolism approach and our efforts to validate candidate hits from the screen that were predicted to be modulators of fatty acid uptake. Following testing using single gene knockdowns of the top genes from the screen, we were not able to identify epigenetic regulators that significantly alter fatty acid uptake. In parallel, we characterised metabolic and genetic parameters of triple-sorted low (TS LOW) and high (TS HIGH) fatty acid uptake sub-populations. However, during the course of the study, we discovered latent contamination by another myeloid cell line, U-937, in our SKK-1 parental cells and TS LOW and TS HIGH sub-populations. Therefore, we interpreted results from the characterisation study with the knowledge that we had mixed cellular populations. I describe the steps we took to first identify the cell line and then our further characterisation of single cell clones of TS LOW and TS HIGH. Interestingly, we observed distinct cytogenetic profiles between single clones of TS LOW and TS HIGH, namely trisomy 8, which is a highly relevant chromosomal aberration in myeloid malignancies. Overall, this study provides a novel approach to investigate epigenetic and metabolic interactions in blood malignancies. We also find metabolically distinct sub-populations that differ by a disease-relevant karyotype.

List of abbreviations

| | |
|-------------------------------|------------------------------------------------------------|
| α-KG | α -ketoglutarate |
| 5-hmC | 5-hydroxymethylcytosine |
| 5-hmC | hydroxymethylcytosine |
| ACC | Acetyl-CoA carboxylase |
| ACC_{1/2} | acetyl-CoA-carboxylase 1/2 |
| AML | acute myeloid leukaemia |
| AMPK | AMP-activated protein kinase |
| ATRA | All-trans retinoic acid |
| BET | bromodomain and extra-terminal |
| BETi | BET inhibitors |
| Cas9 | CRISPR-associated protein 9 |
| cDNA | complementary DNA |
| CFU | colony forming unit |
| CGI | CpG island |
| CHIP | Clonal haematopoiesis of indeterminant potential |
| ChREBP | Carbohydrate response element binding protein |
| CLP | Common lymphoid progenitors |
| CMP | Common myeloid progenitors |
| CGI | CpG island |
| CPM | counts per million |
| CPT₁ | carnitine palmitoyltransferase 1 |
| CRISPR | clustered regularly interspaced short palindromic repeated |
| ddH₂O | double-distilled water |
| DMSO | dimehthyl sulfoxide |
| DNMT | DNA methyltransferase |
| DNMTi | DNMT inhibitors |
| ds | double-stranded |
| ESA | Erythropoiesis-stimulating agents |
| ETC | electron transport chain |
| FA | Fatty acid |
| FABP | fatty acid binding protein |

| | |
|-------------------------|-----------------------------------------------------------------------|
| FACS | Fluorescence-activated cell sorting |
| FADH₂ | flavin adenine dinucleotide |
| FAS | Fatty acid synthase |
| FATP | fatty acid transport protein |
| FDA | Food & Drug Administration |
| FDR | False discovery rate |
| gDNA | genomic DNA |
| GFP | Green fluorescence protein |
| GMP | Granulocyte/macrophage progenitors |
| HDAC | Histone deacetylase |
| HDACi | HDAC inhibitors |
| HDMT | Histone deacetylase |
| HMT | histone methyltransferase |
| HSC | haematopoietic stem cell |
| HSCT | haematopoietic stem cell transplant |
| IDH | socitrate dehydrogenase |
| IGTP | Institut d'Investigació en Ciències de la Salut Germans Trias i Pujol |
| K | Lysine |
| KAT | Histone lysine acetyltransferase |
| LCFA | Long chain fatty acid |
| LMPP | Lymphoid-primed multipotent progenitors |
| logFC | Log-fold change |
| LSC | leukaemia stem cell |
| MAT | Marrow adipose tissue |
| MCFA | Medium chain fatty acid |
| MDS | Multidimensional scaling |
| MDS | myeloid dysplastic syndromes |
| MFI | median fluorescence intensity |
| miRNA | microRNA |
| MPP | Multipotent progenitors |
| NADH | nicotinamide adenine dinucleotide |
| OL allele | off-ladder allele |
| OXPHOS | Oxidative phosphorylation |
| PADI₄ | peptidyl arginine deiminase 4 |
| PBS | Phosphate buffered saline |
| PCR | polymerase chain reaction |
| PMT | Post-translational modification |

| | |
|---------------------|-----------------------------------------------|
| PPAR | Peroxisome proliferator-activated receptors |
| PRC | Polycomb repressive complex |
| R | Arginine |
| RISC | RNA-induced silencing complex |
| RNAi | RNA interference |
| RT | Room temperature |
| RT-qPCR | quantitative real time PCR |
| sAML | secondat acute myeloid leukaemia |
| SFFV | Spleen focus forming virus |
| shRNA | Short hairpin RNA |
| siRNA | small interfering RNA |
| SKK-1::hEpi9 | SKK-1 cells transduced with the hEpi9 library |
| SREBP | Sterol regulatory element-binding proteins |
| STR | short tandem repeats |
| TCA | tricarboxylic acid cycle |
| TET | Ten-eleven translocation |
| TF | Transcription factor |
| TMM | Trimmed mean of M-values |
| trxG | Trithorax-group |
| UCOE | ubiquitous chromatin opening element |
| RNAi | RNA interference |
| RT | Room temperature |
| RT-qPCR | quantitative real time PCR |
| sAML | secondat acute myeloid leukaemia |
| SFFV | Spleen focus forming virus |
| shRNA | Short hairpin RNA |
| siRNA | small interfering RNA |
| SKK-1::hEpi9 | SKK-1 cells transduced with the hEpi9 library |
| SREBP | Sterol regulatory element-binding proteins |
| STR | short tandem repeats |
| TCA | tricarboxylic acid cycle |
| TET | Ten-eleven translocation |
| TF | Transcription factor |
| TMM | Trimmed mean of M-values |
| trxG | Trithorax-group |
| UCOE | ubiquitous chromatin opening element |

Table of contents

| | |
|------------------------------------------------------------------------------------|------------|
| ACKNOWLEDGEMENTS | I |
| ABSTRACT | V |
| LIST OF ABBREVIATIONS | VII |
| INTRODUCTION | 15 |
| 1. HAEMATOPOIESIS AND HAEMATOLOGICAL MALIGNANCIES | 17 |
| 1.1 THE HAEMATOPOIETIC HIERARCHY | 18 |
| 1.1.1 Haematopoiesis: a historical perspective..... | 18 |
| 1.1.2 Modern paradigm of haematopoiesis..... | 22 |
| 1.1.3 Haematopoietic cell types..... | 25 |
| 1.1.4 Haematopoiesis during aging | 25 |
| 1.2 MYELODYSPLASTIC SYNDROMES AND THEIR CLINICAL MANAGEMENT | 25 |
| 1.2.1 Epidemiology and pathogenesis of MDS | 26 |
| 1.2.1 Transformation to secondary AML | 27 |
| 1.2.2 Classification and prognostic scoring of MDS..... | 28 |
| 1.2.3 Diagnostics | 28 |
| 1.2.4 Current therapeutic strategies | 31 |
| 1.2.5 Novel drugs | 33 |
| 1.3 MDS IS PART OF A SPECTRUM OF CLONAL MYELOID DISEASES | 33 |
| 1.3.1 Clonal haematopoiesis of indeterminate potential (CHIP)..... | 34 |
| 1.3.2 Somatic mutations..... | 35 |
| 2. FATTY ACID METABOLISM AND ITS ROLE IN HAEMATOLOGICAL MALIGNANCIES | 39 |
| 2.1 OVERVIEW OF FATTY ACID METABOLISM | 39 |
| 2.1.1 Beta-oxidation..... | 39 |
| 2.1.2 Fatty acid synthesis and the storage of high-energy fuel | 40 |
| 2.2 TRANSCRIPTIONAL REGULATION OF FATTY ACID METABOLISM | 43 |
| 2.3 INTERPLAY BETWEEN EPIGENETIC REGULATION AND FATTY ACID METABOLISM | 45 |
| 2.4 FATTY ACID METABOLISM IS IMPLICATED IN HAEMATOLOGICAL DISEASE | 46 |
| 2.4.1 The role of epigenetic regulation in altered FA metabolism..... | 47 |
| 2.4.2 The bone marrow is the nutrient-providing HSC niche..... | 48 |
| 2.4.3 Metabolism interference with therapy..... | 48 |
| 3. EPIGENETICS: ROLE IN MYELOID DISEASE AND THERAPY | 51 |
| 3.1 EPIGENETICS: A HAEMATOLOGICAL PERSPECTIVE | 51 |
| 3.2 CHROMATIN AS THE BASIS OF EPIGENETIC REGULATION | 52 |
| 3.2.1 Epigenetic regulation in haematopoiesis..... | 54 |
| 3.2.2 Abnormal epigenome in MDS | 55 |
| 3.2.3 Aberrant DNA methylation | 56 |
| 3.2.4 Dysregulation of histone modifications..... | 57 |
| 3.2.5 Histone acetylation..... | 58 |
| 3.3 EPIGENETIC DRUGS FOR MDS | 58 |
| 3.3.1 Hypomethylating agents | 58 |
| 3.3.2 Histone acetylation as a drug target..... | 60 |

| | | |
|-------|----------------------------------------------------------------------------------------------|------------|
| 3.4 | RNA INTERFERENCE | 63 |
| 3.4.1 | shRNA-based knockdown mechanism of action..... | 63 |
| 3.4.2 | shRNA design | 66 |
| 3.4.3 | Applications of RNAi..... | 66 |
| | RATIONALE AND OBJECTIVES..... | 69 |
| 4. | RATIONALE & OBJECTIVES | 71 |
| | RESULTS | 73 |
| 5. | RESULTS I: SHRNA SCREEN | 75 |
| 5.1 | CHAPTER SUMMARY..... | 75 |
| 5.2 | FATTY ACID UPTAKE ASSAY..... | 75 |
| 5.3 | ESTABLISHMENT OF THE SHRNA KNOCKDOWN SCREEN CONDITIONS | 79 |
| 5.4 | GDNA-SEQUENCING SAMPLE PREPARATION | 83 |
| 5.5 | SHRNA SCREEN ANALYSIS | 85 |
| 5.6 | VALIDATION OF THE HEP19 SHRNA SCREEN | 90 |
| 5.7 | DESCRIPTION OF SCREEN HITS CHOSEN FOR FURTHER ANALYSIS | 92 |
| 5.8 | <i>IN VIVO</i> VALIDATION OF THE SHRNA SCREEN..... | 94 |
| 5.9 | PADI4 VALIDATION | 99 |
| 5.10 | PADI4 INHIBITION | 101 |
| 5.11 | PADI4 AND ATRA-INDUCED DIFFERENTIATION | 103 |
| 5.12 | CONCLUSION | 104 |
| 6. | RESULTS II: FATTY ACID UPTAKE PHENOTYPE | 105 |
| 6.1 | CHAPTER SUMMARY..... | 105 |
| 6.2 | SKK-1 CELLS RETAIN FATTY ACID UPTAKE CAPACITY AFTER THREE ROUNDS OF CELL SORTING 105 | |
| 6.3 | TS LOW AND TS HIGH DISPLAY SUBTLE DIFFERENCES IN MITOCHONDRIAL RESPIRATORY CAPACITY | 109 |
| 6.4 | NO SIGNIFICANT DIFFERENCES IN CELL CYCLE OR CELL PROLIFERATION IN TS LOW AND TS HIGH 113 | |
| 6.5 | GENES RELATED TO TYROSINE KINASE RECEPTOR PATHWAYS ARE UP-REGULATED IN TS LOW 114 | |
| 6.6 | STEM CELL MARKERS ARE EXPRESSED IN TS LOW..... | 117 |
| 6.7 | CONCLUSION | 118 |
| 7. | RESULTS III: IDENTIFICATION OF TS LOW AND TS HIGH AS U-937 SUBCLONES | 121 |
| 7.1 | CHAPTER SUMMARY..... | 121 |
| 7.2 | EVIDENCE OF A MIXED POPULATION OF SKK-1 AND U-937 CELLS | 121 |
| 7.3 | TS LOW AND TS HIGH DISPLAY U-937-LIKE IMMUNOPHENOTYPES | 126 |
| 7.4 | CELL LINE-SPECIFIC GENE FUSION DETECTION..... | 129 |
| 7.5 | U-937 GROWS FASTER THAN SKK-1 IN CULTURE..... | 131 |
| 7.6 | SINGLE CELL COLONIES OF TS LOW AND TS HIGH RETAIN FATTY ACID UPTAKE PHENOTYPE 132 | |
| 7.7 | KARYOTYPE PROFILES OF TS LOW AND TS HIGH DIFFER BY TRISOMY 8..... | 134 |

| | | |
|--------|-------------------------------------------------------------------------------------------------------------------------------------------|-----|
| 7.8 | CONCLUSION | 137 |
| | DISCUSSION..... | 139 |
| 8. | DISCUSSION | 141 |
| 8.1 | IDENTIFICATION OF CONTAMINANT U-937 CELLS..... | 142 |
| 8.1.1 | Possible sources of U-937 contamination | 144 |
| 8.1.2 | Contaminant cells are U-937 clones with altered karyotypes | 144 |
| 8.1.3 | Isolation and characterisation of pure U-937 clones can provide a cell culture model for clinically-relevant karyotypic differences | 145 |
| 8.1.4 | The historical issue of misidentified cell lines..... | 146 |
| 8.2 | CHARACTERISATION OF TS LOW AND TS HIGH | 149 |
| 8.2.1 | Stable uptake phenotype: inherent feature or contamination-dependent?..... | 149 |
| 8.2.2 | Transcriptional differences between TS LOW and TS HIGH might reflect differences in cell composition | 150 |
| 8.2.3 | Low OXPHOS capacity in TS LOW and TS HIGH..... | 151 |
| 8.3 | A NOVEL MEANS TO EXPLORE EPIGENETIC-METABOLIC INTERACTIONS | 153 |
| 8.3.1 | Targeting metabolic features of AML cells | 153 |
| 8.3.2 | Mixed results from shRNA screen validation | 154 |
| 8.3.3 | Choice of labelled fatty acid..... | 154 |
| 8.3.4 | Narrow dynamic range of fatty acid uptake assay and cell line | 155 |
| 8.3.5 | Fatty acid uptake as selection criterion for screen..... | 156 |
| 8.3.6 | Advantages and limitations of shRNA knockdown screens | 157 |
| 8.3.7 | A role for PADI4 in fatty acid metabolism?..... | 159 |
| 8.4 | THE ROLE OF DIET IN HAEMATOLOGICAL MALIGNANCIES..... | 161 |
| | CONCLUSIONS..... | 163 |
| 9. | CONCLUSIONS | 165 |
| | MATERIALS AND METHODS | 167 |
| 10. | MATERIALS AND METHODS | 169 |
| 10.1 | CELL LINES AND CELL CULTURE | 169 |
| 10.2 | FATTY ACID UPTAKE ASSAY | 170 |
| 10.3 | FLOW CYTOMETRY AND FLUORESCENCE-ACTIVATED CELL SORTING (FACS) | 171 |
| 10.4 | CELL CYCLE AND PROLIFERATION | 172 |
| 10.4.1 | Proliferation assay..... | 172 |
| 10.4.1 | Cell cycle analysis..... | 172 |
| 10.4.2 | Colony-forming unit (CFU assay)..... | 172 |
| 10.5 | CYTOGENETICS..... | 173 |
| 10.5.1 | Karyotyping | 173 |
| 10.5.2 | Fluorescence <i>in situ</i> hybridization | 173 |
| 10.6 | HIGH-RESOLUTION RESPIROMETRY..... | 174 |
| 10.7 | SEMI-QUANTITATIVE ANALYSIS OF RNA AND DNA LEVELS | 174 |
| 10.7.1 | cDNA synthesis (Reverse Transcriptase) | 174 |
| 10.7.2 | Quantitative reverse transcription PCR (RT-qPCR) | 175 |
| 10.8 | TRANSCRIPTOMIC ANALYSIS..... | 176 |
| 10.9 | DIFFERENTIATION | 177 |

| | | |
|-------------------------------|----------------------------------------------------------------|------------|
| 10.10 | DRUG RESPONSE | 177 |
| 10.10.1 | PADI4 inhibitors | 177 |
| 10.10.2 | Puromycin selection | 178 |
| 10.11 | PROTEIN EXPRESSION ANALYSIS | 178 |
| 10.11.1 | Western blot..... | 178 |
| 10.11.2 | Immunophenotypic analysis..... | 180 |
| 10.12 | SHRNA KNOCKDOWN SCREEN | 181 |
| 10.12.1 | hEpi9 library..... | 181 |
| 10.12.2 | Transfection | 182 |
| 10.12.3 | Infection test | 184 |
| 10.12.4 | Transduction | 184 |
| 10.12.5 | FACS sorting of low and high uptake SKK-1 populations..... | 185 |
| 10.12.6 | PCR and sample preparation for sequencing | 186 |
| 10.12.7 | Test PCR and gel..... | 187 |
| 10.12.8 | Library preparation for determining shRNA enrichment | 189 |
| 10.12.9 | shRNA knockdown screen analysis | 189 |
| 10.13 | SHORT HAIRPIN VALIDATION | 190 |
| 10.13.1 | Plasmids..... | 190 |
| 10.13.2 | PCR amplification of shRNA fragments..... | 190 |
| 10.13.3 | Digestion and ligation | 191 |
| 10.13.4 | Cloning | 192 |
| 10.14 | SINGLE CELL COLONY EXPANSION | 193 |
| 10.15 | IDENTIFIER TEST | 193 |
| 10.16 | STATISTICAL ANALYSIS | 194 |
| 10.17 | LIST OF PRIMERS | 195 |
| 10.18 | LIST OF ULTRAMERS FOR INDIVIDUAL SHRNA KNOCKDOWNS | 198 |
| 10.19 | LIST OF ANTIBODIES | 200 |
| BIBLIOGRAPHY | | 201 |
| 11. BIBLIOGRAPHY | | 203 |
| 12. APPENDIX | | 235 |
| 12.1 | LISTS OF TOP RANKED GENES FROM SHRNA SCREEN | 236 |

Introduction

1. Haematopoiesis and haematological malignancies

Fuil. Sangre. Blut. Blood.

Across languages and cultures, blood conjures a mystical and biological reverence. Ingrained in both our human psyche and animal instincts, its rich, red hue bears an intriguing dichotomy: while our ‘bloodline’ signifies a direct link to our ancestral past, and a hidden force reminiscent of life’s perpetual flow and circularity, to shed blood is a visible mark of bodily harm and loss of vitality. This liquid organ permeates every tissue in the body, carrying life-giving oxygen and nutrients, while also providing sophisticated adaptive and innate immune defences that protect us from otherwise lethal pathogens. The field of clinical haematology is first and foremost concerned with the treatment of blood disorders, and in so doing, has contributed to our overall understanding of organ development. At the apex of the haematopoietic tree—the step-wise conveyor belt of functional blood cells—lie the haematopoietic stem cells. They represent a paradigm for tissue development and are central to blood cell formation. Genetic and epigenetic factors guide haematopoietic stem cells and their progenitors to fully functional blood cells that circulate around the body. In turn, these same genes, when mutated, disrupt the tightly controlled process of blood cell formation, which can result in malignancies to develop. Therapeutic strategies have greatly improved in the last half century with the advent of stem cell transplants and targeted drug therapies. However, myelodysplastic syndromes and other haematological malignancies unfortunately remain largely incurable.

By way of introduction to my PhD thesis, I provide some background to haematopoiesis and associated malignancies. I first give a brief overview of key discoveries that paved the way to our current understanding of how blood cells are produced in the body. I discuss key genes that have been shown to be directly involved in the regulation of haematopoiesis and that, when mutated, drive haematological malignancies, such as myelodysplastic syndromes and acute myeloid leukaemia. I highlight the principle diagnosis methods and

classification systems used in the clinic, which have greatly improved in recent years thanks to enhanced international collaborative efforts between researchers and clinicians. Finally, I point out the major treatments that are currently in place for myelodysplastic syndromes and acute myeloid leukaemia.

1.1 The haematopoietic hierarchy

1.1.1 Haematopoiesis: a historical perspective

Haematopoiesis is the finely tuned process stem cells undergo to differentiate from the multipotential haematopoietic stem cell (HSC) to either common myeloid or lymphoid progenitor cells and finally circulating blood cells. The bone marrow is the site of the majority of blood cell production wherein a vast network of immature and mature blood cell types, as well as non-blood cells and structures, comprise the bone marrow niche. The complex tissue of the haematopoietic systems is responsible for a wide variety of functions for the organism: nutrient and oxygen transport, innate and adaptive immune functions, wound healing and the production of 500×10^9 cells per day (T.M. Fliedner et al., 2002). To produce such large numbers of cells daily, the body relies on a relatively small pool of stem and progenitor cells that exist for decades to produce more specialised cells that survive from days to months. Key to stem cell function is their ability to self-renew and differentiate. The fully functional cells that are formed include erythrocytes, megakaryocytes, platelets, lymphocytes (B and T cells), monocytes, and granulocytes (Doulatov et al., 2012). Our understanding of this elegant system began with early observational studies in the 19th and early 20th centuries and, more recently, has been informed by advanced genetic studies.

Artur Pappenheim's haematopoietic stem tree

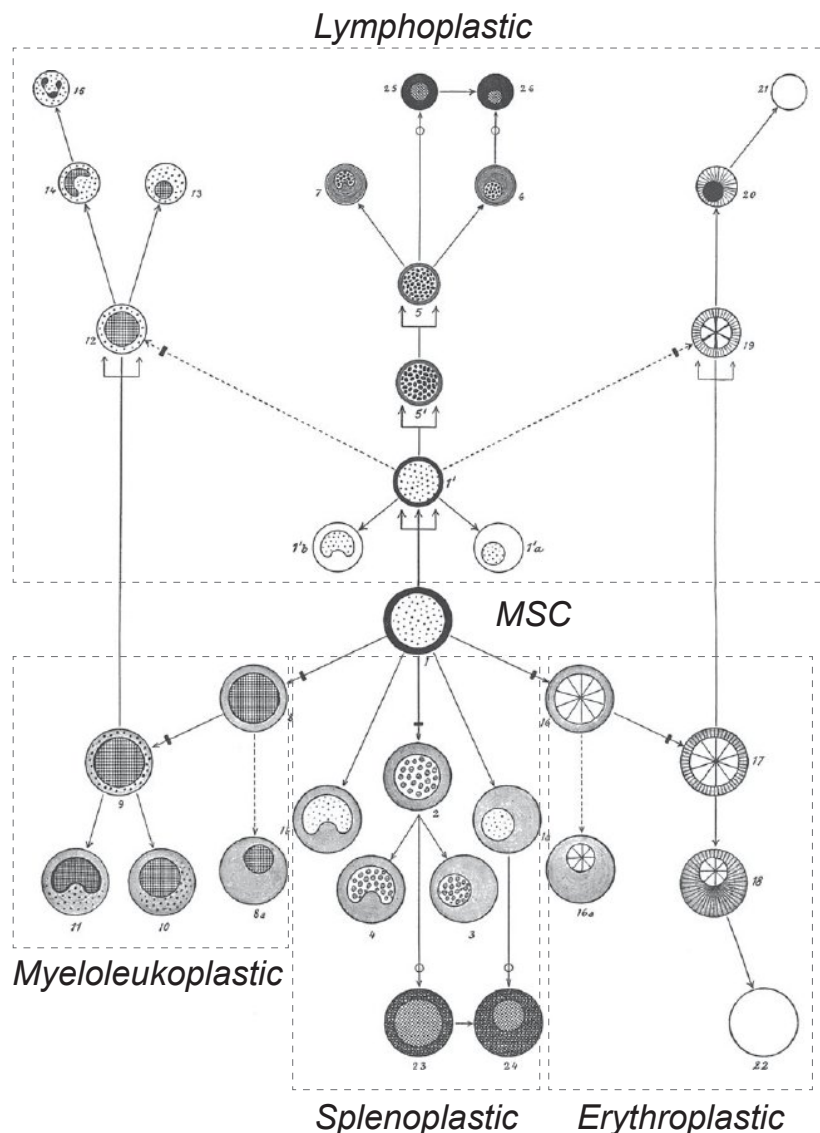


Figure 1: Early interpretations of the stem cell and the haematopoietic hierarchy. Artur Pappenheim's interpretation of haematopoiesis from 1905. The cell in the centre, emphasised by the bold circle, is the hypothesised common progenitor of the entire blood system, which Pappenheim called the stem cell. It is the origin of the 'myeloleukoplasmic branch' (to the left), the 'erythroplasmic branch' (to the right), 'the lymphoplasmic branch' (in the middle and upwards), and the 'splenoplasmic branch' (in the middle and downwards) (Pappenheim, 1905).

The first reference of 'stem cell' came in 1869 when the German scientist, Ernst Haeckel, described the unicellular origin of life as "Stammzelle" (Pappenheim, 1896). Later, he expanded this theory to embryology to describe how single cells give rise to more specialised cells. Although Haeckel's work did not concern blood cell formation, but rather embryology, future researchers interested in haematology were to take inspiration from this hierarchy model. With the help of Paul Ehrlich's vital staining techniques that

distinguished red and white blood cells, early anatomical work reported on the vast network of cells in the bone marrow that displayed differences in morphology and granularity. Artur Pappenheim postulated that red and white blood cells originated from a single stem cell (Pappenheim, 1905) (**Figure 1**). In 1905, Pappenheim produced a diagram illustrating his stem cell fate model featuring a multipotent stem cell in the middle that resembles current representations; a remarkable achievement considering the limited microscopic and staining technologies available at the time. In parallel to these findings, the Russian scientist, Alexander Maximow, was the first to describe the unitarian theory of haematopoiesis, whereby all blood cell types are derived from a common stem cell (Maximow, 1909). Indeed, Pappenheim and Maximow have both been credited with first using the term 'stem cell' in the context of haematology (Ramalho-Santos & Willenbring, 2007). Maximow took advantage of the advances in microscopy of his time and applied his artistic talents to create exquisitely detailed drawings of blood cells, which are still in use by doctors-in-training today (**Figure 2**). However, the concept of a single cell origin of multiple blood cell lineages was to remain theoretical for decades to come.

Major breakthroughs in haematology came during the 'atomic era' of haematologists in the 1940's and 1950's, owing to observations that structural alterations occurred in blood cells following irradiation. The atomic bomb that fell on Japan in 1945 caused widespread health complications. As a consequence, researchers began to investigate the biological effects of radiation, during which time, animal experiments revealed the lowest lethal dose of radiation that eliminated the blood-forming system. One of these scientists, Theodor Fieldner, experimented with ^3H -thymidine labelling methods, which involved injections of bone marrow cells labelled by tritiated thymidine into animals followed by analysis with radiochemical assays (Theodor M. Fliedner, 1998). In this way he was able to distinguish quiescent stem cells from dividing progeny as well as show that stem cells localised to the bone marrow endothelium, thus introducing the concept of the stem cell niche (T. Fliedner et al., 1968). This was followed by the seminal finding that irradiated mice could be transplanted with healthy bone marrow cells to replace the damaged blood-forming cells. This paved the way for the Nobel prize-winning breakthrough by E. Donnall Thomas in 1957 when he performed the first bone marrow transplants in humans (Thomas et al., 1957). Taken together, these studies proved the existence of blood-forming stem cells and their ability to regenerate. However, it was still unclear whether blood cell lineages derive from a single cell of origin or from a multi-stem cell system.

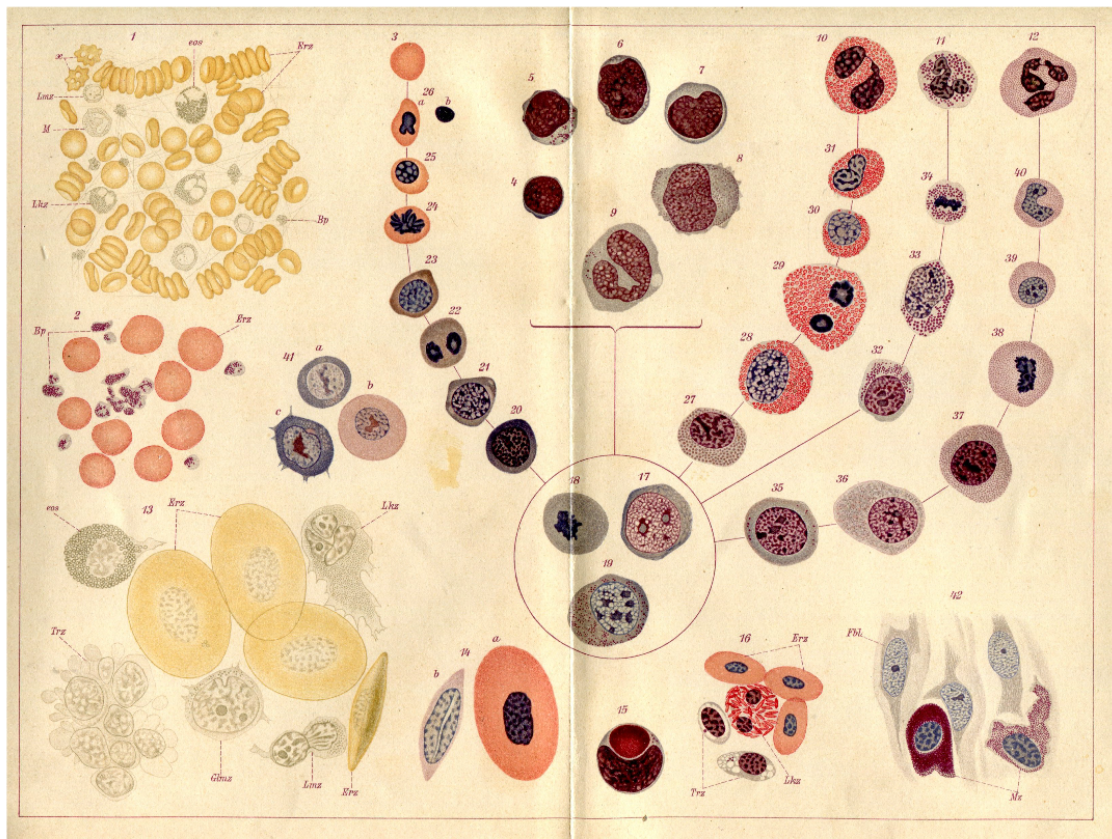


Figure 2: The haematopoiesis scheme of Alexander Maximov. Maximov's gifted artistry complemented his scientific curiosity. This was exemplified with many detailed drawings of blood cells that he directly interpreted from microscopy and staining techniques. The circle indicates the stem cells from which lymphocytes (top right) and erythrocytes (middle left) emerge. This drawing is taken from his book *The Essence of Histology* (1914). Mounts of his drawings can be viewed at the University of Chicago.

The unitarian theory of haematopoiesis was finally demonstrated empirically by McCulloch and Till in 1961, who are best known for identifying HSC. Their work involved first lethally irradiating mice so that the bone marrow cells were completely ablated, after which they transplanted fresh bone marrow cells intravenously. They found that the survival of the animals was directly proportional to the number of transplanted cells, indicating the importance of the cells' regenerative capacity (McCulloch & Till, 1960). Later, they discovered macroscopic nodules of cells in the spleen of transplanted mice that could be easily counted and were directly proportional to the number of transplanted cells (Till & McCulloch, 1961). The nodules contained colonies of proliferating haematopoietic cells of different types, such as erythroid cells, megakaryocytes, granulocytes, and macrophages, which they referred to as 'colony-forming units' (CFUs). CFUs were later shown to have the ability to form heterogeneous colonies after serial transplantation into secondary animal recipients (Becker et al., 1963), thus highlighting the now typical characteristics of stem cells: extensive proliferation, ability to differentiate and capacity to self-renew (Siminovitch et al., 1963).

1.1.2 Modern paradigm of haematopoiesis

Since the early irradiation and transplantation experiments of the 20th century, haematopoiesis has become a paradigm for both tissue organisation and stem cell biology. The functional studies of McCulloch and Till greatly informed how researchers study the haematopoietic system today by utilising CFU assays and murine models to identify primitive progenitor cells.

The immunophenotype comprises a variety of cell surface antigens that are present on HSCs and progenitors. Markers can be simultaneously detected by multi-colour flow cytometry in order to identify the presence and proportion of cell types in a heterogeneous population. In mice, HSCs are identified by the absence of lineage-specific cell surface markers (Lin) and high surface expression of stem-cell antigen 1 (SCA1) and KIT, and are collectively known as Lin⁻SCA1⁺KIT⁺ (LSK) cells (Okada et al., 1992).

Although the hierarchical structure of murine haematopoiesis resembles that of human, HSC markers differ substantially between the two species. Functional assays using humanised murine models have been used to investigate the immunophenotype of human HSCs. Transgenic mouse models express human growth factors that allow for human HSC to engraft and the generation of myeloid and lymphoid progenitors (Ishikawa et al., 2005; Vose et al., 2001).

In vivo studies have revealed that human HSC are enriched in cells expressing Lin⁻CD34⁺CD90⁺CD38⁻ (Baum et al., 1992; W. Craig et al., 1993), which were partly observed in *in vitro* colony-forming experiments (Ishikawa et al., 2005; Vose et al., 2001). Some marker and light scatter combinations are used consistently. For instance, CD45 gating combined with light scatter is used to delineate lymphocytes, monocytes and maturing myeloid cells (Harrington et al., 2012). Overall, however, the immunophenotype of human HSCs is dynamic and, in the clinical setting, patients present with heterogeneous profiles. A representative immunophenotype profile of neutrophil maturation is shown in **Figure 3**, highlighting the dynamics of antigen expression and cell morphology.

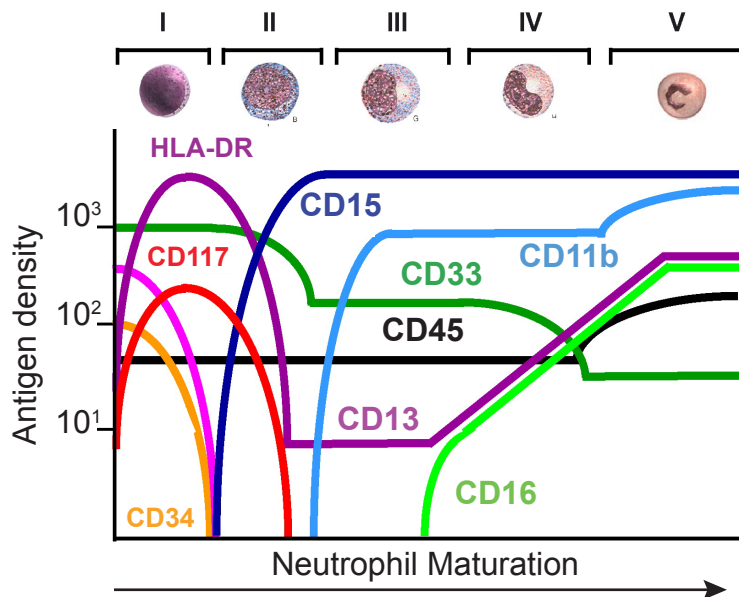


Figure 3: Intensities of various myeloid antigens of myeloid maturation and the corresponding cytological morphology. The maturation stages are as follows: I myeloblasts, II promyelocytes, III myelocytes, IV metamyelocytes/bands, V neutrophils. Adapted from (Loken et al., 2008).

Changes in CD34 and CD38 expression have been reported as part of changes in cell cycle and development states (M. Ogawa, 2002). Further, human HSC are extremely rare; only one in 10^6 are transplantable from the bone marrow (Wang et al., 1997). Therefore, as human HSC must be isolated from bulk differentiated cells, accurate identification is challenging. HSCs can now be functionally defined by two principal characteristics: 1) long-term self-renewal, or the ability to give lifelong rise to identical progeny, and 2) multipotency, or the capacity to differentiate into all blood cell lineages upon serial transplantation into an irradiated secondary recipient, and must do so at a single cell, or clonal, level (Majeti et al., 2007; Wilson & Trumpp, 2006).

The ‘classic model’ of haematopoiesis described discrete compartments of cells with identical potential to differentiate (Orkin & Zon, 2008) (**Figure 4A**). Recently, the updated ‘punctuated continuum’ model postulates that each of these discrete compartments is comprised of heterogeneous pools of cells that are variably primed to give rise to their respective lineages (Liggett & Sankaran, 2020; Pietras et al., 2015) (**Figure 4B**).

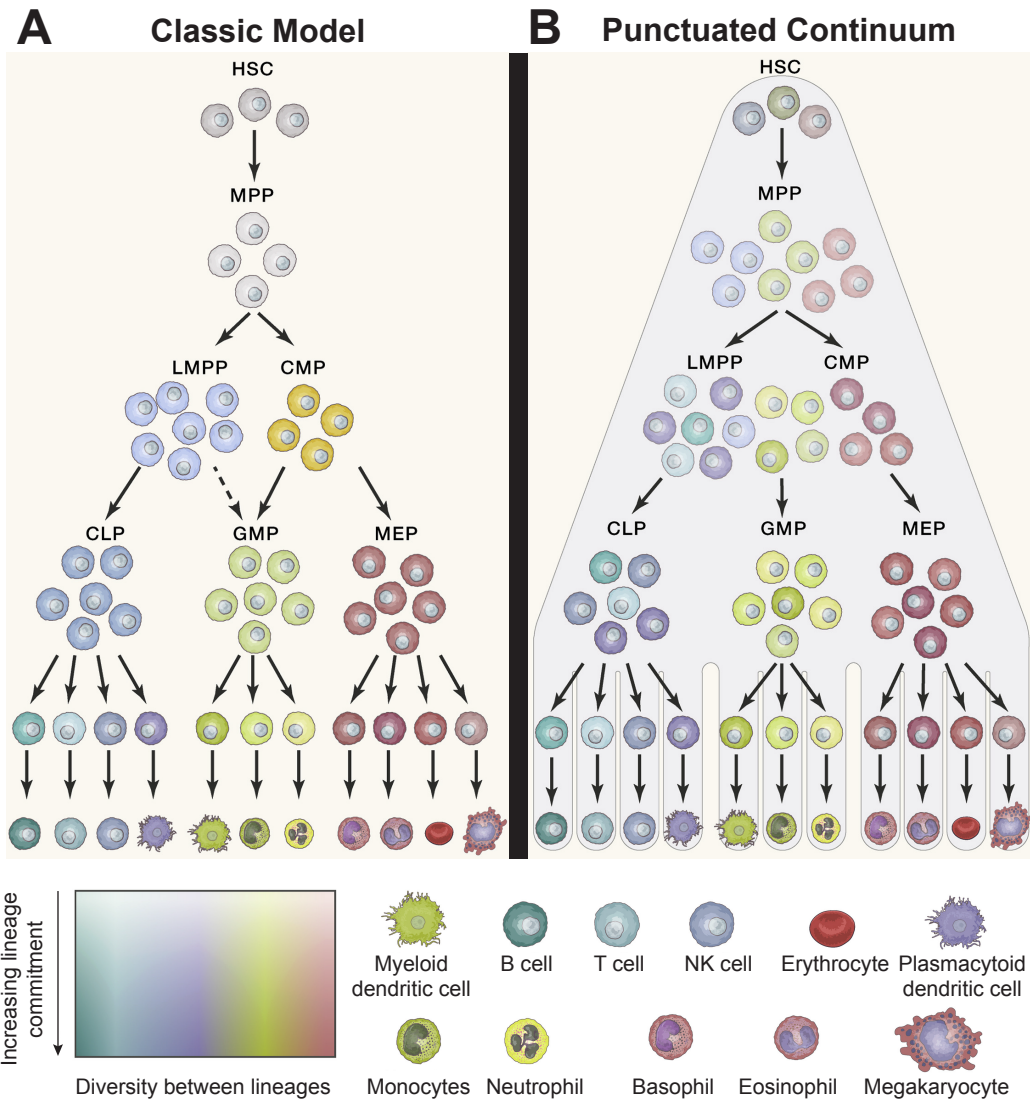


Figure 4: The evolving models of haematopoiesis. A) The “classic model” of haematopoiesis describes discrete stages containing cells of uniform potential, as illustrated by the cell colours. Stepwise cell fate decisions are made and are depicted transformations of one phenotype to another as distinct intervals. HSC, haematopoietic stem cell; MPP, multipotent progenitor; CMP, common myeloid progenitor; MEP, megakaryocyte/erythroid progenitor; GMP, granulocyte/macrophage progenitor; CLP, common lymphoid progenitor; LMPP, lymphoid-primed multipotent progenitor. (Orkin and Zon, 2008). B) The “punctuated continuum” model shares the discrete phenotypic transformations of the classic model but differs in its representation of cell states. Instead of homogenous, single lineage-primed progenitors, each state contains heterogeneous pools of cells that are variably primed to give rise to different haematopoietic lineages, as indicated by the variation in colour. The magnitude of this lineage commitment increases with colour intensity as cells proceed along the differentiation hierarchy (Pietras et al., 2015).

1.1.3 Haematopoietic cell types

Haematopoietic cells that are not capable of self-renewal, but give rise to differentiated cells, are termed multipotent progenitors (MPP) and lie directly downstream of the HSC. MPP-specific immunophenotype features include the loss of CD90 (Pang et al., 2011). It is at this point that cells lose their complete multipotency and become either lymphoid, myeloid, megakaryocytic or granulocytic precursors. Lymphoid-primed multipotential progenitors (LMPP) are the first lymphoid-restricted compartment, which, in turn, give rise to common lymphoid progenitors (CLP) and granulocyte/macrophage progenitors (GMP), but have little potential for megakaryocyte/erythroid progenitors (MEP) (Dias et al., 2008). The CLP lineages consist of T, B, and NK cells, which perform adaptive and innate immune functions. Common myeloid progenitors (CMP) and GMP give rise to the myeloid lineages, which broadly function in oxygen transport and innate immunity. Monocytes, neutrophils, eosinophils, basophils, and dendritic cells provide a general defence against pathogens and initiate adaptive immune responses. Erythrocytes, or red blood cells, are responsible for carrying oxygen around the body. **Figure 4** also outlines the different precursor lineages that lead to mature blood cells.

1.1.4 Haematopoiesis during aging

Aging has a clear effect on the self-renewal capacity of HSC and decreases in CD34⁺ cells have been reported. There is decreased bone marrow cellularity, decreases in lymphocytic lineages, red cell abnormalities such as anaemia and higher incidence of haematological malignancies (discussed below) (Beerman et al., 2010). Clear differences are observed between the HSC compartments of healthy young and old people. Older age groups display bias towards myeloid progenitors that have a more active cell cycle, but less engraftment potential, which contribute towards age-related degeneration of the haematopoietic system. Unfortunately, this predisposition can lead to myeloid malignancies and immune system decline (Pang et al., 2011). The sequence of developmental events can be tracked by differential expression of cell surface markers (Ding et al., 2017). Since their discovery over the last century, cell surface markers have proven to be an invaluable tool to understand the haematopoietic system, from both a developmental and pathological standpoint.

1.2 Myelodysplastic syndromes and their clinical management

Haematological malignancies, or leukaemias, affect the normal function of blood cells by disrupting haematopoiesis. There are many sub-types of leukaemia that can be broadly classified into 'myeloid' and 'lymphoid,' depending on which blood cell lineage is affected,

and ‘acute’ and ‘chronic’, depending on the speed of disease onset and progression. The four major groups of leukaemia are acute myeloid leukaemia (AML), chronic myeloid leukaemia (CML), acute lymphoblastic leukaemia (ALL), and chronic lymphocytic leukaemia (CLL). Within those broad categories, leukaemia is further divided into sub-classes that affect specific progenitor cells. Ultimately, however, all leukaemias develop from undifferentiated stem or progenitor cells. Myelodysplastic syndromes (MDS) and acute myeloid leukaemia (AML) are groups of haematological disorders affecting the myeloid compartment caused by abnormal differentiation and uncontrolled proliferation of malignant leukaemic stem cell (LSC) clones at the expense of normal haematopoiesis (Sperling et al., 2017). In the case of MDS, there is an initial expansion of the HSC pool followed by exhaustion that leads to a reduction in circulating blood cells. AML is characterised by massive proliferation of dysfunctional cells that disrupt the normal output of healthy blood cells. Although most AML cases develop *de novo*, MDS can act as a precursor malignancy that transforms to secondary AML (sAML).

1.2.1 Epidemiology and pathogenesis of MDS

AML is the most common type of acute leukaemia in adults (Germing et al., 2008) and MDS is the most frequent haematopoietic disorder in the elderly (Kuendgen et al., 2006; Sekeres, 2011). Advanced age is the main contributing risk factor of acute myeloid malignancies, with the median age of diagnosis at around 70 years and 92% of MDS patients aged over 50 years (Cogle et al., 2011; Germing et al., 2008). Annual incidences of 3-5 cases per 100,000 population have been reported, rising to 20 cases per 100,000 individuals aged older than 70 years (McQuilten et al., 2014). However, underreporting of MDS is likely, as several iterations of classification systems have been developed since the 1980s and the condition itself has been a notifiable cancer since only 2001 (B. M. Craig et al., 2012). As a result, the true incidence of MDS may be closer to 65 per 100,000 in people over 65 years (Germing et al., 2008). In contrast, MDS is rare among young people, accounting for just 5% of haematological malignancies in children under 14 years (Germing et al., 2008). Prognosis for MDS varies with median survival ranging from six months to five years, depending on genetic characteristics (Arber et al., 2016). MDS are clonal stem cell disorders where a genetic aberration in one HSC or progenitor cell can result in the evolution of the whole disease. Both MDS and AML are characterised by proliferation of HSCs, genetic abnormalities, ineffective haematopoiesis and various cytopenias (Bennett et al., 1982).

Cytopenia, or reduced counts of mature blood cells, in at least one myeloid lineage is required for diagnosis of MDS. Consistent with peripheral cytopenia, of which anaemia

is most common, patients present with a wide range of symptoms, including fatigue (Efficace et al., 2015), which comes with an altered sense of well-being; recurring infections related to neutrophil dysfunction (Pomeroy et al., 1991); and autoimmune abnormalities, such as rheumatic heart disease, that affect up to a quarter of MDS patients (Anderson et al., 2009). MDS develops with increased numbers of myeloid progenitors, or blast cells, and reduced overall normal haematopoiesis leading to cytopaenia (Sperling et al., 2017)

1.2.1 Transformation to secondary AML

Like MDS, AML is a group of disorders affecting the myeloid lineage of blood cells in the bone marrow. In AML HSCs undergo genetic mutations that result in ineffective haematopoiesis and dysfunctional blood cells due to impaired differentiation (Shih et al., 2012). *De novo* AML occurs without any previous neoplasm, is more common in younger patients and is associated with better overall survival (Lindsley et al., 2015).

Around 30% of MDS patients transform to secondary AML (sAML) (Steensma & Bennett, 2006). sAML is characterised by further increases in blast cell counts above 20% in the bone marrow, as defined by WHO classification (Swerdlow et al., 2017), along with subsets of co-occurring genetic mutations and epigenetic abnormalities, many of which are shared with MDS (Sperling et al., 2017).

MDS and sAML patients develop aberrant genetic and epigenetic changes that distinguish them from healthy cells (Shen et al., 2011; Shih et al., 2012) (figure 4). Specifically, LSCs in late stage MDS acquire mutations that confer uncontrolled growth, such as *NRAS*, and inhibition of apoptosis, such as *TP53*. Together with epigenetic abnormalities, these oncogenic mutations cause blast cell numbers to increase and inhibit differentiation, which is characteristic of the MDS to sAML transformation (Sperling et al., 2017).

The heterogeneous mutational landscape of MDS and sAML makes it difficult to devise exact molecular signatures of disease progression. It is unclear whether the transformation to sAML is brought about by an accumulation of mutational events (Lindsley et al., 2015) or a single ‘tipping point’ mutation (Shukron et al., 2012). However, it appears that there is overall increased mutational burden in sAML compared to MDS (Kim et al., 2017).

LSCs show spontaneous apoptosis *in vitro* but increased proliferation *in vivo* (Lane et al., 2009), indicating intrinsic factors of the cells and extrinsic factors in the bone marrow environment may contribute to their survival. Indeed, an abnormal stem cell niche may favour the outgrowth of mutant clones, such as disruptions to the bone marrow architecture and the immune signalling pathways that take place there (Pronk & Raaijmakers, 2019).

1.2.2 Classification and prognostic scoring of MDS

MDS were originally classified in preleukaemic conditions by the French-American-British (FAB) group (Bennett et al., 1976). The classification was based on morphological abnormalities of myeloid lineage cells, or “myelodysplasia”, and the number of blasts, or immature myeloid lineage cells. This groundwork led the path for future classification systems of MDS sub-types, as the morphological and haematological approach proved to be reproducible and hold prognostic value. Currently, MDS and AML diagnoses are established by the proportion of blasts, in either the bone marrow or the peripheral blood. In MDS, blast counts are between 5 and 20% and are over 20% in AML (Swerdlow et al., 2017). Increasing blast counts signify ineffective haematopoiesis, with the accumulation of undifferentiated and dysfunctional cells. The initial FAB classification described five sub-types of MDS, which has since been revised under the World Health Organisation (WHO). In 2016, the WHO released an updated classification for MDS that provides a more refined criteria for clinical diagnostics and decision-making and is now the standard for MDS classification (Swerdlow et al., 2017). The classification was expanded to include genetic and cytogenetic abnormalities that reflect recent findings. Six sub-types of MDS were described: 1) MDS with single lineage dysplasia (MDS-SLD); 2) MDS with multi-lineage dysplasia (MDS-MLD); 3) MDS with ring sideroblasts (MDS-RS), which includes the sub-groups single- and multi-lineage dysplasia (MDS-RS-SLD and MDS-RS-MLD); 4) MDS with excess blasts (MDS-EB), which includes the sub-groups MDS-EB₁ and MDS-EB-2; 5) MDS with isolated del(5q); and 6) MDS, unclassifiable (MDS-U).

In 1997, a working group set up the International Prognostic Scoring System (IPSS) that integrated large amounts of clinical data as part of a risk assessment system for MDS (Greenberg et al., 1997). A revised IPSS (IPSS-R) was later developed to include wider clinical features, such as refining blast percentages at the lower levels and revising the weights given to cytogenetic abnormalities, that improved prognostic prediction of survival and risk of sAML transformation (Greenberg et al., 2012). IPSS-R provides five risk categories based on five prognostic sub-groups: cytogenetic abnormalities; marrow blast percentage; and depth of cytopaenia, as calculated by haemoglobin levels (<10 g/dL), platelet counts (<100 x 10⁹/L), and absolute neutrophil count (<1.8 x 10⁹/L). Among additional variables that are also taken into consideration, such as marrow fibrosis and serum lactate dehydrogenase, the prognostic score is adjusted for the age of the patient.

1.2.3 Diagnostics

The diagnosis of MDS is currently based on a combination of cytology, cytogenetics and cytometry techniques with the help of the aforementioned prognostics protocols. Genetic

and flow cytometry methods complement diagnoses and are considered as part of the IPSS-R or WHO guidelines.

Complete blood counts give valuable information about the degree of cytopaenia in the peripheral blood. Notably, anaemia is almost always present, and half of patients have reduced white blood cell counts (Swerdlow et al., 2017). Dysplasia, or abnormal morphology, of bone marrow and peripheral blood cells is a common feature of MDS (Huang et al., 2008). Red blood cells may appear as macrocytic, while white blood cell lineages may appear enlarged, have abnormal nuclear shape, or, in the case of granulocytes, reduced granulation (Huang et al., 2008). Essential to evaluating MDS is the examination of bone marrow aspirates and biopsies. Bone marrow aspirates are performed to measure blast counts and cellular morphology. Hypercellularity of the bone marrow, in the form of increased blast numbers, is usually evident. Bone marrow biopsies determine the cellular structure of bone marrow by extracting sections from the iliac crest of the spine (Bain, 2001).

86% of the known cytogenetic abnormalities can be assigned a prognostic score, according to the original IPSS (Greenberg et al., 1997). Characterisation of cytogenetic and molecular abnormalities is carried out using karyotyping and fluorescence *in situ* hybridisation (FISH) techniques. Cytogenetic abnormalities have been well established as prognostic factors in MDS and are very heterogeneous (Schanz et al., 2012). IPSS-R describes 19 different cytogenetic alterations with assigned prognostic subgroups, for example: very good, loss of Y chromosome; good, deletion of the q-arm of chromosome 5 (del(5q)); intermediate, gain of chromosome 8 (trisomy 8); poor, loss of chromosome 7; very poor, complex karyotype (three or more abnormalities) (Hirai, 2003; Stengel et al., 2019) (**Figure 5**).

Indeed, additional cytogenetic changes commonly emerge in MDS patients during the course of the condition, which are associated with increased risk of sAML transformation and worse overall survival (Jabbour et al., 2013). However, more than half of patients with myelodysplastic syndromes have a normal karyotype, and patients with identical chromosomal abnormalities are often clinically heterogeneous (Haase et al., 2007). Flow cytometry is principally used to detect abnormal immunophenotypes, as determined by the detection of cell surface antigens by measuring abnormal increases or decreases in populations, along with the expression of mature and immature lineage markers (Bento et al., 2017).

Specifically, antibody combinations such as CD45/CD34/CD117/HLA-DR and CD45/CD34/CD123/HLA-DR distinguish myeloid progenitor cells from other cell

populations (Papaemmanuil, 2014). A good correlation between the percentage of blasts, as determined by morphological evaluation of the bone marrow aspirate, and CD34+ cells, as determined by flow cytometry has been reported (Porwit et al., 2014; van de Loosdrecht et al., 2013).

There can be poor reproducibility for detecting dysplasia in the clinic. In cases of minimal dysplasia, such as MDS with isolated del(5q), flow cytometry offers a pattern recognition approach to detect dysplastic characteristics, as clones with an abnormal immunophenotype may display normal morphology, such as abnormal myeloid progenitor cells (Ogata, 2002; Stachurski et al., 2008). Overall, while blast count and cell morphology examinations remain indispensable for diagnosis, flow cytometry is a useful complementary tool for diagnosis and for following the disease course.

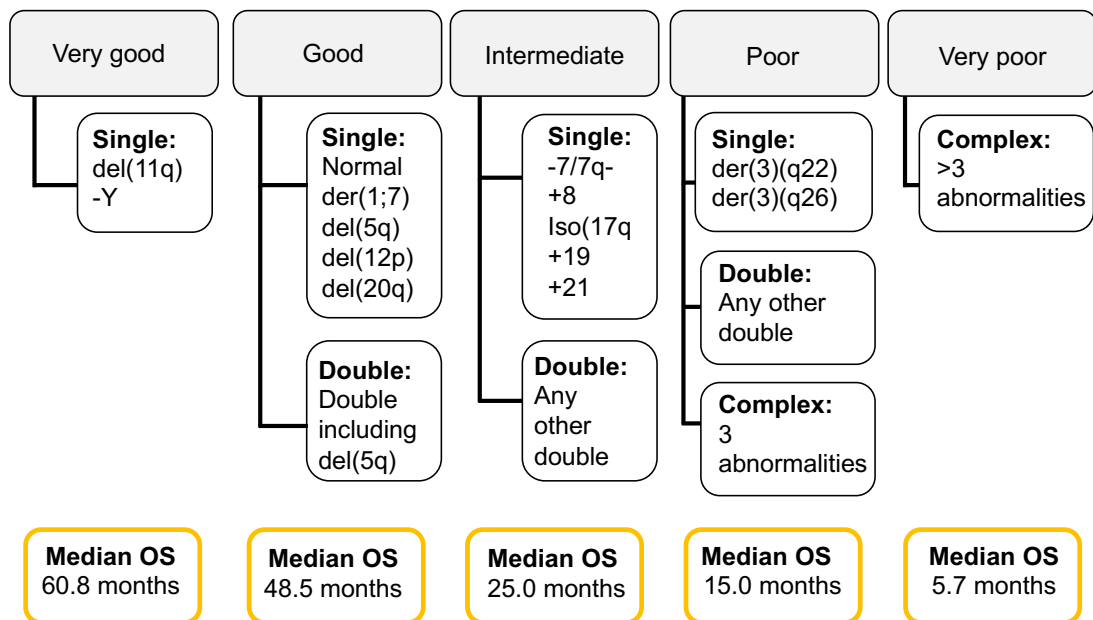


Figure 5: IPSS-R cytogenetic risk stratification of MDS patients. The revised international prognostic scoring system (IPSS-R) classifies MDS patients into five sub-groups based on cytogenetics: very good, good, intermediate, poor and very poor. Single, double and complex (three or more) chromosomal abnormalities contribute towards disease severity and overall survival (OS). Adapted from (Schanz et al., 2012).

1.2.4 Current therapeutic strategies

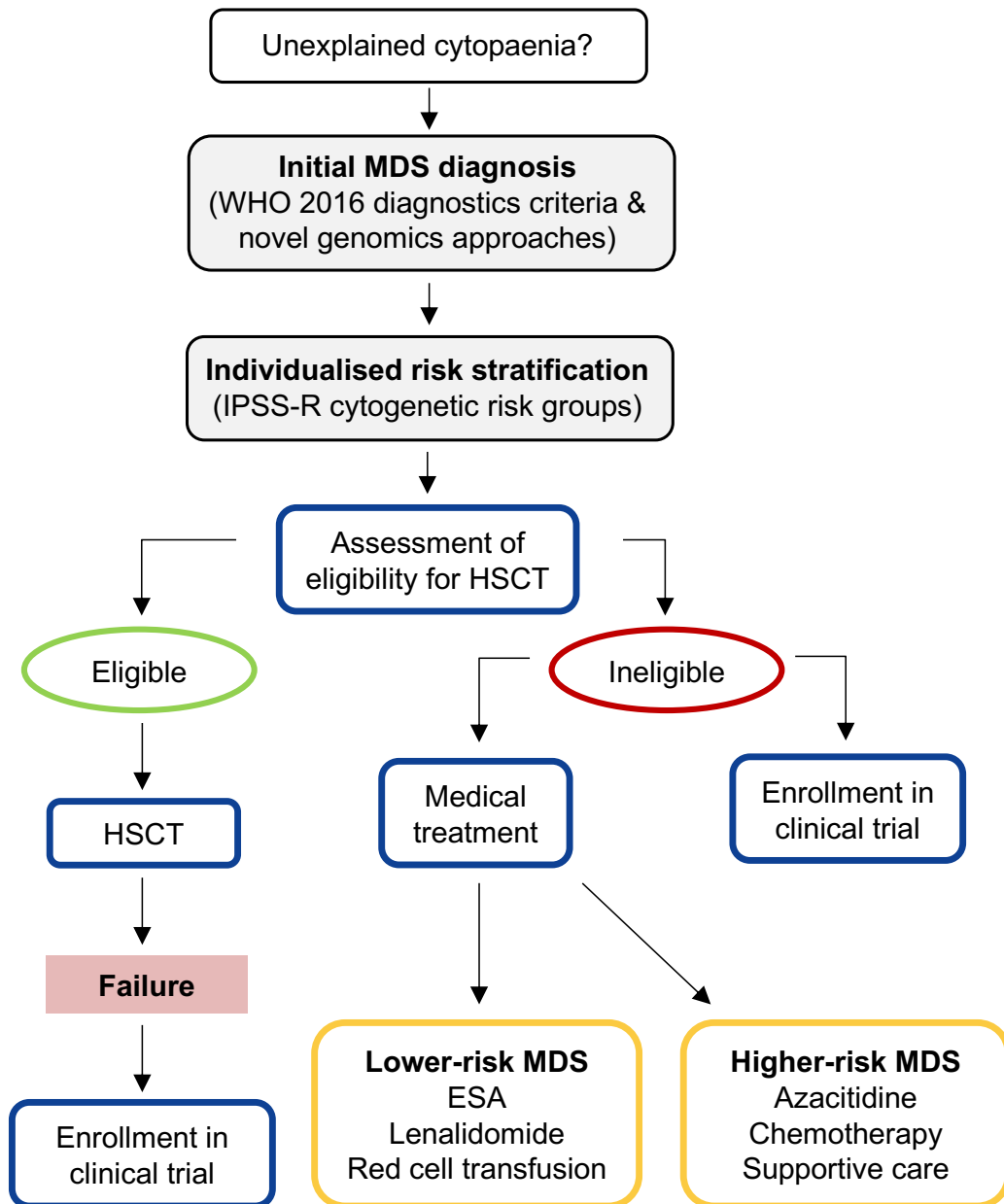
Without treatment intervention, high-risk MDS and sAML patients have a life expectancy of about 9 months (Greenberg et al., 2012). Allogeneic haematopoietic stem cell transplantation (HSCT) is the only curative treatment for MDS. However, the process is invasive and is associated with significant morbidity (Saber & Horowitz, 2016). This is of special concern for elderly people, for whom the treatment is often unsuitable and pharmaceutical therapies are sought. Nowadays, chemotherapy is used less frequently; however, cytarabine, which induces DNA damage in cancer cells, can be prescribed to HSCT-ineligible patients under 60 years with greater than 10% bone marrow blasts (Malcovati et al., 2013). The main pharmaceutical treatment lines available for MDS include initial supportive therapy, which aims to alleviate cytopenic symptoms by increasing blood cell counts, and hypomethylating agents (discussed in greater detail in section 1.3).

The treatment objectives for low-risk MDS is to lessen the clinical manifestations of cytopaenia and improve quality of life for the patients (**Figure 6**). Anaemia is one of the main outcomes of ineffective haematopoiesis due to low red blood cell counts and, as one of the main cytopaenias in MDS, affects over 50% of patients (Bowen & Hellstrom-Lindberg, 2001). Red blood cell transfusions are administered to most MDS patients during the course of the disease (Cazzola et al., 2008). Erythropoietic stimulating agents (ESA) stimulate the production of red blood cells and reduce transfusion dependence. Recently, the recombinant form of human erythropoietin, epoetin alfa, has been approved in Europe to treat low-risk MDS patients with anaemia (Gascón et al., 2019). Two-thirds of MDS patients with del(5q)-associated anaemia respond to lenalidomide, which reactivates genes with haploinsufficiency encoded on the deleted 5q arm (Giagounidis et al., 2014).

Hypomethylating agents, namely azacitidine, represent the best treatment strategy for high-risk MDS patients who are ineligible for HSCT. Worryingly, however, chemoresistance and relapse among treatment responders is common (Santini et al., 2014). The heterogeneous mutational burden of LSCs means that reliance on target-specific drugs is limited; therefore, more general, broad-acting therapies have mainly been used to date. It is believed that hypomethylating agents mainly function to reactivate tumour suppressor genes by reducing global DNMT3A-mediated methylation. Work in

our lab is ongoing to elucidate azacitidine's cytotoxic effects in MDS- and sAML-derived cell lines (Diesch et al, in review).

Figure 6: A representative MDS treatment algorithm. Patients with unexplained



cytopaenia symptoms are assessed following WHO and IPSS-R guidelines. While some patients may require only continuous monitoring and symptom relief, others must be assessed for allogeneic haematopoietic stem cell transplant (HSCT) eligibility. Approximately two-thirds and one-third of MDS patients are considered low-risk and high-risk, respectively. The median age is 70 years, of whom only a minority are eligible for HSCT. For lower risk patients, the choice of treatment is largely based on disease subtype. For example, erythropoiesic-stimulating agents (ESA) regain red blood count, following anaemia, and lenalidomide is effective in patients with del(5q). The majority of patients are treated with hypomethylating agents, primarily azacitidine, but only a minority have a benefit. Therefore, enrolment in clinical trials should be considered. Adapted from Bejar, 2014 and Cazzola, 2020.

1.2.5 Novel drugs

The limited efficacy of hypomethylating agent monotherapies and the strict inclusion criteria for HSCT means that novel drugs are urgently needed. Indeed, a number of new strategies for MDS are showing promising results.

Numerous combinatorial treatments with azacitidine are being considered. Recently, APR-246 in combination with azacitidine has been given therapy designation status by the FDA. Clinical trials with APR-246, a mutant p53 reactivator, in combination with azacitidine are ongoing and have shown high response rates in high-risk MDS patients, albeit only in those with the deactivating p53 mutation (Cluzeau et al., 2019; Sallman et al., 2019). The selective BCL-2 inhibitor, venetoclax, has been approved for AML treatment and is showing promise in MDS. Recently, it was reported that venetoclax in combination with azacitidine increased response and prolonged survival compared to azacitidine treatment alone in MDS patients (Ball et al., 2020).

There are several targeted monotherapies in late-stage clinical trials stages as well as several combinatorial therapies. Targetable mutations include *TP53*, *IDH1* and *IDH2*, which are found in 5-10% of MDS patients, and drugs specific for these mutations are in clinical trials. Enasidenib has been approved for the treatment of AML with *IDH2* mutation and is showing promise for MDS patients. A recent phase 1 trial was the first to report positive outcomes in high-risk MDS patients with *IDH2* mutations. Overall, there were haematological improvements observed, including in those patients with previous treatment with hypomethylating agents (Stein et al., 2020).

Chimeric antigen receptor (CAR) T cell therapies have revolutionised treatment strategies for lymphoid leukaemias, such as paediatric and adult ALL (Mardiana & Gill, 2020). So far, the success of CAR T therapies has not translated to myeloid malignancies, mainly due to the heterogeneous immunophenotypes of the various myeloid-derived leukaemias, which often overlap with healthy HSCs. Recently, CD123-positive stem cells in high-risk MDS patients were shown to be metabolically distinct from normal CD123-positive HSCs, suggesting a potential therapeutic CAR T target (Stevens et al., 2019).

1.3 MDS is part of a spectrum of clonal myeloid diseases

MDS is part of a spectrum of clonal myeloid diseases starting with asymptomatic expansion of mutated HSC clones and ending with transformation to full-blown sAML. MDS is driven by a number of driver mutations that contribute to the heterogeneous disease outcome.

Clonal haematopoiesis of indeterminate potential (CHIP) describes the expansion of clonal populations of blood cells from a single HSC with one or more somatic mutations. It is a frequent consequence of ageing, which when accompanied by driver mutations, can result in haematological malignancies (Steensma, 2018). Although it is accepted that the accumulation of mutations directly results in the onset of MDS, genetic mutations are not included in the WHO classification system or IPSS-R prognostic scoring. MDS-specific mutations have been found in normal HSC of people without MDS (Steensma et al., 2015). MDS-associated mutations were first reported as prognostic indicators independently of IPSS-R in 2011 (Bejar et al., 2011). Since then, the expansion of genetic information has revealed a much broader disease landscape.

1.3.1 Clonal haematopoiesis of indeterminate potential (CHIP)

Mutated stem cells are provided with a selective growth advantage, which can lead to CHIP. The CHIP model of cancer evolution, as proposed by Steensma and colleagues, refers to the expansion of LSCs with one or more somatic mutations but without the resulting symptoms related to haematological malignancies (Steensma et al., 2015) (

Figure 7). There are normal peripheral blood counts and no evidence of WHO-defined criteria for a haematological malignancy. Crucially, however, there is a variant allele frequency (VAF; the percentage of mutated DNA sequence reads at a given genetic locus) greater than 2% of a leukaemia-associated mutation. For this purpose, VAF is a surrogate measure for the number of bone marrow cells that contain the mutation.

CHIP-related mutational burden appears to increase with age, as CHIP is present in 10-15% of individuals aged over 70 years (Sperling et al., 2017). As of now, VAF cut-offs that demarcate MDS-relevant somatic mutations have not been clinically validated and so await further development, most likely with increased sequencing power (Sperling et al., 2017). The most common mutations affect *DNMT3A*, *TET2*, and *ASXL1*; however, usually only one mutation is detected in individuals with CHIP (Bowman et al., 2018).

Although the overall blast cell count remains low and there is little effect on normal blood cell function, individuals with CHIP have increased risk of developing blood malignancies. In scenarios where the fitness of clones increases, mutated cells and their progeny continue to proliferate among the bulk cell population, resulting in the production of mature, but malignant, blood cells. The mutated clones proliferate and replace normal

cells, becoming under the control of the niche and immune system. Eventually, this expansion of mutated cells can lead to cytopenia resulting in blood disorders, such as MDS and AML.

Alternatively, a reservoir of mutated cells can develop that do not adversely affect the organism immediately but may contribute to future malignancies (Corces-Zimmerman & Majeti, 2014). Therefore, mutated blasts can expand in the bone marrow for years before the onset of clinical symptoms (**Figure 7**). The current challenge lies in the detection and characterisation of CHIP as a means to predict the onset of MDS, and potentially sAML.

1.3.2 Somatic mutations

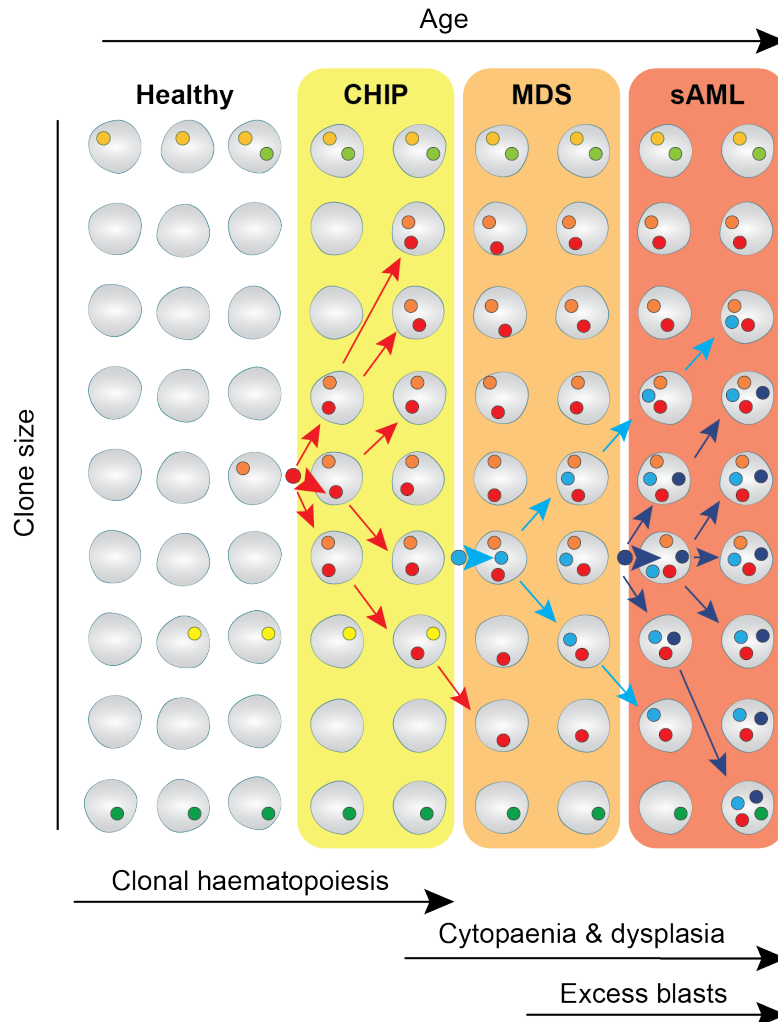
Somatic mutations occur both as part of the normal course of aging and as a result of environmental mutagens. Despite the substantial effects that even one mutation can have on disease outcome, most confer a neutral effect overall, as non-coding regions are mainly affected (López-Otín et al., 2013). Early predictors of malignancies can be found in small quantities of clones with specific somatic mutations. Driver mutations associated with blood malignancies can be detected in healthy asymptomatic individuals with normal, or close to normal, blood counts. Mutated clones proliferate and replace normal cells, becoming under the control of the niche and immune system. Evidence that mutations arise from ageing alone comes from the observation that most mutations are C-to-T transitions at CpG dinucleotides, indicating deamination of methylated cytosines (Makishima et al., 2016).

Genetic mutations in MDS can be grouped into broad classes: epigenetic regulators, spliceosomal machinery, cohesion, DNA processing enzymes, transcription factors and tumour suppressor genes (Steensma et al., 2015)

Figure 7). Epigenetic regulators and RNA splicing-encoding genes are most frequently mutated. *SF3B1* and *TET2* mutations initiate clonal expansion and are the most commonly affected genes in MDS, affecting 20-25% patients (S. Ogawa, 2019). *SF3B1* mutations cause aberrant RNA splicing that results in abnormal erythropoiesis and macrocytic anaemia. Loss-of-function mutations in *TET2* cause decreased demethylation, resulting in the activation of genes involved in stem cell self-renewal and differentiation (Feng et al., 2019). The splicing factor, *SRSF2*, and the epigenetic regulators *ASXL1*, *RUNX1* and *DNMT3A* are mutated in at least 10% of MDS patients (Steensma, 2018). Inactivation of the hallmark

| Introduction I

tumour suppressor gene, *TP53*, occurs in 5-10% of MDS patients in advanced stages of the disease and is significantly associated with the del(5q) subtype and complex karyotypes (Cumbo et al., 2020; Sugimoto et al., 1993). Loss-of-function mutations in the p53 transcription factor disrupt normal cell cycle regulation, highlighting its role in leukaemogenesis (Parker et al., 2000).



| | Epigenetic | Splicing | Transcription factor | Signalling |
|------------------------------------------------------------------------------|----------------------------------------------|--------------|-----------------------------|------------------------------------------|
| Background mutations ● ● ● ● unrelated to haematopoiesis expansion | | | | |
| Early mutations initiate clonal expansion ● | <i>DNMT3A</i> <i>TET2</i> <i>ASXL1</i> | <i>SF3B1</i> | | <i>JAK2</i> |
| Late mutations contribute to disease ● ● | <i>IDH1/2</i> <i>EZH2</i> | <i>SRSF2</i> | <i>RUNX1</i> <i>TP53</i> | <i>FLT3</i> <i>NRAS</i> <i>KIT</i> |

Figure 7: Clonal haematopoiesis in MDS and transformation to sAML. Clonal haematopoiesis, the over-representation of a single clone in the blood or bone marrow, can begin in early life (white area). Background mutations unrelated to haematopoiesis can arise as part of the natural ageing process and can increase in clonal size. Mutations (red circle) can sporadically arise and lead to increased HSC self-renewal, clonal expansion and the development of CHIP (yellow area). During this period, there are little overt clinical features of disease. Mutant clones enlarge and give rise to an expanding population of cells that acquire additional genetic mutations (light blue). These mutations confer a selection advantage that allow mutated cells to out-compete healthy ones, thereby promoting the progression to myelodysplastic syndromes (MDS). Secondary mutation events (dark blue) can lead to cytopenia (reduced blood cell numbers), dysplasia and excess blast counts. Eventually, these events can lead to secondary acute myeloid leukaemia (sAML). Overall, the risk of developing CHIP, MDS and sAML increases with age. Adapted from Sperling et al., 2017 and Steensma et al., 2015.

2. Fatty acid metabolism and its role in haematological malignancies

Fatty acid (FA) metabolism has gained greater attention in the context of leukaemia in recent years (Maher et al., 2018). The early discoveries of Otto Warburg posited that cancer cells relied on aerobic glycolysis and was a result of mitochondrial injury. Today, a more complex picture has emerged whereby cancer cells exhibit metabolic plasticity that is dependent on the tumour niche in which they find themselves. In particular, FA metabolism has gained attention in recent years for its role in driving leukaemogenesis and providing protective features for LSC.

This brief review endeavours to highlight the changes in FA metabolism that distinguish malignant leukaemic cells from healthy cells. Firstly, by way of background, I would like to provide a summary of anabolic and catabolic FA metabolism and an overview of key transcriptional regulators. The bidirectional relationship between epigenetics and metabolism is an expanding field of study and I will point to some of the relevant epigenetic regulators and to the reciprocal effects of FA metabolism on epigenetic mechanisms. Finally, I will outline our current understanding regarding the role FA metabolism plays in haematological malignancies, namely MDS and AML.

2.1 Overview of fatty acid metabolism

2.1.1 Beta-oxidation

Oxidative phosphorylation (OXPHOS) generates 36 moles of ATP from one mole of glucose compared to two moles of ATP produced from glycolysis alone (Heiden et al., 2009). Though OXPHOS is a far more efficient process, glycolysis is faster and so may favour rapid proliferation of cancer cells. The tricarboxylic acid cycle (TCA) utilises acetyl-CoA derived from the step-wise breakdown of glucose to pyruvate during glycolysis in the cytosol and the sequential breakdown of FA from beta-oxidation in the mitochondria. From there, the TCA yields nicotinamide adenine dinucleotide (NADH) and flavin adenine dinucleotide (FADH₂). To generate ATP, these high-energy molecules provide electrons that are transferred to O₂ along the electron transport chain of complex proteins in the mitochondria. In the context of haematological malignancies, leukaemic cells often utilise FAs under metabolically stressed conditions, and the NADH and FADH₂ that are

| Introduction II

generated support ATP production, redox homeostasis and biosynthesis. Regulation of both anabolic and catabolic processes in FA metabolism is exerted on the levels of FA transporters, mitochondrial biogenesis and intermediate enzymes.

FAs are degraded by beta-oxidation in the mitochondria providing energy in the form of ATP and acetyl-CoA for protein acetylation and anabolic reactions. Several membrane-associated proteins including CD36, membrane-associated FA-binding proteins (FABP) and a number of FA transport proteins facilitate FA uptake into the cell (Stremmel et al., 2001). In particular, CD36 plays an important role in the regulation of FA uptake due to its ability to translocate between intracellular endosomes and the plasma membrane (Luiken et al., 2003). This intracellular translocation is dependent on FA availability, the energy status of the cell as well as its transcriptional activation (Bastie et al., 2005). Once in the cell, FAs undergo conversion into long-chain acyl-CoA catalysed by fatty acyl-CoA synthase. Acyl-CoA is transported into the mitochondria by the carnitine palmitoyltransferases, CPT₁ and CPT₂, that are located at the outer and inner mitochondrial membranes, respectively (McGarry et al., 1977). Acyl-CoA is subsequently converted into acetyl-CoA through beta-oxidation, which then enters the TCA cycle (Kunau, 1995). Beta-oxidation is inversely coupled to FA synthesis and regulated by ACC₂-derived malonyl-CoA, which inhibits mitochondrial FA uptake by CPT₁. Conversely, malonyl-CoA decarboxylase decreases the inhibition of CPT₁ by decarboxylating malonyl-CoA to acetyl-CoA, leading to an elevated rate of FA oxidation (McGarry et al., 1977; Ruderman & Dean, 1998). Importantly, beta-oxidation enzymes are susceptible to negative feedback inhibition in which the intermediates they produce inhibit their activity (Kunau, 1995).

2.1.2 Fatty acid synthesis and the storage of high-energy fuel

Lipids originate from dietary sources or are generated by *de novo* FA biosynthesis occurring mainly in the liver and adipose tissue (reviewed in Heil et al., 2019). Acetyl-CoA is the precursor of FA synthesis and is produced in the mitochondria from FA oxidation (**Figure 8**). Acetyl-CoA is converted within the tricarboxylic acid (TCA) cycle to citrate and subsequently transported into the cytoplasm by the citrate transporter. In the cytoplasm, citrate is cleaved by citrate lyase regenerating acetyl-CoA that can then be used for FA synthesis. The first and rate-limiting step of FA synthesis is the ATP-dependent carboxylation of acetyl-CoA to malonyl-CoA catalyzed by acetyl-CoA-carboxylase 1 (ACC₁). The remaining steps are catalyzed by the FA synthase (FAS) complex, which leads to a series of reactions until the 16-carbon long chain FA (LCFA) palmitic acid is

synthesised. Further elongation and desaturation take place at the endoplasmic reticulum membrane (Salti & Goodridge, 1996).

ACC exists in two isoforms, ACC₁ and ACC₂ (Abu-Elheiga et al., 1997), and is activated by citrate and conversely inhibited by palmitoyl-CoA and malonyl-CoA by allosteric regulation (Trumble et al., 1995). Regulatory phosphorylation of ACC is conferred by AMP-activated protein kinase (AMPK), an important cellular sensor of low energy states, that phosphorylates both ACC₁ and ACC₂ leading to their inhibition (Munday et al., 1988; Winder et al., 1997). Conversely, proline hydroxylation by PHD₃ activates ACC₂ (German et al., 2016). In addition to the short-term and transient regulation through post-translational modifications, long-term mechanisms include changes in gene expression of genes encoding key FA synthesis enzymes and occur in response to dietary factors. For instance, consuming a carbohydrate-rich diet increases ACC₁ and FAS expression, which then promotes FA formation (Kim, 1997). Conversely, fasting decreases FA synthesis by inhibiting ACC₁ and FAS expression (Pape et al., 1988).

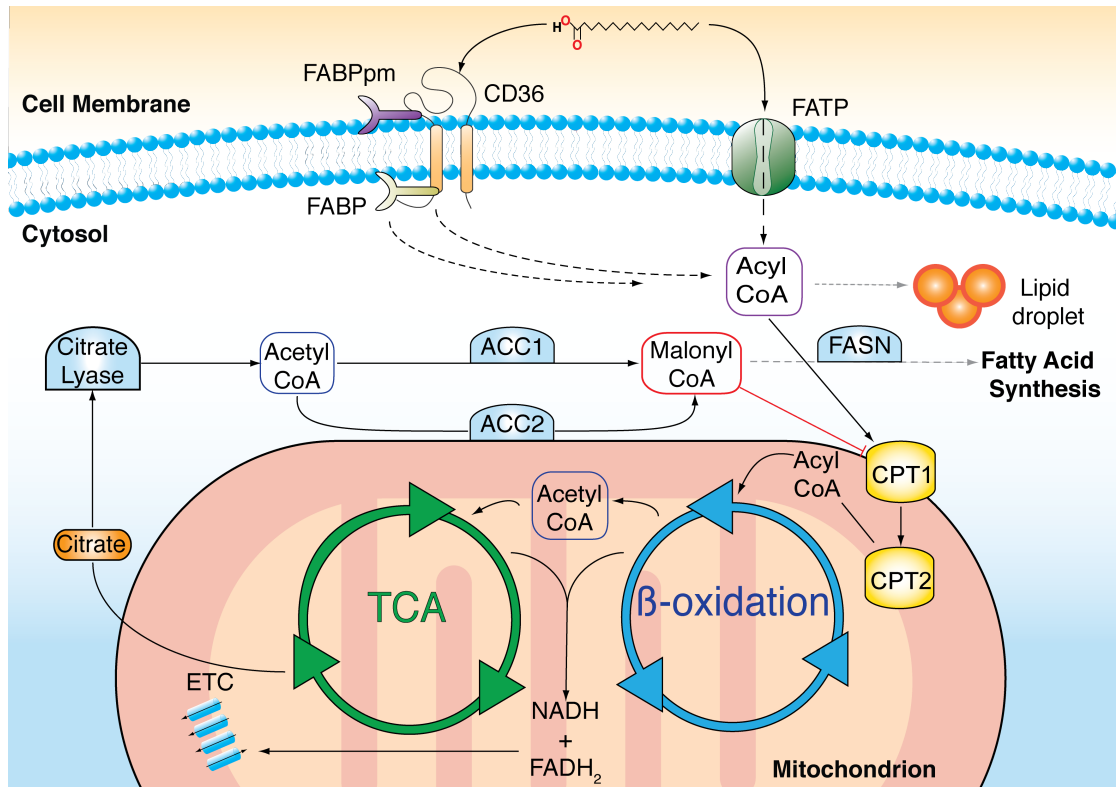


Figure 8: A schematic representation of fatty acid metabolism. Long chain fatty acids, such as palmitic acid, are actively transported across the cell membrane by membrane-bound transporters, such as CD36 and fatty acid transport protein (FATP). Fatty acid binding proteins (FABPpm, membrane-associated; FABP, cytosolic) facilitate the transfer. In the cytosol, fatty acids can either be stored in lipid droplets or undergo enzymatic conversion to FA-acyl-CoA that can enter the mitochondria via the carnitine palmitoyltransferases I and 2 (CPT1, CPT2) transporters, located on the outer and inner mitochondrial membranes, respectively. The activation of CPT1 is a survival signal and inhibits the oligomerisation of the pro-apoptotic Bcl-2 family proteins, Bak and Bax. Inside mitochondria, FA-acyl-CoA molecules are broken down in a series of enzymatic reactions known as beta-oxidation. FADH₂ and NADH are released and are used as co-factors in the electron transport chain (ETC) to produce ATP. Acetyl-CoA is released and enters the tricarboxylic acid cycle (TCA), where it is oxidised for citrate production. Citrate is transported to the cytosol where it is converted to acetyl-CoA. Acetyl-CoA carboxylase 1 (ACC1) -mediated conversion of acetyl-coA to malonyl-CoA is the rate-limiting step in fatty acid synthesis. Malonyl-CoA in particular when produced by ACC2, inhibits CPT1 and thus limits beta-oxidation.

2.2 Transcriptional regulation of fatty acid metabolism

Both anabolic and catabolic processes of FA metabolism are under the control of transcription factor (TF) regulation (

Figure 9). Peroxisome proliferator-activated receptors (PPAR) are key TFs involved in increased FA oxidation (reviewed in (Poulsen et al., 2012). PPARs act as heterodimers with RXR and are activated by binding DNA and FA ligands (Aagaard et al., 2011; Forman et al., 1997). PPAR α and PPAR β/γ are involved in increased FA uptake and activation of mitochondrial beta-oxidation in various cell types, while PPAR γ is mainly expressed in adipose tissue and is a potent inducer of adipogenesis (reviewed in Poulsen et al., 2012). FA metabolism genes that are induced by PPARs include *CD36*, *FATP*, *ACSL1* (acyl-CoA synthetase), *MLYCD* (malonyl-CoA decarboxylase) and *CPT1* (reviewed in Desvergne & Wahli, 1999; Mandard et al., 2004). Likewise, peroxisome proliferator-activated receptor-gamma co-activator alpha (PGC-1 α) is involved in increased overall FA oxidation as well as mitochondrial biogenesis. In response to low energy sources, AMPK and SIRT1 activate PGC-1 α through phosphorylation and deacetylation, respectively (Jager et al., 2007; Rodgers et al., 2005). PGC-1 α is a potent activator and a target of several other metabolism-related TFs involved in the up-regulation of oxidative metabolism, including PPAR α and PPAR δ (Vega et al., 2000), FoxO1 (Puigserver et al., 2003), nuclear respiratory factors (NRF)1 and NRF2 (Wu et al., 2016), as well as the lipogenic regulator ChREBP (Chambers et al., 2013). FoxO1 enhances FA oxidation by increasing expression of acyl-CoA oxidase and PPAR δ , repressing *ACC2* and by promoting FA uptake through translocation of *CD36* to the plasma membrane (Bastie et al., 2005). NRF1 and NRF2 are principal promoters of mitochondrial biogenesis and thus increase the β -oxidation capacity of the cell (Scarpulla, 1997). NRF1 further regulates several FA oxidation regulators such as PPAR α , *Lipin1* and PGC-1 β (Hirotzu et al., 2012).

Anabolic regulators of FA metabolism play a role in countering the effects of higher oxidation in times of plentiful nutrient supply by increasing FA synthesis and storage. A build-up of FAs, especially LCFAs, or cholesterol can be toxic to cells and so feedback loops are in place to control intracellular levels. Sterol regulatory element-binding proteins (SREBP) are required for the control of *de novo* FA and cholesterol synthesis (Bengochea-Alonso & Ericsson, 2007; Espenshade & Hughes, 2007). SREBPs are bound to the endoplasmic reticulum from where they translocate to the nucleus in response to depleted intracellular FA or cholesterol levels (Sakai et al., 1996). The SREBP-1c isoform has been shown to upregulate the expression of several genes involved in FA synthesis including citrate lyase, *ACC1* and *FAS* (reviewed in Foufelle & Ferré, 2002). Carbohydrate response

| Introduction II

element binding protein (ChREBP) is a glucose-responsive TF. While FAs inhibit ChREBP activity (Dentin et al., 2005), glucose enhances ChREBP nuclear translocation and DNA binding by decreasing phosphorylation (Kawaguchi et al., 2001). Glucose has been shown to induce ChREBP gene expression in the liver (Dentin et al., 2004), that in turn induces lipogenic genes such as ACC1 and FAS (Ishii et al., 2004). Taken together, both FA synthesis as well as their beta-oxidation is regulated on the transcriptional level.

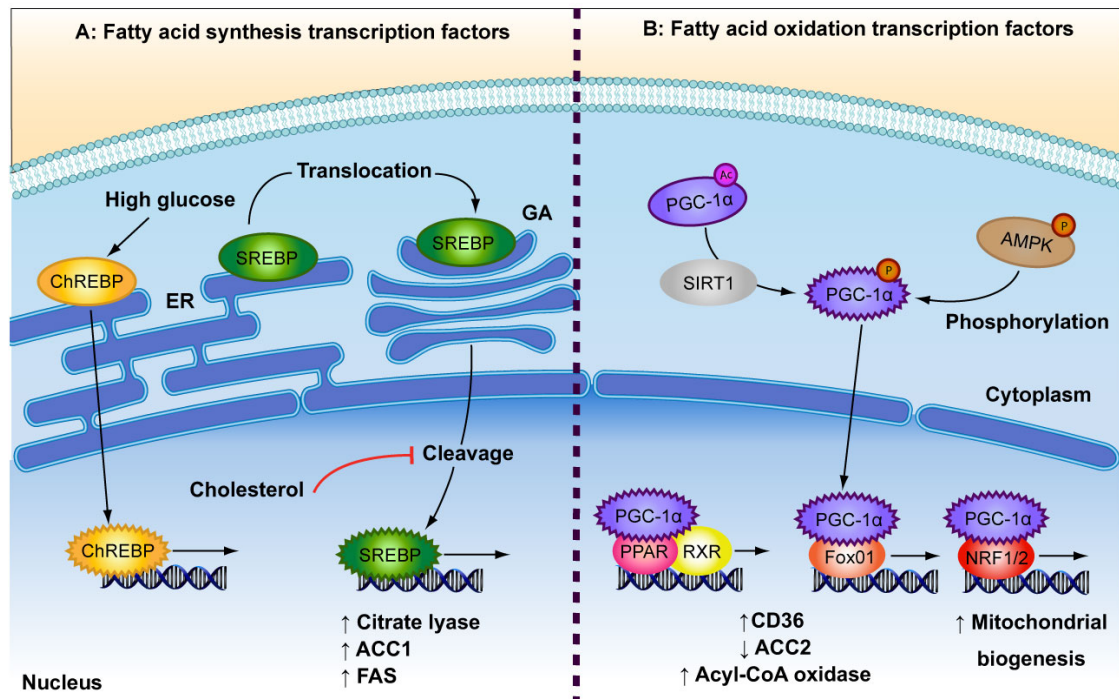


Figure 9: The main transcriptional factors involved in fatty acid (FA) synthesis and beta-oxidation. A: In response to high glucose concentrations carbohydrate responsive element-binding protein (ChREBP) is transported to the nucleus. Sterol regulatory element-binding protein (SREBP) is bound to the endoplasmic reticulum (ER) where it is translocated to the golgi apparatus (GA). SREBP is cleaved to produce its active transcription factor form, a process that is inhibited by high levels of cholesterol. Both ChREBP and SREBP are involved in FA synthesis by increasing expression of citrate lyase, acetyl-CoA carboxylase (ACC1) and fatty acid synthase (FAS). B: The low energy sensors, AMPK and SIRT1 activate peroxisome proliferator-activated receptor-gamma coactivator 1 alpha (PGC-1 α) that after translocation to the nucleus where it interacts with several transcription factors: Peroxisome proliferator-activated receptor (PPAR) and retinoid X receptor (RXR) which heterodimerise upon ligand binding; forkhead box protein O1 (FoxO1); and nuclear respiratory factor 1 (NRF1/2). These events result in up-regulation of FA oxidation by increasing expression of FA transporters and rate-limiting enzymes (CD36, ACC2, acyl-CoA oxidase) and by increasing overall mitochondrial biogenesis.

Illustration by Raquel Casquero

2.3 Interplay between epigenetic regulation and fatty acid metabolism

While TF-mediated regulation in metabolism is generally transient, epigenetic factors may confer prolonged alterations and possibly transmit these to the next generation. The molecular basis of epigenetic mechanisms are modifications of chromatin, of which DNA methylation is best studied and frequently related with gene silencing (**discussed in section 1.2**). Diets rich in fat have been shown to affect methylation states of metabolism genes in both rodents and humans. For instance, several studies in rodent offspring have shown that higher maternal dietary fat intake caused persistent DNA hypermethylation and down-regulation of the *Fads2* gene, which encodes FA desaturase in FA synthesis (Kelsall et al., 2012; Niculescu et al., 2013). Similar diet-induced epigenetic changes found in adult rodents could be reversed by decreasing fat intake (Hoile et al., 2013). Maternal high-fat diet has also been reported to induce hypermethylation of the *PGC-1 α* promoter in skeletal muscle cells. Interestingly, the resulting decreased expression can be counteracted by maternal exercise, further highlighting the plasticity of FA metabolism (Laker et al., 2014).

Acetyl-CoA is generated from glucose via glycolysis and from FAs via beta-oxidation and is substrate for histone acetylation (Takahashi et al., 2006). Indeed, high levels of glucose have been shown to increase histone acetylation (Wellen & Thompson, 2012), while a converse reduction in acetyl-CoA synthesis results in rapid histone deacetylation (Takahashi et al., 2006). In this way, acetyl-CoA is an important link between energy metabolism and chromatin regulation (Rathmell & Newgard, 2009; Wellen & Thompson, 2012). FAs also affect acetyl-CoA levels and thus histone acetylation. On the one hand, *de novo* FA synthesis uses acetyl-CoA as substrate, and therefore competes with histone acetylation for the same acetyl-CoA pool. Lowering the rate of FA synthesis, by reducing ACC1 expression, increases global histone acetylation and gene expression (Galdieri & Vancura, 2012). On the other hand, stimulating FA oxidation, and thereby increasing acetyl-CoA levels, leads to increased histone acetylation (McDonnell et al., 2016).

Epigenetic factors interact with non-chromatin substrates to regulate FA metabolism. This has been observed in the inhibition of PPAR γ by histone deacetylase 3 (HDAC3) and SIRT1 (Jiang et al., 2014; Qiang et al., 2012). Interestingly, metabolic enzymes can also more directly act to bring about changes in chromatin structure and gene transcription. AMPK has been shown to phosphorylate H2B histones to activate transcription of AMPK-responsive genes, such as *CPT1c*, during metabolic stress (Bungard et al., 2010). Similarly, AMPK phosphorylation of the methyltransferase enzyme, EZH2, represses polycomb

repressive complex 2 (PRC2) -mediated methylation, thereby up-regulating tumour suppressor genes (Wan et al., 2018). Further, it has been reported that almost all glycolytic enzymes are RNA-binding proteins, thereby linking metabolism and gene transcription (Beckmann et al., 2015). Overall there is a complementary interplay between epigenetic regulation and FA metabolism that is mediated by the provision of acetyl-CoA and the regulation of metabolic gene expression.

2.4 Fatty acid metabolism is implicated in haematological disease

It has been well documented that cancer cells, including leukaemic, can be distinguished metabolically from normal cells (Berger et al., 2017; Kohli & Passegué, 2014). Otto Warburg proposed that cancer cells exhibit increased glycolysis in the presence of oxygen in a process known as the 'Warburg effect', thereby providing the cells with a more readily accessible source of ATP (Warburg, 1956) (Shlush et al., 2017). Initially, this idea led researchers to think of cancer in terms of metabolic dysfunction due to mitochondrial injury. Instead, what is becoming evident is that metabolic plasticity may be a cellular adaptation to increased energy demands of proliferating cells and a harsh tumour microenvironment in which there may be limited nutrient and oxygen supply. These unfavourable conditions require cancer cells to modulate their metabolism to one that promotes survival and proliferation. In response to treatments, metabolic adaptations can lead to drug resistance.

Many MDS and AML patients do not respond to current pharmacological therapies, while among those individuals who show initial response, many subsequently relapse (Shlush et al., 2017). Although the reasons for resistance and relapse remain unclear, it has been widely reported that reservoirs of chemoresistant cells originate among LSCs, which have the capacity to clonally expand and eventually replace normal HSCs (Ding et al., 2017; Lagadinou et al., 2013). LSCs have been observed to exhibit plasticity in FA metabolism so that adaptations to environmental challenges, such as drug treatments, can be mounted (Farge, Saland, Toni, et al., 2017; Ye et al., 2016). Identifying specific metabolic traits relating to FA metabolism may provide clues for targetable genes or pathways. Much progress has been made in determining the genetic factors of MDS and sAML, however less is known about the metabolic changes that may contribute to disease progression and therapy resistance. While the majority of cancer cells rely on anaerobic glycolysis for their energy supply, LSCs have been reported to preferentially utilise OXPHOS (Lagadinou et al., 2013).

Dysregulation of FA metabolism has been implicated in a variety of diseases and a prominent role in cancer is emerging. FA synthesis is required for anabolic reactions such as membrane biosynthesis and generation of signalling molecules. From the oxidation of FAs, ATP yield is more than twice that of glucose or amino acids, making FAs an important fuel.

2.4.1 The role of epigenetic regulation in altered FA metabolism

It is now well accepted that epigenetic changes contribute to haematological cancers (Pastore & Levine, 2016). Altered DNA methylation patterns are a hallmark of AML, partly due to dysregulation of DNMT-encoding genes (discussed in section 1.3.2). In recent years links between epigenetic regulation and an altered FA metabolism have been emerging in AML. FABP4 has a dual role in increasing FA uptake and signalling to the epigenetic regulators, which together create a favourable environment for AML proliferation (Yan et al., 2017). Mechanistically, FABP4 up-regulation increases IL-6 expression and STAT3 phosphorylation leading to DNMT1 overexpression and silencing of the cell cycle inhibitor p15 (Yan et al., 2017). Conversely, forced DNMT1 expression caused increased FABP4 expression in AML, pointing towards a possible metabolic-epigenetic feedback loop (Yan et al., 2018). The epigenetic silencing of the ACC2 gene is a key step that drives the reliance of AML cells on FA oxidation. Repression of the ACC2 by SIRT1-dependent histone deacetylation allows for simultaneous beta-oxidation and FA synthesis to take place (Corbet, 2017). This 'futile cycle' of both up-regulated lipolysis and dysregulated lipogenesis is a hallmark of malignant haematologic cells (Aadra P. Bhatt, 2012). Indeed, the ACC2 activator, PHD3, has been shown to be down-regulated in around 80% of AML patients, resulting in higher beta-oxidation (German et al., 2016).

Healthy haematopoietic and leukaemia stem cells have been traditionally defined and delineated by immunophenotyping cell markers (Bennett et al., 1976). However, metabolic heterogeneity among these cell populations is becoming increasingly evident. CD36-positive leukaemia stem cells were shown to have elevated FA uptake and beta-oxidation (Ye et al., 2016). In addition to increased FA uptake, higher rates of anaerobic glycolysis contribute to increased beta-oxidation in AML cells by promoting a decreased electrochemical gradient on the mitochondrial membrane and uncoupling of the electron transport chain (Samudio et al., 2010). While we are just at the beginning of understanding the significance of metabolic changes in leukaemia, increased reliance on FAs as fuel is becoming apparent.

2.4.2 The bone marrow is the nutrient-providing HSC niche

The bone marrow microenvironment provides nutrients and growth signals to both healthy HSCs and disease clones. The bone marrow is composed of an array of different cell types including adipocytes and mesenchymal stem cells and is the pertinent site of interest in leukaemia (Medyouf, 2017). Adipocytes account for approximately 70% of the tissue mass of the bone marrow (Hardaway et al., 2014). AML blasts undergo spontaneous apoptosis *in vitro*, but proliferate *in vivo* in the bone marrow (Lane et al., 2009), indicating that the bone marrow environment contributes to extrinsic growth-promoting factors. Indeed, bone marrow adipocytes protect acute monocytic leukaemia cells by disrupting apoptosis. Adipocytes supply leukaemia cells with FA ligands that induce PPAR γ -controlled FA oxidation genes, thereby promoting cell survival (Tabe et al., 2017). Further evidence of metabolic cross-talk involves secreted FABP4 that, in addition to its aforementioned involvement in *DNMT1* overexpression, acts as carrier proteins for FA transport between adipocytes and AML blasts (Shafat et al., 2017). Adipocytes also produce adipokines such as leptin and adiponectin, which modulate FA metabolism of nearby cells (VanSaun, 2013). Interestingly, AML cells also exhibit higher rates of beta-oxidation when co-cultured with mesenchymal stem cells (Samudio et al., 2008) and a study in mice showed that osteoblast cells induce leukaemogenesis in HSCs via FOXO1 (Kode et al., 2016). Overall, AML cells take advantage of the growth-promoting environment of the bone marrow.

2.4.3 Metabolism interference with therapy

As discussed in section 1.2.4, HSCT remains the only curative option for AML (Farge, Saland, de Toni, et al., 2017). Although AraC killed both resting and proliferating cancer cells, the remaining resistant cells were characterised by increased FA oxidation and up-regulated CD36. In another study, CD36-positive leukaemia cells were shown to be relatively more drug-resistant to AraC *in vivo* and *in vitro* compared with CD36-negative cells (Ye et al., 2016). Moreover, high expression of CD36 and CPT1a recorded in different cohorts of AML patients was associated with poor prognosis and shorter overall survival (Perea et al., 2005; Shi et al., 2016). Although predicting AML patient response to drugs based on cellular metabolic profiles remains elusive, these observations point towards a key role of FA metabolism, particularly increased beta-oxidation. This might explain why obesity is a leading risk factor for most cancers (Lichtman, 2010). In the context of leukaemia, excess adipose tissue increases the risk of disease onset (Naveiras et al., 2009) and is associated with poorer outcome due to chemotherapy resistance (Behan et al., 2009; Ye et al., 2016). Coupled with these findings is the increased proportion of adipose tissue

in the bone marrow as people age, which incidentally correlates with increased rates of disease incidence (Stenderup et al., 2003). Taken together, the accumulation of bone marrow adipose tissue and incidence of obesity represent probable risk factors for acquiring AML and subsequent therapy resistance.

Efforts have been made to target FA metabolism as a therapeutic strategy. For instance, the FA uptake protein CD36 has been evaluated as a potential target. Sulfo-N-succinimidyl oleate (SSO) is a FA analogue that inhibits CD36 function (Kuda et al., 2013) and has been shown to perturb cell growth *in vitro* (Coort et al., 2002) and reduce CPT1 activity (Campbell et al., 2004). However, its toxicity *in vivo* deems SSO unsuitable for therapeutic use. As an alternative strategy, inhibitory CD36-specific antibodies increase sensitivity of chronic myelogenous leukaemia cells to the first-line drug imatinib (Landberg et al., 2018). Etomoxir irreversibly inhibits CPT1 and thus beta-oxidation (Abdel-aleem et al., 1994) and has been successfully used for the treatment of cardiac conditions (Bristow, 2000). In AML, etomoxir sensitises cells to apoptosis-inducing treatments (Samudio et al., 2010). Another CPT1 inhibitor, ST1326, was shown to inhibit proliferation, survival and chemoresistance in leukaemia cell lines and primary cells by driving cells to apoptosis and causing toxic accumulation of cytosolic palmitate (Ricciardi et al., 2017).

The findings that LSC preferentially utilise OXPHOS, compared to normal HSC, and that BCL-2 inactivation inhibits OXPHOS in LSCs have encouraged researchers to investigate LSC-directed therapy strategies that target mitochondrial metabolism (Lagadinou et al., 2013). Recent work from the Craig Jordan lab has shone light on the contribution of FA metabolism in resistance to combined azacitidine and venetoclax therapy in AML patients (Pollyea et al., 2018). Preliminary data has shown resistant LSCs were re-sensitised to treatment when key FA metabolism genes were knocked down, including CPT1a (Jones et al., 2018, 2019). Azacitidine monotherapy has been shown to inhibit SREBP signaling and reduce the expression of genes involved in FA uptake, independent of demethylating activity (Poirier et al., 2014). Collectively, these studies indicate that inhibition or reversal of increased FA oxidation has been shown to be a suitable therapeutic intervention, in particular when combined with other cytotoxic drugs.

3. Epigenetics: role in myeloid disease and therapy

Epigenetic regulation is concerned with the concept of modifying genes by chemical and chromatin conformational changes that are not associated with changes in the DNA sequence. In this chapter I present some of the factors giving credence to the notion that MDS is a prototypical epigenetic disease. I then introduce the basic concepts that govern epigenetic regulation. MDS is particularly responsive to therapies that target epigenetic mechanisms, and I outline established drugs as well as novel strategies in the pipeline. As our study employed a shRNA knockdown genetic screen that targeted epigenetic regulators, I give an overview of RNA interference (RNAi) technologies.

3.1 Epigenetics: a haematological perspective

There are some compelling data to support the notion that MDS is an epigenetic disease (as reviewed in J.-P. J. Issa, 2013). Epigenetic abnormalities co-occur with cytogenetic changes in MDS, and together, contribute to the full manifestation of the disease. As discussed in section 1.2.1, the accumulation of mainly epigenetic changes may represent a tipping point to transformation to sAML (Sperling et al., 2017). MDS has been consistently characterised by an abnormal epigenome. Effector enzymes with epigenetic regulatory functions are among the most commonly mutated genes in MDS (Haferlach et al., 2014; Shih et al., 2012). DNA methylation plays an important role in regulating haematopoiesis. Disrupted DNA methylation and histone modifications lead to increased apoptosis and aberrant differentiation that is typical of MDS (J.-P. Issa, 2010).

Mutations in *TET2* and *DNMT3A* disrupt normal methylation patterns, while mutations in *IDH1/2* and *ASXL1* can lead to altered histone modifications. Induced mutations in mice have recapitulated MDS disease state (Challen et al., 2012; Moran-Crusio et al., 2011). Such disruptions have been exemplified in the clinic where hypermethylation states have been reported among MDS patients versus healthy, and are associated with poorer outcomes (Jiang et al., 2009). Epigenetic changes are inherently reversible, which, remarkably, is an observation that is borne out in sensitivity to drugs that modify the epigenome among MDS patients. The hypomethylating agent, azacitidine, is the primary pharmaceutical therapy for high-risk MDS and for which there is a 50% response rate (Fenaux & Ades,

2009). However, resistance is still common and complete remission is rare, which may be due to the inability to eliminate mutated clones that persist due to other non-epigenetic mechanisms. Together, there are strong indications that MDS represents an epigenetic disease, in which mutations in epigenetic regulators and abnormal epigenome drive disease progression. Patient sensitivity to epigenetic drugs, albeit limited, highlights key targetable pathways that may be coupled with other cytotoxic therapies.

3.2 Chromatin as the basis of epigenetic regulation

DNA is organised around histone protein complexes into chromatin. Chromatin mainly exists in two degrees of compaction. Heterochromatin is mostly compacted and is mostly transcriptionally repressed. In contrast, euchromatin is a more 'open' structure that allows greater gene transcription to take place. The three-dimensional conformation of chromatin dictates the degree of interaction between enhancers, or *cis*-acting regulatory elements, and promoter regions, thus providing a layer of transcription regulation (Hu & Tee, 2017).

The nucleosome is the principle component of chromatin, which comprises DNA wound around an octamer complex of core histones: H2A, H2B, H3, and H4 (McGinty & Tan, 2015). Post-translational modifications alter histone chemistry at their N-terminus 'tails' by various histone modifying enzymes. Enzymes that mediate histone methylation and acetylation and DNA methylation, termed 'writers', include acetyltransferases, methyltransferases, kinases and ubiquitinases. Enzymes that remove these modifications, termed 'erasers', include deacetylases, demethylases and deubiquitinases (Bannister & Kouzarides, 2011). 'Readers', such as bromodomain and extra-terminal (BET), are protein domains that recognise specific histone modifications. Thus, the action of epigenetic regulators is reversible, allowing for dynamic modulation of gene activity through changes to chromatin structure, which change the relative distance to regulatory sequence elements, such as enhancer regions, and access to DNA by transcription factors (Eberharter & Becker, 2002). Overall, the level of gene transcription is determined by relative accessibility of transcription factors to DNA. This accessibility can be covalently regulated by two broad functions: methylation or acetylation of histone tails, and methylation of DNA.

Histone acetylation is regulated by histone lysine acetyltransferases (KAT) and deacetylases (HDAC) by altering the charge on lysine (K) residues between neutral and positive, respectively, mainly at the N-termini of H3 and H4 tails. Acetylation is generally associated with open chromatin and active gene expression by relaxing DNA and histone

interactions, whereas deacetylation is associated with a more closed chromatin structure and repressed gene expression, due to stabilisation of the chromatin structure (Eberharter & Becker, 2002). The BET family of proteins, such as BRD2, BRD3 and BRD4, contain two bromodomains that recognise K residues of acetylated histone tails to recruit transcriptional machinery and chromatin remodelling, through which transcription is enhanced (Marmorstein & Zhou, 2014). Broadly speaking, BRDs regulate RNA transcription and cell cycling by activating RNA polymerase II (Dhalluin et al., 1999).

Histone methylation is carried out by broad action histone methyltransferases (HMT). Methylation occurs mainly on K residues 4, 9, 27 and 36, which can be mono- di-, or trimethylated, or on arginine (R) residues 2, 17, and 36, which can be mono-, symmetrically-, or asymmetrically di-methylated (Barski et al., 2007; Musselman et al., 2012). Methylation can be reversed directly via erasers, such as histone demethyltransferases (HDMT), or indirectly by blocking further methylation (Kohli & Zhang, 2013). For instance, arginine residue demethylation is catalysed by peptidyl arginine deiminase 4 (PADI4) which converts arginine to citrulline, thus blocking further methylation (Cuthbert et al., 2004). In contrast to acetylation, histone methylation does not affect charge, but rather directs a wide range of reader proteins that recruit transcription factors, such as chromatin remodelling complexes (Hyun et al., 2017; Yun et al., 2011). Further, histone methylation is highly site-specific; the resulting changes can have either activating or repressive consequences for gene expression, depending on the state and site of methylation states, which is determined by the cellular context (Musselman et al., 2012).

On the level of DNA, DNMTs catalyse the addition of a methyl group to the fifth carbon of cytosines to yield 5-methylcytosines. *De novo* methylation is carried out by DNMT3A and DNMT3B, while DNMT1 maintains methylation states (Jaenisch & Bird, 2003). Active demethylation is carried out by hydroxylation of 5-methylcytosine to 5-hydroxymethylcytosine (5-hmC) by ten-eleven translocation (TET) enzymes, such as *TET2* (Lister et al., 2009). As DNA strands are hemi-methylated, passive demethylation can occur in the absence of DNMT1 activity over several rounds of DNA replication with the loss of 5-mC (Kohli & Zhang, 2013).

DNA methylation normally occurs at CpG dinucleotides; however, CpG's when concentrated in CpG islands (CGI) at promoter regions remain demethylated (Schübeler, 2015). When CGI become hypermethylated, robust transcriptional repression is induced by transcription factor blocking. DNA methylation determines the degree of accessibility of transcription factors at their respective binding motifs. Indeed, binding sites of transcription factors related to lineage commitment and differentiation, such as GATA1,

GATA2, and RUNX1, have been shown to be sites of both differential methylation and dynamic chromatin conformation. More recently, differential methylation at CGI-adjacent areas, CGI shores, and even CpG-scarce regions, has been correlated with gene expression levels. In contrast, hypomethylation of these regions is correlated with open chromatin state and transcription factor accessibility that allow for transcriptional activity to take place (Langstein et al., 2018).

Taken together, these modifications are the basis of heritable phenotypic differences that dictate important genes in organism development and, in the context of haematopoiesis, cell fate decisions.

3.2.1 Epigenetic regulation in haematopoiesis

Haematopoiesis is a regulated process on both epigenetic and transcriptional levels. Transcription factor binding determines the sequential gene expression patterns that lead to the activation and repression of lineage-specific genes, which is directed by epigenetic factors, such as DNA methylation and histone modifications.

Advances in genome-wide methylation studies have revealed distinct DNA methylation patterns at different stages of differentiation during haematopoiesis that demarcate myeloid and lymphoid lineage decisions (Ji et al., 2010; Trowbridge et al., 2009). In general, myelopoiesis is associated with a loss of methylation. Genes methylated in MPP of mice were reported to become unmethylated in a lineage-specific manner, such as neutrophil-specific genes, *Mpo*, that encodes the microbe toxin, myeloperoxidase, and *Cxcr2* that encodes a chemokine to allow chemotaxis (Bröske et al., 2009). In contrast, lymphopoiesis depends more on global methylation maintenance, as evidenced by a reduction in lymphoid progeny in mice with reduced *Dnmt1* activity (Bröske et al., 2009). Induced depletion of *TET2* was shown to disrupt normal myeloid differentiation (Rasmussen et al., 2015). A principle characteristic of HSC is their life-long ability to self-renew. When *DNMT1* activity is removed in mice, HSC and progenitors were reduced in the bone marrow and differentiation patterns were disrupted, suggesting maintenance of DNA methylation plays a direct role in regulating HSC self-renewal and cell fate decisions (Bröske et al., 2009).

Polycomb repressive complexes (PRC) 1 and 2 are histone writers that regulate transcriptional silencing by modifying chromatin through their multimeric enzyme complexes. Although PRCs have a diverse range of transcriptional target sites across many tissues, they are recognised as general regulators of stem cells, with involvement in stem cell renewal and differentiation (A. P. Bracken, 2006). PRC2 is responsible for all di- and tri-methylation of lysine 27 of H3 (H3K27me2/me3) (Valk-Lingbeek et al., 2004). Gene

repression is brought about via a component of PRC2, enhancer of zeste 2 (EZH2), that functions as a histone methyltransferase (Trojer, 2016). High *EZH2* expression is associated with proliferating cells, but not resting cells, during lymphopoiesis, suggesting a role in lineage-specific cell cycle regulation (Hervioux et al., 2016). Recruitment of the PRC1 component, CBX, to the H3K27me3 mediates heterochromatin compaction. Subsequently, the RING1 subunit of PRC1 mono-ubiquitylates H2A at lysine 119 (H2AK119ub1), which promotes repression by inhibiting RNA polymerase II-dependent transcriptional elongation prior to transcription and then initiating chromatin compaction (Sashida & Iwama, 2012).

Interestingly, the PRC-induced H3K27me3 mark is offset by the Trithorax-group (trxG), which mediates the activating H3K4me3 mark associated with open chromatin and gene activation (Bernstein et al., 2006). Genes in loci that contain both marks are so-called 'bivalent' domains that indicate flexible activation and repressive mechanisms. HSC contain many bivalent gene sequences (Cedar & Bergman, 2011). Genome-wide changes of gene expression and histone modifications have shown HSC genes are 'primed' for subsequent activation or repression during lineage commitment (Weishaupt et al., 2010). In this way, PRCs are thought to regulate pluripotency maintenance and self-renewal of HSC by dynamically repressing cell fate regulators during haematopoiesis (Adrian P. Bracken & Helin, 2009). For this reason, PRC1 and 2 are recognized as general stem cell regulators via histone methylation-induced alterations to chromatin accessibility. Overall, there is a multi-faceted system of epigenetic regulatory mechanisms that ensure the tight functioning of blood cell formation.

3.2.2 Abnormal epigenome in MDS

Given the central role epigenetic factors play in the normal running of haematopoiesis, it is not surprising that age-related functional decline of HSC has been strongly linked to epigenetic dysregulation. Positioned atop the haematopoiesis hierarchy, HSCs are poised as potential sources of clonal mutations that can lead to haematological malignancies, such as MDS. Genetic mutational patterns consistent with MDS and AML have been observed in healthy, mainly elderly populations as part of population-based studies (Genovese et al., 2014; Jaiswal et al., 2014). These studies provided some of the first measurable indications of CHIP, the asymptomatic condition preceding haematological malignancies that is evidenced in around 10% of people aged over 65 years (as discussed in section 1.3.1). Commonly mutated genes involved in the progression of CHIP to MDS and sAML are involved in epigenetic regulation. Genes affected include the epigenetic regulators *TET2* and *DNMT3A*, and the spliceosome factor, *ASXL1*.

3.2.3 Aberrant DNA methylation

The correlation between DNA hypermethylation and MDS disease progression have provided the rationale for using hypomethylating agents for therapeutic use. However, the exact mechanisms by which methylation levels contribute to MDS burden and sAML transformation are unclear. DNMT3A establishes *de novo* DNA methylation and it is thought that heterozygous mutant *DNMT3A* acts as a dominant negative over wild type *DNMT3A*, thereby reducing overall methyltransferase activity (Russler-Germain et al., 2014).

HSC of conditional *Dnmt3a*-knockout mice display reduced self-renewal capacities and differentiation (Challen et al., 2012; Ettou et al., 2012). Double knockouts of *Dnmt3a* and *Dnmt3b* pointed to a synergistic effect on methylation levels, with *Dnmt3a* activity appearing as the main driver of global methylation. DNA methylation-mediated silencing causes inactivation of the tumour suppressor gene, *p15^{INK4B}*, in a large percentage of MDS patients, of whom 70% patients develop sAML (Tien et al., 2001). Indeed, the methylation state of *p15^{INK4B}* is an early prognostic marker of MDS and is likely to be a driver event in MDS pathogenesis.

The aforementioned TET family of enzymes carry out antagonistic biochemical functions to DNMT3A (López-Moyado & Rao, 2020), despite their mutated forms being heavily implicated in MDS. Indirect demethylation is catalysed by TET by converting 5-mC to 5-hmC in a Fe⁺⁺ and α -ketoglutarate (α -KG)-dependent reaction, after which 5-hmC is converted to unmodified cytosine (Nakajima & Kunimoto, 2014). Of these enzymes, TET2 is commonly mutated in MDS. 5-hmC is not recognized by DNMT3A and so undergoes passive demethylation. 5-hmC is representative of an epigenetic mark, as it is mainly located at CGI at promoters and transcription binding sites where it is associated with active gene expression (Ehrlich & Ehrlich, 2014). *TET2* deficiency has been shown to cause 5-hmC depletion and widespread hypermethylation in mice, where upregulated oncogenes and downregulated tumour suppressor genes may have contributed to the observed leukaemogenesis (Rasmussen et al., 2015). Deletion of *TET2* in CD34+CD38+ haematopoietic progenitor cells resulted in increased monocyte expansion, suggesting a role in myeloid differentiation or lineage commitment (Itzykson et al., 2013)

Isocitrate dehydrogenase (IDH) is a key enzyme in the citric acid cycle that catalyses the conversion of isocitrate to 2-oxoglutarate. Mutations in the encoding genes, *IDH1* and *IDH2*, have been identified in around 5% of MDS cases (DiNardo et al., 2016). Gain-of-function *IDH1/2* mutations result in the production of 2-hydroxyglutarate, an oncometabolite that diffuses to the nucleus. There it acts as a competitive inhibitor of α -

KG, which interferes with TET2 activity and histone demethylases (Xu et al., 2011). Thus, the epigenetic landscape is altered by promoting DNA and histone hypermethylation. As a consequence, differentiation is blocked and LSC proliferate (Lu et al., 2012). Taken together, abnormal DNA methylation patterns in MDS are brought about by mutations in HSC directly and indirectly affecting the addition and removal of methyl groups to DNA.

3.2.4 Dysregulation of histone modifications

Genes involved in histone modifications are also implicated in MDS pathogenesis. Namely, components of both the aforementioned PRC1 and 2, and a number of their associated proteins, incur loss-of-function mutations. This results in decreased levels of histone methylation, specifically H3K27me3.

EZH2 mutations occur in around 5% of MDS patients (Haferlach et al., 2014), where they are associated with poor prognosis (Nikoloski et al., 2010). Mechanistically, loss of *Ezh2* in mice has been shown to promote MDS development by activating inflammatory cytokine responses resulting in impaired HSC (Sashida et al., 2014). *RUNX1* mutations are one of several that are significantly associated with *EZH2* mutations and occur in 10-20% of MDS patients (Harada et al., 2004). The *RUNX1* transcription factor physically binds to the *BMI1* component of PRC1, thereby recruiting PRC2 to gene promoters to repress gene transcription (Yu et al., 2012) (ref). Although mutations are not a direct cause of myeloid malignancies, HSC self-renewal is disrupted in animals with mutated *Runx1* (Jacob et al., 2010). In a PRC1-independent mechanism, *RUNX1* positively or negatively regulates the *PU.1* gene, which is involved in the development of all haematopoietic lineages. Disruption of *RUNX1* activity results in *PU.1* downregulation with various lineage-specific consequences, including an increased percentage of granulocytes in the bone marrow of mice (Huang et al., 2008).

BCOR is a component of the PRC1 complex variant, PRC1.1 (Z. Wang et al., 2018). This non-canonical PRC1 complex first binds to target sites independent of histone methylation to add the ubiquitination marker, H2AK119ub1, to histones and subsequently recruit PRC2 and H3K27me3 (Sashida et al., 2019). *BCOR* mutations occur in about 5% of cases of MDS, often co-occurring with *RUNX1* mutations, and are associated with a poor prognosis (Haferlach et al., 2014). *Bcor* loss results in myeloid progenitor expansion and leukaemogenesis in mice (Kelly et al., 2019). Although not a component of PRC1/2, *ASXL1* forms a complex with BRCA1-associated protein 1 (BAP1) that physically interacts with PRC2 to deubiquitinate histone H2A (Abdel-Wahab et al., 2012). *ASXL1* gain-of-function mutations increase the deubiquitination activity of BAP1, which is associated with decreased H3K27me3 globally. *ASXL1* is mutated in approximately 20% of MDS patients,

thus representing one of the top mutated genes (Haferlach et al., 2014). Together, mutations in *EZH2*, *RUNX1*, *BCOR*, and *ASXL1* mutations lead to dysregulation of a number of important haematopoietic lineage genes by disrupting PRC1/2 activity and thus, affecting overall histone methylation levels.

3.2.5 Histone acetylation

Unlike MDS-associated increases in DNA methylation, there is relatively little known about the global effects of altered histone acetylation in the disease context. Age-associated increases in global acetylation in animals occur due to multiple alterations in cellular metabolism, including altered levels of acetyl-CoA, a key metabolite utilized by KATs, and mutations in HDAC-encoding genes (Peleg et al., 2016), which may be congruous to cancer situations. In haematopoiesis, the relatively higher rates of glycolysis in pluripotent cells compared to differentiated cells are associated with greater availability of acetyl-CoA and concurrent increases in histone acetylation (Moussaieff et al., 2015). KAT mutations in myeloid malignancies relating to sporadic translocations have been reported, while HDAC mutations are rare (Wouters & Delwel, 2016).

3.3 Epigenetic drugs for MDS

It has been repeatedly demonstrated that MDS and AML are responsive to epigenetic-altering drugs (Jones, 2016). As many epigenetic alterations are mediated by enzymes, disease-relevant epigenetic modifications are frequently reversible. Thus, due to this plasticity, epigenetics provides numerous opportunities for targeted treatments that affect inherent properties of disease determinants. Namely, treatments that are currently available or in the pipeline take advantage of altering either methylation maintenance or histone-modifying proteins; namely, DNMT inhibitors (DNMTi), HDAC inhibitors (HDACi) and bromodomain and extra-terminal inhibitors (BETi).

3.3.1 Hypomethylating agents

DNA methylation plays important roles in both regulating normal haematopoiesis and disease progression in MDS (López-Moyado & Rao, 2020), and has, therefore, provided rationale for use as a therapy marker. The heterogenous mutational burden of LSCs means that reliance on target-specific drugs is limited. More general, broad-acting therapies, such as hypomethylating agents, have been the most successful strategies used to date.

The azanucleosides, 5-azacytidine (azacitidine) and 5-aza-2'-deoxycytidine (decitabine), are nucleoside analogues that have become the mainstay of MDS treatment for intermediate- to high-risk MDS patients who are ineligible for HSCT. Although originally

investigated at high doses for MDS treatment, later studies reported increased efficacy at low doses with higher remission rates and lower blast counts (Quintás-Cardama et al., 2010). Subsequently, both drugs were shown to induce differentiation and act as hypomethylating agents at low doses (Christman et al., 1983; Jones & Taylor, 1980). For this reason, they are considered the first epigenetic drugs.

The clinical efficacies of azacitidine and decitabine were later confirmed in clinical trials, which eventually led to their approval by the US Food and Drug Administration (FDA) and the European Medicines Agency approval as treatment for MDS (Lübbert et al., 2016; Silverman et al., 2002). Further clinical trials have shown efficacy of azacitidine across different MDS patient groups ((Fenaux et al., 2009; Kaminskas, 2005). Azacitidine represents the best treatment for high-risk MDS patients ineligible for HSCT (Goetze, 2009).

The exact mechanisms of azacitidine-induced effects have yet to be elucidated. It is thought that the main mechanism of action of hypomethylating agents is the re-activation of gene transcription by demethylating promoter regions of tumour suppressor genes by inhibiting DNMT activity (Stresemann & Lyko, 2008). In this way, tumour suppressor gene expression is increased, along with genes related to cell differentiation and apoptosis, thereby dampening MDS progression (Quintás-Cardama et al., 2010).

Upon azacitidine incorporation into DNA, adducts are formed between DNA and DNA methyl-transferases, thereby preventing DNA methylation. Interestingly, despite its known hypomethylating effects, only 10% of azacitidine is incorporated into DNA, with around 80-90% being incorporated in RNA. Little is known regarding the RNA-associated effects of azacitidine; however, ongoing work in our laboratory points to a novel role for azacitidine in disrupting RNA translational machinery (Diesch et al., in revision).

Resistance

Azacitidine treatment is associated with increased survival in patients with abnormal cytogenetic features and high-risk mutations and decreased risk of transformation to sAML. The survival outcome from a 2009 trial was reported to be a median overall survival of 24.5 months in azacitidine-treated patients (Fenaux & Ades, 2009). Crucially, however, these results have not been replicated since then; reported overall survival has been in the range of 13 to 16 months (Zeidan et al., 2017). In contrast to results for azacitidine, clinical trials for decitabine have so far not been able to show an overall survival benefit in patients with MDS (Cazzola, 2020). Unfortunately, mutated driver genes are not significantly inhibited and so continue to push ineffective haematopoiesis (Unnikrishnan et al., 2017). Therefore, azacitidine treatment is not curative and mechanisms underlying resistance to

azacitidine remain open questions. Approximately only half of MDS patients respond to azacitidine treatment (Fenaux et al., 2009). Among responders, response to treatment is not apparent until six months (Gore et al., 2013). Importantly, azacitidine response seldomly persists; a large proportion of initial responders eventually relapse within a two-year period (Prébet et al., 2011). There is much speculation as to the kinds of resistance mechanisms in place.

Aberrant global methylation is a key feature of MDS and there is a general increase in methylation in MDS cells compared to normal HSC cells (Figueroa et al., 2009), yet hypomethylating agents have had limited effect in targeting this driver of the disease. MDS and sAML patients with different cytogenetic or genetic alterations have been shown to have distinct DNA methylation patterns (Figueroa et al., 2010), suggesting the possibility of response stratification. Indeed, distinct DNA methylation patterns at disease-relevant genes, such as *ASXL1*, *EZH2* and *RUNX1*, have been reported to have prognostic value in MDS patients (Reilly et al., 2019). However, so far, azacitidine response has been shown to be mainly independent of cytogenetics. Although there are relatively little data concerning karyotype and response compared to molecular markers, MDS patients with chromosome 7 abnormalities were reported to have a slightly more favourable response to azacitidine (Raj et al., 2007). Crucially, there has been a lack of correlation between global hypomethylation following azacitidine treatment and response. It was found that there was no difference in global methylation levels following azacitidine treatment between MDS patients resistant to azacitidine and those who achieved complete remission (Blum et al., 2007). Initially, MDS patients with *TET2* mutations were reported to show greater response to DNMT inhibition compared to *TET2* wild type (Bejar et al., 2014), suggesting a dependency on aberrant methylation. However, this finding has been seldom repeated. Indeed, univariate analyses examining *TET2*, *DNMT3A*, *IDH1/2*, *ASXL1*, and other poor-risk factors, have shown no single biomarker is a predictor of response (Kuendgen et al., 2018; Voso et al., 2015). Differentiated myeloid cells are associated with decreased methylation (Bröske et al., 2009), suggesting hypomethylating agents may exert sub-optimal efficacy than what they potentially would in a more methylated compartment. Overall, although hypomethylating agents represent the best treatment strategy for high-risk MDS, chemoresistance and relapse among treatment responders is common (Santini et al., 2014).

3.3.2 Histone acetylation as a drug target

The role of histone acetylation in the regulation of oncogene transcription provides a strong basis for therapeutic targets. Several clinical trials are ongoing to determine the

efficacy of BETi and HDACi in MDS. Overall, however, it is clear that a deeper knowledge of acetylation status in MDS is required.

BET inhibitors

BETi have gained increasing attention in recent years as potent modulators of genes involved in disease progression across several cancers (Ribeiro et al., 2019). BRD4 is the most studied BET protein in the context of therapy targets. BRD4 recruits an interaction complex containing P-TEFb, JMJD6 and Mediator proteins, which together stabilise their interaction to instigate rapid transcription factor binding as well as chromosomal restructuring (Shi & Vakoc, 2014). Further, BRD4 has been shown to occupy large enhancer elements. These so-called ‘super enhancers’ regulate gene transcription through synergistic interactions between transcription factors and coactivators upstream of gene promoters (Lovén et al., 2013). These distal *cis*-acting interactions drive expression of genes that are relevant in haematological malignancies, such as the oncogenes, *MYC* and *BCL2* (Lovén et al., 2013). Similarly, rearrangements and fusions involving the mixed lineage leukaemia (*MLL*) gene are drivers of haematological malignancies. Due to *MLL* fusion partners binding directly to RNA polymerase II, *MLL* sub-types of leukaemia have been shown to be sensitive to BETi (Dawson et al., 2011; Winters & Bernt, 2017).

BRD4 is considered the first ‘druggable’ BET protein. The BRD4-specific small-molecule BETi, JQ1 and I-BET, were first reported by independent groups in 2010 (Filippakopoulos et al., 2010; Nicodeme et al., 2010). Inhibition is mediated by competitive binding with acetylated proteins that causes displacement of BRD4 from chromatin. BRD4 inhibition with specific BETi has been shown to substantially decrease *MYC* activity in haematopoietic cell lines (Dawson et al., 2011; Zuber et al., 2011).

As AML progression relies on aberrant chromosomal states, it may be a particularly suitable disease type for BRD4 inhibition. The reliance of AML on BRD4 was highlighted by a genetic screening method in mice, in which JQ1-mediated BRD4 inhibition caused anti-leukaemic effects (Zuber et al., 2011). This discovery solidified BRD4 as a candidate target for haematological malignancies. Indeed, JQ1 has recently been shown to induce HSC expansion and recovery of the haematopoietic system in mice following stem cell transplantation (Wroblewski et al., 2018). It is thought that the susceptibility of AML to BRD4 inhibition may lie in the targeting of cell lineage-specific transcription factors that determine cell fate (Roe & Vakoc, 2016).

Although most of the BETi in clinical trials are being studied in the context of AML, some include MDS as an indication condition (Reyes-Garau et al., 2019). Results from phase 1 and 2 clinical trials indicate good tolerability and modest efficacy as a monotherapy.

However, enhanced antitumoral activity of BETi in combination with other drugs suggests a role in combinatorial therapies (Pan et al., 2020).

Histone deacetylase inhibitors

Distinct from the activity of BET, the removal of acetyl groups by HDAC promotes DNA compaction, resulting in less accessibility for transcription factor binding. Disruption to the balance between KAT and HDAC activity can result in hypoacetylation, which plays an important role in the progression of haematological malignancies by repressing the activity of genes involved in normal cellular development (Johnstone & Licht, 2003).

HDACs are encoded by 18 genes and divided into four classes (class I-IV). There are currently clinical trials running for HDACi treatment of haematological malignancies that target each class (P. Wang et al., 2020). HDACs are heavily involved in multilineage development, including HSC, CMP and CLP. Although mutations of HDACs have not been detected in AML, HDAC proteins have been reported to recruit to promoter regions by fusion proteins, causing gene silencing that contributes to leukaemogenesis (Johnstone & Licht, 2003).

HDACi aim to restore the normal process of histone acetylation, thus activating gene expression that promotes differentiation and apoptosis (J. Zhang & Zhong, 2014). Thus far, one of the main barriers observed in the first generation of HDACi was apparent toxic effects, which was believed to be brought about by the deacetylation of non-histone proteins and activity against several HDAC isoforms (Suraweera et al., 2018). More recent iterations of HDACi have concentrated on isoform specificity.

HDACs can have opposing functional properties, thus making it a challenge to employ HDACi as monotherapies. HDAC1 and HDAC2 behave as oncorepressors during the initiation of acute promyelocytic leukaemia, while they act as oncogenes in established leukaemia cells (Santoro et al., 2013). While FDA-approved HDACi therapies exist for lymphoma and multiple myeloma, clinical trials, both as monotherapy and in combination, are ongoing for MDS and AML (Chandhok & Prebet, 2019). Early combinatorial trials with azacitidine show promising clinical activity and safety for MDS (Pan et al., 2020). Crucially, however, data concerning acetylation status in MDS are lacking. Therefore, a deeper understanding of the mechanistic consequences of HDAC activity is required in order to better devise therapies that target this aspect of epigenetic regulation.

3.4 RNA interference

The number of identified genes related to survival in myeloid malignancies has increased in recent years due to screening technologies, such as RNAi and clustered regularly interspaced short palindromic repeats (CRISPR)/Cas9. These technologies have attracted increased attention for their usefulness as both valuable research tools and cutting-edge therapeutic agents. Indeed, this has been highlighted most recently with the awarding of the 2020 Nobel Prize for Chemistry to Emmanuelle Charpentier and Jennifer Doudna “for the development of a method for genome editing” as part of their pioneering work in developing CRISPR/Cas9 (Jinek et al., 2012). RNAi is a regulatory mechanism that is present in most eukaryotic organisms. It involves the acute inactivation of gene activity using small double-stranded (ds) RNA molecules that are directed towards specific mRNA sequences. In this way, gene transcription is fine-tuned and, further, allows the organism to respond to dsRNA from endogenous and exogenous pathogenic nucleic acids (Jaronczyk et al., 2005).

Here I focus on RNA interference (RNAi) technologies that have revolutionised the way genotype-to-phenotype relationships are uncovered. I first describe the molecular mechanisms with which RNAi operates and then give an outline of the design criteria for short hairpin RNA (shRNA) knockdown screens that we and others have used.

3.4.1 shRNA-based knockdown mechanism of action

The development of RNAi as a means of targeted gene knockdown was awarded the Nobel Prize for Physiology or Medicine in 2006 to Andrew Z. Fire and Craig Mello for their seminal work with *C. elegans* (Fire et al., 1998). Crucially, they found that only a small amount of interfering RNA was required to initiate gene silencing and that this effect could spread between cells. Small double-stranded (ds) RNAs are introduced to cells that utilise cellular RNAi silencing machinery by processing products of endogenous microRNAs (miRNAs).

There are two main variants of RNAi: small interfering RNA (siRNA) and short hairpin RNA (shRNA). siRNA is double-stranded RNA, which is used to transiently silence gene activity (Elbashir et al., 2001). siRNAs are synthesised and introduced directly to the cell. In contrast, shRNAs induce stable silencing of target genes and are synthesised in the cell by DNA vector-mediated production.

shRNA are 19-22 base pairs in length and contain a stem structure composed of an antisense ‘guide’ sequence that is complementary to target mRNA, and a ‘passenger’ sense strand to complete the double-stranded nucleic acid (**Figure 10**). Cells are transduced

using a virally produced vector from which shRNAs are transcribed in the nucleus using a modified RNA polymerase II or III U6 promoter (Xia, 2003). Primary-miRNA (pri-miRNA), containing the stem loop structure, is first transcribed from the shRNA-encoding gene. Pri-miRNA is then cleaved by the Microprocessor complex, comprising Drosha and DGCR8, to form pre-shRNA. This dsRNA is then exported to the cytosol by Exportin 5 where the loop that links the two strands is removed by the RNase III enzyme, Dicer, leaving an RNA duplex molecule called small interfering RNA (siRNA). siRNA is then loaded into RNA-induced silencing complex (RISC) where the passenger strand is cleaved. The single-stranded guide sequence then directs RISC to the complementary target mRNA where transcription is inhibited by either mRNA degradation or translational silencing (Gautam et al., 2016; Yates et al., 2013).

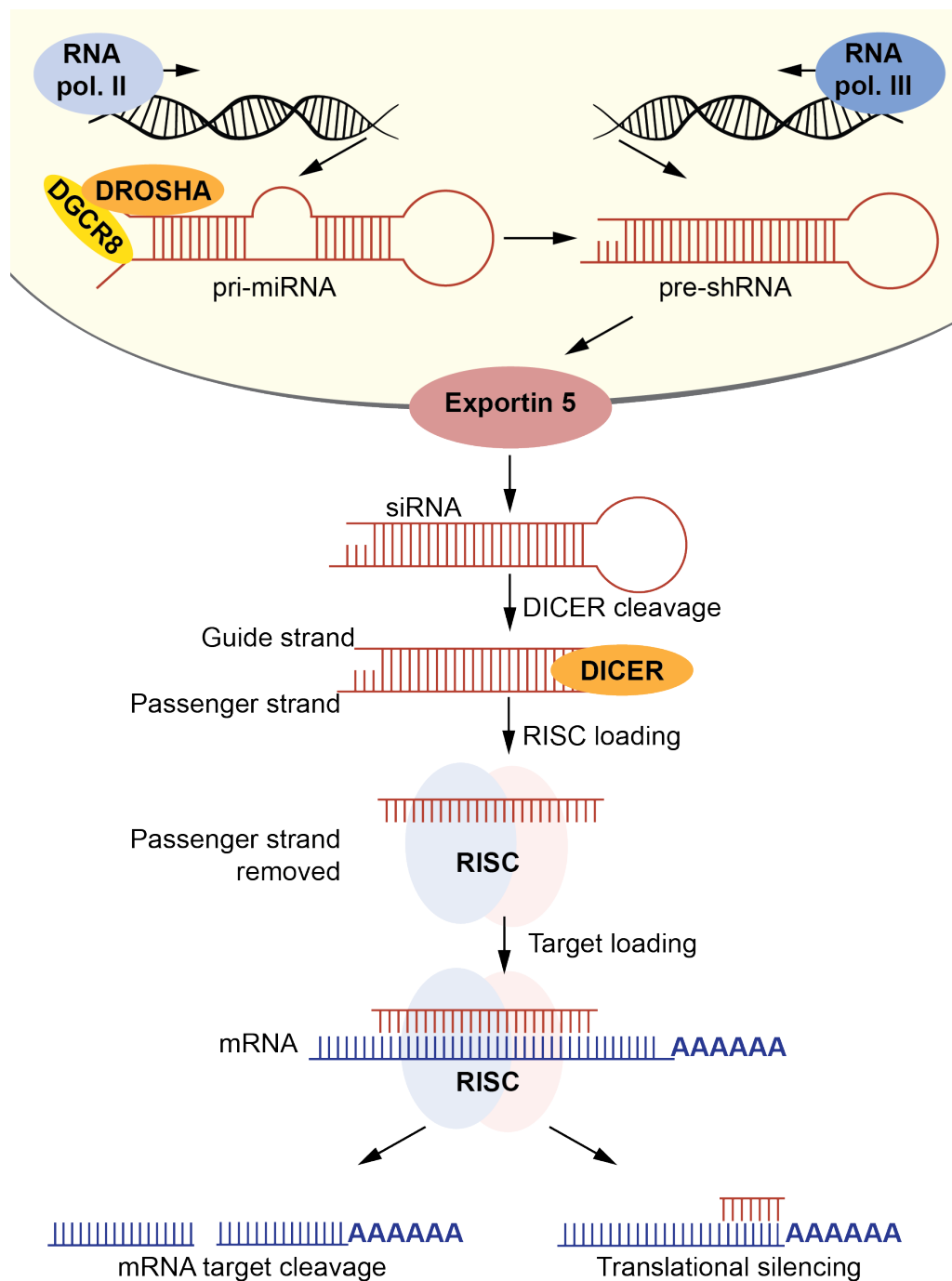


Figure 10: shRNA mechanism of action. Following transduction of lentiviral plasmid into the target cells, shRNA is transcribed by either RNA polymerase II or III in the nucleus. First, primary-microRNA (pri-miRNA) is produced, which is then cleaved by Drosha and DGCR8 to form pre-shRNA. Pre-shRNA is exported out to the cytoplasm through the Exportin 5 transporter, where it is processed by Dicer into shRNA. shRNA is loaded onto the RNA-induced silencing complex (RISC) where the passenger strand is discarded. The shRNA-RISC complex is guided by the guide strand to complementary target mRNA. Target mRNA is then inhibited by either degradation or translational silencing.

3.4.2 shRNA design

A number of recent developments in shRNA vector design have enhanced the potency and stability of gene silencing and minimised the risk of off-target effects. Lentiviral vectors are normally used as they are less toxic than adenoviral-mediated transductions and can be used in dividing and non-dividing cells (Moore et al., 2010). The expression of shRNAs is driven by constitutive promoters and the choice of the promoter that transcribes the shRNAs can have a bearing on the potency of gene silencing. In this thesis, the spleen focus forming virus (SFFV) was used, which has been previously shown to exert strong transcriptional ability in a lentiviral vector (Winiarska et al., 2017). A fluorescent marker, such as green fluorescent protein (GFP), is placed on the same transcript as the shRNA on the vector so that the level of fluorescence in the cell correlates directly with the level of shRNA expression. Epigenetic silencing by DNA methylation of elements of the vector may hinder effective and stable silencing of the target genes. To counter this, a ubiquitous chromatin opening element (UCOE) is placed upstream of the SFFV promoter that is resistant to methylation and has been shown to improve the stable expression of transgenes in lentiviral vectors (F. Zhang et al., 2010; Diesch et al., in revision). Although shRNAs are designed to instruct degradation of complementary mRNA, off-target effects can occur whereby other mRNA transcripts are inadvertently affected. This can happen if the guide sequence is identical, or nearly identical, to a non-target mRNA (Sharma & Rao, 2009). Further, binding of the 'seed region' of the shRNA can cause unwanted depletion of non-target protein (Schlabach et al., 2008). The seed region is essential for binding to target mRNA and so it is important that it is unique to the target of interest. However, compared with exogenously synthesised siRNA, shRNA are less likely to produce off-target effects and, because of their relatively short length, they do not induce immune responses (Zimmer et al., 2019). The activity of Dicer can be inaccurate by cleaving at imprecise sites in commonly used shRNA stem designs (Gu et al., 2012). The placement of synthetic shRNA stems during the endogenous synthesis of miRNA can improve Dicer accuracy. These so-called 'shRNAmir' structures have been shown to enhance knockdown potency and single-copy integration of the shRNA (Fellmann et al., 2013).

3.4.3 Applications of RNAi

Loss-of-function screening has become a valuable tool in cancer research as a means to uncover gene function. As virtually any gene can be silenced, RNAi technologies have contributed significantly to our understanding of gene function.

Notably, valuable discoveries have been made using high throughput shRNA screens in the context of haematological malignancies (as reviewed in Liu, 2020). The Zuber

laboratory has developed several pooled shRNA libraries which they employ to uncover clinically relevant genetic interactions in AML (Fellmann et al., 2013). RNAi screens facilitated their discovery of the aforementioned BRD4 as a therapeutic target for BETi (Zuber et al., 2011) and later, PRC2-mediated mechanisms underlying BETi resistance (Rathert et al., 2015). Broad-acting epigenetic drivers of leukaemogenesis have been identified for the *MLL* fusion AML sub-type, involving the SIRT1 histone deacetylase (Chen et al., 2015) and MOF histone acetyltransferase (Valerio et al., 2017).

The modest efficacy of most epigenetic drugs to date has set the demand for compounds that effectively eradicate LSC. Recently a targeted shRNA screen assisted in identifying epigenetic dependencies in LSCs in an *ex vivo* mouse model (MacPherson et al., 2020). Similarly, by taking advantage of LSC-specific glutamine metabolism dependencies, AML cells were shown to be sensitized to FLT inhibition in *FLT*-mutated AML (Gregory et al., 2016). Using an shRNA screen directed towards glucose and TCA cycle genes, vulnerabilities in creatine metabolism were discovered that could be exploited in therapy-resistant AML with aberrant *EVI1* expression (Fenouille et al., 2017). Taken together, RNAi screens have been shown as valuable tools in identifying potential therapeutic targets that are LSC-specific and relevant in particular disease subtypes.

Rationale and objectives

4. Rationale & objectives

Leukaemia affects the normal function of blood cells by disrupting differentiation and haematopoiesis at the level of stem cells. Leukaemic stem cells acquire genetic mutations, which clonally expand, and display metabolic plasticity that allows them to proliferate over normal haematopoietic stem cells and evade challenges mounted by chemotherapies. Fatty acid metabolism has been observed to play a significant role in disease progression and drug resistance in haematological malignancies (Tabe et al., 2020). Genes encoding for epigenetic regulators are frequently mutated in myeloid malignancies and are associated with the transformation of MDS to sAML. Genetic and epigenetic factors are thought to contribute to the altered metabolism of leukaemic stem cells but have remained largely elusive. Markers of altered metabolism may provide new targets for therapy and biomarkers of disease that are unique to diseased cells. Novel methods of interrogating the interplay between epigenetic regulation and altered metabolism are needed. The aim of my PhD thesis has been to investigate the role of fatty acid metabolism in haematological malignancies with the following objectives:

1. Devise a methodology to simultaneously investigate epigenetic and metabolic properties of haematological cell lines centred on a shRNA knockdown screen coupled with fluorescence-based fatty acid uptake assay.
2. Investigate epigenetic regulators involved in fatty acid metabolism, specifically fatty acid uptake, in the MDS/sAML cell line, SKK-1.
3. Metabolically and transcriptionally characterise sub-populations of SKK-1 cells based on their distinct low and high fatty acid uptake phenotypes.

Results

5.1 Chapter summary

There has been relatively little research regarding the epigenetic regulation of lipid metabolism in the context of leukemia. We therefore devised a novel shRNA knockdown screen/FACS approach to attempt to uncover epigenetic-metabolic axis. Specifically, we decided to take a targeted approach to uncover regulatory factors that may be involved in lipid metabolism. This involved knocking down 912 epigenetic and regulatory genes with the use of a pooled library of 7296 shRNA hairpins called hEPI9 (kindly provided by Dr. Johannes Zuber). Transduced cells were subsequently sorted into two populations based on their fatty acid uptake. By separating low and high fatty acid uptake cells following shRNA knockdown we attempted to identify genes that were functionally associated with the metabolic phenotype.

5.2 Fatty acid uptake assay

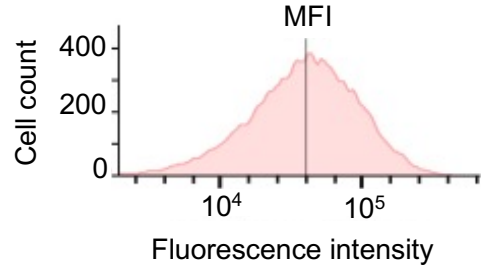
We wished to characterise MDS-derived sAML cell lines on the level of fatty acid metabolism using a simple metabolic read-out that could separate cells based on low and high fatty acid uptake. For this we have used fatty acid uptake as a proxy for cellular metabolic activity. Fatty acid uptake was measured by flow cytometry using two BODIPY-tagged fatty acids analogues: a red fluorescence-labelled laurate and a green fluorescence-labelled palmitate. These fatty acid analogues formed the basis of the approach we employed to distinguish the two lipid metabolism-related phenotypes. Green fluorescence-labelled palmitate has been shown to bind to FABPs and localise to mitochondria (Thumser & Storch, 2007) and its uptake is inhibited by blocking the activity of the CD36 fatty acid transporter (Paulus et al., 2017). Fluorescence-labelled laurate has been previously used to detect lipid droplets *in vitro* (Wang et al., 2010). Thus, fluorescence labelled-fatty acids represent a simple means to visualise and measure fatty acid uptake in live cells.

We measured fatty acid uptake as a function of median fluorescence intensity (MFI). Uptake was distributed along a Gaussian curve, indicating a spectrum of fatty acid uptake capacities (**Figure 11A**). Fluorescent palmitate was taken up by SKK-1 and MOLM-13 cells in a dose-dependent manner (**Figure 11B** and **11C**). To see if the assay was applicable to other haematologically relevant cell lines, we introduced another MDS-derived cell line,

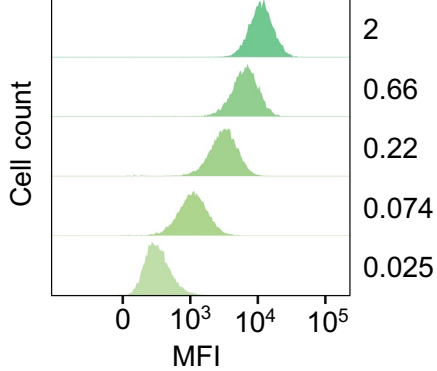
| Results I

SKM-1, along with an AML-derived cell line, THP-1 and observed how fluorescence-labelled laurate was taken up. Again, we observed that fatty acid uptake was shown in a dose-dependent manner in all three cell lines (**Figure 11D**). Similarly, when we incubated SKK-1 and MOLM-13 cells with the fluorescent palmitate, fatty acid uptake was directly correlated with incubation time (**Figure 11E**). For subsequent experimentation, we chose the intermediate concentration of 0.5 μM and an incubation time of 60 minutes to avoid saturation. We further determined that the detection of the BODIPY signal is transient and cannot be detected when re-analysing cells after five days (data not shown).

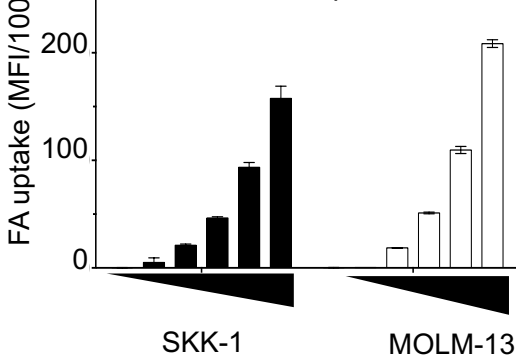
A Uptake of fluorescence-labelled palmitate by SKK-1 cells



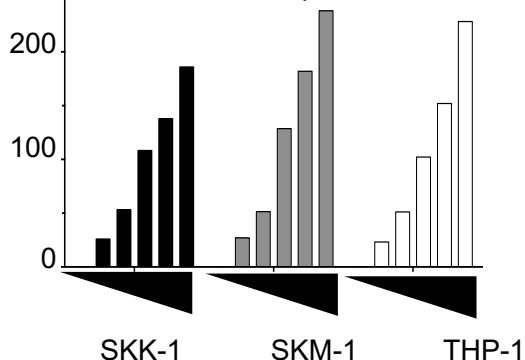
B Palmitate uptake μ M



C Palmitate uptake



D Laurate uptake



E Palmitate uptake

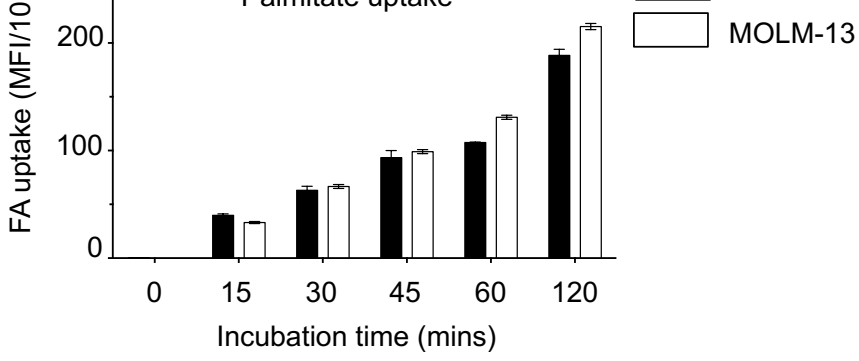


Figure 11: FACS-based detection of fluorescence-labelled laurate and palmitate fatty acids. A) representative flow cytometry histogram showing a Gaussian-like distribution with indicated median fluorescence intensity (MFI), when cells were incubated with fluorescent BODIPY-labelled palmitate or laurate. B) Representative FACS histogram showing median fluorescence intensity (MFI) of the BODIPY dye relative to cell count in SKK-1 cells. C) Two MDS/sAML-derived cell lines (SKK-1, MOLM-13) take up fluorescence-labelled palmitate in a dose-dependent manner following incubation for 60 minutes with a range concentrations of fatty acids: 0, 0.025, 0.075, 0.22, 0.66, 2 μ M. From this measurement, a concentration of 0.5 μ M of palmitate was chosen for subsequent uptake tests. Data are represented as MFI +/- standard deviation of three samples for each concentration. D) Two MDS/sAML-derived cell lines (SKK-1, SKM-1) and one AML-derived cell line (THP-1) take up fluorescence-labelled laurate in a dose-dependent manner following incubation for 60 minutes with a range concentrations of fatty acids: 0, 0.025, 0.075, 0.22, 0.66, 2 μ M. From this measurement, a concentration of 0.5 μ M of laurate was chosen for subsequent uptake tests. Data are represented as MFI. E) SKK-1 and MOLM-13 cells were incubated with 0.5 μ M fluorescence-labelled palmitate for the indicated amount of time. From this measurement, an incubation time of 60 minutes was chosen for subsequent uptake tests. Data are represented as MFI +/- standard deviation of three samples for each incubation time.

Since fatty acid oxidation ultimately takes place in the mitochondria, we decided to test whether fatty acid uptake capacity of SKK-1 and MOLM-13 cells is linked to mitochondrial uptake and activity. Therefore, we analysed palmitate uptake after pre-treatment with etomoxir, which is a widely used inhibitor of fatty acid uptake into mitochondria (Pike et al., 2011). As controls we used insulin and the activator of AMP kinase, AICAR, that both activate cell membrane-bound fatty acid transporters (Chabowski et al., 2005). Both SKK-1 and MOLM-13 cells treated with etomoxir had a substantial reduction in fatty acid uptake compared to the non-treated control, AICAR and insulin treatment showed a slight, but significant, increase in fatty acid uptake (**Figure 12A** and **Figure 12B**).

Overall, we found that both fluorescence-labelled laurate and palmitate were taken up in a dose- and time-dependent manner and that fatty acid uptake could be modulated with inhibiting and stimulating compounds.

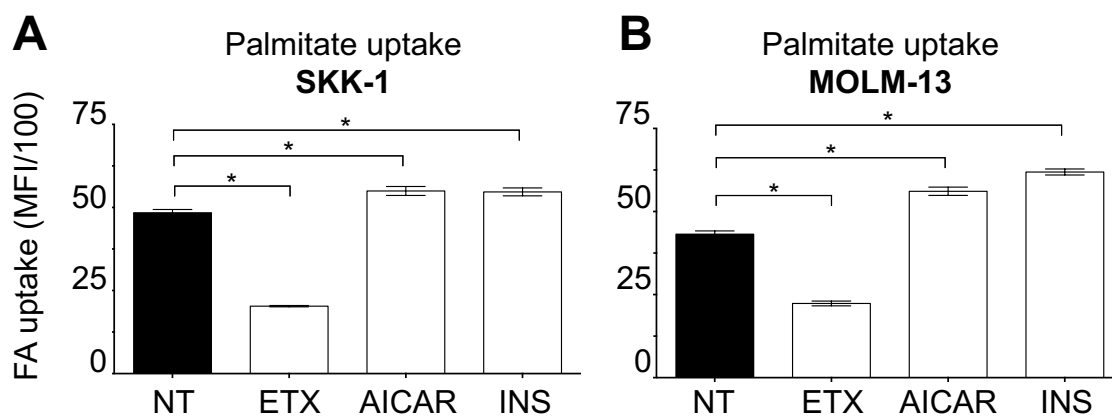


Figure 12: Fatty acid uptake is modulated with Etomoxir, AICAR and insulin. After pre-treatment A) SKK-1 and B) MOLM-13 cells with Etomoxir (Etx, 50 μ M), AICAR (200 μ M) or insulin (Ins, 200 nM), palmitate uptake in was analysed as described in Figure 1. Measurements were taken in triplicate. Data are represented as the median fluorescence intensity (MFI), vertical bars indicate standard deviation, $n = 3$. * $p < 0.05$ (one-way ANOVA).

5.3 Establishment of the shRNA knockdown screen conditions

In order to associate epigenetic regulators with fatty acid uptake, we coupled a shRNA-based knockdown screen to the fatty acid uptake assay. For this, we employed the hEpi9 shRNA library, which consists of 7296 hairpins cloned into the lentiviral cSGEP vector that target 912 genes (eight hairpins per gene) (**Figure 13**). The genes constitute a variety of enzymatic and effector activities (**Figure 14**). The backbone of the cSGEP vectors contained a GFP-expressing marker. GFP has an excitation peak at 395 nm and emission peak at 509 nm, and the green-labelled palmitate has an excitation peak at 503 nm and emission peak at 512 nm. Therefore, in order to avoid interfering fluorescence signals on the flow cytometer, we decided to use the red-labelled laurate for the subsequent fatty acid uptake portion of the screen.

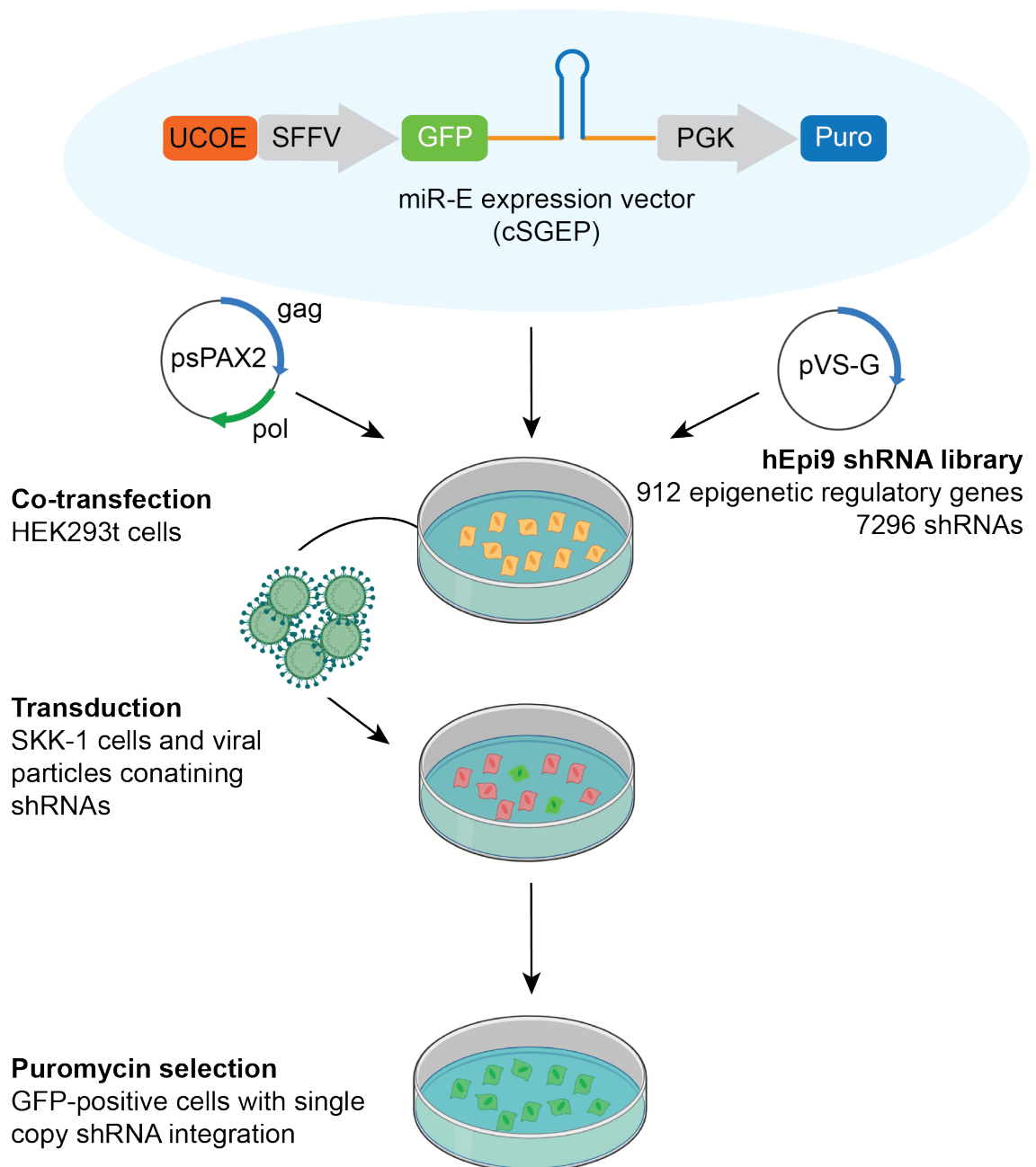


Figure 13: Chromatin regulators associated with low and high fatty acid uptake are identified with optimised shRNA knockdown screen. Schematic workflow outlining the transfection, transduction and selection steps for stably knocking down SKK-1 cells with 7296 shRNAs targeting 912 chromatin regulator genes. HEK293t cells were co-transfected with a pool of miR-E expression (cSGEP) lentiviral vectors containing the shRNA guide sequences along with packaging plasmids psPAX2 and pVSG-G. UCOE was introduced to improve expression of the SFFV promoter. Also present on the cSGEP vector are genes encoding green fluorescence protein (GFP), PGK promoter and puromycin resistance. SKK-1 cells were then transduced with the harvested viral particles. Puromycin was later added to select for the successfully transduced cells with puromycin resistance and GFP expression (explained in greater detail in Material and Methods section).

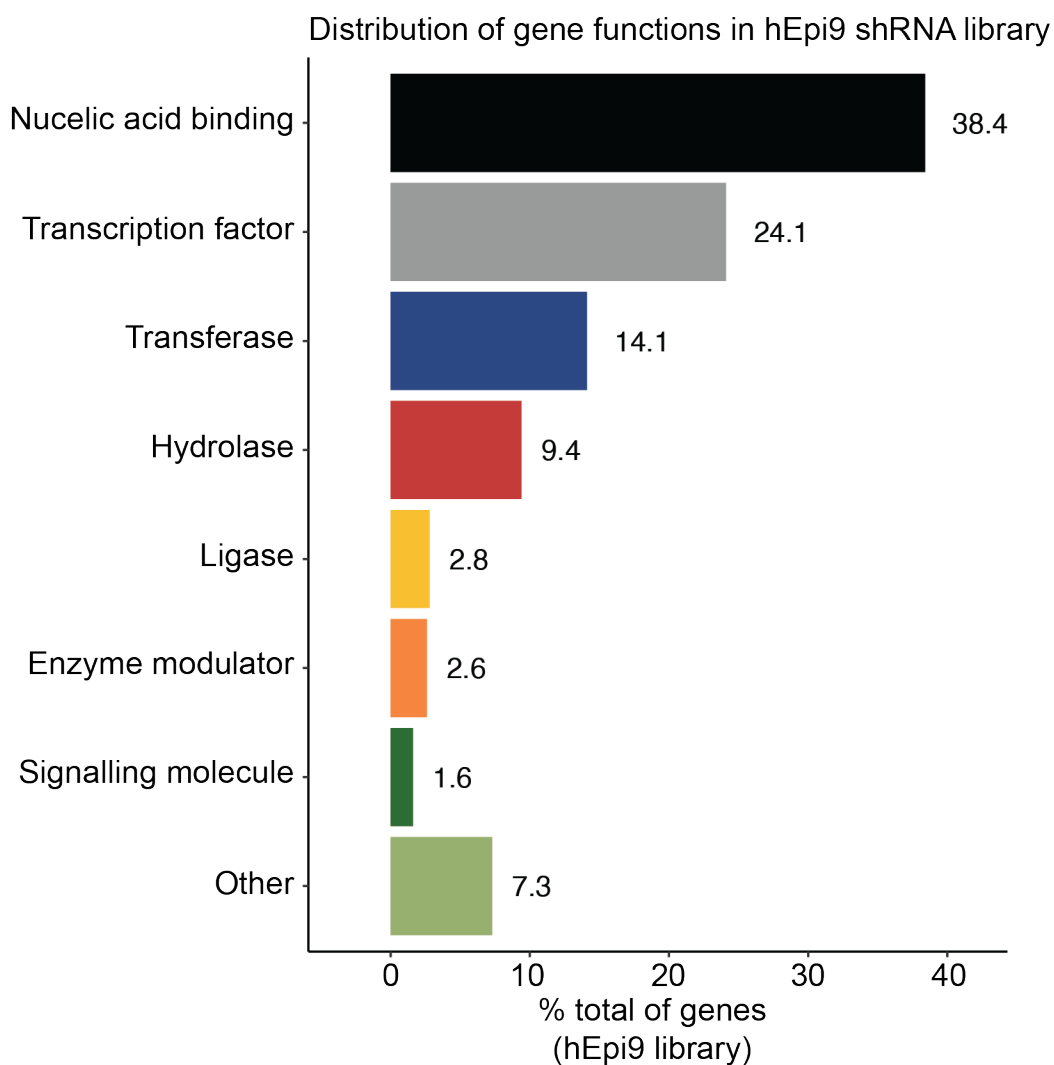


Figure 14: Distribution of gene functions in hEpi9 shRNA library. Bar plot showing the percentage distribution of the broad biological functions of the 912 genes in the hEpi9 shRNA library.

Following the hEpi9 shRNA library-mediated knockdown of SKK-1 parental cells with the hEpi9 shRNA library, we sorted the lowest and the highest 10% of knockdown cells based on their uptake of fluorescently labelled laurate (**Figure 15**). We refer to these cells as single-sorted low (SS LOW) and single-sorted high (SS HIGH), respectively. Therefore, when comparing SS LOW versus SS HIGH populations, enriched and depleted hairpins could be associated with low and high fatty acid uptake, respectively.

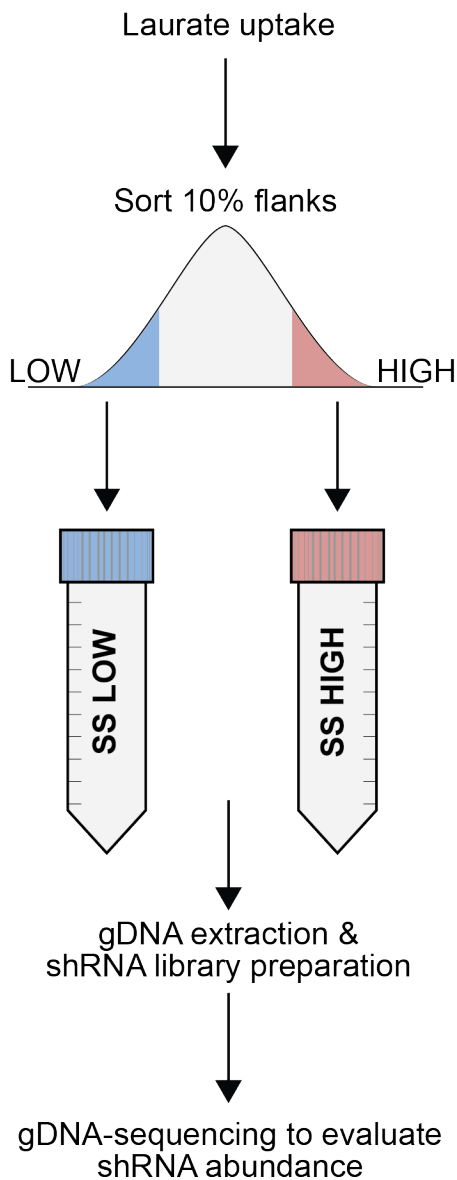


Figure 15: Schematic of FACS strategy for separating cells based on fatty acid uptake. Following knockdown with the hEpi9 short hairpin RNA (shRNA) library, SKK-1 cells were incubated with fluorescence-labelled laurate after which the lowest and highest 10% sub-populations were sorted based on fatty acid uptake. The sorted populations were termed single-sorted LOW (SS LOW) and single-sorted HIGH (SS HIGH). Three replicates of each population were sorted on three separate days. On three separate days. After the sorted cell populations were collected, genomic DNA (gDNA) was extracted and prepared for sequencing from which read counts of enriched and depleted shRNAs from each replicate were analysed.

Previous work carried out by Jeannine Diesch in our lab established that 10-13% GFP-positive SKK-1 cells was indicative of single copy integration of the lentiviral particles, i.e. one cSGEP plasmid per cell. We chose 400 μ L as the optimal viral titre, as 10% of SKK-1 cells transduced with hEpi9 were GFP-positive one day post-infection (**Figure 16A**). Similarly, based on previous work in the lab, we used 1.2 μ g/mL puromycin for selecting successfully transduced SKK-1 cells, as it was found to be the minimum concentration at which non-transduced cells died. A similar concentration of puromycin was found to kill other AML cells, such as KG-1 (**Figure 16B**). The same puromycin concentration was used for selecting KG-1 cells with *PADI4* knockdown (as detailed in section 10.9).

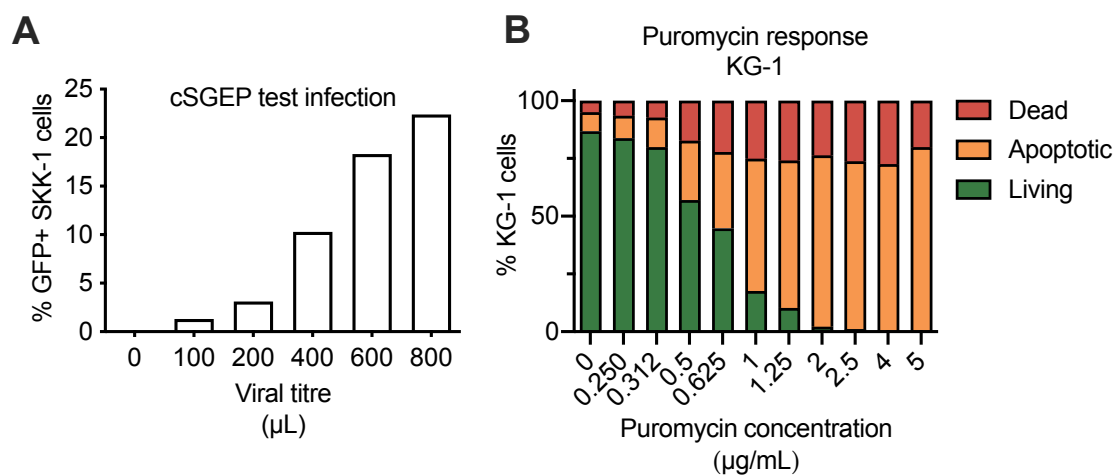


Figure 16: Optimisation of conditions for viral infection and puromycin selection. A) Bar plot shows the percentage of GFP-positive SKK-1 cells one day post-infection with a range of volumes of the lentiviral cSGEP control vector. The titre of virus particles that results in 10-13% infection efficiency in SKK-1 cells was chosen. B) Bar plot shows the percentages of living, apoptotic and dead KG-1 cells (y-axis) after a 3-day treatment with a range of puromycin concentrations (x-axis), as determined by flow cytometry. The concentration of puromycin that kills KG-1 cells not transfected with lentiviral shRNAs was determined.

5.4 gDNA-sequencing sample preparation

Prior to FACS sorting of the SKK-1 knockdown cells based on the differential uptake of fluorescence-labelled laurate, we optimised the sorting conditions. To ascertain whether the cells were still viable after the FACS sorting and determine the time needed to collect the required number of cells, we carried out a test FACS sort of SKK-1 cells using two different nozzle sizes, 70 and 85 nm. We saw that cells were viable and culturable after the sort using both nozzle sizes. Therefore, we chose 70 nm nozzle size as this allowed for an acquisition rate of up to 20,000 events per second, thus allowing for approximately eight million cells to be acquired over two hours.

Following the transduction of SKK-1 cells with the hEpi9 library (SKK-1:hEpi9), cells were selected for 14 days at which point over 86% of the total population was GFP-positive (**Figure 17A** and **Figure 17B**). Once the SKK-1:hEpi9 cells had grown to sufficient numbers, reaching approximately 140 million, they were taken to the FACS facility for the sort. This allowed us to have sufficient numbers of sorted cells so that we could maintain 1000x representation of each hairpin for adequate coverage during sequencing, as explained in section 10.12 of Materials and Methods.

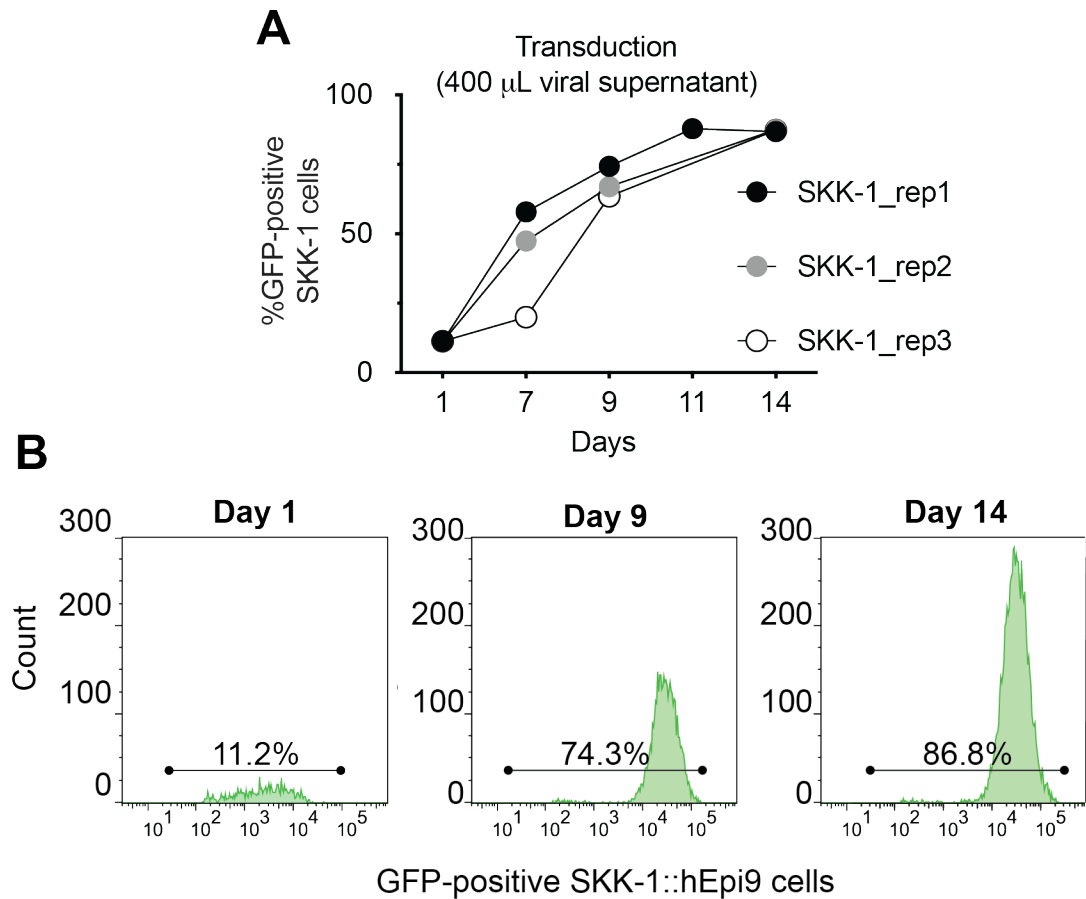


Figure 17: Measurements of GFP-positive SKK-1::hEpi9 cells following transduction. A) Line graph shows the increased percentage of green fluorescent protein (GFP)-positive SKK-1 cells (y-axis) over a period of 14 days (x-axis), as measured by flow cytometry. Three replicates of SKK-1 cells transduced with the hEpi9 shRNA (SKK-1::hEpi9) library were selected with puromycin over a 14-day period. B) Representative flow cytometry histograms on three selected days showing cell counts (y-axis) and fluorescence intensities (x-axis) of one of the replicates (SKK-1_rep1) following transduction with the hEpi9 shRNA library. Indicated percentages are GFP-positive cells.

After the sort, we performed a purity control test to make sure the cells were intact and they retained low and high uptake phenotypes. This involved re-analysing the sorted SS LOW and SS HIGH populations. SS LOW were characterised by low MFO, and SS HIGH were characterised with higher MFI, showing that both sorted populations had good purity. Thus, we did not observe any carry-over between the two populations.

5.5 shRNA screen analysis

Throughout the shRNA screen analysis, we analysed the data by way of comparing SS LOW versus SS HIGH using the R package EdgeR (**Figure 18A**) (Dai et al., 2014). Therefore, when comparing SS LOW with SS HIGH, knockdowns of enriched shRNA-associated genes were considered to be associated with low fatty acid uptake. Conversely, knockdowns of depleted shRNA-associated genes were considered to be associated with higher fatty acid uptake (**Figure 18B**).

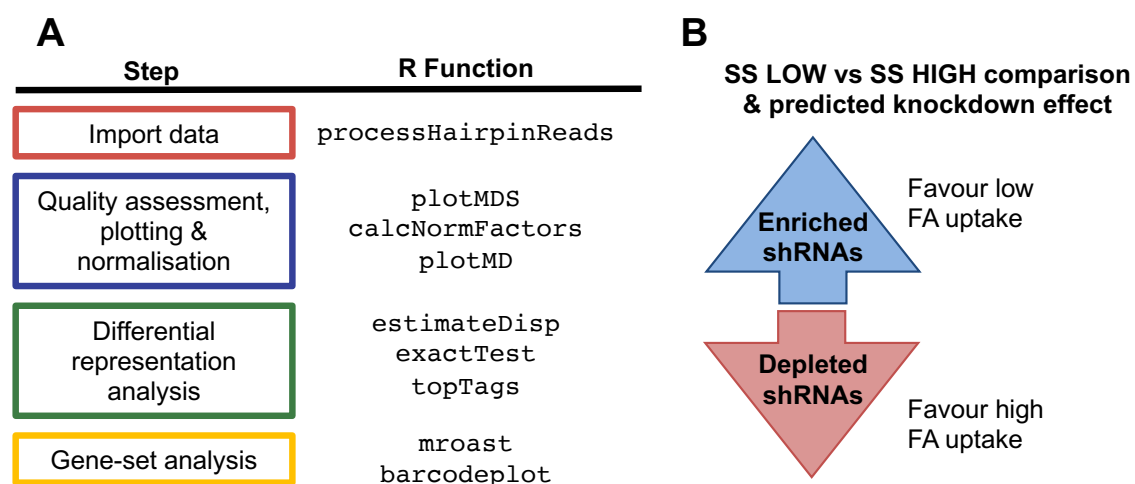


Figure 18: In silico analysis of the shRNA count data carried out comparing SS LOW and SS HIGH. A) Summary of EdgeR and limma workflow to first calculate the relative abundance of the individual shRNAs and then to integrate these counts by gene-wise analysis to calculate the top genes associated with low and high fatty acid uptake. B) Using the SS LOW versus SS HIGH comparison, enriched shRNAs and genes were associated with low fatty acid uptake and depleted shRNAs and genes were associated with high fatty acid uptake.

Upon receiving the count data from the gDNA sequencing run, we carried out a descriptive analysis of the screen to get an idea of how the count data looked. The cumulative counts of each shRNA across all six samples were obtained, where some shRNAs were over-represented (**Figure 19A**). To see the distribution of the count data, we transformed the raw counts to logarithmic counts per million (log-CPM), as count data is not normally distributed. Distributions of log-CPM values were similar across all samples for both unnormalised and normalised counts (**Figure 19B**). Counts were normalised by the trimmed mean of M-values (TMM) method (Robinson & Oshlack, 2010). A multidimensional scaling plot shows clustering of the replicates from each day of sorting in the first dimension of the leading logFC, while SS LOW and SS HIGH sample groups clustered in the second dimension (**Figure 19C**).

| Results I

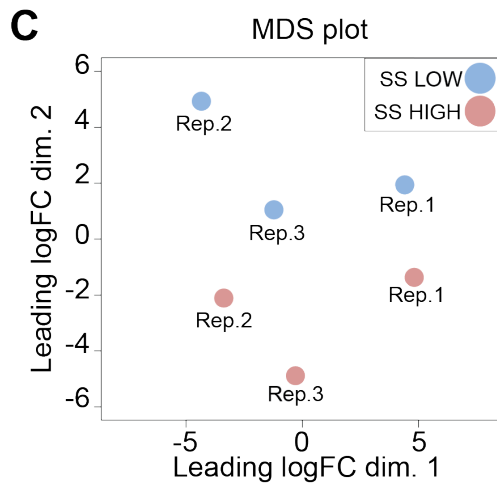
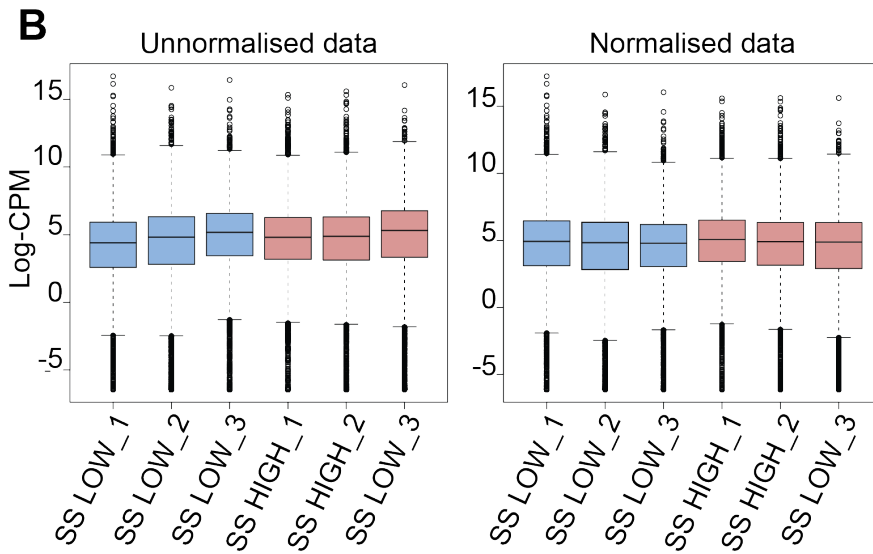
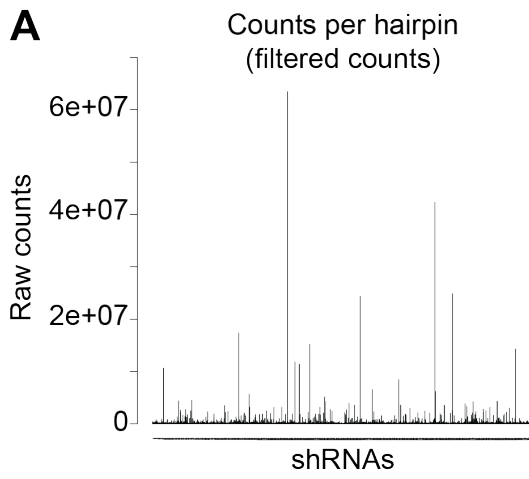


Figure 19: Descriptive analysis of shRNA read counts and similarity between SS LOW and SS HIGH replicates. A) Bar plot representing the cumulative number of read counts (y-axis) across all 7296 shRNA hairpins (x-axis). B) Box plot representing the density distributions of unnormalised and normalised (TMM method) read counts (log-CPM) of all hairpins that were matched per sample. Blue: SS LOW₁, SS LOW₂, SS LOW₃. Red: SS HIGH₁, SS HIGH₂, and SS HIGH₃. The inter-quartile range defines the height of the box. Whiskers extend to 1.5x the inter-quartile range. Horizontal black lines in each box represent the mean log-CPM of each sample. Outliers are represented as individual points. C) Multidimensional scaling (MDS) plot showing the relationships between the three replicates (Rep.1-3) of SS LOW and SS HIGH over dimensions 1 and 2 (Leading LogFC dim 1 and Leading LogFC dim 2).

We generated a mean-difference plot to visually summarise the read counts of the individual hairpins, which comprised log-FCs from the exact test and the average log-CPM values that were generated from the plotMD function (**Figure 20A**). The significantly enriched and depleted hairpins in SS LOW are highlighted in red and blue, respectively (p -value < 0.05). 204 and 168 hairpins were found to be significantly enriched and depleted, respectively, in SS LOW (**Figure 20B**).

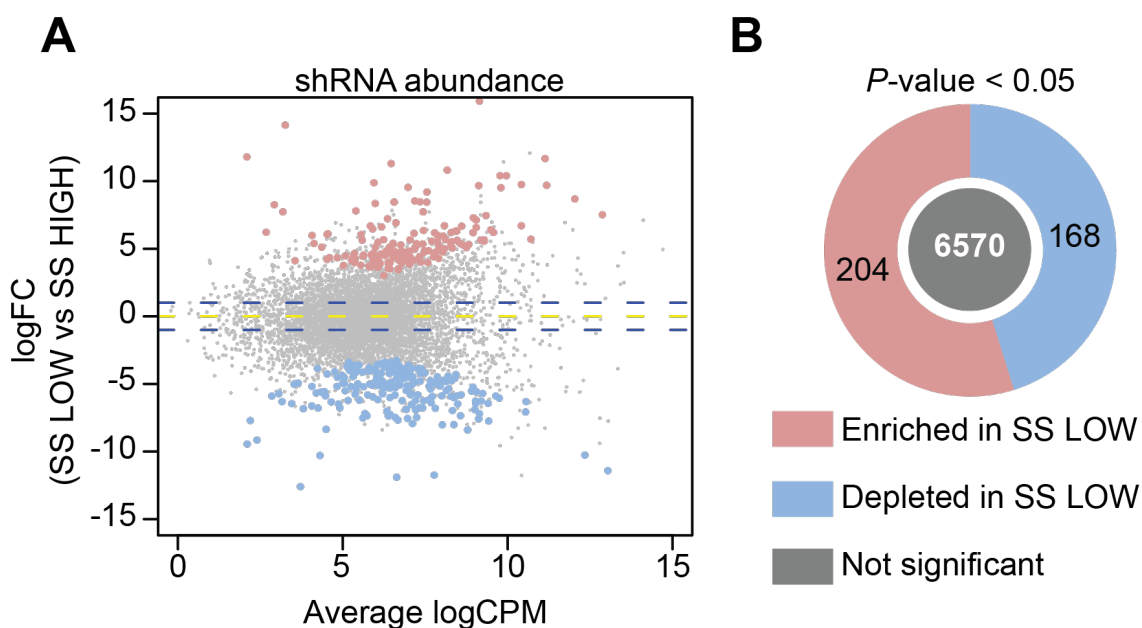


Figure 20: Differential abundance of individual shRNAs comparing SS LOW versus SS HIGH. A) shRNA hairpins are represented on a plot as calculated by the plotMD function. Shown are the logfold-change (logFC, y-axis) versus the average log₂ count per million (Average log CPM, x-axis) of the differences in hairpin abundance when comparing SS LOW versus SS HIGH. Significantly enriched shRNAs are indicated in red and those significantly depleted are in blue (p-value < 0.05). Horizontal blue lines delineate 1-fold change and each point represents one hairpin. The grey dots represent hairpins whose abundance was not significantly different. B) Following Fisher's Exact Test, 168 shRNAs were enriched and 204 shRNAs were depleted SS LOW and SS HIGH. 6570 shRNAs were not significantly enriched or depleted.

Next, we performed a ROAST gene set analysis to summarise the results from the multiple shRNAs targeting the same gene (Wu et al., 2010). For this, a ranked list of significantly differentially abundant genes was generated according to p-value, which consisted of genes containing counts from six or more hairpins with an absolute mean logFC greater than 1. 52 and 104 genes were found to be significantly enriched and depleted, respectively (**Figure 21A**). The list of all significantly enriched and depleted genes can be found in **Table 18** and **Table 19** in the appendix section.

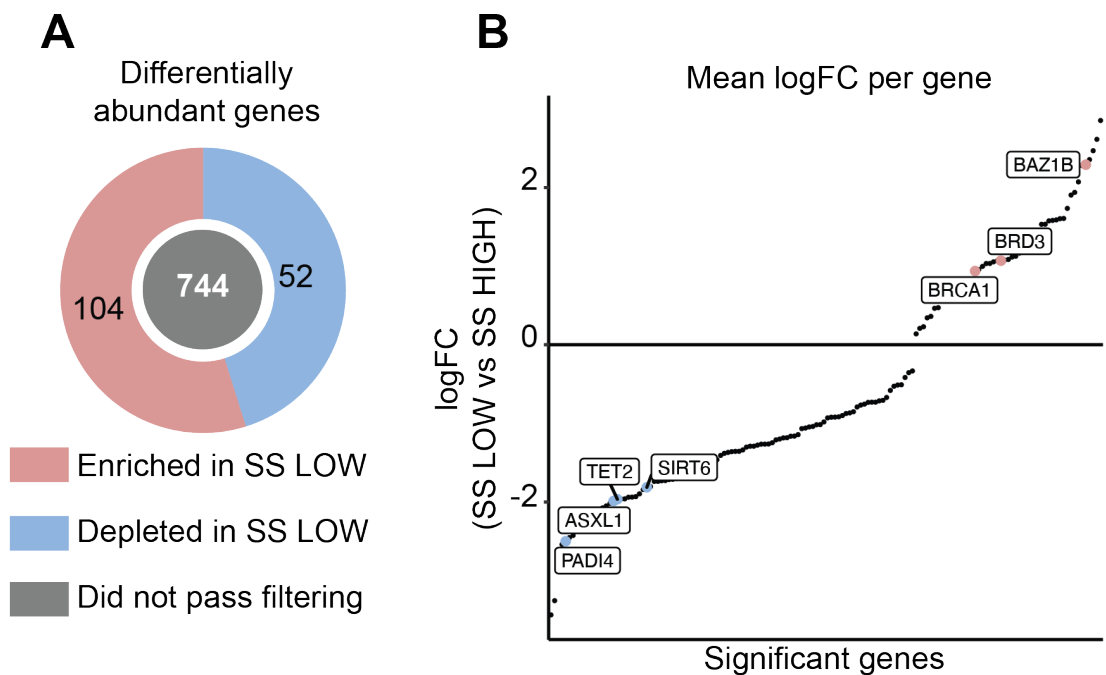


Figure 21: Top hits from the shRNA knockdown screen were selected for further validation. A) Of the 912 genes, 52 gene knockdowns were significantly enriched, and 104 gene knockdowns were significantly depleted when comparing SS LOW versus SS HIGH. The criteria comprised a log fold-change of 1, p-value < 0.05 and each gene having six or more hairpins in the same direction (either enriched or depleted). 744 gene knockdowns were not significantly differentially abundant. B) Plot displays significantly enriched and depleted genes (x-axis) and mean log fold-change (logFC, y-axis), as calculated by gene set analysis using the mroast function. Selected genes with mean log-fold changes greater than 1 or less -1 are shown. Outlined are enriched low fatty acid uptake-associated gene knockdowns (BAZ1B, BRD3 and BRCA1) and depleted high fatty acid uptake-associated gene knockdowns (PADI4, ASXL1, TET2 and SIRT6) that were chosen for further validation.

5.6 Validation of the hEpi9 shRNA screen

From the list of enriched and depleted genes constructed from the ROAST gene set analysis, seven genes were considered for further validation (**Figure 21B**). These genes were chosen from the ranked list based on their p-value rank alone or previously known relevance in haematological disease or fatty acid metabolism and were associated with either low fatty acid uptake (enriched hairpins) or high fatty acid uptake (depleted hairpins). The contribution of the individual hairpins of each of the seven genes chosen for further validation are visually summarised with barcode plots (**Figure 22**).

Details of each of the chosen genes are described in **Table 1**. These included: three enriched low fatty acid uptake-associated knockdowns, *BAZ1B* (Bromodomain adjacent to zinc finger domain, 1B), *BRD3* (Bromo domain containing 4) and *BRCA1* (breast cancer type 1 susceptibility protein), and four depleted high fatty acid uptake-associated knockdowns, *PADI4* (peptidyl arginine deiminase 4), *ASXL1* (additional sex combs-like 1, transcriptional regulator), *TET2* (tet methylcytosine dioxygenase 2), and *SIRT6* (Sirtuin 6). *CD36* (cluster of differentiation 36 or fatty acid translocase (FAT)), *CPT1a* (carnitine palmitoyltransferase 1A) and *SIRT1* (Sirtuin 1) were also included as controls, as each have been previously shown to be directly involved in fatty acid uptake specifically or fatty acid metabolism in general (described below).

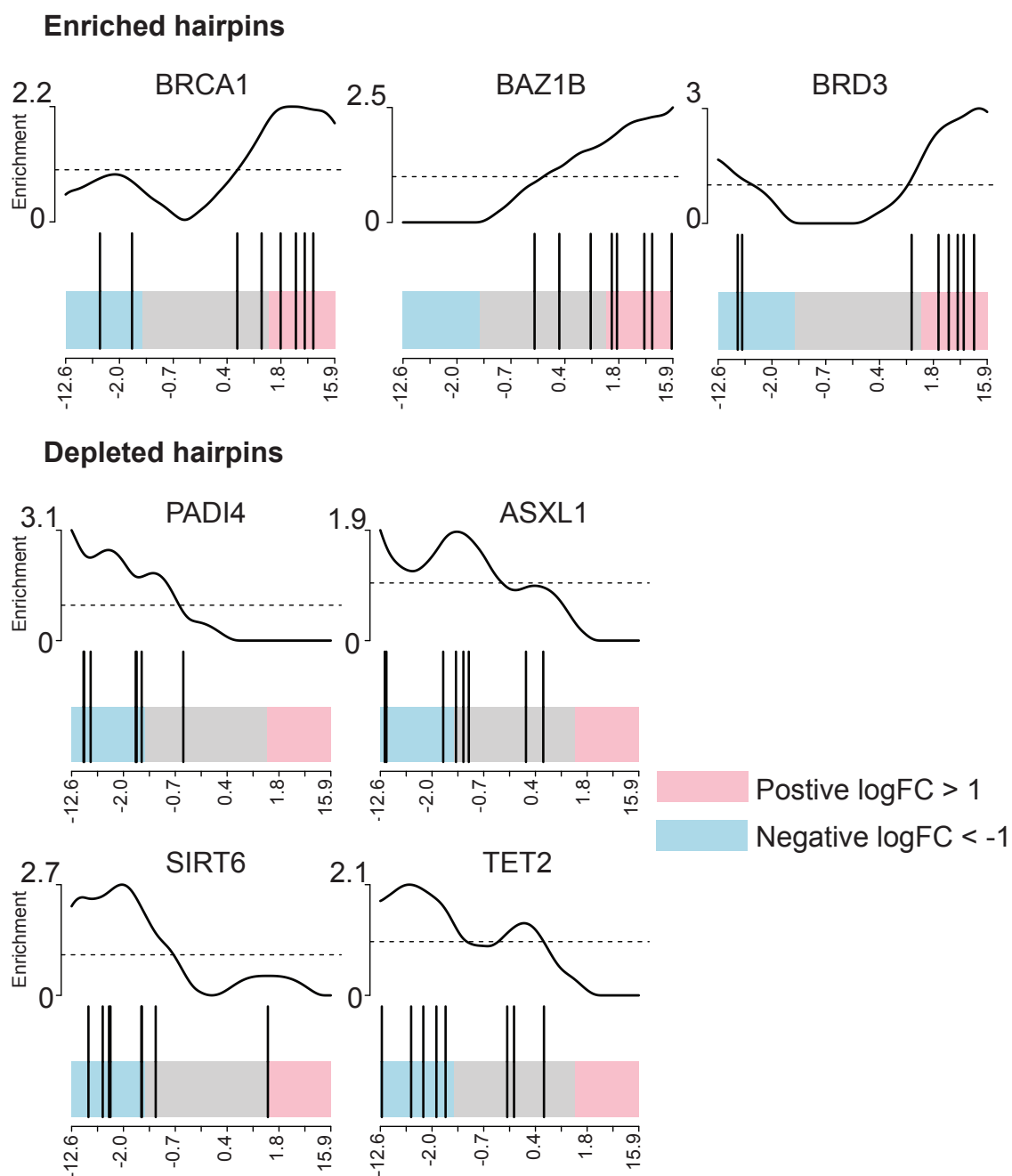


Figure 22: Barcode plots of individual hairpin enrichment. Variation in enrichment and depletion of shRNA clones of selected genes in SS LOW versus SS HIGH, as determined by gene-set analysis. X-axis shows log fold-change (logFC), blue box delineates logFC < -1 and pink box delineates logFC > 1. Vertical black bars represent individual hairpins. The worm graph on top shows relative enrichment among the eight hairpins of each gene. Enriched gene knockdowns chosen for validation: *BRCA1*, *BAZ1b* and *BRD3*. Depleted gene knockdowns chosen for validation: *ASXL1*, *PADI4*, *SIRT6*, and *TET2*.

5.7 Description of screen hits chosen for further analysis

PADI4 has been specifically linked to stem cell maintenance (Christophorou et al., 2014). *PADI4* acts to suppress or activate gene expression in cancer by post-translational modifications of proteins or chromatin decondensation via the citrullination of arginine residues on histones (Song et al., 2016). *ASXL1* regulates transcription and epigenetic marks via recruitment of polycomb complex proteins (Gelsi-Boyer et al., 2012). *ASXL1* mutations are some of the most common found in myeloid malignancies, resulting in increased aggressiveness and poorer outcome in patients (Katoh, 2013). Similarly, aberrant *TET2* activity is common in MDS and AML (Weissmann et al., 2012). *TET2* is involved in active DNA methylation by oxidising methylcytosine to 5-hydroxymethylcytosine (Ito et al., 2011). Sirtuins have broad functions across genomic stability and energy metabolism, mainly through nicotinamide adenine dinucleotide (NAD⁺)-dependent deacetylation of histones (Kugel & Mostoslavsky, 2014). *SIRT6* deficiency has been reported to result in increased expression of genes involved in long-chain fatty acid uptake and reduced fatty acid oxidation, highlighting *SIRT6* has a negative regulator of fatty acid synthesis (Kim et al., 2010). The best characterised sirtuin, *SIRT1*, was chosen as control for high fatty acid uptake due to its role as a key regulator in lipid metabolism through deacetylation of transcriptional regulators (Cantó & Auwerx, 2009). Upon changes in cellular NAD⁺ levels, *SIRT1* has been shown to act as a metabolic switch, inhibiting fat storage and activating lipolysis (Simmons et al., 2015).

BAZ1B encodes a bromodomain family member protein that is strongly involved in chromatin organisation via phosphorylation of the Tyr₁₄₂ residue on H₂A histone family member X (Xiao et al., 2009). *BRD3*, another bromodomain family member, is a transcriptional and epigenetic regulator by associating with acetylated lysines on transcriptional factors and histones (Carretta et al., 2017). Along with tyrosine kinase receptor pathways, *BRD3* has been shown to be critical for the survival of AML cells (Carretta et al., 2017) and its down regulation has been associated with reduced growth capacity of cancer cells (Asangani et al., 2014). Indeed, bromodomains are widely used therapeutic targets in leukaemia. Although most often associated with breast cancer, the *BRCA1/2* pathway has been shown to prevent the onset of certain classes of leukaemias and lymphomas that involve gene rearrangements (Friedenson, 2007). *BRCA1* interacts with acetyl-coenzyme A (CoA) carboxylase (*ACC1*) in its inactive, phosphorylated form, thereby inhibiting fatty acid synthesis by preventing dephosphorylation. RNA-silencing of *BRCA1* has been shown to reverse this inhibition of fatty acid synthesis (Koobotse et al., 2018; Moreau et al., 2006). Further, the loss of *BRCA1* in cardiomyocytes alters lipid

metabolism by reduced expression of the fatty acid transporters, CD36 and CPT1a and the fatty acid oxidation regulating enzyme ACC2, resulting in overall lower fatty acid oxidation (Singh et al., 2013). *CD36* and *CPT1a* were chosen as low fatty acid uptake controls for their widely reported roles in fatty acid transport on the cellular and mitochondrial membranes, respectively (Jogl & Tong, 2003; Stremmel et al., 2001).

Table 1: Selected genes from shRNA knockdown screen for further validation and controls predicted to modulate fatty acid uptake.

| Gene | Gene product function | Relevance | p-value | Mean logFC |
|-----------------------------------------------------|------------------------------------|--------------------------------------------------------------------|---------------------------|------------|
| High fatty acid uptake-associated knockdowns | | | | |
| <i>PADI4</i> | Arginine deaminase | Stem cell maintenance | 0.0023 | - 2.50 |
| <i>ASXL1</i> | Transcriptional regulator | Mutations associated with MDS and AML | 0.0406 | -1.99 |
| <i>TET2</i> | DNA demethylation | Strongly associated with AML | 0.0115 | -1.96 |
| <i>SIRT6</i> | Deacetylase | Involved in lipid metabolism regulation | 0.0003 | -1.81 |
| <i>SIRT1</i> | Deacetylase | Regulates increased FA oxidation | 0.0116 | -1.143 |
| Low fatty acid uptake-associated knockdowns | | | | |
| <i>BAZ1b</i> | Chromatin remodeling | Chromatin organisation | 0.0132 | 2.29 |
| <i>BRD3</i> | Transcription regulation | Strongly associated with AML | 0.0443 | 1.07 |
| <i>BRCA1</i> | DNA repair | Interacts with ACC1 (rate-limiting enzyme in fatty acid synthesis) | 0.0315 | 0.94 |
| <i>CD36</i> | Cell membrane-bound FA transporter | Directly involved in fatty acid uptake | <i>Chosen as controls</i> | |
| <i>CPT1a</i> | Mitochondria-bound FA transporter | Rate-limiting step in fatty acid oxidation | | |

5.8 *In vivo* validation of the shRNA screen

To validate the chosen hits from the shRNA screen, we initially performed single knockdowns in SKK-1 cells of each gene of interest with two hairpins per gene. We chose the two hairpins on the basis of highest logFC from the screen results, so that hairpins with highest potency were used. In parallel, we included the three controls mentioned above: the fatty acid metabolism regulator, *SIRT1*, and the fatty acid transporters *CD36* and *CPT1a*. Using RT-qPCR we assessed knockdown efficiency by comparing the mRNA levels of the respective genes versus cells transduced with the cSGEP control vector containing the luciferase hairpin. We aimed for a knockdown effect greater than 50%, based on mRNA levels relative to the cSGEP control, to qualify genes as sufficiently knocked down. Sufficiently reduced transcription levels of the knockdown genes provide greater chance of reduced activity of their respective encoded proteins. Following confirmation of the knockdowns, we wished to validate low and high fatty acid uptake-associations from the genetic screen by performing fatty acid uptake assays with the cSGEP-compatible red fluorescence-labelled laurate. Thus, we would check if knockdowns had significant effects on uptake versus the cSGEP control.

All but one of low uptake-associated knockdowns (shCD36_1) had a mean knockdown effect of greater than 50% (**Figure 23A**). However, our fatty acid uptake assay revealed that none of the low uptake-associated knockdown SKK-1 cells displayed significantly reduced levels of fatty acids compared to the cSGEP control (**Figure 23B**).

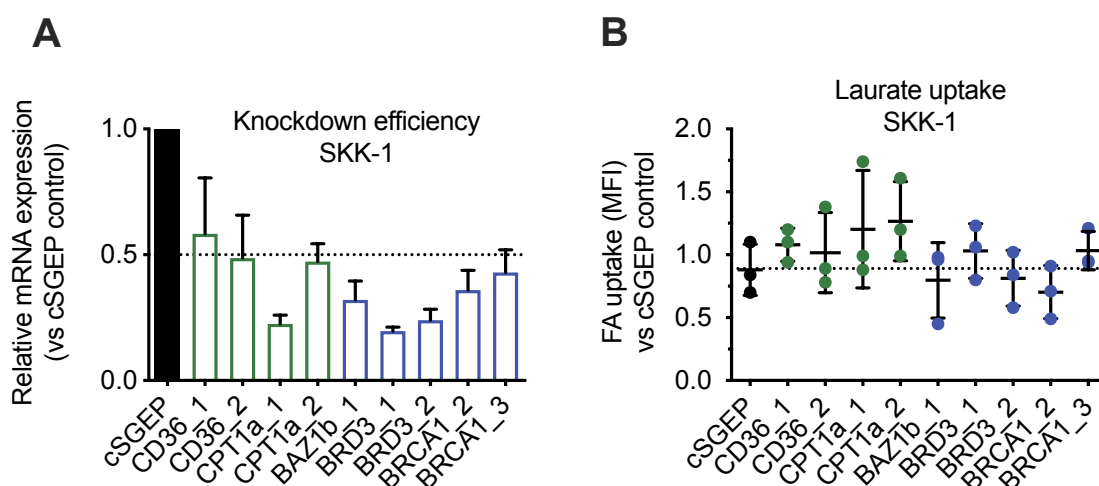


Figure 23: Candidates and controls for lower fatty acid uptake could not be validated. A) RT-qPCR shows relative mRNA expression (versus cSGEP control vector) of knockdown genes relating to low fatty acid uptake-associated hairpins (in blue) and control knockdowns targeting CD36 and CPT1a fatty acid transporters (in green). Values were normalised to the housekeeping gene GAPDH. Results are presented as the mean \pm standard deviation ($n = 3$). Dotted line represents 50% knockdown effect. B) To assess the effect of the knockdowns on fatty acid uptake, SKK-1 cells knocked down with low fatty acid uptake-associated hairpins were incubated with fluorescent BODIPY-labelled $0.5 \mu\text{M}$ laurate for 60 minutes, washed and uptake was assessed by flow cytometry. Results are compared to the SKK-1::cSGEP control vector and expressed as median fluorescence intensity (MFI) relative to the experimental mean (dotted line represents mean of MFIs across all measurements; $n=3$).

We observed similar non-significant differences for the fatty acid transporter controls, CD36 and CPT1a, which were expected to cause a reduction in fatty acid uptake. We therefore decided to investigate CD36 and CPT1a expression in other MDS and AML cell lines to see if greater expression of these transporters would be associated with a greater effect on fatty acid uptake when knocked down. TF-1 emerged as the cell line with substantially greater expression in both CD36 and CPT1a expression compared to SKK-1 and other cell lines (Figure 24A and Figure 25A). Despite strong knockdown effects for both genes in TF-1 (Figure 24B and Figure 25B), we observed a mixed effect on fatty acid uptake. For both genes one of the two short hairpins had the opposite expected effect with cells taking more fatty acids than the control (Figure 24C and Figure 25C).

Thus, we did not observe a significant decrease of fatty acid uptake, neither among the selected top hits from the shRNA screen, nor among the fatty acid transporters upon knocking them down.

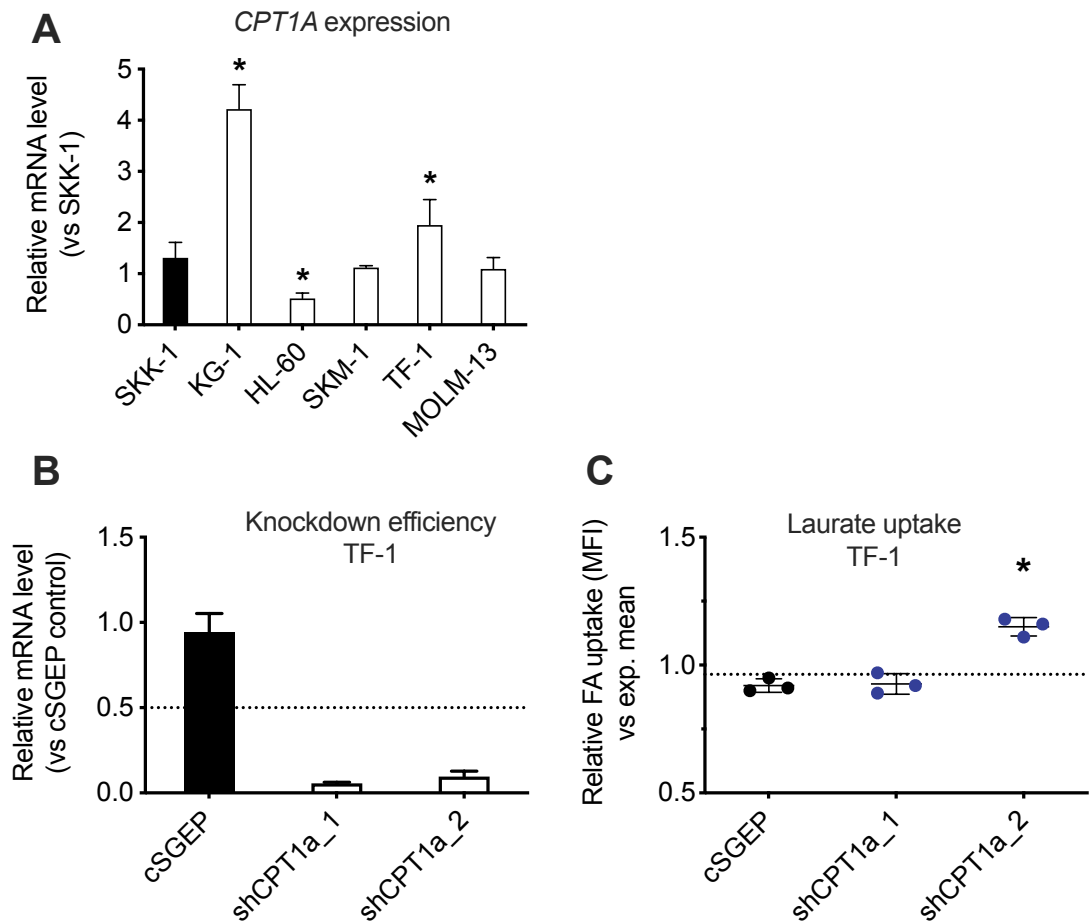


Figure 24: CPT1a knockdown in TF-1 cells does not reduce fatty acid uptake. A) RT-qPCR shows relative mRNA expression (versus SKK-1 cells) of CPT1a in six MDS and AML cell lines (SKK-1, KG-1, HL-60, SKM-1, TF-1 and MOLM-13). * $p < 0.05$ (one way ANOVA). B) RT-qPCR shows relative mRNA expression (versus cSGEP control vector) following single gene knock down using two shRNAs targeting CPT1a in TF-1. Values were normalised to the housekeeping gene GAPDH. Results are presented as the mean \pm standard deviation ($n = 3$). Dotted line represents 50% knockdown effect. C) Plot representing uptake of fluorescence-labelled laurate in TF-1 cells knocked down with two CPT1a shRNAs. Results are expressed as median fluorescence intensity relative to the experimental mean (dotted line represents mean of MFIs across all measurements; $n=3$). Fatty acid uptake in the knocked down cells was compared to TF-1::cSGEP control vector. * $p < 0.05$ (one way ANOVA).

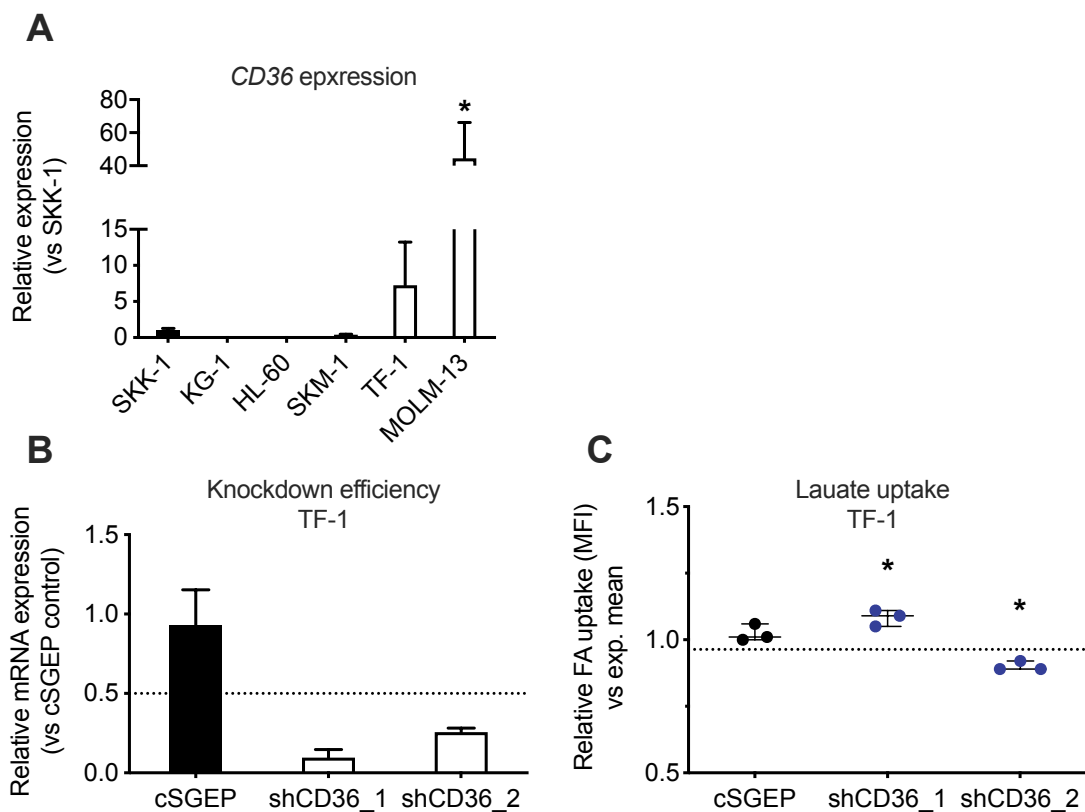


Figure 25: CD36 knockdown in highly expressing TF-1 cells has inconsistent effects on FA uptake. A) RT-qPCR shows relative mRNA expression (versus SKK-1 cells) of CD36 in six MDS and AML cell lines (SKK-1, KG-1, HL-60, SKM-1, TF-1 and MOLM-13). * $p < 0.05$ (one way ANOVA). B) RT-qPCR shows relative mRNA expression (versus cSGEP control vector) following single gene knock down using two shRNAs targeting CD36 in TF-1. Values were normalised to the housekeeping gene GAPDH. Results are presented as the mean \pm standard deviation ($n = 3$). Dotted line represents 50% knockdown effect. C) Plot representing uptake of fluorescence-labelled laurate in TF-1 cells knocked down with two CD36 shRNAs. Results are expressed as median fluorescence intensity relative to the experimental mean (dotted line represents mean of MFIs across all measurements). Fatty acid uptake in the knocked down cells was compared to TF-1::cSGEP control vector. * $p < 0.05$ (one way ANOVA).

Among the high uptake-associated knockdowns, all but one (shTET_1) had a mean knockdown effect of greater than 50% in SKK-1 cells (**Figure 26A**). Compared to the cSGEP control, shPADI4_2, shBAZ1b_1, and the controls, shSIRT1 and shSIRT1_2, trended towards increased fatty acid uptake (**Figure 26B**). However, only shPADI4_2 was associated with a statistically significant difference in fatty acid uptake.

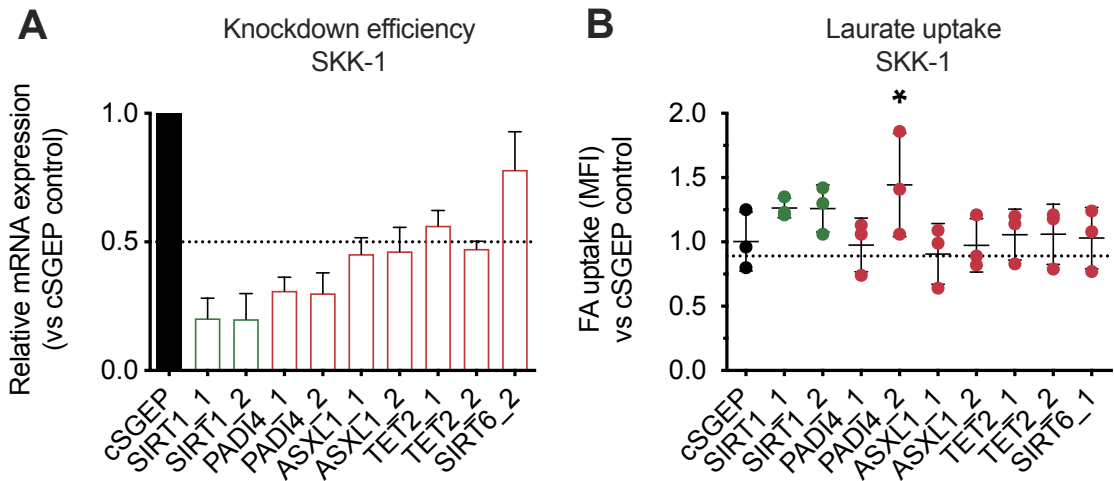


Figure 26: Evaluation of knockdown efficiencies and fatty acid uptake following single gene knockdown of selected high fatty acid uptake-associated hits from the shRNA knockdown screen in SKK-1 cells. A) RT-qPCR shows relative mRNA expression (versus cSGEP control vector) of knocked down genes relating to high fatty acid uptake-associated hairpins (in red) and a knockdown control targeting the positive regulator of fatty acid oxidation, SIRT1 (in green). Values were normalised to the housekeeping gene GAPDH. Results are presented as the mean \pm standard deviation ($n = 3$). Dotted line represents 50% knockdown effect. B) To assess the effect of the knockdowns on fatty acid uptake, SKK-1 cells knocked down with high fatty acid uptake-associated hairpins were incubated with fluorescent BODIPY-labelled 0.5 μ M laurate for 60 minutes, washed and uptake was assessed by flow cytometry. FA (fatty acid) uptake results are compared to the SKK-1::cSGEP control vector and expressed as median fluorescence intensity (MFI) relative to the experimental mean (dotted line represents mean of MFIs across all measurements; $n = 3$). $p < 0.05$ (one way ANOVA).

Overall, a mixed picture emerges from the fatty acid uptake validation assays and the predicted phenotypes following the knockdowns. PADI4 was chosen for further analysis as we found one of its hairpins to have the greatest effect on fatty acid uptake among the candidate hits from the genetic screen when knocked down in SKK-1. Importantly, a second hairpin targeting PADI4 had no effect on fatty acid uptake indicating that we need to consider the possibility of unwanted off-target effects that might create or neutralize the phenotype of interest.

5.9 PADI4 validation

Since the effect of PADI4 gene knockdown caused only a mild increase in laurate uptake in SKK-1 cells, we decided to investigate if PADI4 gene expression in other AML cell lines was greater, therefore potentially eliciting a greater phenotypic response when knocked down. Indeed, KG-1 and TF-1 showed approximately 20-40 times more *PADI4* expression on the mRNA level compared to SKK-1 (**Figure 27A**). Therefore, we performed *PADI4* gene knockdowns in KG-1 and TF-1 cells using the same short hairpins as used for SKK-1. Knockdown effects for the two short hairpins were greater in KG-1 than TF-1 where the knockdown effect was less than 50% (**Figure 27B** and **Figure 27D**). As was observed in the shCD36 knocked down TF-1 cells, the two PADI4 hairpins caused opposing fatty acid uptake profiles in TF-1 cells: the shPADI4_1 caused slightly lower, but not significant, laurate uptake, while shPADI4_2 caused significantly higher fatty acid uptake (**Figure 27C**). Although we saw an upward trend in fatty acid uptake in shPADI4 knockdown KG-1 cells, the difference versus cSGEP control was not significant (**Figure 27E**).

Overall, like we saw in the previous knockdowns, the effect on fatty acid uptake phenotype following *PADI4* knockdown was mild and hairpin-dependent. However, we observed significant increases in laurate uptake in SKK-1 and TF-1 knocked down with shPADI4_2.

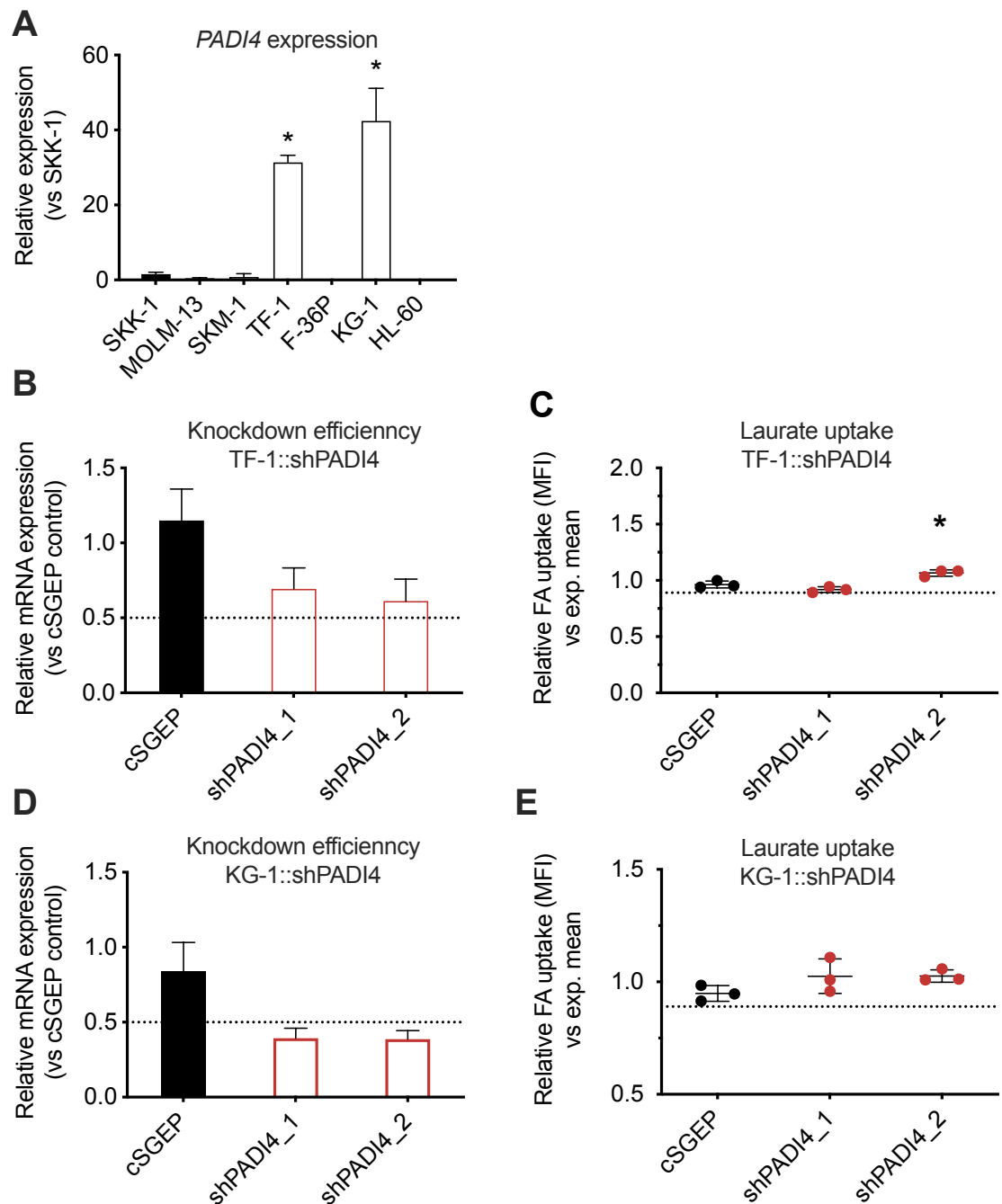


Figure 27: PADI4 expression is highest in TF-1 and KG-1 among MDS and AML cell lines with slight increase in fatty acid uptake when PADI4 is knocked down. Evaluation of PADI4 expression across different MDS and AML cell lines, knockdown efficiencies and fatty acid uptake following shRNA transfections in TF-1 and KG-1 cell lines. A) RT-qPCR shows relative mRNA expression (versus SKK-1 cells) of PADI4 in seven MDS and AML cell lines (SKK-1, MOLM-13, SKM-1, TF-1, F36-P, KG-1, and HL-60) following single gene. * $p < 0.05$ (one way ANOVA). RT-qPCR shows relative mRNA expression (versus cSGEP control vector) following single gene knock down using two shRNAs targeting in B) TF-1 and D) KG-1. Values were normalised to the housekeeping gene GAPDH. Results are presented as the mean \pm standard deviation ($n = 3$). Dotted line represents 50% knockdown effect. Plot representing uptake of fluorescence-labelled laurate in C) TF-1 and E) KG-1 cells knocked down with two PADI4 shRNAs. Results are expressed as median fluorescence intensity relative to the experimental mean (Dotted line represents mean of MFIs across all measurements). In each case, fatty acid uptake in the knocked down cells was compared to TF-1::cSGEP or KG-1::cSGEP controls. * $p < 0.05$ (one way ANOVA).

5.10 PADI4 inhibition

Although short hairpin knockdowns of *PADI4* in SKK-1, TF-1 and KG-1 cells showed indications that laurate uptake was being increased, we could not observe a clear and consistent phenotype. For this reason, we decided to use an orthogonal method of PADI4 inhibition that was not involving hairpins. Specifically, we wanted to see if non-lethal doses of a PADI4-specific pharmacological inhibitor would cause an increased uptake phenotype by reducing the activity of PADI4, as was originally predicted with the short hairpins. We performed a dose response curve of the PADI4 inhibitor, GSK484, across a broad concentration range in SKK-1, TF-1 and KG-1 cells. From this, a non-lethal dose of the compound was established, i.e. the concentration at which cell viability was not affected. Using DAPI and MitoTracker as markers of live cells, we established 12.5 μ M as the non-lethal dose concentration for GSK484 across all three cell lines (**Figure 28A**). Following treatment with GSK484, we found that laurate uptake increased in SKK-1 and TF-1, the two cell lines in which PADI4 inhibition by gene knockdown caused significantly increased fatty acid uptake (**Figure 28B**). Taken together, treatment with GSK484 - the most potent and specific inhibitor of PADI4 - was associated with a positive effect on laurate uptake in SKK-1 and TF-1 cells without affecting cell viability.

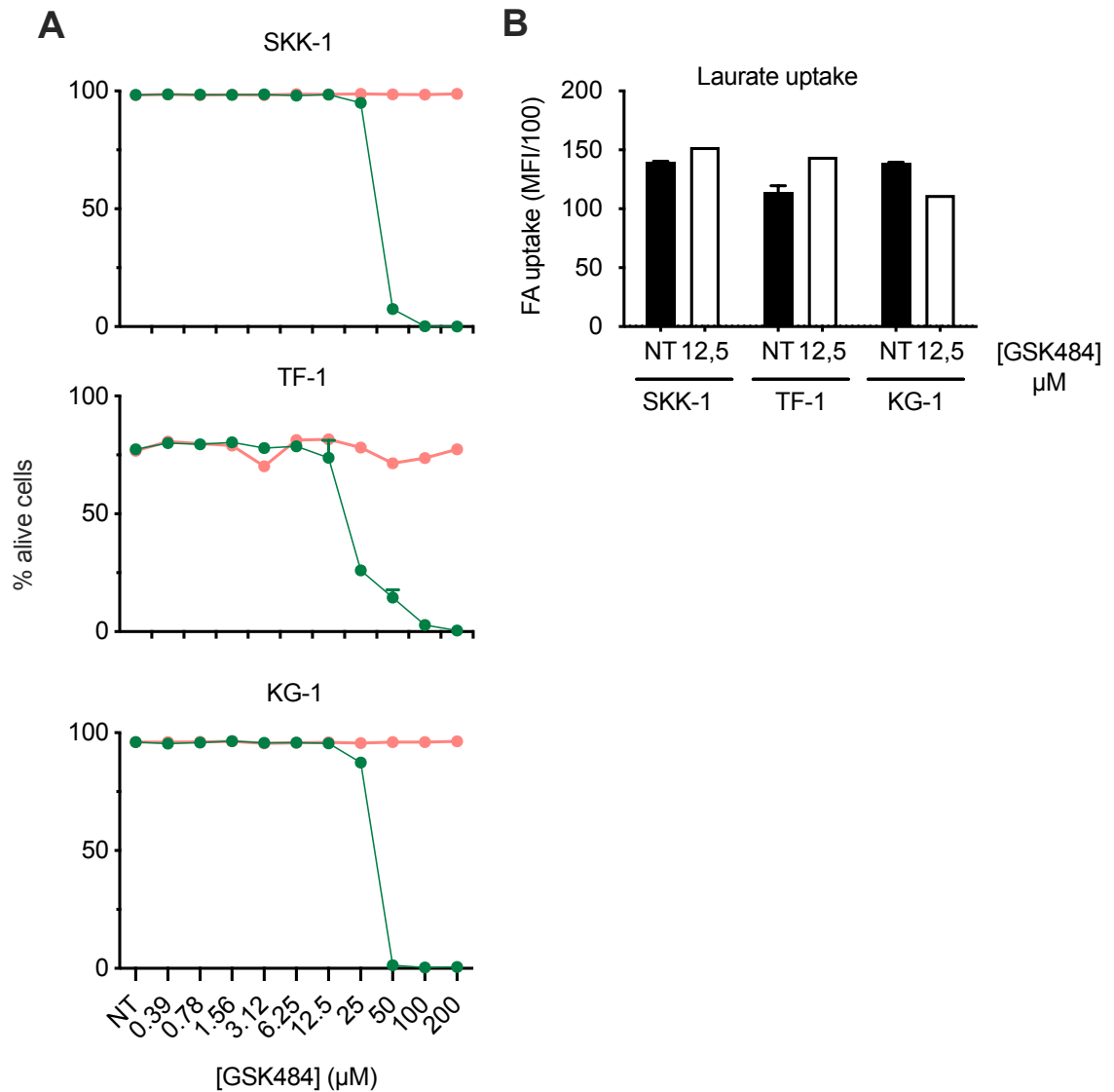


Figure 28: GSK484 treatment is associated with increased laurate fatty acid uptake in SKK-1 and TF-1 but not KG-1 cells. A) Dose response curves for SKK-1, TF-1, and KG-1 cells treated with various concentrations of GSK484 (0-200 μM). Graph depicts alive cells (%) against each of the drug concentrations, as calculated from DAPI and MitoTracker staining. Data points are mean values \pm standard deviation for $n=2$. Green and red points represent treated cells and DMSO vehicle controls, respectively. B) Plot representing uptake of fluorescence-labelled laurate in SKK-1, TF-1 and KG-1 cells treated with 12.5 μM GSK484 and non-treatment with DMSO alone (NT). Fatty acid (FA) uptake results are expressed as median fluorescence intensity (MFI/100). NT results are presented as the mean \pm standard deviation ($n = 2$) and single measurements of the treated samples were taken.

5.11 PADI4 and ATRA-induced differentiation

Next, we wanted to check if increased *PADI4* expression might be associated with lower fatty acid uptake. Thus, we used an established protocol for differentiating the myeloblastic cell line, HL-60, to granulocyte-like cells (Song et al., 2016), to investigate whether *PADI4* expression and, by extension, fatty acid uptake were affected.

CD38 cell surface marker expression was used as a marker of differentiation over the three-day treatment with all-trans retinoic acid (ATRA). Indeed, CD38 expression increased relative to the vehicle control indicating progression of differentiation (**Figure 29A**). In parallel, we measured *PADI4* expression levels, which increased as differentiation progressed (**Figure 29B**). In addition, we measured fatty acid uptake in both the DMSO control and ATRA-treated HL-60 cells. We found that the ATRA-treated cells took up significantly less fatty acids than the DMSO controls during the course of the differentiation protocol. Taken together, we saw a correlation between increased *PADI4* expression and reduced fatty acid uptake in differentiated HL-60 cells.

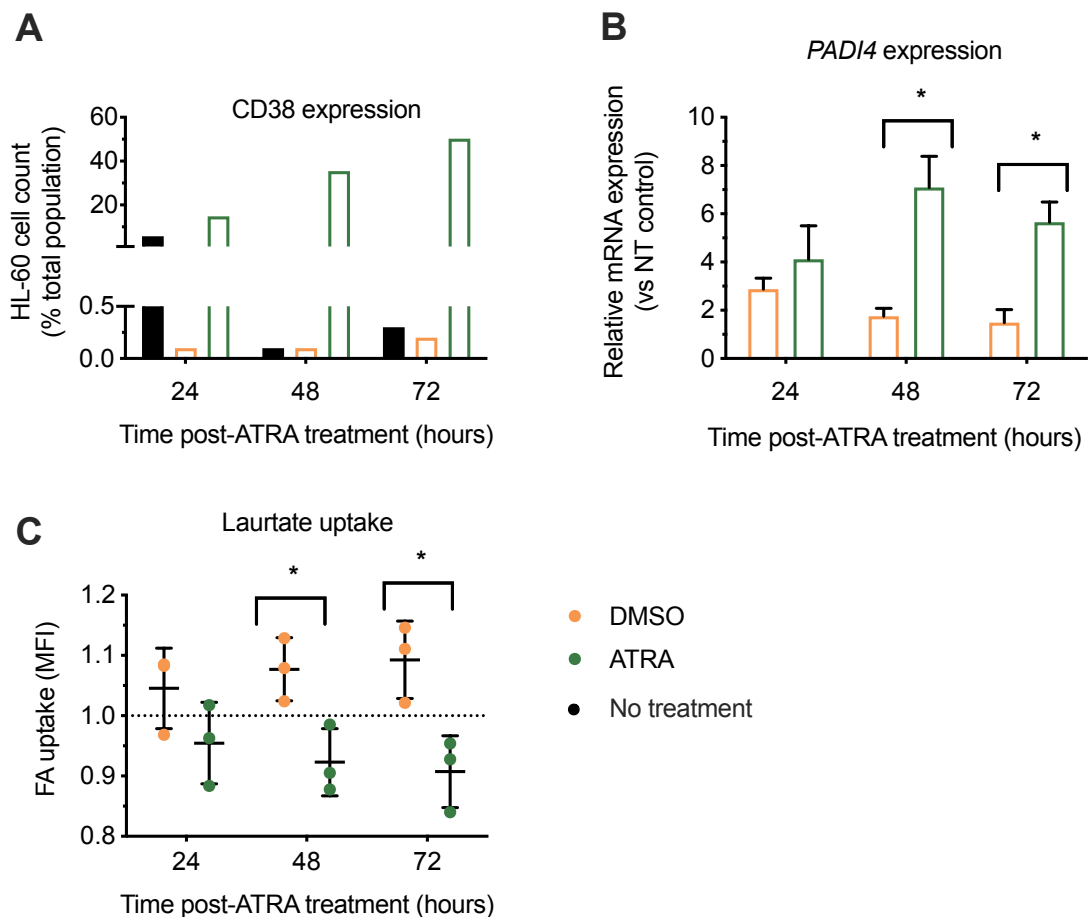


Figure 29: ATRA-induced differentiation of HL-60 is associated with increased *PADI4* expression. A) Bar plot shows CD38 expression of non-treated (NT), DMSO vehicle-treated, and all trans retinoic acid-treated (ATRA) HL-60 cells over the course of 72 hours post-ATRA treatment, as measured by flow cytometry. B) RT-qPCR shows relative mRNA expression of *PADI4* in ATRA-treated HL-60 cells (versus DMSO-treated cells) over the course of 72 hours. Values were normalised to the housekeeping gene GAPDH. Results are presented as the mean \pm standard deviation ($n = 3$). C) Plot representing uptake of fluorescence-labelled laurate in DMSO- and ATRA-treated HL-60 cells treated. FA (fatty acid) uptake results are compared to the DMSO-treated HL-60 cells and expressed as median fluorescence intensity (MFI) relative to the experimental mean (mean of MFIs across all measurements; $n = 3$). * $p < 0.05$ (multiple T test).

5.12 Conclusion

Taken all together, by combining a genetic loss-of-function screen with fatty acid uptake as a read-out for metabolic activity, we were able to rank 912 tested genes based on the representation of hairpin-containing clones in cell populations with different uptake capacities. The validation of several selected hits failed. The only exception was *PADI4* for which some genetic and pharmacologic inhibitions indicated a possible positive influence on fatty acid uptake. The impact of *PADI4* inhibition was mild and variable between cell lines and different hairpins. As such we have decided to not pursue the analysis of *PADI4* further in the context of fatty acid metabolism.

6. Results II: Fatty acid uptake phenotype

6.1 Chapter summary

Fatty acid metabolism has gained increasing interest in haematological diseases in recent years as a means to uncover LSC-specific vulnerabilities. In parallel to our shRNA knockdown screen, we decided to characterise our low and high uptake sub-populations of sorted SKK-1 cells. After three rounds of sorting we noticed that SKK-1 cells retained their low and high fatty acid uptake capacities over time. We therefore wanted to metabolically and genetically characterise these sub-populations to investigate the factors that contribute to their distinct phenotypes.

6.2 SKK-1 cells retain fatty acid uptake capacity after three rounds of cell sorting

Following optimisation of the fatty acid uptake assay for separating low and high fatty acid uptake cells for the shRNA knockdown screen, we wondered whether different uptake capacities of the cell populations would revert to those of the parental populations or remain stable. Therefore, we decided to test if the cells could be phenotypically separated based on their fatty acid uptake capacity. For this, we separated the lowest and highest 10% fatty acid uptake populations in SKK-1, SKM-1 and THP-1 cells by cell sorting. In the case of SKK-1 cells, we carried out three rounds of cell sorting based on palmitate uptake (**Figure 30**).

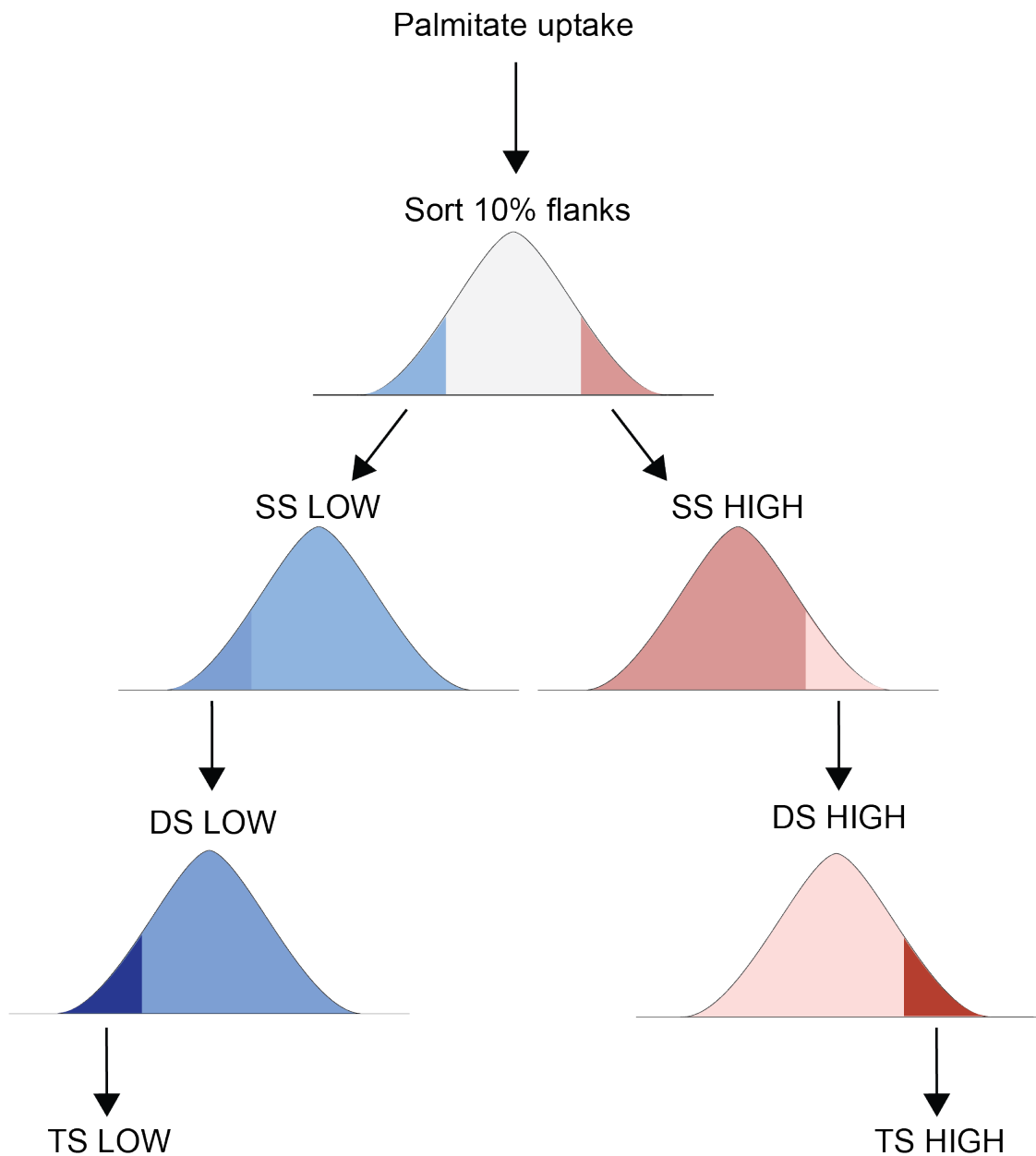


Figure 30: Schematic of the three rounds of FACS for separating SKK-1 cells based on fatty acid uptake. Three rounds of sorting were carried out for the characterisation of TS LOW and TS HIGH. SKK-1 cells were incubated with fluorescence-labelled palmitate after which the lowest and highest 10% sub-populations were sorted based on fatty acid uptake to yield single-sorted low (SS LOW) and single-sorted high (SS HIGH). Subsequent rounds of sorted yielded double-sorted LOW (DS LOW) and double-sorted HIGH (DS HIGH), and finally triple-sorted LOW (TS LOW) and triple-sorted HIGH (TS HIGH).

After each round, cells were grown in culture and their palmitate uptake was re-analyzed. When we re-analysed sorted cells after two rounds of sorting another week in culture, the two separated low and high uptake SKK-1 populations retained substantially different capacities to take up palmitate (**Figure 31A**). We observed a lesser uptake difference in SKM-1 and no difference in THP-1 cells (**Figure 31A**). Curious to understand the nature of the particular behaviour of SKK-1 cells, we carried out two subsequent rounds of sorting repeatedly isolating the 10% cells with lowest and highest fatty acid uptake capacity. We denoted these 'triple-sorted' populations as TS LOW and TS HIGH. Following one week of culture after the third sort, the difference between TS LOW and TS HIGH was in a similar range as single-sorted cells (

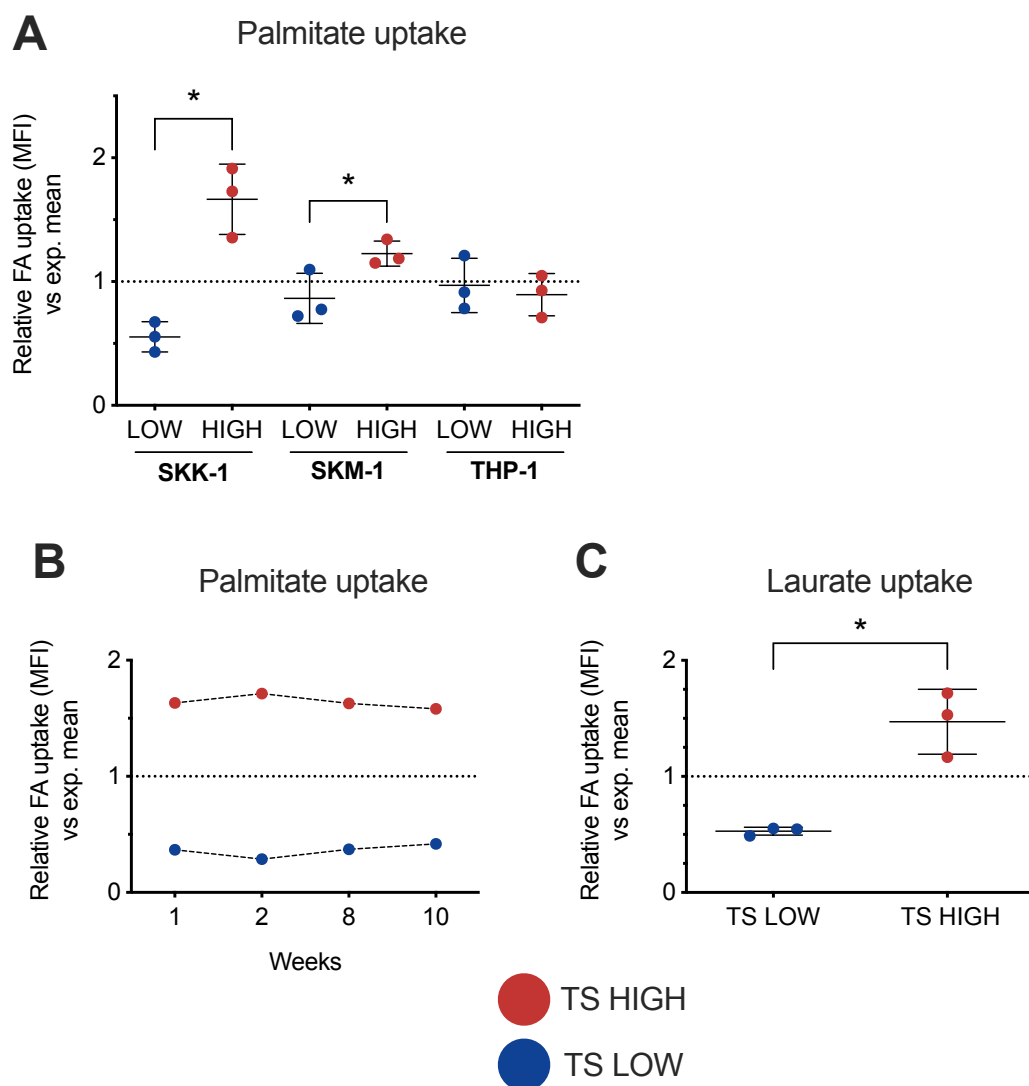


Figure 31B). Over a period of 10 weeks, we observed that the respective uptake capacities of TS LOW and TS HIGH were retained (**Figure 31C**). We confirmed similar phenotypic differences in TS LOW and TS HIGH cells upon exposure to the medium chain fatty acid laurate (**Figure 31C**). Taken together, these results suggested that the MDS/AML

| Results II

cell line SKK-1 contains sub-populations of cells with distinct and stable metabolic properties.

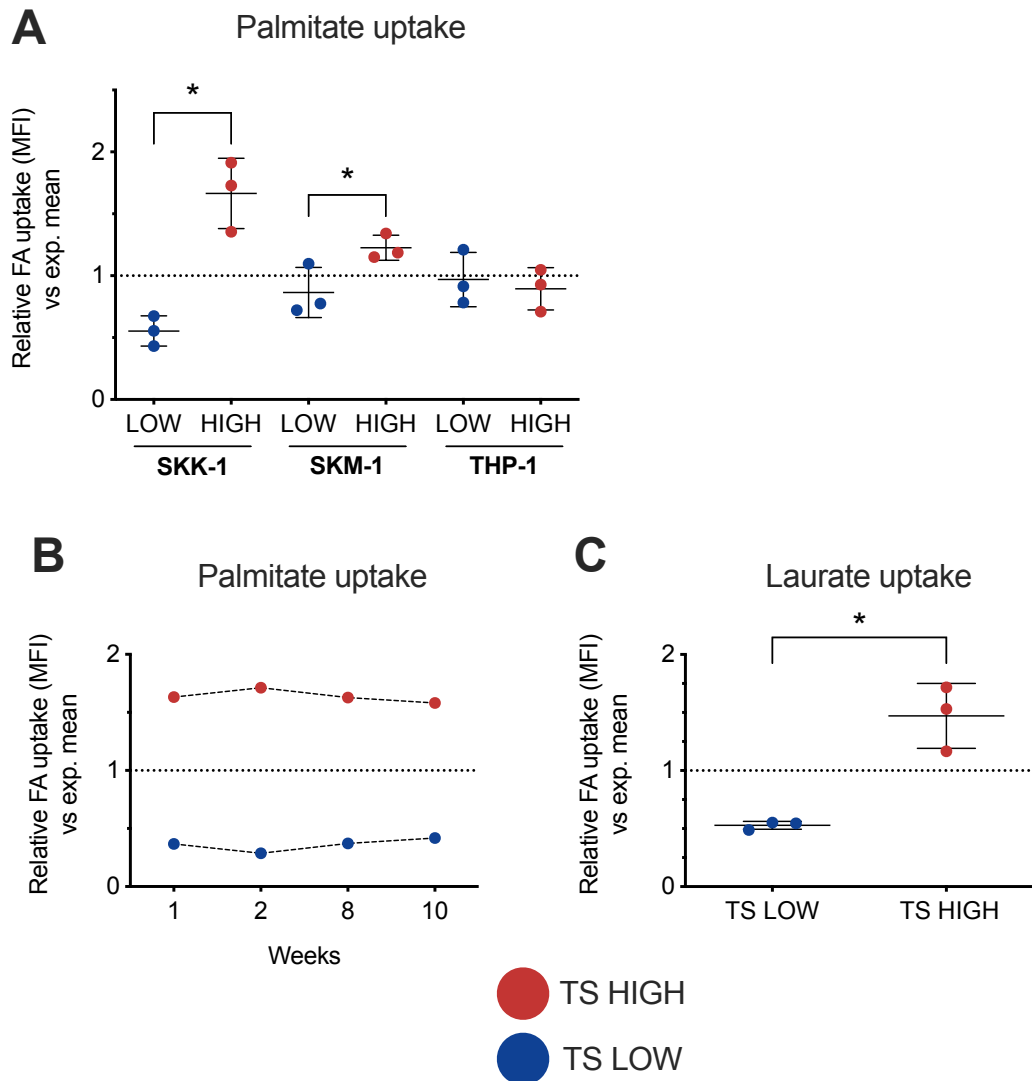


Figure 31: SKK-1 cells can be separated into two stable sub-populations with differential fatty acid uptake capacity. A) Graph represents uptake of fluorescence-labelled palmitate in double-sorted SKK-1, SKM-1 and THP-1 cells. After incubation with 0.5 μ M BODIPY-labelled palmitate for 60 min, 10% of cells with lowest and highest intracellular fluorescence intensity were isolated by cell sorting. After one week in culture, the fatty acid uptake capacity of cells was re-analyzed during three consecutive days using the same conditions. Data shown are the median fluorescence intensities (MFI) of individual experiments ($n = 3$) normalized to the experimental mean of all experiments (dotted line), vertical bars indicate standard deviation. * $p < 0.05$ (paired t-test). (B) The palmitate uptake capacity of triple-sorted low uptake SKK-1 (TS LOW) and triple-sorted high uptake SKK-1 (TS HIGH) cells was analyzed as in (D) at indicated time points. Data shown are the MFIs of individual experiments normalized to the mean of each experiment (dotted line). (C) TS LOW and TS HIGH cells show similar uptake behaviour with a medium chain fatty acid. Cells were analysed after incubation with 0.5 μ M BODIPY-labeled laurate for 60 mins. Data are from three independent measurements and plotted as in (D). * $p < 0.05$ (paired t-test).

6.3 TS LOW and TS HIGH display subtle differences in mitochondrial respiratory capacity

As fatty acids are ultimately transported to the mitochondria where fatty acid oxidation takes place, we decided to characterise mitochondrial function in TS LOW and TS HIGH cells by performing high-resolution respirometry. The respiratory capacity of SKK-1 cells compared to liver-derived HepG2 cells and adipose tissue was found to be generally low (figure) (Cantó, 2015; Jeger, 2015). While TS LOW and TS HIGH were similar in routine (basal respiration), proton leak and residual oxygen consumption, TS HIGH displayed an elevated maximal respiratory capacity of the electron transport system (**Figure 32A**). Since alterations in mitochondrial content could account for the difference in maximal respiratory capacity between TS LOW and TS HIGH, we investigated mitochondrial content based on the ratio of mitochondrial and nuclear DNA. However, we did not observe mitochondrial content to differ significantly between the two cell populations (**Figure 32B**).

To further compare mitochondrial activity in TS LOW and TS HIGH, we analysed mitochondrial complex expression on the levels of both mRNA and protein. Surprisingly, we observed higher transcriptional and protein expression of complex IV (MTCO₁) in TS LOW (**Figure 32C**).

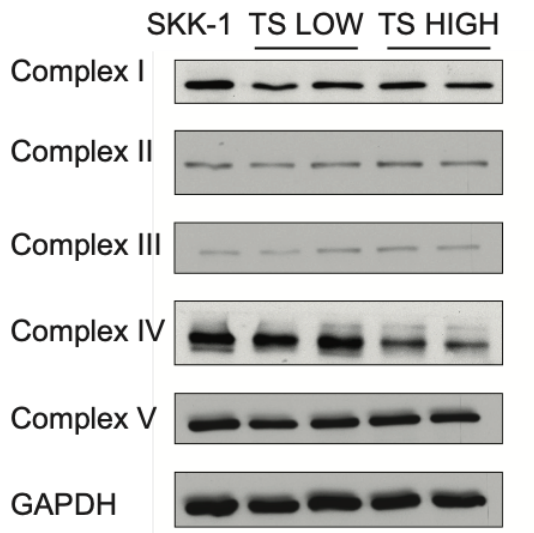
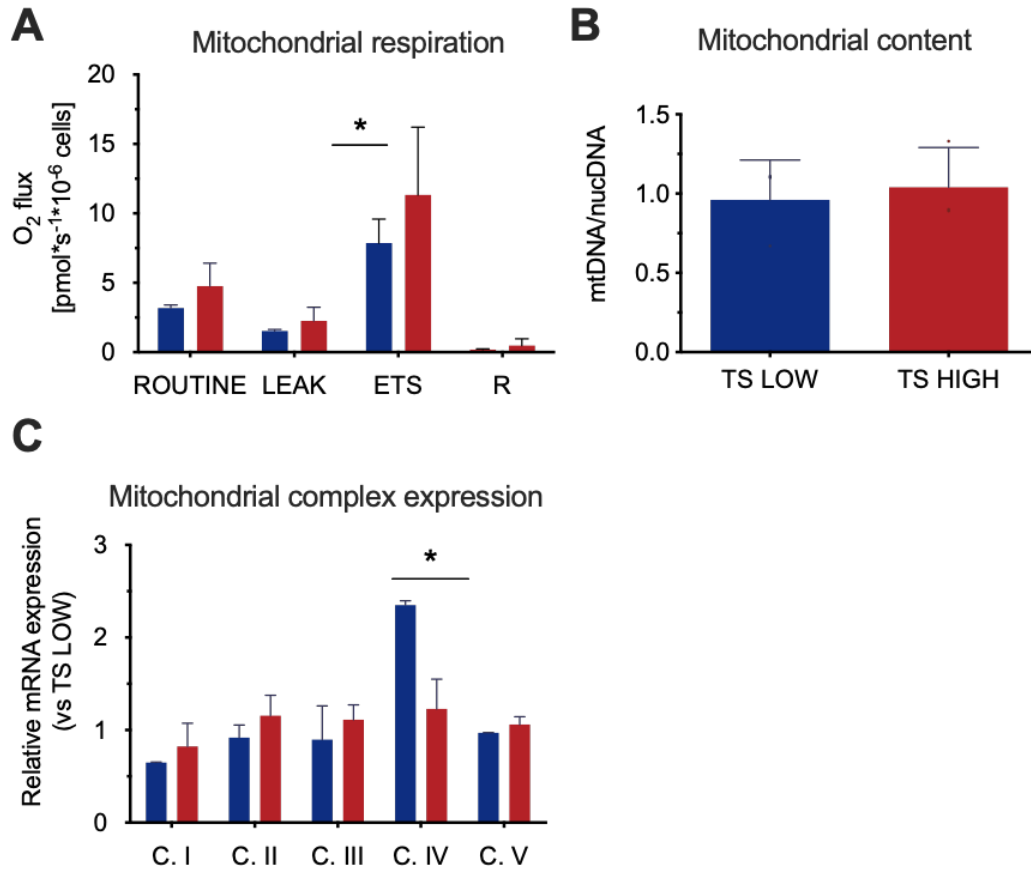


Figure 32: Subtle differences are observed in mitochondrial respiration between TS LOW and TS HIGH. A) The oxygen consumption of TS LOW and TS HIGH cells was measured by high-resolution respirometry. Basal respiration (Routine), proton leak (Leak), maximal respiratory capacity of the electron transport chain (ETS) and residual oxygen consumption (ROX) were analyzed by the sequential addition of oligomycin (1.25 μM), FCCP (3 μM) and rotenone/antimycin A (0.5 μM and 5 μM , respectively). Data are represented as the mean of six measurements taken on three separate days for each cell line, vertical bars indicate standard deviation. * $p < 0.05$ (two-way ANOVA). B) Relative mitochondrial content was measured as the ratio of expression of the mitochondrial DNA-encoded (mtDNA) MT-CYB gene and nuclear DNA-encoded (nucDNA) APP gene as determined by semi-quantitative PCR. Error bars indicate standard deviation of three independent experiments. C) RT-qPCR shows relative mRNA expression of mitochondrial OXPHOS respiratory complexes (complexes I, II, III, IV and V) in TS LOW and TS HIGH. Values were normalised to the housekeeping gene GAPDH. Results are presented as the mean \pm standard deviation ($n = 3$). * $p < 0.05$ (one-way ANOVA). D) Western blot image of mitochondrial OXPHOS respiratory complex and GAPDH expression in SKK-1, TS LOW and TS HIGH cells. Individual antibodies comprising the following sub-units of respiratory complex proteins were used: ubiquinone oxidoreductase subunit A9 (complex I), succinate dehydrogenase complex flavoprotein subunit A (complex II), ubiquinol-cytochrome C reductase core protein (complex III), cytochrome c oxidase subunit I (complex IV) and ATP synthase F₁ subunit alpha (complex V). GAPDH was used as loading control.

| Results II

When looking at lipid metabolism gene expression, we found that genes encoding the mitochondrial membrane-bound fatty acid transporters, *CPT1a* and *CPT2*, and the positive activator of fatty acid oxidation, *PPARA*, were up-regulated in TS HIGH (**Figure 33**). Taking into account our earlier observation of ETX-mediated inhibition of fatty acid uptake (**Figure 12**), overall these results suggest that the transport of fatty acids into mitochondria promotes cellular fatty acid uptake. TS LOW and TS HIGH have a similar mitochondria content. TS HIGH cells displayed a subtle increase in maximal respiratory capacity, despite higher complex IV expression in TS LOW that could have been indicative of a higher capacity to generate ATP.

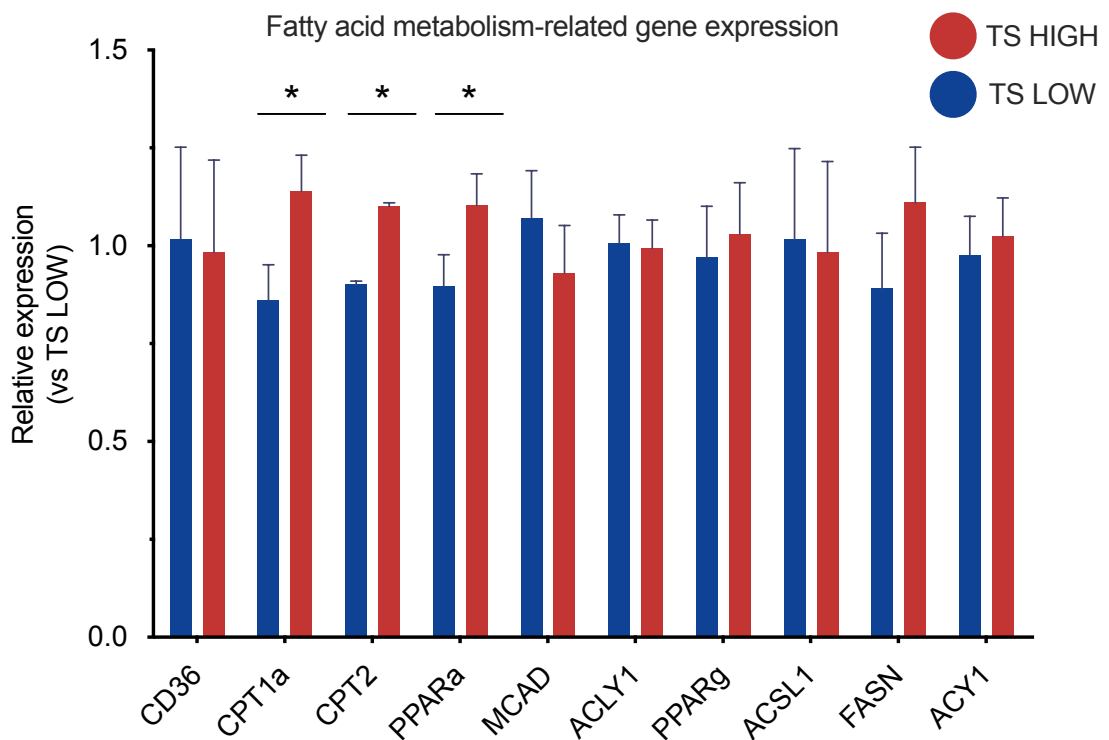


Figure 33: Gene expression of mitochondrial fatty acid transporters and a fatty acid oxidation regulator is up-regulated in TS HIGH. RT-qPCR shows relative mRNA expression of lipid metabolism-related genes in TS LOW and TS HIGH. Values were normalised to the housekeeping gene GAPDH. Results are presented as the mean \pm standard deviation ($n = 3$). Lipid metabolism genes analysed: fatty acid translocase (CD36), carnitine palmitoyltransferase 1A (CPT1a), carnitine palmitoyltransferase 2, (CPT2), peroxisome proliferator-activated receptor alpha (PPAR α), medium-chain acyl-CoA dehydrogenase (MCAD), ATP-citrate synthase 1 (ACLY1), peroxisome proliferator-activated receptor gamma (PPAR γ), acyl-CoA synthetase, long chain family member 1 (ACSL1), fatty acid synthetase (FASN) and aminoacylase-1 (ACY1). * $p < 0.05$ (student's t-test).

6.4 No significant differences in cell cycle or cell proliferation in TS LOW and TS HIGH

After we observed subtle differences in mitochondrial respiration in TS LOW and TS HIGH, we wanted to see if this translated to differences in cell cycle or proliferation. Cell cycle did not differ when measured as a function of DNA content (**Figure 34A**). Ki67 expression is used as a measure of cells' proliferation capacity, however we did not observe any significant differences (**Figure 34B**). Finally, we examined colony forming units (CFU) as a means to estimate proliferation capacity of the cells. The methylcellulose assay is a means of determining the ability of HSC and progenitors to proliferate and differentiate into colonies. The colonies were enumerated. The morphology of the colonies was uniform. Again, CFUs did not differ between the two cell populations (**Figure 34C**). These results indicate that TS LOW and TS HIGH proliferate at similar rates, despite observable differences in mitochondrial respiration.

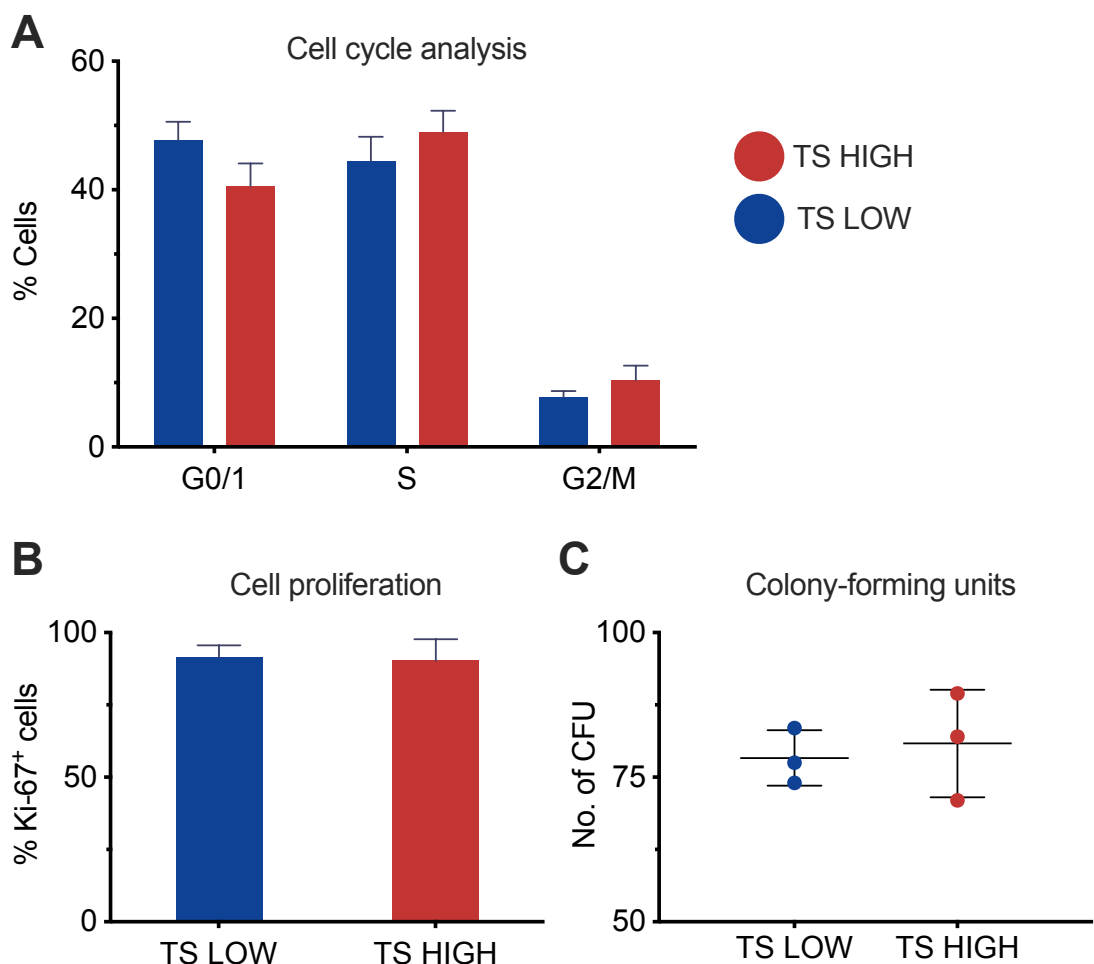


Figure 34: No significant differences in cell cycle or cell proliferation between TS LOW and TS HIGH. A) Cell cycle analysis of TS LOW and TS HIGH, as calculated using the univariate cell cycle model in FlowJo software (version). Bar plots represent the percentage of total cells in G₀/1, S and G₂/M cell cycle phases. Cells were stained with DAPI and analysed by flow cytometry (n=3). B) Bar plot represents Ki67 expression in TS LOW and TS HIGH expressed as percentage of total Ki67-expressing cells, as measured by flow cytometry (n=3). C) Plot represents colony-forming units (CFU) from TS LOW and TS HIGH following 14 days growth in methylcellulose media (n=3). The CFU assay was performed to measure cells' proliferation capacity.

6.5 Genes related to tyrosine kinase receptor pathways are up-regulated in TS LOW

Next, we investigated whether the metabolic differences between TS LOW and TS HIGH would be associated with transcriptional and genetic differences. We analysed genome-wide gene transcription with massive parallel sequencing of mRNA extracted from three replicates of TS LOW and TS HIGH cells. A principal component analysis of the data showed a high percentage of variance (76%) between TS LOW and TS HIGH samples along the first principal component (PC₁) (**Figure 35A**). Our transcriptomic analysis using DESeq2 (Love et al., 2014) revealed a total of 855 differentially expressed genes based on a log₂ fold-change cut-off of 2 and p-value equal or below 0.05. Of these, 789 genes were up-regulated in TS LOW and 66 were down-regulated compared to TS HIGH (**Figure 35B** and **Figure 35C**). To get an overview of the biological functions of differentially expressed genes, we performed a gene ontology (GO) enrichment analysis with the lists of significantly up- and down-regulated genes with log₂ fold-changes of equal or greater to 2. GO terms over-represented among up-regulated genes in TS LOW related to cell surface signalling pathways and, in particular, signalling through receptor tyrosine kinase (**Figure 35D**). Among the up-regulated genes of this GO term were several members of the FLT family, the fibroblast growth factor receptors, *FGFR1* and *FGFR2*, and the key regulator of myeloid progenitor cells, *KIT* (**Figure 35D**). Down-regulated GO terms included genes relating to long chain fatty acid transport and the immunological activation of several myeloid lineage cells (**Figure 35D**). Differentially expressed genes associated with fatty acid transport included genes encoding the regulatory transcription factor of fatty acid oxidation *PPAR γ* ; the lipid droplet membrane-associated, *PLIN2*; and the long chain fatty acid lipase, *ACSL1* (**Figure 35E**).

Taken together, our expression analysis identified a number of fatty acid transport-related genes higher expressed in TS HIGH cells that are likely to contribute to the metabolic difference between both cell populations. In addition, we found that lower capacity to take up fatty acids was associated with higher expression of genes encoding receptor tyrosine

kinases, an indicator of increased aggressiveness in leukaemia. Notably, the number of differentially expressed genes was heavily skewed towards higher expression in TS LOW. Further, the number of differentially expressed genes were over-represented on chromosome 19 in TS LOW compared to the expected, suggesting chromosomal differences between TS LOW and TS HIGH may exist (**Figure 36**).

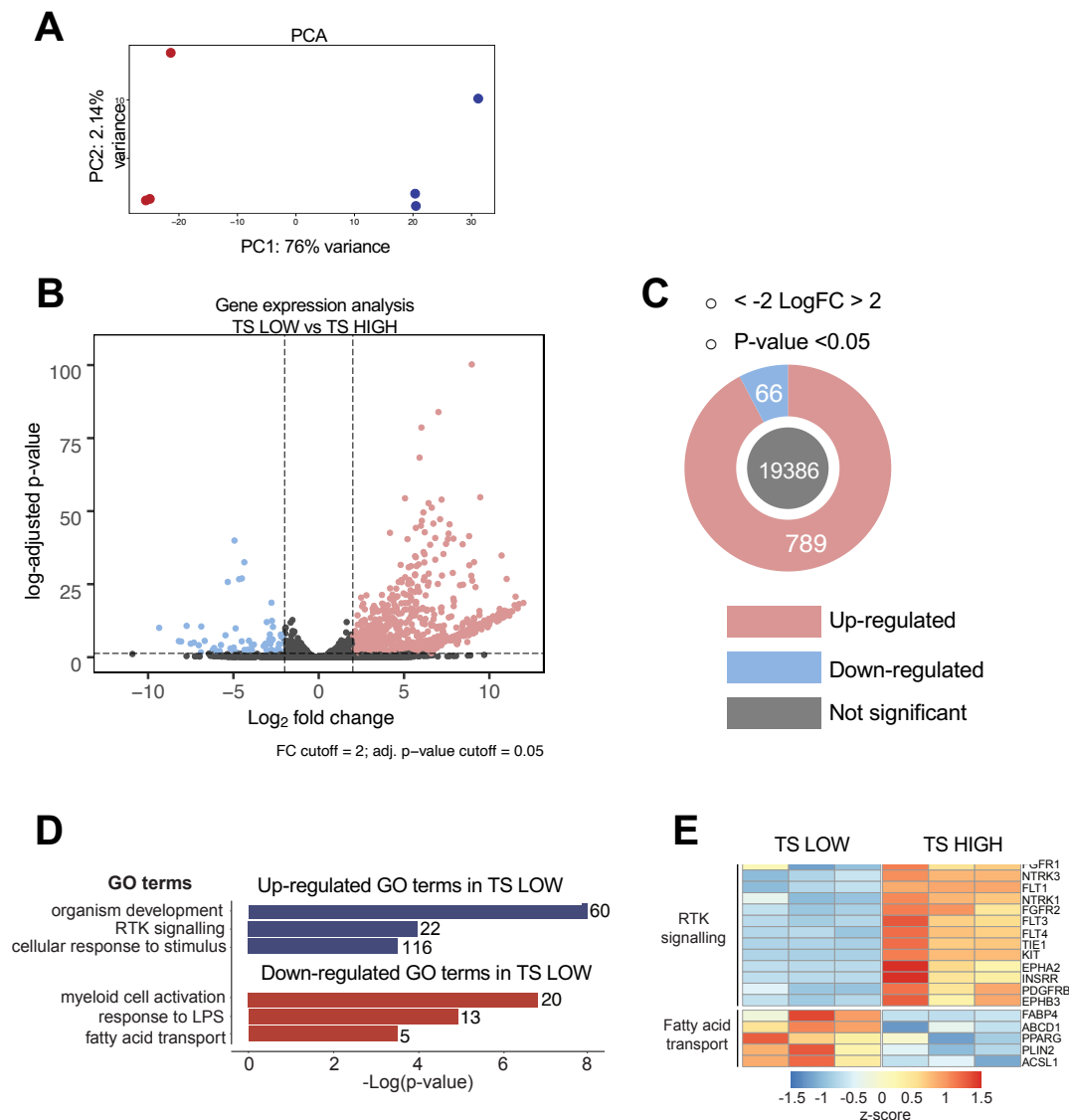


Figure 35: RNA-seq and GO analysis reveal differentially expressed genes (DEGs) in TS LOW and TS HIGH. A) Principal component analysis (PCA) scatter plot of log-transformed normalised RNA-seq data transcripts in TS LOW and TS HIGH. PCA plot shows variance of the three biological replicates of each of the two cell lines. The percentages on each axis represent the percentages of variation explained by the principal components. B) Volcano plot showing differential gene expression between TS LOW and TS HIGH, with fold difference between log₂ normalised expression in TS LOW (n=3) and TS HIGH (n=3) plotted versus log-adjusted p-value. Horizontal dashed line defines the significance threshold (p-value<0.05) and vertical dashed lines define the +2 and -2 log₂ fold-change. C) Significant differentially expressed genes are highlighted in red (789 up-regulated in TS LOW) and blue (66 down-regulated in TS LOW). D) Gene ontology analysis for up- and down-regulated genes in TS LOW, with associated -log p-values and the number of genes per biological process. Significant terms included up-regulated in TS LOW receptor tyrosine kinase signalling pathway (GO:007169) and down-regulated long-chain fatty acid transport (GO:0015909). E) Expression heat map of sample-to-sample distances. Displayed are genes relating to the gene ontology terms long chain fatty acid transport and a selection of genes from receptor tyrosine kinase signalling pathway.

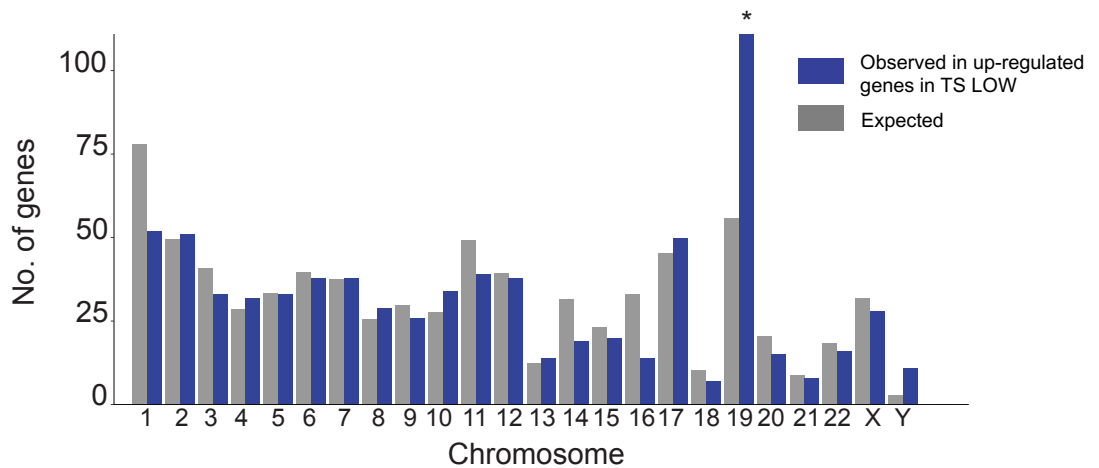


Figure 36: Significantly increased gene expression on chromosome 19 in TS LOW. Bar plots represent the distribution of up-regulated genes in TS LOW (versus TS HIGH) on each chromosome, as calculated from RNA-seq analysis. The number of differentially expressed genes on chromosome 19 is significantly different than the expected number of genes. Chi-square test; * $p < 0.005$.

6.6 Stem cell markers are expressed in TS LOW

We found KIT to be one of the top up-regulated genes in TS LOW. KIT protein (also called CD117) is involved in stem cell maintenance and differentiation and in the activation of a number of metabolism-related regulatory pathways (as reviewed in Foster et al., 2018). In the context of haematology, the protein is known as CD117 and serves as an important myeloid stem cell marker. Thus, we decided to further investigate KIT for its association with low fatty acid uptake. Using PCR of cDNA, we confirmed the increased expression of CD117 in TS LOW compared to TS HIGH cells (**Figure 37A**). We further validated this difference on the protein level using flow cytometry. Up to 35% of the total TS LOW cell population expressed CD117 and this proportion was substantially and significantly higher than in TS HIGH (**Figure 37B**).

We took advantage of the fact that parental SKK-1 cells were found to be only partially positive for CD117 at the time of these tests and used the combined detection of palmitate uptake and CD117 expression to further examine the relationship between both parameters. CD117-negative SKK-1 cells showed significantly higher fatty acid uptake compared to CD117-positive SKK-1 cells (**Figure 37C**).

To investigate whether this relationship between low fatty acid uptake and CD117 expression could be extended to other stem cell markers, we analyzed CD123 and HLA-DR in TS LOW and TS HIGH cells by similar means (data not shown). CD123- and HLA-DR-positive LSCs and are found in both MDS and AML patients (Li et al., 2014). Similar to CD117, TS LOW cells contained a higher proportion of CD123- and HLA-DR-positive

| Results II

populations compared to TS HIGH (**Figure 37D**). Taken together, we were able to confirm the association of low fatty acid uptake in TS LOW and TS HIGH cells with the expression of a number of stem cell markers. This might suggest that the metabolic phenotype is linked to disease-relevant parameters such as stemness.

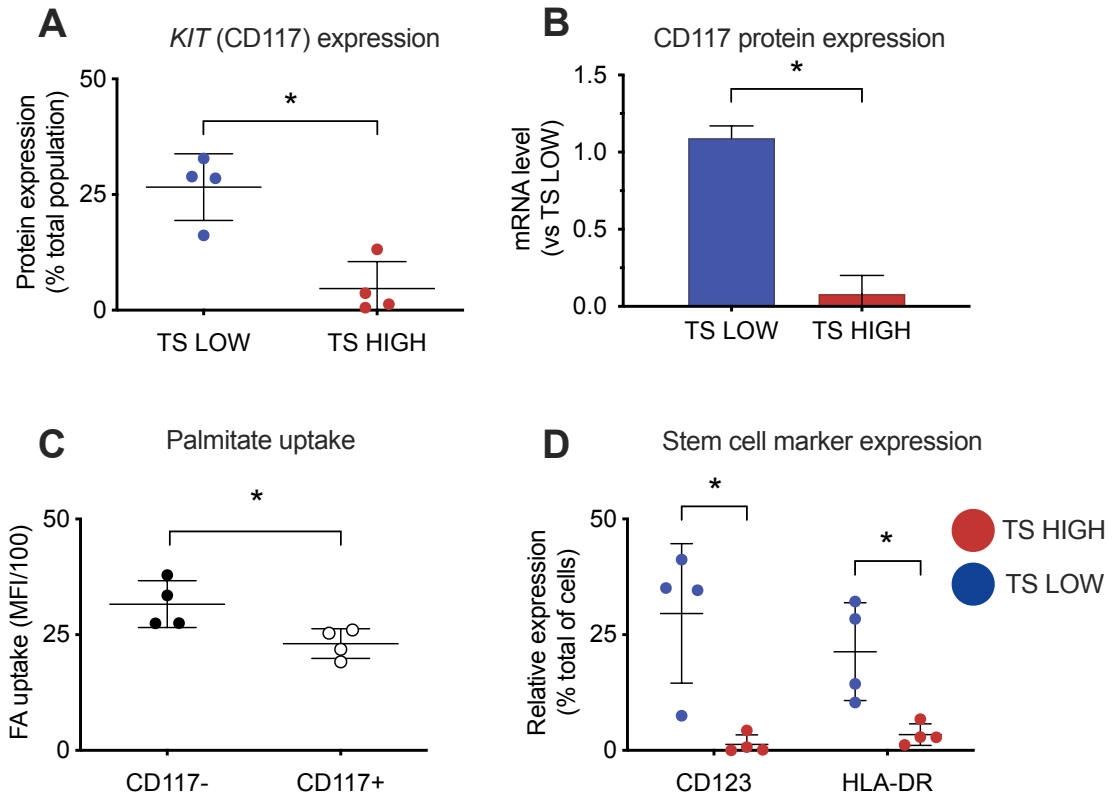


Figure 37: Increased stem cell marker expression in TS LOW on both transcriptional and protein levels. A) RT-qPCR shows relative mRNA expression of *KIT* in TS LOW and TS HIGH. Values were normalised to the housekeeping gene *GAPDH*. Results are presented as the mean \pm standard deviation ($n = 3$). B) Plot represents *KIT*-encoded CD117 protein expression in TS LOW and TS HIGH cells as percentage total cells. Expression was measured by flow cytometry ($n=3$). C) CD117-positive and CD117-negative SKK-1 parental cells assessed by flow cytometry on four separate days for fatty acid (FA) uptake with fluorescent BODIPY-labelled $0.5 \mu\text{M}$ palmitate. FA uptake was measured as median intensity fluorescence (MFI). D) Plot represents CD123 and HLA-DR protein expression in TS LOW and TS HIGH cells as percentage total cells. Expression was measured by flow cytometry ($n=3$). * $p < 0.05$ (student's t-test).

6.7 Conclusion

Taken together, we provide a detailed analysis of the MDS-derived sAML cell line SKK-1 and report that SKK-1 cells can be separated into stable sub-populations with distinct metabolism based on different capacities to take up long- and medium-chain fatty acids. Low fatty acid uptake is associated with clinically relevant parameters such as up-regulation of stem cell markers. Furthermore, we noted a number of cytogenetic

alterations shared by both TS LOW and TS HIGH cells that were not observed previous cytogenetic analysis of SKK-1 cells (Drexler, 2010; Palau et al., 2017), suggesting that either the SKK-1 cell line is genetically unstable or that the triple sorting process has enriched for other cells that have been present as latent contamination. This has been further investigated and results are described in Chapter 4.

7. Results III: Identification of TS LOW and TS HIGH as U-937 subclones

7.1 Chapter summary

TS LOW and TS HIGH cells differed substantially from SKK-1 cells in karyotype. Furthermore, TS LOW and TS HIGH cells differed between each other in at least one chromosome. SKK-1 cells have been carefully characterised in our lab (Palau et al., 2017) and thus it was not clear how the differences in TS LOW and TS HIGH appeared. In particular, we considered two possible explanations. A drastic genetic drift over time due to time in culture or -induced selection of latent sub-populations.

7.2 Evidence of a mixed population of SKK-1 and U-937 cells

Following our characterisation of TS LOW and TS HIGH cells, we decided to verify the identity of the cell lines by short tandem repeat (STR) profile analysis. We compared the STR profiles with that of the original SKK-1 cell stock, from which the sorted populations originally derived. STR profiling is a widely used technique to identify human cell lines by unique signatures based on the allelic number of 16 highly conserved microsatellite sequences. Cell lines with shared STR profiles of 80% or greater similarity are considered to be related (Masters et al., 2001). In this way, the identity of our different cell populations could be clarified.

When comparing with STR profiles on the publicly available Cellosaurus database from the Swiss Institute of Bioinformatics, we found that DS HIGH, TS LOW and TS HIGH cell lines matched perfectly with another independent cell line, the lymphoma-derived U-937 (Table 2). Interestingly, however, the original SKK-1 stock, from where TS LOW and TS HIGH are derived, matched with the SKK-1 STR profile.

We then looked at other frozen cell stocks: two working stocks of parental SKK-1 (one grown in short-term culture, two weeks; one grown in long-term culture, 10 weeks), single-sorted SKK-1 (SS LOW and SS HIGH), double-sorted SKK-1 (DS LOW and DS HIGH), and bona fide U-937, as control (Table 2).

We found that U-937 was undetectable in the original and 'short culture' parental SKK-1 stocks, as well as the SS LOW and SS HIGH. U-937 began to be detected in the 'long

| Results III

culture' SKK-1 cells, where we found mixed STR profiles of both SKK-1 and U-937. We found a similar mix in DS LOW. On the other hand, the STR profiles of DS HIGH, TS LOW and TS HIGH indicated U-937. As STR profiling has a limit of detection of up to 10% (M. Yu et al., 2015), it is possible that U-937 cells had been growing at undetectable levels in parental stocks, such that the predominant immunophenotype and karyotype were those of SKK-1.

Table 2: STR profiles of SKK-1, U-937, single-, double- and triple-sorted LOW and HIGH cells.

| Micro-satellite | U-937 | SKK-1 (original) | SKK-1 (short culture) | SKK-1 (long culture) | SS LOW | SS HIGH | DS LOW | DS HIGH | TS LOW | TS HIGH |
|-----------------|--------|------------------|-----------------------|----------------------|--------|---------|------------------|---------|--------|---------|
| D8S1179 | 12, 13 | 12, 13 | 12, 13 | 12, 13 | 13 | 13 | 12, 13 | 12, 13 | 12, 13 | 12, 13 |
| D21S11 | 27, 29 | 29, 32 | 29, 32 | 27, 29 | 29, 32 | 29, 32 | 27, 29 | 27, 29 | 22 | 22 |
| D7S820 | 9, 11 | 11, 12 | 11, 12 | 9, 11 | 11, 12 | 11, 12 | 9, 11 | 9, 11 | 9, 11 | 9, 11 |
| CSF1PO | 12 | 11, 12 | 11, 12 | 11, 12 | 11, 12 | 11, 12 | 11, 12 | 11*, 12 | 12 | 12 |
| D3S1358 | 16 | 16, 17 | 16, 17 | 16, 17 | 16, 17 | 16, 17 | 16 | 16 | 16 | 16 |
| TH01 | 6, 9,3 | 9 | 9 | 6, 9,3 | 9 | 9 | 6, 9, 9,3 | 6, 9,3 | 6, 9,3 | 6, 9,3 |
| D13S317 | 10, 12 | 10 | 10 | 10, 12 | 10 | 10 | 10, 12 | 10, 12 | 10, 12 | 10, 12 |
| D16S539 | 12 | 9, 11 | 9, 11 | 9, 11, 12 | 9, 11 | 9, 11 | 9, 11, 12 | 12 | 12 | 12 |
| D2S1338 | 17, 20 | 19, 20 | 19, 20 | 17, 19, 20 | 19, 20 | 19, 20 | 17, 19, 20 | 17, 20 | 17, 20 | 17, 20 |
| D19S433 | 14, 16 | 12, 14 | 12, 14 | 12, 14, 16 | 12, 14 | 12, 14 | 12, 14, 16 | 14, 16 | 14, 16 | 14, 16 |
| vWA | 15 | 14, 16 | 14, 16 | 14, 15, 16 | 14, 16 | 14, 16 | 14, 15, 16 | 14, 15 | 14, 15 | 14, 15 |
| TPOX | 8, 11 | 9, 11 | 9, 11 | 8, 11 | 9, 11 | 9, 11 | 8, 9, 11 | 8, 11 | 8, 11 | 8, 11 |
| D18S51 | 13, 14 | 13, 14 | 13, 14 | 13, 14 | 13, 14 | 13, 14 | 13, 14 | 13, 14 | 13, 14 | 13, 14 |
| AMEL | X | X, Y | X, Y | X | X, Y | X, Y | X, Y* | X | X | X |
| D5S818 | 12 | 12 | 12 | 12 | 12 | 12 | 12 | 12 | 12 | 12 |
| FGA | 22, 25 | 21, 23 | 21, 23 | 21, 22, 23, 25 | 21, 23 | 21, 23 | 21*, 22, 23*, 25 | 22, 25 | 22, 25 | 22, 25 |

*Small peak

To see if cells of distinct origins could be detected using STR analysis, we analysed three samples comprising the original SKK-1 cell line and TS HIGH in three exact concentrations of gDNA in the following ratios: 1:1, 1:4 and 4:1 (**Table 3**). From the electropherogram visualisation of results, we can see that in a 4:1 mixed ratio population of SKK-1 and TS HIGH, both cell lines contribute peaks at loci in a cell line-specific manner (Figure 38). Due to the qualitative nature of STR profiling, however, only the predominant loci peaks are considered for cell line identification. Therefore, given the tri-allelic patterns observed

| Results III

in pre-mixed SKK-1 and TS HIGH populations, this may be indicative of multi-cell populations in SKK-1 (long culture) and DS LOW. Taken together, it is possible to visualise mixed populations by the STR method.

Table 3: STR profiles of pre-mixed populations of parental SKK-1 and TS HIGH. The two cell populations were mixed in the following ratios: 1:1, 1:4, and 4:1, respectively.

| Micro-satellite | SKK-1 (original): TS HIGH ratio | | |
|-----------------|---------------------------------|----------------|----------------|
| | 1:1 | 1:4 | 4:1 |
| D8S1179 | 12 ,13 | 12 ,13 | 12 ,13 |
| D21S11 | 27, 29, 32 | 27, 29, 32 | 27, 29, 32 |
| D7S820 | 9, 11, 12 | 9, 11, 12 | 9, 11, 12 |
| CSF1PO | 11, 12 | 11, 12 | 11, 12 |
| D3S1358 | 10, 12 | 10, 12 | 10, 12 |
| TH01 | 6, 9, 9.3 | 6, 9, 9.3 | 6, 9, 9.3 |
| D13S317 | 16, 17 | 16, 17 | 16, 17 |
| D16S539 | 9, 11, 12 | 9, 11, 12 | 9, 11, 12 |
| D2S1338 | 17, 19, 20 | 17, 19, 20 | 17, 19, 20 |
| D19S433 | 12, 14, 16 | 12, 14, 16 | 12, 14, 16 |
| vWA | 14, 15, 16 | 14, 15, 16 | 14, 15, 16 |
| TPOX | 8, 9, 11 | 8, 9, 11 | 8, 9, 11 |
| D18S51 | 13, 14 | 13, 14 | 13, 14 |
| AMEL | X, Y | X, Y | X, Y |
| D5S818 | 12 | 12 | 12 |
| FGA | 21, 22, 23, 25 | 21, 22, 23, 25 | 21, 22, 23, 25 |

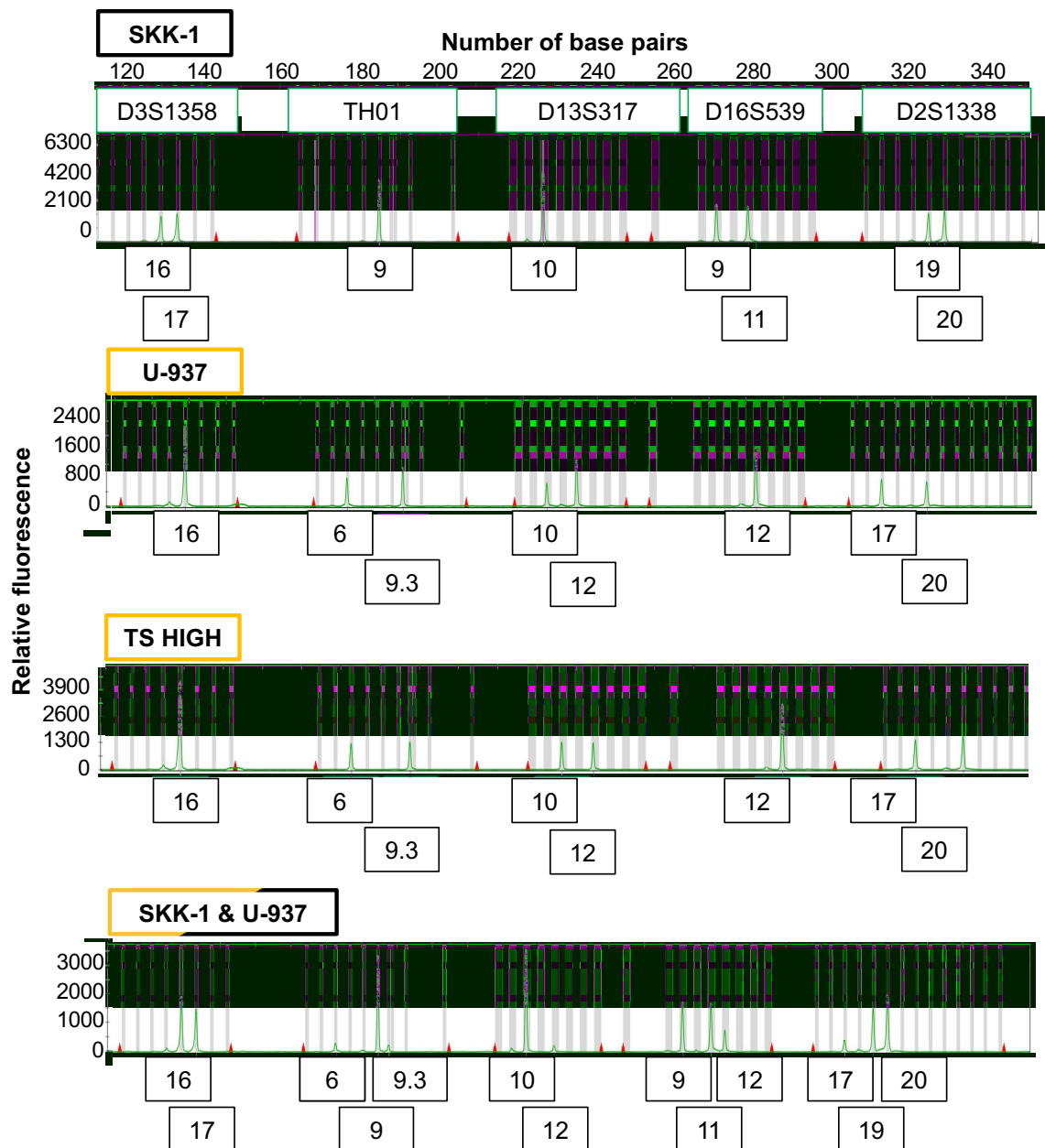


Figure 38: Representative electropherograms of SKK-1, U-937, TS HIGH and a mixed population of SKK-1 and TS HIGH. Electropherograms of five of the 16 microsatellite loci are shown for SKK-1, U-937, TS HIGH and a mixed population of SKK-1 and TS HIGH (4:1 ratio) are shown, as measured by short tandem repeat (STR) profiling. The x-axis is the number of base pairs, the y-axis is the relative fluorescence and the boxes represent the number of microsatellites per locus. The black box indicates cells identified as SKK-1, the yellow box indicates cells identified as U-937, and the black-yellow box indicates cells that contain SKK-1 and U-937 STR profiles.

7.3 TS LOW and TS HIGH display U-937-like immunophenotypes

We have previously shown that TS LOW and TS HIGH differed by their cell surface marker expression, most notably stem cell markers. We decided to revisit these data and see if these differences could explain cell-specific immunophenotype differences between SKK-1 and U-937 cells. We directly compared the immunophenotypes of SKK-1, TS LOW, TS HIGH and U-937 where we found cell-specific signatures (**Figure 39**). We found SKK-1 to have high expression of the stem cell markers CD117, CD123, CD10 and HLA-DR, whereas TS LOW, TS HIGH and U-937 had low expression of these markers. Conversely, we found low expression of CD36 in SKK-1 and medium to high expression in TS LOW, TS HIGH and U-937. With these five cell surface markers, clear immunophenotypic differences could be seen where TS LOW and TS HIGH had more U-937-like cell surface marker expression compared to SKK-1. The haematopoietic marker, CD45, was common in all four cell lines. Indeed, we noticed that during a 'long culture' of eight weeks, cell surface marker expression fluctuated over time in SKK-1, TS LOW and TS HIGH (**Figure 40**). Interestingly, we observed that expression of the three stem cell markers (CD117, CD123 and HLA-DR) decreased over time in all three cell lines, while CD36 tended to increase. This observation highlighted immunophenotypic changes over time that may be indicative of the U-937 cell line expanding within the SKK-1 population.

| | SKK-1 | TS LOW | TS HIGH | U-937 |
|--------|-------|--------|---------|-------|
| CD45 | | | | |
| CD117 | | | | |
| CD123 | | | | |
| HLA-DR | | | | |
| CD10 | | | | |
| CD36 | | | | |

Expression level

(% cell population)

| | |
|---------------|--------|
| HIGH | >70% |
| MEDIUM | 30-70% |
| LOW | 5-30% |
| ZERO | <5% |

Figure 39: U-937-specific immunophenotype evident in TS LOW and TS HIGH. Cell surface marker expression (percentage of total cell population) of SKK-1, TS LOW, TS HIGH and U-937 cell lines, as measured by flow cytometry.

| Results III

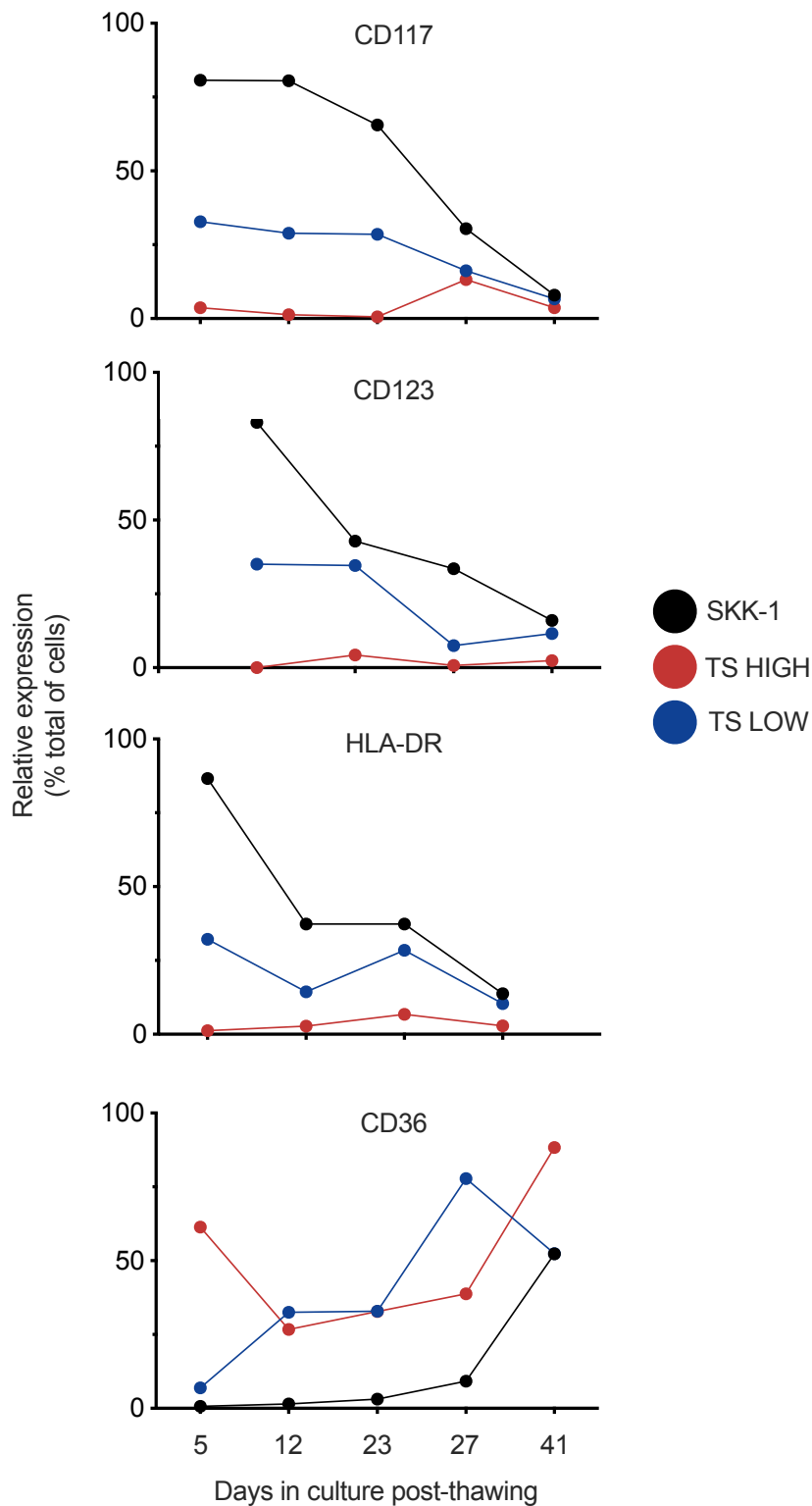


Figure 40: Stem cell marker expression decreased over time while SKK-1, TS LOW and TS HIGH cells were in culture. Plots represent cell surface marker expression (CD117, CD123, HLA-DR and CD36) in SKK-1 (long culture stock), TS LOW and TS HIGH cells while in culture over a period of 41 days. Expression was measured using flow cytometry and is expressed as percentage of the total cell.

7.4 Cell line-specific gene fusion detection

Next, we aimed to take advantage of cell-specific gene fusions for SKK-1 and U-937 cells with which we could further uniquely identify presence in the TS LOW and TS HIGH cell populations. Gene fusions are a common characteristic of both myeloid and lymphoid leukaemias and occur due to chromosomal translocations, which can result in the expression of oncogenes. Indeed, gene fusions have been investigated as part of diagnostic protocols across different leukaemias due to their disease subtype specificity (Laforêt et al., 2013; Strefford et al., 2001). The gene fusion occurs due to a translocation occurring at (10;11)(p13;q14) (Laforêt et al., 2013). When comparing gene fusion expression across the four cell lines, we found *ETV6-NTRK3* gene fusion expressed only in SKK-1 (**Figure 41A**). To see if gene fusion expression could be used as a measure of SKK-1 contribution in TS LOW and TS HIGH populations, we interpolated TS LOW and TS HIGH *ETV6-NTRK3* expression on a standard curve and saw that their expression values appeared on the lower end of input mRNA concentrations (**Figure 41B**). This suggested that trace levels of *ETV6-NTRK3* may be present in TS LOW and TS HIGH. Similarly, for the U-937-specific gene fusion, *MLLT10-PICALM*, we observed expression in TS LOW, TS HIGH and U-937, and none in SKK-1 (**Figure 41C**). Again, to see if gene fusion expression could be used as a measure of U-937 contribution in TS LOW and TS HIGH populations, we interpolated TS LOW and TS HIGH *MLLT10-PICALM* expression on a standard curve and saw that their expression values appeared on the higher end of input mRNA concentrations (**Figure 41D**). This suggested that the contribution of U-937 cells in the TS LOW and TS HIGH populations was indeed high.

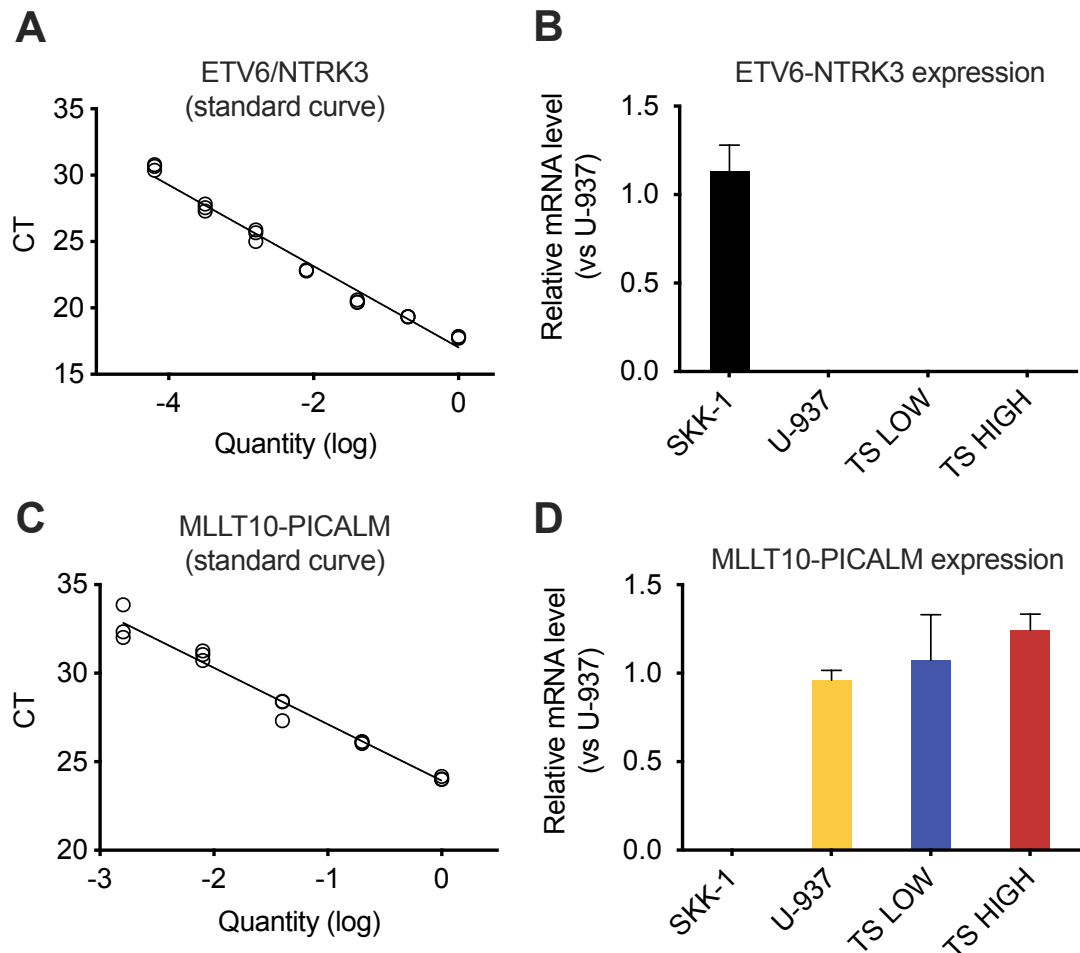


Figure 41: SKK-1- and U-937-specific gene fusions are associated with the detection of U-937 in TS LOW and TS HIGH cells. A) Plot represents a standard curve of ETV-NTRK3 expression in SKK-1 cells, with serially diluted input concentrations (x-axis) calculated from the log of starting mRNA levels. Each point represents the threshold cycle of one of three replicates at each concentration of the standard curve. Indicated on the curve are the interpolated Ct values of ETV-NTRK3 expression in TS LOW (blue) and TS HIGH (red). B) RT-qPCR shows relative mRNA expression of the SKK-1-specific ETV6-NTRK3 gene fusion across SKK-1, U-937, TS LOW and TS HIGH cell lines. Values were normalised to the housekeeping gene GAPDH. Results are presented as the mean \pm standard deviation ($n = 3$). C) Plot represents a standard curve of MLLT10-PICALM expression in U-937 cells. Indicated on the curve are the interpolated Ct values of MLLT10-PICALM expression in TS LOW (blue). Ct values for TS HIGH were lower than those for U-937 and so could not be interpolated. D). RT-qPCR shows relative mRNA expression of the U-937-specific MLLT10-PICALM gene fusion across SKK-1, U-937, TS LOW and TS HIGH cell lines. Experimental details are as in A).

7.5 U-937 grows faster than SKK-1 in culture

Next, we compared the growth rates of U-937, SKK-1, TS LOW and TS HIGH cells to determine the feasibility of U-937 cells to expand and out-grow SKK-1 cells in a mixed culture. After a four-day period (96 hours) in culture, we saw that U-937, TS LOW and TS HIGH cells had higher cell numbers compared to SKK-1 (**Figure 42**). Further, we observed faster ‘yellowing’ of the growth media for U-937, TS LOW and TS HIGH, hinting at a faster utilisation of glucose and, therefore, a faster growth rate.

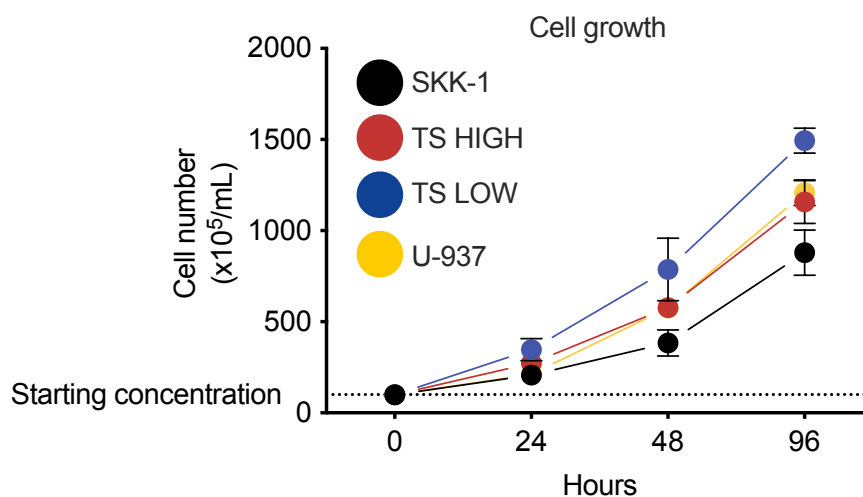


Figure 42: U-937, TS LOW and TS HIGH cells grow at a faster rate than SKK-1 under normal culture conditions. Plot represents growth of SKK-1, U-937, TS LOW and TS HIGH cells under normal growth conditions over a period of 96 hours. Cells were seeded at 1×10^5 /mL in triplicate. Cell counts were taken at the indicated time points in duplicate.

7.6 Single cell colonies of TS LOW and TS HIGH retain fatty acid uptake phenotype

We decided to expand single cell colonies of TS LOW and TS HIGH to carry out further phenotypic and genetic characterisation. We performed this by first plating cells at a low cell density so as to ensure single cells grew from single wells. In this way, purified colonies would give us a better idea of the exact composition of the mixed populations. First, of the colonies that grew, we noticed that colonies grew at different rates, indicating that this may be reflective of the different growth rates observed between the cell lines. However, when we repeated the gene fusion detection test by RT-qPCR, no SKK-1-specific ETV6-NTRK3 gene fusion expression was detected in TS LOW or TS HIGH (**Figure 43A**). On the other hand, the U-937-specific MLLT10-PICALM gene fusion was detected in all of the TS LOW- and TS HIGH-derived colonies (**Figure 43B**). We then investigated palmitate uptake of five TS LOW and TS HIGH expanded single cell colonies. We compared uptake values of the TS LOW colonies with the overall mean TS HIGH uptake and, similarly, we compared uptake values of the TS HIGH colonies with the overall mean TS LOW uptake. We found that three colonies each from TS LOW and TS HIGH had significantly lower and higher mean fatty acid uptake, respectively (**Figure 43C**). Therefore, we found that most of the TS LOW and TS HIGH colonies had retained their respective fatty acid uptake behaviour.

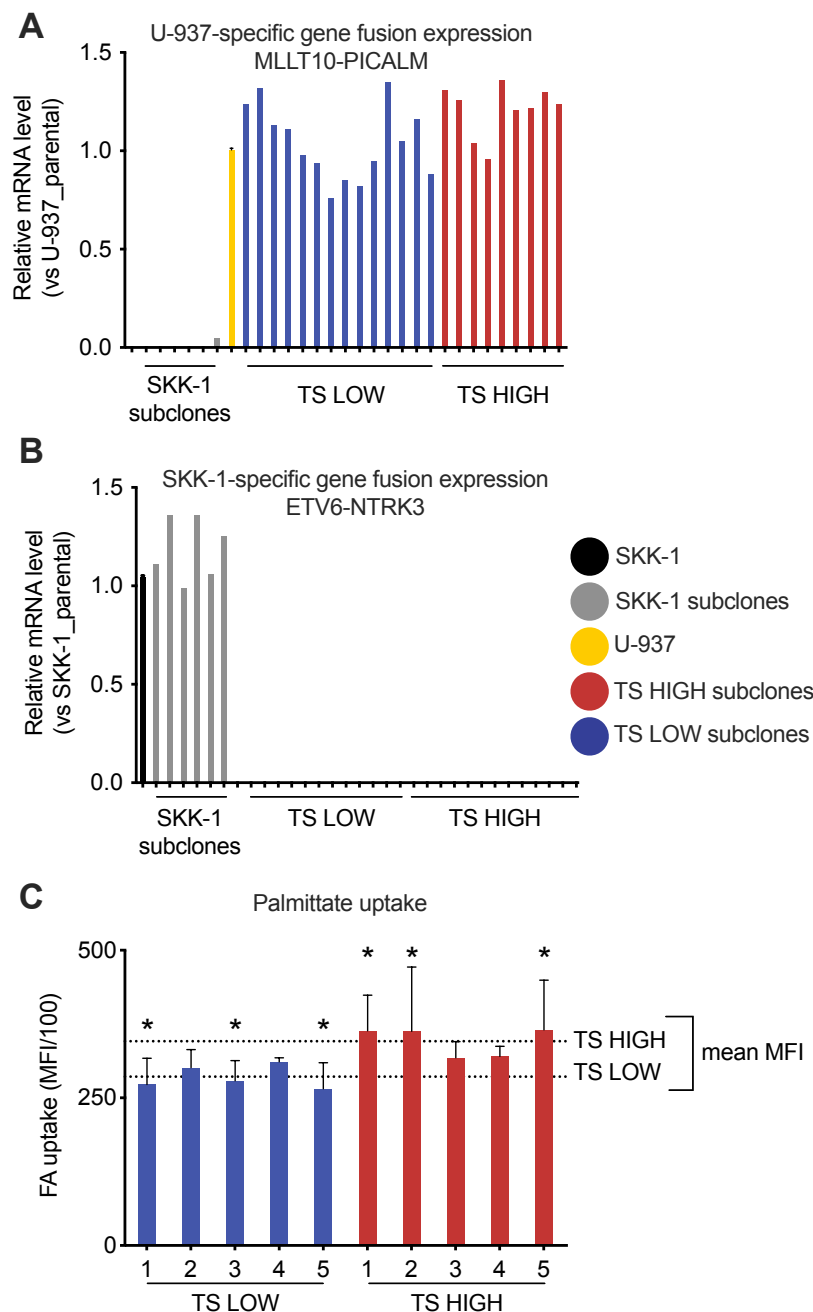


Figure 43: TS LOW and TS HIGH expanded single cell colonies express a U-937-specific gene fusion and retain their respective fatty acid uptake capacities. A) RT-qPCR shows relative mRNA expression of the SKK-1-specific ETV6-NTRK3 gene fusion across SKK-1 and U-937 bulk cells and 11 TS LOW and 12 TS HIGH expanded single cell colonies. Values were normalised to the housekeeping gene GAPDH. Results are presented as the mean \pm standard deviation ($n=3$ for bulk parental cell and $n=1$ for single cell colonies). B) RT-qPCR shows relative mRNA expression of the U-937-specific MLLT10-PICALM gene fusion across SKK-1 and U-937 bulk cells and 11 TS LOW and 12 TS HIGH expanded single cell colonies. Values were normalised to the housekeeping gene GAPDH. Results are presented as the mean \pm standard deviation ($n=3$ for bulk parental cell and $n=1$ for single cell colonies). C) To assess if single cell colonies retain their fatty acid (FA) uptake capacities, five TS LOW and TS HIGH expanded single cell colonies were incubated with fluorescent BODIPY-labelled $0.5 \mu\text{M}$ palmitate for 60 minutes, washed and uptake was assessed by flow cytometry on three separate days. TS LOW results are compared to the overall TS HIGH FA uptake mean and TS HIGH results are compared to the overall TS LOW FA uptake mean. $*p < 0.05$ (one-way ANOVA).

7.7 Karyotype profiles of TS LOW and TS HIGH differ by trisomy 8

We performed conventional karyotyping and fluorescence in situ hybridization (FISH) in TS LOW and TS HIGH and in two of the expanded sub-clones, TS LOW sub-clone 3 (sc3) and TS HIGH sub-clone 5 (sc5), to see if cytogenic differences could be detected and if these differences were similar to either SKK-1 or U-937 parental cell lines. Notably, the karyotypes of TS LOW and TS HIGH, and their sub-clones, TS LOW_sc3 and TS HIGH_sc5, differed greatly from those of the parental cell lines (**Table 2**). Indeed, we found highly complex karyotype profiles that did not resemble any other cell line.

Regarding the expanded sub-clones, we observed the presence of a partial trisomy 8 in TS LOW_sc3 that was not present in TS HIGH_sc5 (**Figure 44E** and **Figure 44F**). The third partial chromosome 8 in TS LOW_sc3 had a deletion at 8q24 portion, which contained the MYC gene locus. Trisomy 8 is one of the most common chromosomal abnormalities in MDS and AML (Bakshi et al., 2012). Similarly, we also found a complete trisomy 18 in TS LOW_sc3, as determined by a probe targeting the 18q21 locus encoding *BCL2* (**Figure 44A** and **Figure 44B**). *BCL2* overexpressed in MDS, contributing to disease by blocking cell death (Parker, 2000). Second, while both sub-clones have a trisomy 7, TS LOW_sc3 displayed a deletion in 7q36 arm of chromosome 7 (7q36), which corresponds to the *EZH2*-encoding locus (**Figure 44C** and **Figure 44D**). *EZH2* encodes for histone methyltransferase and a loss-of-function mutation is associated with both MDS and sAML (Haferlach et al., 2014).

Overall, there appears to be an increase in chromosomal number in TS LOW_sc3, with alterations at genetic loci that are relevant in myeloid malignancies.

Table 4: Cytogenetic analysis reveals presence of trisomy 8 in TS LOW, but not in TS HIGH, and a distinct karyotype to the parental SKK-1 cells. Shown are the representative karyotype profiles of TS LOW and TS HIGH, as measured from 20 cells in metaphase. Also shown is the conventional karyotype of SKK-1, as previously described in Drexler, 2010).

| Cell line | Karyotype |
|--------------------|-------------------------------------------------------------------------------------------------------------------------------------------------------------------------------------------------------------------------------------------------------------------------------------------------|
| SKK-1 | 47, XY, add(4)(p16), add(7)(q35),+8, add(12)(p13),add(18)(p11)[10] |
| TS LOW | 55-59, XX, -Y, +1, add(1)(p13), add(1)(q12), add(2)(q37), +3, add(3)(q12), add(3)(q24), -5, add(6)(p25), +7, del(7)(q22), +8, add(10)(p11.2), add(10)(q26), del(11)(q23), add(12)(p11.2), add(13)(q22), add(16)(p11.2), +18, +20, +21X3 +mar1,+mar2,+mar3,+mar4,+mar5[cp20] |
| TS HIGH | 55-59, XX,-Y, +1, add(1)(p13), add(1)(q12), add(2)(q37), +3,add(3)(q12), add(3)(q24), -5, add(6)(p25), +7, del(7)(q22), add(10)(p11.2), add(10)(q26), del(11)(q23), add(12)(p11.2), add(13)(q22), add(16)(p11.2), +18, +20, +21X3, +mar1,+mar2,+mar3,+mar4,+mar5[cp20] |
| TS LOW_sc3 | 58,XX,-X, -1, t(1;5)(p22;q31.1), -2, add(2)(q37), add(3)(q12), der(3)t(1;3)(q21;q27), -4, -5,-6, add(6)(p25), del(7)(q22.3q36.3), del(8)(q21.2), -9, -10, add(10)(p13), -11, del(11)(q23), -12, add(12)(p12), -13, add(13)(p11.2), -14, 15, add(16)(p11.1), -17, -19, -22, +6mar |
| TS HIGH_sc5 | 56,XX,-X, -1, t(1;5)(p22;q31.1), -2, add(2)(q37), add(3)(q12), der(3)t(1;3)(q21;q27), -4, -5, -6, add(6)(p25), -8, -9,-10, add(10)(p13), -11, del(11)(q23), -12, add(12)(p12), -13, add(13)(p11.2), -14, -15, add(16)(p11.1), -17, -18, -19, -22, +6mar |
| U-937 | 63(58-69)<3n>XXY, t(1;12)(q21;p13), -2, -4, der(5)t(1;5)(p22;q35), -6, +7, -9, add(9)(p22), t(10;11)(p14;q23), i(11q), i(12p), add(16)(q22), add(19)(q13) -20, -21, +3mar |

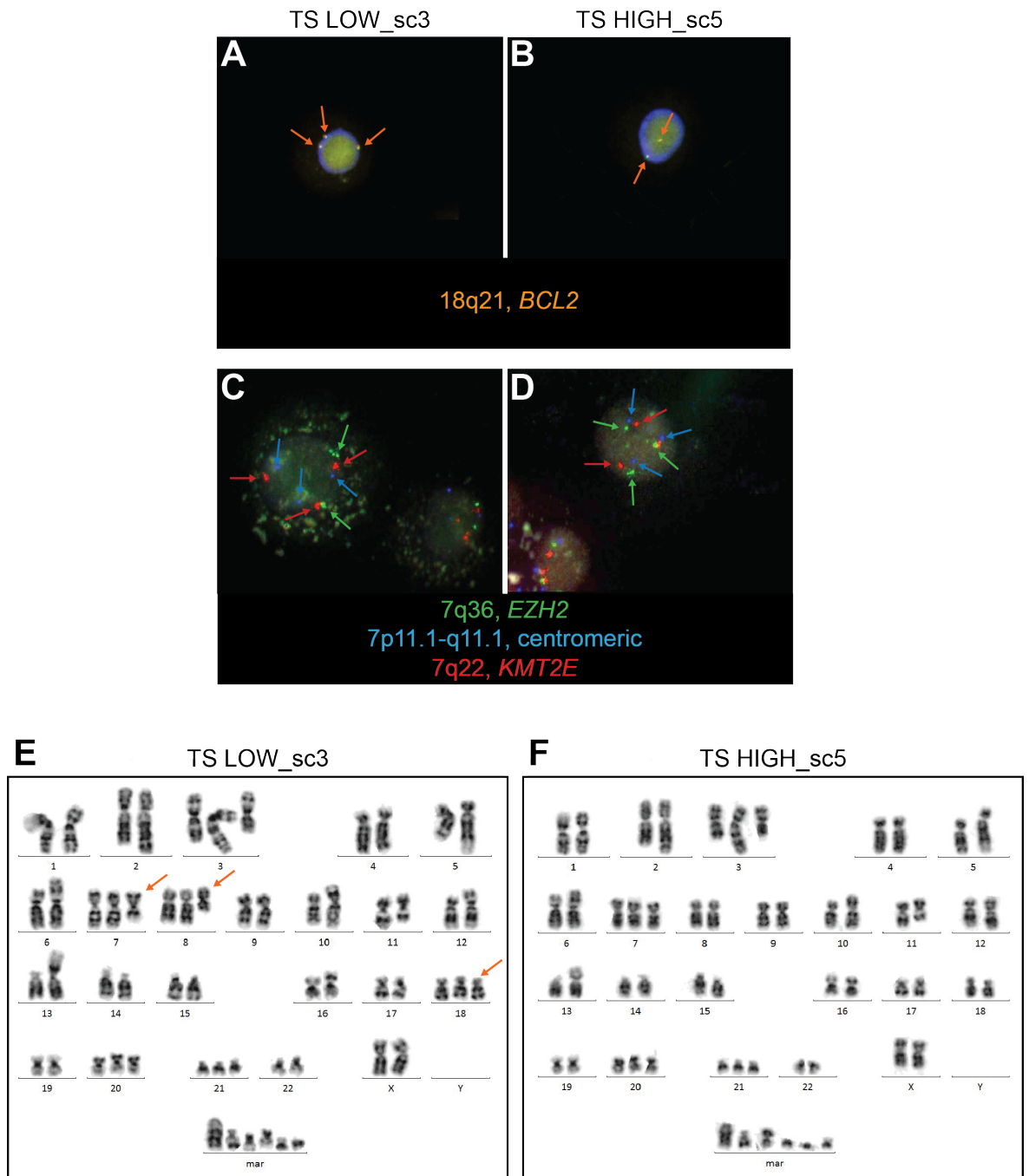


Figure 44: Fluorescence in situ hybridisation (FISH) analysis reveals cytogenetic differences at chromosomes 7 and 8 between TS LOW and TS HIGH sub clones. Fluorescence microscopy images showing the detection of several genetic loci at chromosomes 18 and 7. A) TS LOW_sc3 and B) TS HIGH_sc5 were hybridised with BCL2 locus detection probe (green/orange signal) at 18q21 as indicated by the arrows. Similarly, C) TS LOW_sc3 and D) TS HIGH_sc5 were hybridised with the EZH2 locus detection probe (green) at 7q36, KMT2E (orange) at 7q22, and the centromeric region (blue) at 7p11.1-q11.1). Arrows indicate each of the loci. Karyotype images of E) TS LOW_sc3 and F) TS HIGH_sc5 showing cytogenetic differences: partial trisomy chromosomes 7 and 8, and complete trisomy 18.

7.8 Conclusion

Taken together, it appears that SKK-1 parental cells had contained low-levels of U-937 cells meant that expanded over time. We traced back in time to any potential exposure our SKK-1 cells may have had to other cell lines. We concluded that neither the parental or the sorted populations had been directly or proximally exposed to U-937 cells, either within our laboratory group or neighbouring groups. Similarly, we confirmed with the FACS facility that previous users had not sorted U-937 cells, therefore ruling out contamination during FACS processing. Therefore, SKK-1 cells most likely had contained latent contamination of U-937 since arriving in our lab. Interestingly, sub-clones of U-937 have distinct uptake phenotypes and disease-relevant differences in their cytogenetic profiles. We are currently carrying out further experimentation to determine the significance of this finding in terms of cytology, mutational profile and drug sensitivity (Maher, et al., in preparation).

Discussion

8. Discussion

Our running hypothesis that leukaemia cells could be separated based on their lipid metabolism and characterised thereafter changed course once we discovered the presence of a cell line other than SKK-1 in our TS LOW and TS populations.

Clones derived from the lymphoma U-937 cell line were the surprise guests in this story, which I discuss in terms of their identification and their potential as a means to study chromosomal aberrations in haematological malignancies. I then consider how the presence of these contaminants in mixed cell populations affects the interpretation of results from chapter 3 where we characterised TS LOW and TS HIGH. Taking a methodological point of view, I present an analysis of the genetic screen we performed, discuss technical limitations and suggest modifications for future improvements and alternative approaches to dissect the interaction between epigenetic regulation and metabolism. Finally, I reflect on the broader context of our results and elude to the importance of metabolism as a function of diet for myeloid diseases.

8.1 Identification of contaminant U-937 cells

We found strong evidence that U-937 cells emerged and expanded among SKK-1 parental cells and TS LOW and TS HIGH populations over the course of this study. From our STR analysis, we were able to construct a map to outline the contribution of SKK-1 and U-937 in each of the tested samples over time (**Figure 45**). This finding was principally based on STR profile analysis and substantiated with immunophenotypic and karyotypic profiling and cell line-specific gene fusion expression. Using similar forensic science methods for identifying human individuals, STR profiling is a reliable and accurate way to assess the identity and purity of a given cell line (Masters et al., 2001). A minimum of eight core STR loci plus the sex-determining locus, amelogenin, is recommended for optimal discriminating power for identifying and comparing STR profiles (Capes-Davis et al., 2013). For our study, we performed an extended cell line authentication protocol that incorporates 16 distinct loci to create a fingerprint with a random match probability of 1 in 1×10^{18} (Reid et al., 2013). However, given the sensitivity limit of this technique in determining a minority cell line in a mixed population is 5-10% (Y. Huang et al., 2017; Masters et al., 2001; M. Yu et al., 2015), it is plausible that U-937 went undetected in the original SKK-1 parental population for some time during culturing. Indeed, from our retrospective analysis of frozen stocks, it is apparent that U-937 cells only emerged over time within parental SKK-1 and sorted cells. Although multiple cell lines within a population were not fully identifiable by STR alone, we observed multiple peaks at several microsatellite loci in SKK-1 (long culture), DS LOW and the pre-mixed control samples, indicating that mixed populations were detectable.

Despite the accuracy of STR profiling in identifying bulk populations of cell lines, there may still be ambiguity where cell line subclones differ in STR profiles but display identical immunophenotypes, chromosomal markers and biological behaviours (Parson et al., 2005). Therefore, it was prudent that we take a holistic approach in order to verify U-937 contamination. Since STR profiling is a mainly qualitative approach to cell identification, we decided that single cell analysis of TS LOW and TS HIGH would be useful to check the heterogeneity of subclones on the levels of cytogenetic aberrations and gene fusion expression, and to see if the fatty acid phenotypes were still present, as was observed in the bulk populations.

Cells expressing SKK-1-specific gene fusions were not detected in either TS LOW or TS HIGH, indicating that these populations consist predominantly of U-937-derived cells. Similarly, we did not detect mRNA from U-937-specific fusion genes in the parental SKK-1 bulk population. Based on the same criterium, single-cell clones grown from parental

SKK-1 cells were clearly identified as SKK-1 and not U-937. However, it is again possible that the level of U-937 contamination in the original SKK-1 population may have been below detection limit.

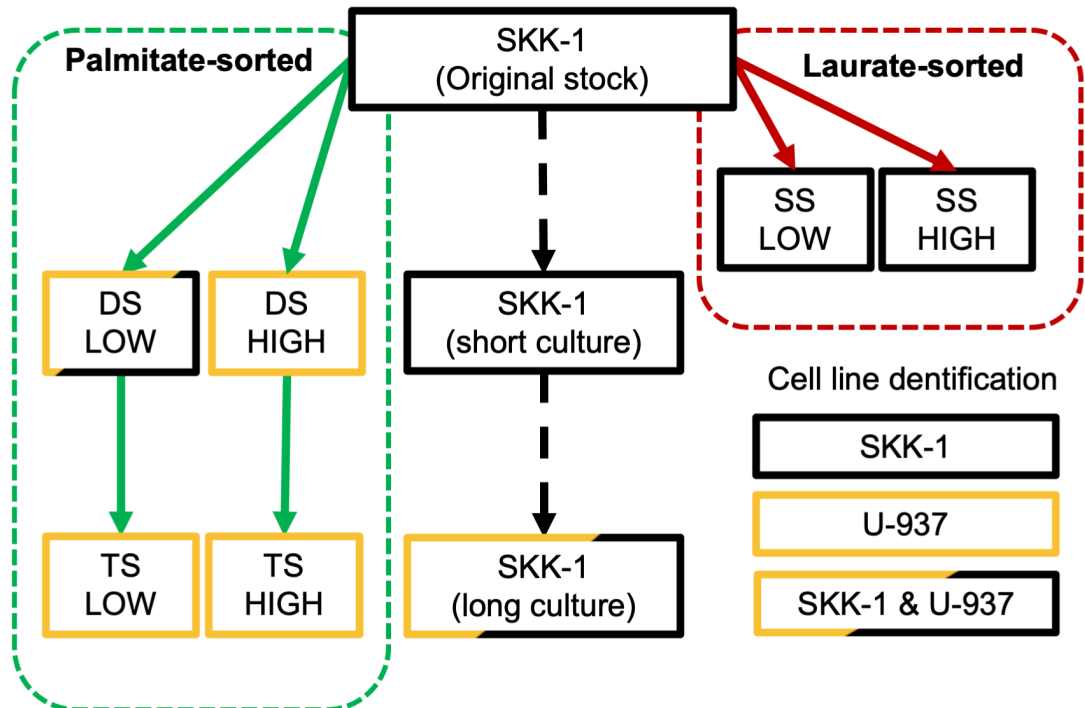


Figure 45: Schematic representation of the contribution of SKK-1 and U-937 cells in parental and sorted populations of SKK-1, as determined by STR profiling. Colour-coded boxes indicate the identification of parental and single- (SS), double- (DS), and triple- (TS) sorted cell lines, bases either on palmitate (green dashed line) or laurate (red dashed line) uptake, as determined by STR profiling. Black boxes indicate pure SKK-1, yellow boxes indicate pure U-937, and black-yellow boxes indicate a mixture of the two cell lines, according to allelic peaks on the electropherogram.

8.1.1 Possible sources of U-937 contamination

We can consider two hypotheses as to how U-937 cell entered our SKK-1 population: first, it is conceivable that we originally received SKK-1 cells with low-levels of contaminating U-937 cells. Second, and less likely, it is possible that cross-contamination occurred during the course of cell culture. Both ideas are substantiated by the observations of U-937's fast growth rates and historical reputation as widespread contaminants.

It has been previously reported that U-937 can be easily expanded from single cells by limiting dilutions (Kameoka et al., 1995). Indeed, our observation of U-937's faster growth rate compared to SKK-1 may support greater single clone expansion capacity. Likewise, long-term passaging creates a selection environment for highly proliferative cells, thereby introducing a growth bias that inhibits slower growing cells (Hirsch & Schildknecht, 2019). In this way, U-937 may have had a significant growth advantage over SKK-1 during expansion. Furthermore, the process of cell sorting may have introduced a selection pressure that could have allowed the expansion of U-937 relative to SKK-1 cells. It is possible that the repeated rounds of cell sorting that we carried out further accelerated U-937 expansion. It is worthwhile to point out that the lab of origin of SKK-1 cells have also used U-937 cells in their studies (Kurimoto et al., 2013; Maimaitili et al., 2018).

At present we cannot fully exclude the possibility that the contamination happened in our hands. Possible moments in which this could happen are inadvertent cross-contamination in the cell culture lab or at the flow cytometry facility. In these cases, the source of the U-937 cells would be unclear as we did not identify any occasions in which U-937 were cultured at the same time as SKK-1 cells in our lab nor did we find users who had sorted cells at the flow cytometry facility prior to us. Taken together, the most likely scenario is that the original stock of SKK-1 was latently contaminated with U-937 cells that expanded over time allowing TS LOW and TS HIGH cells to dominate.

8.1.2 Contaminant cells are U-937 clones with altered karyotypes

Our initial observations of fluctuations in cell surface antigen expression of TS LOW and TS HIGH bulk cells provided evidence that these cell populations were changing while in culture. Although genetic and transcriptional heterogeneity can occur in cancer cell lines, consensus immunophenotypes are considered a defining characteristic of haematological cell lines (Hans G Drexler, 2010), as well as being used for assigning cells to haematopoietic lineages *in vivo*. Therefore, the detection of multiple cell surface antigens using flow cytometry provides a valuable way to identify and compare cell lines on a cell-by-cell basis.

As part of our immunophenotypic characterisation of TS LOW and TS HIGH, we chose a panel of antibodies that target a wide range of cell surface markers routinely used in the

clinical setting. During regular monitoring of the cells, it was evident that the two cell lines were undergoing immunophenotypic changes that were distinct from SKK-1. Later, when comparing to U-937, we discovered that the immunophenotypes of TS LOW and TS HIGH resembled the consensus profile of U-937 (Hans G Drexler, 2010). Major alterations to cell surface antigen expression in cell lines of single origin under normal culture conditions are not common. Induced differentiation with compounds such as ATRA and vitamin D₃ stimulates changes in cell surface markers on haematopoietic cell lines with differentiation capacity, as the cells undergo changes in phenotype and morphology (Sanchez et al., 2014). As we did not treat the cells with differentiation-inducing compounds, this did not explain the observed reduction in stem cell marker expression.

Similar to the observed changes in cell surface antigens, we also found complex karyotypes of TS LOW and TS HIGH that were distinct from those of both SKK-1 and U-937. A notable deviation from the published karyotype profiles of SKK-1 and U-937 included the loss of the Y-chromosome, even though both cell lines were originally derived from male donors (Hans G Drexler, 2010). The Y-chromosomes are frequently lost during cell culture, which has previously been shown in U-937 (Lee et al., 2002). As karyotypic changes can be brought about over the course of increasing passage numbers (MacLeod et al., 1997), we initially thought that genetic changes were brought about due to the extended time the cells had been in culture, as well as the stress cell sorting by FACS may have exerted. In addition, chromosomal instability has been described as essential to the evolution of cancer (Heng et al., 2013), and so we thought that these changes could be an inherent property of the cell lines. Previously, however, subclones of U-937 with differences in both tandem repeats and chromosomal aberrations have been identified following long periods in culture (Lee et al., 2002; Parson et al., 2005). Further, chromosomal instability and loss of heterozygosity has been previously attributed to U-937 (Stacey et al., 1992), highlighting the likelihood of U-937's appearance in SKK-1. Since such inadvertent changes to both the immunophenotype and karyotype under normal culture conditions are unlikely, our results showing the loss of the SKK-1-like immunophenotype and karyotype in SKK-1 parental, TS LOW and TS HIGH over an extended period of culturing suggests the U-937 cell line expanded within these populations.

8.1.3 Isolation and characterisation of pure U-937 clones can provide a cell culture model for clinically-relevant karyotypic differences

In the context of haematological disease, irregular karyotypes represent one of the most powerful determining factors that predict patient survival and therapy response (Daneshbod et al., 2019). In particular, risonomy of chromosome 8 is associated with poor

prognosis in AML and is one of most common chromosomal aberrations in MDS (Bakshi et al., 2012), representing the sole genetic aberration in 11% of MDS cases (Paulsson & Johansson, 2007). Strikingly, our results reveal that the one of the main karyotypic differences is the presence and absence of trisomy 8 in TS LOW and TS HIGH, respectively. This was observed in both bulk populations and subclones, further pointing to the genetic instability of U-937. Although trisomy 8 has been previously observed in subclones of U-937 (Lee et al., 2002), the consensus karyotype of U-937 does not include this aberration.

The exact mechanism with which trisomy 8 contributes to disease burden is unknown. 20% of decitabine-treated MDS patients showed cytogenic abnormalities following relapse, including trisomy 8 (Qin et al., 2011), suggesting an association with drug resistance. Dysregulation of genes encoded on abnormal chromosomes may have consequences for disease outcome due to increased gene dosage, such as the oncogene *MYC* in trisomy 8 in AML (Bakshi et al., 2012), which when dysregulated leads to uncontrolled proliferation and inhibition of myeloid differentiation (Mertens et al., 1995). In this instance, however, we did not detect any up-regulated genes in TS LOW that are commonly associated with trisomy 8 in AML or MDS. Further, as our RNA-seq results show, an additional copy of a chromosome 8 in TS LOW does not lead to increased differentially expressed genes directly on that chromosome. In addition, gene dosage itself may not necessarily be associated with trisomy 8 in AML, but rather changes in global gene expression, such as increased expression of several leukaemogenesis-associated *HOXA* genes encoded on chromosome 7 (Kok et al., 2010).

While analysis of the TS LOW and TS HIGH subclones reveals genetic instability, both cell types retained their respective low and high fatty acid uptake capacities. For this, work is ongoing in our lab to elucidate the transcriptional, metabolic and drug response consequences of the observed cytogenic differences between TS LOW_sc3 and TS HIGH_sc5 subclones (Maher et al., in preparation). It remains to be seen if TS LOW-associated trisomies—partial trisomy 7 and 8 and complete trisomy 18—can be directly associated with changes in lipid metabolism, namely decreased fatty acid uptake, and azacitidine sensitivity. Therefore, our U-937 subclones represent a potential model to study disease-relevant genetic aberrations.

8.1.4 The historical issue of misidentified cell lines

One of the main lessons learned from this study concerns the importance of cell line purity. Because our cell line of interest, SKK-1, was compromised from the beginning of the project, we are mindful to interpret the data from the perspective of a mixed cell population. Cross-contamination of cell lines has been problematic in cellular biology

research since the establishment of the first human cancer cell line in the 1950s, the historically important cervix carcinoma-derived HeLa cell line (Gey, 1954). Around the time HeLa cells were established, karyotyping and immunophenotyping methods for identifying cell lines were garnering interest, with reports beginning to highlight cell lines that differed from their stated species of origin (Brand & Syverton, 1962). Soon after, HeLa cells were found to have contaminated 18 other independent human cell lines (Gartler, 1967). Of these, the haematopoietic cell line, J-111, first published in 1955 as an acute monocytic leukaemia cell line, was found to be HeLa (Nelson-Rees & Flandermeyer, 1976). Remarkably, publications continued to use J-111 as a model for different leukaemia subtypes up to the 1990s, despite having a completely distinct morphology to common haematopoietic cell lines (Hans G Drexler, 2010).

Since then, instances of cellular cross-contamination have continued to be reported where it is estimated that between 20-36% of publications using cell lines that have been cross-contaminated or misidentified (Bian et al., 2017; Hukku et al., 1984; Masters et al., 2001). Worryingly, in 2016, over 40,000 articles were published that cited literature containing contaminated cell lines (Horbach & Halffman, 2017).

During the last two decades, valuable contributions by Hans Drexler, Amanda Capes-Davis and others have highlighted the problem where scientists have failed to ensure their cell lines are pure and of a single origin. In response to this chronic and widespread problem, the International Cell Line Authentication Committee (ICLAC), chaired by Dr. Capes-Davis, have established a curated register of misidentified cell lines that is regularly updated (Capes-Davis et al., 2010). The issue has been problematic across a wide range of cancer cell lines (Y. Huang et al., 2017). At the time of writing, 509 cell lines are misidentified with no known authentic stock, of which U-937 has been long known to be one of the most common contaminating cell lines (according to the ICLAC website). Haematopoietic cell lines seem to be particularly susceptible to cross-contamination and misidentification, with up to 15% of leukaemia- and lymphoma-derived cells lines having been falsely identified (H G Drexler et al., 2003). Indeed, four cell lines that were originally described as monocytic leukaemia cell lines were misidentified and are, in fact, *bona fide* U-937 (Ohta et al., 1986).

It is important that researchers using cell lines be cognizant of the historic pervasiveness of cell line cross-contamination and misidentification, of which U-937 has been prevalent. Cell line misidentification and cross-contamination has negative repercussions for scientific reproducibility and quality, as well as a waste of time and valuable resources. Cell lines are model systems used instead of primary samples and so must faithfully

| Discussion

correspond to the disease systems they are purported to represent. Therefore, it is imperative that laboratories take the necessary precautions to ensure their cell lines are pure and of a single origin.

8.2 Characterisation of TS LOW and TS HIGH

In this study, we originally employed a cytometry-based sorting strategy to separate the MDS/sAML cell line, SKK-1, into distinct populations based on their fatty acid uptake capacity. We report that after three consecutive rounds of sorting TS LOW and TS HIGH populations display stable low and high fatty acid uptake phenotypes. Metabolic and transcriptomic characterisation of TS LOW and TS HIGH cell lines revealed significant differences, which may underlie the difference in fatty acid uptake capacities. Specifically, we observe that TS LOW is associated with a more stem cell-like immunophenotype and a lower OXPHOS capacity, compared to TS HIGH. Importantly, however, we must interpret these results in light of the fact that these subpopulations contained both SKK-1 cells as well as contaminant U-937-derived cells.

8.2.1 Stable uptake phenotype: inherent feature or contamination-dependent?

The SKK-1 cell line is derived from a patient who developed sAML following MDS (Matsuoka et al., 2005). and represents one of the few cell lines representative of this leukaemic transformation that is easily grown in culture. For this reason, we chose SKK-1 as a disease model to further characterise and study fatty acid metabolism. After each of the three rounds of sorting, the respective uptake phenotypes of the low- and high-sorted cells remained stable, suggesting genetic factors influencing the difference. Although we do not rule out the possible contribution of epigenetic factors, we suspect that the observed difference would have been more transient and fluctuate over time were epigenetic regulation prominent.

The original stock of SKK-1 was identified by STR profiling but, as we have shown, it is likely U-937 cells were present at low and undetectable levels. Since we are not able to guarantee we were working with pure cultures of SKK-1 from the beginning of the study, we cannot attribute the observed uptake phenotypes to inherent properties of SKK-1 alone, even after the first round of sorting when there were undetectable levels of U-937. Similarly, we cannot attribute the phenotypes solely to U-937, as we cannot rule out the influence of SKK-1 in TS LOW and TS HIGH. Therefore, two issues require some attention in the context of this discussion: first, whether U-937 contamination is the main contributor to the observed metabolic and genetic differences, and second, whether these observed differences are independent of the contaminating cells and, indeed, are inherent properties of both SKK-1 and U-937.

Apart from TS LOW and TS HIGH, other AML cell lines did not appear to be amenable to wide separation into stable phenotypes. Sorted SKM-1 cells showed subtle but consistent

differences in fatty acid uptake, while we did not see noticeable differences when we sorted THP-1. This suggests that, in the context of this study, the ability to separate cells into stable phenotypes may be an inherent metabolic heterogeneities of both SKK-1 and U-937. Nevertheless, further characterisation of isolated subclones will be required to investigate whether pure SKK-1 and U-937 parental cells are capable of being separated into distinct phenotypes, independent of a mixed population. The identity of the subclones will need to be confirmed by means of STR, immunophenotype and karyotype.

On the other hand, the presence of U-937 cells may have altered the metabolism of the mixed population through genetic instability. As previously discussed in section 5.1.2, the U-937 cell line is inherently genetically unstable. The blend of different U-937 subclones with complex karyotypes may have caused significantly altered gene expression and, in this way, metabolically distinct subclones emerged in the form of TS LOW and TS HIGH cells. In addition, altered gene expression in some cells may have caused the secretion of paracrine factors that affect lipid metabolism in the bulk population. It is known that AML cells secrete cytokines, such as interleukins and interferons, that affect cell survival and differentiation in an autocrine manner (Kupsa et al., 2012). For instance, patient AML cell-derived interleukin-6 and -8 were shown to cause increased low-density lipoprotein uptake in AML cell lines (Bhuiyan et al., 2017). In the same study, these factors were shown to autostimulate low density lipoprotein uptake in the AML cells themselves, suggesting a strong role for intracellular metabolic signalling. It remains to be seen if a similar relationship could exist between altered gene expression and secretory factors in the context of TS LOW and TS HIGH that affects fatty acid uptake.

Taken together, we need to consider the differences of TS LOW and TS HIGH in the context of contributing factors from the contaminating U-937 cells and intrinsic characteristics of SKK-1 and U-937. However, as U-937 appear to be the dominant cells in TS LOW and TS HIGH, it is likely that the differences observed are U-937-related.

8.2.2 Transcriptional differences between TS LOW and TS HIGH might reflect differences in cell composition

The transcriptomic characterisation of TS LOW and TS HIGH cell lines revealed significant differences. We observed that TS LOW is associated with a stem cell-like gene expression signature associated with a corresponding immuniphenotype. In TS LOW, genes relating to long chain fatty acid transport were down-regulated. This included *FABP4*, which plays a major role in lipid transport in the cytoplasm (Tabe et al., 2017). Terms relating to cell surface receptors and receptor tyrosine kinase receptors were apparent among those up-regulated in TS LOW. Our study revealed up-regulation of *KIT*

at both the transcriptional and protein levels in TS LOW. CD117, encoded by *KIT*, is a cell surface receptor on HSC and progenitor cells that, upon interaction with its ligand stem cell factor, provides cellular signals for survival, proliferation and differentiation of both normal HSCs and malignant stem cells (Wells et al., 1996). CD117 co-expression with CD123 and HLA-DR cell surface markers on TS LOW highlighted a more stem cell-like phenotype compared to TS HIGH. In contrast, loss-of-function mutations in *KIT* have been shown to regulate mitochondrial activity via the PGC α transcription factor, hinting at its potential relevance in metabolism regulation (Z. Huang et al., 2014). Further, *FLT3*, another receptor tyrosine kinase, was found to be up-regulated in TS LOW. *FLT3* with an internal tandem mutation is found in up to one-third of AML cases and predicts poor prognosis (Lin et al., 2016; Sumiyoshi et al., 2017). This mutation results in constitutive expression of its gene product that causes increased proliferation of LSCs (Kiyoi et al., 1998).

KIT, *FLT3* and many of the other genes found upregulated in TS LOW in respect to TS HIGH are expressed SKK-1 but not U-937 cells. As such, the observed transcriptomic differences might have been caused by differences in the ratio of remaining SKK-1 cells in the two U-973 dominated populations.

8.2.3 Low OXPHOS capacity in TS LOW and TS HIGH

Indications that TS LOW and TS HIGH rely more on glycolysis than OXPHOS for energy was also suggested from our respirometry analysis. The spare reserve capacity is defined as the difference between basal and maximal respiratory rates, as determined by oxygen consumption rates after the addition of oligomycin to inhibit ATP synthase activity and FCCP to uncouple ATP synthesis from the electron transport chain. AML cell lines and LSCs were both previously shown to have lower spare reserve oxidative capacity than normal HSCs (Sriskanthadevan et al., 2015). This is in agreement with our observation that the more stem-like TS LOW showed lower maximal oxidative capacity than TS HIGH, hinting that TS LOW is representative of LSCs on the metabolic level. Increased mitochondrial respiration has been associated with increased mitochondrial mass (Sriskanthadevan et al., 2015) and LSCs have been shown to have higher mitochondrial mass than normal HSCs (Škrčić et al., 2011). However, we did not observe significant differences in mitochondrial content, despite the observed higher oxidative capacity in TS HIGH. Low mitochondrial content was also evident when we prepared mitochondria isolates from TS LOW and TS HIGH cells for respirometry analysis. Large quantities of at least 200×10^6 cells are normally required for optimal yields of mitochondria for analysis (Jung et al., 2009; Sriskanthadevan et al., 2015), however we did not detect sufficient amounts of mitochondria needed, despite using more than with this quantity of TS LOW

| Discussion

and TS HIGH cells (data not shown). Further, the previously discussed up-regulation of *FLT3* in TS LOW may suggest a propensity towards glycolytic metabolism. Constitutive activation of *FLT3* is associated with increased glycolysis by activating the glycolysis enzyme hexokinase 2 and a subsequent decrease in mitochondrial respiration (Ju et al., 2017).

Taken together, the metabolism of TS LOW and TS HIGH cells may be more glycolytic than we previously estimated, with low reliance on OXPHOS for energy and an apparent low number of mitochondria. There are subtle, but significant, differences in oxidative respiration between TS LOW and TS HIGH difference, which may account for the differences in fatty acid uptake.

8.3 A novel means to explore epigenetic-metabolic interactions

The interplay between epigenetics and metabolism has gained increasing attention in recent years, as researchers attempt to solve the regulatory underpinnings of metabolic pathways and, in turn, how altered metabolism can affect epigenetic processes. Indeed, the overarching aim of the innovative training network, ChroMe, a H2020 Marie Skłodowska Curie Action, that I have been a part of during my PhD studies, was to highlight epigenetic-metabolic cross-talk in biology and explore its role both from basic biology and disease-centred standpoints. The network of 15 PhD students and their supervisors in research centres across Europe have attempted to unravel some of the questions in research areas such as circadian rhythm, histone variants and mitochondrial biology, among others.

From the outset of my doctoral project, we were faced with the task of devising a strategy that allowed us to explore metabolic consequences of perturbed epigenetic regulators in the context of leukaemia. A number of prominent articles at the time led us to lipid metabolism as a highly relevant area of study with the potential to identify new points for therapeutic intervention (summarised in Maher et al., 2018). Hence, we decided to focus on lipid metabolism and to use a simple metabolic read-out as proxy of its activity. Specifically, we utilised flow cytometry to measure the intracellular accumulation of fluorescence-labelled fatty acids. As flow cytometry allows for the simultaneous detection of multi-colour fluorophores, we predicted that other analytes of interest, such as cell surface markers, could be measured simultaneously and coupled with fatty acid uptake. Further, this approach provided a simpler means to detect fatty acid uptake than established methods that require more complex equipment, such as stable isotope measurement by mass spectrometry (Schönfeld & Wojtczak, 2016), or unspecific staining of intercellular fatty acids by Nile red (Kim et al., 2004). In this way, the hEpi9 shRNA library afforded us the opportunity to investigate the phenotypic consequences of knocking down a wide range of epigenetic genes.

8.3.1 Targeting metabolic features of AML cells

Relapse following intensive treatments is common in several cancer types, including AML, due to resistant clones. Immunotherapy approaches that target cell-specific antigens have been developed in recent years, particularly for lymphomas. However, unlike lymphoid neoplasms, it has proven difficult to identify cell surface markers that are expressed sufficiently differently on myeloid LSCs compared to healthy myeloid cells as a means to specifically target cancer cells (Valent et al., 2019). Indeed, only a few antibody-based drugs targeting critical cell surface markers are available for treating myeloid neoplasms.

Targeting unique metabolic features of cancer cells could be an effective means of drug therapy without damaging healthy cells.

Although azacitidine is one of the most effective treatment strategies for MDS and AML, only 50% of patients show a response, most of whom go on to relapse (Santini et al., 2014). The exact reasons for resistance are unknown, but may include a reduction in drug efflux, support structures of the bone marrow niche or poor penetration of the drug to the microenvironment (Housman et al., 2014; Qin et al., 2011). Fatty acid metabolism has been implicated in increased azacitidine resistance, and, similarly, azacitidine has been shown to induce changes in lipid homeostasis (Poirier et al., 2014). Metabolic features of AML cells are being considered as potential therapeutic targets in combination with existing therapies. Up-regulation of fatty acid transporters and beta-oxidation has been associated with increased drug resistance and poorer survival in patients (Perea et al., 2005; Shi et al., 2016). Central to beta-oxidation is the mitochondria membrane-bound transporter, carnitine palmitoyltransferase 1 (CPT1). Etomoxir inhibits beta-oxidation by blocking CPT1 activity (Abdel-aleem et al., 1994) and has been shown to sensitize AML cells to treatment and reduce proliferation (Ricciardi et al., 2015; Samudio et al., 2010). In addition, inhibiting mitochondrial complex activity in AML cells has been reported to also inhibit glycolysis activity (Lagadinou et al., 2013). Thus, targeting differences in fatty acid metabolism may represent an alternative and viable strategy.

8.3.2 Mixed results from shRNA screen validation

We originally employed the hEpi9 library of short hairpins in a genetic screen to knockdown 912 epigenetic regulatory and chromatin remodeler genes on a by-cell basis to investigate effects on fatty acid uptake. Following single gene knockdowns of selected candidates based on the shRNA knockdown screen in SKK-1, we could not validate genes with significant effects on fatty acid uptake. Further, the fact that knockdowns of known regulators of fatty acid uptake such as the CD36 and CPT1a transporters did not cause significant reductions in laurate uptake in SKK-1, KG-1 or TF-1 cells indicated that the assay might not have been variable and robust enough. The choice of a labelled MCFA as substrate, together with the low OXPHOS rate observed in SKK-1 cells, may further have contributed to a narrow dynamic range of the uptake assay. We would have expected these changes in uptake to be an indirect consequence of diminished epigenetic regulator activity; nevertheless, we did not observe significant effects on fatty acid uptake.

8.3.3 Choice of labelled fatty acid

While palmitate was our preferred choice for studying differences between TS LOW and TS HIGH in this study, we used a red-labelled laurate, a 12-carbon medium chain fatty acid

(MCFA), for separating cells for the shRNA knockdown screen. The decision was mainly due to fluorescence detection constraints on the flow cytometer when combining green-labelled palmitate and GFP-positive shRNA-expressing cells. In contrast to LCFAs, there is relatively little in literature regarding the transport mechanisms of laurate across the cellular membrane. It is thought that MCFAs move by a combination of active and passive transport, depending on the carbon chain length. A study across a range of human cell lines showed that uptake of the 18-carbon fatty acid, oleate, was enhanced when co-treated laurate, suggesting that there is little competition for transport between MCFAs and LCFAs (Kitaura et al., 2015). Rodents fed with an MCFA-rich diet were shown to have increased mitochondrial enzyme activity in muscle but no change in fatty acid binding protein, which, in contrast, increased with an LCFA-rich diet (El-Brolosy & Stainier, 2017).

A drawback of our knockdown approach was the lack of control target genes known to regulate fatty acid uptake. The use of palmitate as substrate may have provided clearer phenotypes following knockdowns of the palmitate transporters, CD36 and CPT1a. In general, the longer the chain length of a fatty acid, the more membrane-bound active transporters are recruited (Freudenberg et al., 2012). Therefore, the mixed associations we observed with CD36 and CPT1a knockdowns and MCFA uptake may be explained by a predominance of passive transport across both cellular and mitochondrial membranes. The reduction in fatty acid transporter activity – targets that were predicted to associate most with fatty acid uptake – via shRNA interference may not have inhibited MCFA uptake to measurable levels. This is contrast to the significant reduction we observed in LCFA uptake when we inhibited CPT1a with the compound inhibitor, ETX, thereby preventing mitochondrial LCFA uptake and blocking fatty acid oxidation.

Indeed, doubts have been raised as to the suitability of MCFAs to study uptake transporters. In a study using labelled laurate to investigate the involvement of FABP in fatty acid uptake in skeletal muscle *in vitro*, the researchers concluded that the MCFA may not have been representative of physiological conditions (Ishizawa et al., 2015).

Overall, LCFAs are the most physiologically relevant fatty acids. Due to the involvement of various transport proteins for the uptake of palmitate, this fatty acid may be a more suitable substrate to study epigenetic regulation of lipid metabolism. To overcome the differences in MCFA and LCFA uptake in future studies, we would explore the possibility of conjugating a red fluorophore with palmitate.

8.3.4 Narrow dynamic range of fatty acid uptake assay and cell line

It was evident from our mitochondrial respiration tests that SKK-1 cells display low OXPHOS capacity and, as a consequence, it is likely that fatty acids are not the preferred

| Discussion

fuel source in growth conditions with high glucose and glutamine, such as in RPMI growth media. Therefore, utilising fatty acid uptake capacities as the principle metabolic read-out may not have represented a large enough dynamic range under the given culture conditions and choice of cell line.

Studies have shown that cell lines can be primed to utilise fatty acids as a preferred fuel source under chronic low glucose conditions, as shown by increased rates of fatty acid oxidation (Weightman Potter et al., 2019). Incorporating a similar a nutrient conditioning approach to the uptake assay could yield a broader range of fatty acid uptake capacities that are more sensitive to perturbations to chromatin regulators. Further, the bone marrow is a hypoxic environment, as measured by low oxygen tension (Spencer et al., 2014). LSCs are adapted to utilise OXPHOS under hypoxic conditions of the bone marrow, whereas normal HSCs rely on aerobic glycolysis, as has been evidenced in leukaemia cell lines (Goto et al., 2014). Therefore, growth conditions that resemble physiologically relevant metabolic stress, such as that found in the hypoxic bone marrow niche, are required. These conditions comprise low serum concentration, lipoprotein-deficient media and hypoxic conditions (2% oxygen) to replicate *in vivo* conditions (Lisec et al., 2019).

In addition, cell lines that demonstrate OXPHOS capacity are desirable in order to better study fatty acid metabolism in the context of AML. However, most cancer cell lines tend towards a more glycolytic metabolism where sugar is more readily converted to energy. In particular, aerobic glycolysis may be brought about by hypoxic conditions in the tumour environment (see review (Jose et al., 2011), which is not directly replicable in regular cell line growth conditions. In contrast, THP-1 cells have been shown to utilise OXPHOS under hypoxic conditions and display higher growth capacity than in normoxic conditions (Goto et al., 2014; Sukanuma et al., 2010), suggesting that it may represent a more appropriate cell line to study fatty acid metabolism. Further, THP-1 cells undergo a shift from glycolysis to OXPHOS when glycolysis is inhibited (MIWA et al., 2013).

Overall, cell culture conditions and cell line choice may have a significant influence in order to improve the dynamic range of our fatty acid uptake assay and gain more physiologically relevant insight.

8.3.5 Fatty acid uptake as selection criterion for screen

Typically, cellular fitness is used in genetic screens as the phenotypic readout, whereby increased cell viability is inferred as positive and decreased viability as negative. In general, cell viability is a clear indicator of gene perturbations. As previously discussed, the dynamic range of our fatty acid uptake assay may not represent a robust phenotypic

readout to detect genes directly affecting uptake activity. However, as fatty acids are not crucial factors to cell survival, especially in environments of high glucose, we estimate that cell viability would not greatly differ in cell populations characterised by low and high fatty acid uptake. For this reason, we believe that fatty acid uptake is more suitable readout than a cell viability readout for the purpose of our knockdown screen. Further, our metabolic readout represents a novel means to both delineate and validate sample groups.

8.3.6 Advantages and limitations of shRNA knockdown screens

ShRNA knockdown screens are relatively simple to perform, however, interpreting statistically significant hits from noise can be a challenge. We applied an arbitrary cut-off for fold-enrichment and significance to select the top candidates. A more comprehensive statistical approach incorporating the biological significance of the target genes, such as known interactions with lipid metabolism pathways, may have provided a more informed list of candidate regulators. A p-value of 0.05 was chosen as cut-off for determining the top significant hits for both individual hairpins and gene-wise enrichment analysis. This p-value corresponds to a 5% chance of detecting false positive results. Although 5% is scientifically acceptable when comparing two sample groups, we would expect 364 individual hairpins and 45 of genes to be falsely identified as positive hits by using this significance level. A second screen containing a pooled library of selected top hits could be performed as an additional validation and a way to improve statistical power.

In our search for epigenetic regulators of fatty acid uptake, our scope was limited to the 912 target genes of the hEpi9 library. In future studies, we would consider performing an unbiased, genome-wide screen in order to incorporate a broader spectrum of candidate regulators.

For instance, recently, a pooled genome-wide CRISPR screen with cells carrying a loss-of-function of a *de novo* fatty acid synthesis enzyme, fatty acid synthase (*FASN*), revealed a novel regulator of lipid uptake (Aregger et al., 2019). The researchers incorporated a genetic interaction mapping approach, which uses pairwise perturbations of genes, such as depletions or overexpression, to explore the functional relationship between two genes by studying how the phenotype of one gene affects another. Such a method may reveal more closely linked metabolism-epigenetics interactions.

The silencing activity directed to mRNA during shRNA knockdown means that residual protein function can remain. An argument in favor is that such a partial inhibition might resemble what can be achieved with drugs in the clinical setting. Debate is ongoing surrounding the merits of either knockdown or knockout screens in investigating novel gene functions. Variable knockdown efficiencies and off-target effects are well-

| Discussion

documented in shRNA-based screening (Smith et al., 2017). In contrast, knockout approaches, such as the prokaryotic immune system-derived clustered regularly interspaced short palindromic repeated (CRISPR)-associated protein 9 (Cas9), ablates gene function completely (Doudna & Charpentier, 2014). For measuring gene essentiality across different cell lines, the CRISPR technology has been shown to out-perform a comparable shRNA-based knockdown screen, showing less variation in data, reduced off-target effects and improved consistency across samples (Evers et al., 2016). However, gene compensation may arise in response to a gene knockout, whereby RNA or protein can compensate for the loss of function of another gene (Deplus et al., 2014). This may be in the form of upregulation of related genes with redundant functions or genes within the same regulatory network.

Perhaps paradoxically, more pronounced gene activation has been observed following gene knockouts compared to gene silencing. For instance, gene silencing-mediated reduction in the demethylating enzyme, *Tet1*, resulted in less methylated cysteines and increased morphological changes in mouse embryonic stem cells compared to *Tet1* knockout in the same system (Dawlaty et al., 2011). The authors suggested a compensatory mechanism involving the functionally similar *Tet2* in the knockout, but not knockdown cells.

Off-target effects of RNA interference are sources of erroneous results in genetic screens and can be caused by two main modes: non-specific effects on non-target genes by mRNA destabilisation or activation immune response and apoptotic pathways (Rao et al., 2009; Singh et al., 2011). The micro RNA backbone (“miR-E”) encoded on the cSGEP expression vector used in this study has been optimised to increase guide strand incorporation, thereby maximising on-target knockdowns and minimising off-target effects (Chang et al., 2009; Fellmann et al., 2013). To further buffer off-targets effects, eight hairpins targeting each gene were included in the hEpi9 shRNA library. Indeed, off-target effects are not exclusive to RNA interference, as guide strand incorporation on non-target loci has also been reported in CRISPR-based knockout screens (Fu et al., 2013).

Taken together, there are merits and disadvantages to using RNAi over CRISPR/Cas9, or other gene deletion methods, to elucidate genotype-to-phenotype associations. While RNAi represents a clinically significant approach to gene perturbation by only partially knocking down gene activity, the residual activity of *the epigenetic regulators may have been sufficient such that changes in fatty acid uptake were not observable. Our shRNA knockdown represents a novel approach to the problem. With adaptations to the assay

and a genome-wide approach with a second targeted validation screen, a wider range of candidate regulators may be uncovered.

8.3.7 A role for PADI4 in fatty acid metabolism?

PADI4 emerged as the only candidate gene to have a potential effect on fatty acid uptake. *PADI4* has not been associated with lipid metabolism regulation previously. We decided to further investigate this gene as it ranked highly on the list of enriched up regulated genes in TS LOW. *PADI4* has a dual mechanism in regulating gene expression and protein activity through the conversion of arginine and monomethyl-arginine to citrulline (**Figure 46**). First, *PADI4*-mediated citrullination of histones causes demethylination of arginine residues, resulting in chromatin decompaction and changes in gene expression (Christophorou et al., 2014; Song et al., 2016). Second, post-translational modification of non-histone proteins, such as DNMT3a and P300, by citrullination can cause changes in protein conformation resulting in either stabilisation or loss-of-function (Liu et al., 2006). For example, citrullination of *de novo* DNMT3A stabilises the protein and increased DNA demethylase activity (Jiang et al., 2013).

Of the five known PADI isotypes, *PADI4* is mainly expressed haematopoietic and immune cells, namely monocytes, macrophages and lymphocytes (Mondal & Thompson, 2019). Specifically, *PADI4* is thought to assist in monocyte differentiation (Jiang et al., 2013). *PADI4* has also been prominently associated with immunological conditions, such as rheumatoid arthritis and neutrophil extracellular trap formation in macrophages (Lewis et al., 2015). In addition, *PADI4* has been reported to be overexpressed in a variety of malignant blood and tissue samples (Jang et al., 2012), thus marking it out as a potential therapeutic target. Consistent with our observation that ATRA treatment induces *PADI4* expression and a decrease in fatty acid uptake, translocation of *PADI4* to the nucleus has been reported under the same conditions (Cook et al., 2018), suggesting a direct role in gene regulation. Induced overexpression of *PADI4* reduced the viability of HL-60 cells with concomitant expression of the p53 proto-oncogene and accumulation of the apoptosis-related protein, Bax (Liu et al., 2006).

Analysing histone citrullination has been previously shown to be a reliable method of measuring *PADI4* enzyme activity (Zhou et al., 2018). A limitation of our validation experiments was that we did not measure citrullination levels in our knockdown cells, which may have revealed the intercellular impact of *PADI4*.

In addition to aforementioned DNMT3A and p53, there may be other several citrullinated proteins that are relevant in AML. One such candidate highly relevant in glucose

metabolism is alpha enolase (ENO1), which is a key glycolytic enzyme that is active in hypoxic conditions. ENO1 was found to be a novel citrullinated enzyme in cancer cell lines, however citrullination can result in diverse ENO1 functions depending on the citrullination site (Jang et al., 2012). In addition, citrullinated ENO1 peptides were shown to induce an immune response that specifically targeted ENO1-expressing tumour cells in transgenic mice (Cook et al., 2018), suggesting that ENO1 is a good anti-tumour target. Indeed, ENO1 is one of the most over expressed genes in AML (Hands Schuh et al., 2018). It would therefore be interesting to investigate the potential involvement of PADI4 overexpression as a means to reprogramme AML cells to increased glycolysis and reduce fatty acid uptake. Taken together, further investigation into the role of PADI4 in haematological malignancies and its potential interaction with cellular metabolism is warranted.

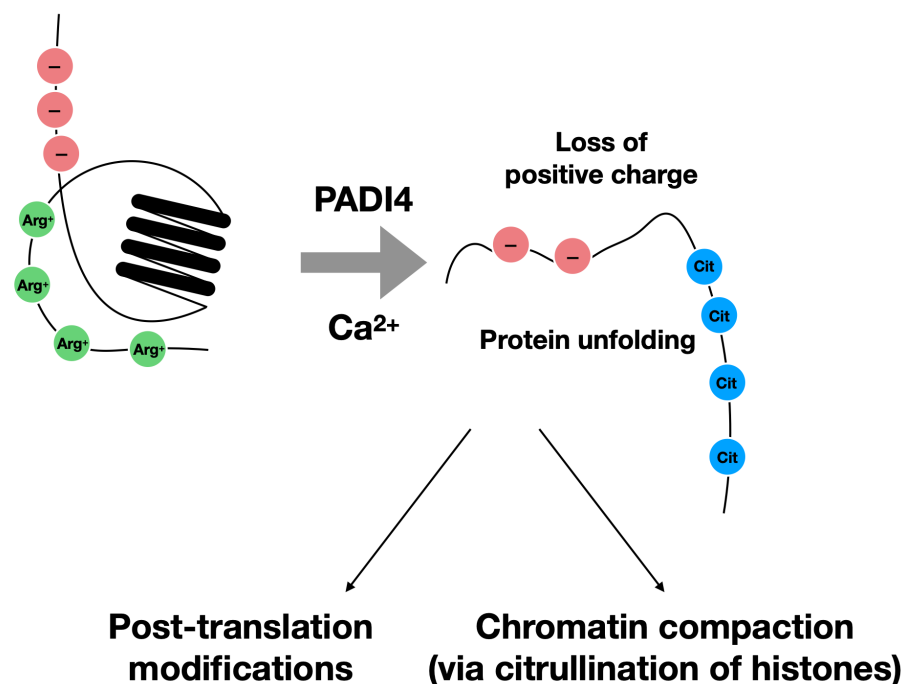


Figure 46: Peptidyl arginine deiminase 4 (PADI4) acts to both suppress and activate gene expression in cancer. PADI4 catalyses the conversion of positively charged arginine residues to citrulline, which causes proteins to change conformation resulting in altered protein activity and, in the case of histones, chromatin compaction.

8.4 The role of diet in haematological malignancies

A deeper understanding of lipid metabolism properties specific to the MDS to sAML leukaemia sub-type is needed. From the perspective our study, it would be interesting to investigate how the low and high fatty acid uptake phenotypes observed in cell line models correlate with those of LSCs and normal HSCs from primary patient samples. Although we observed clear differences in fatty acid uptake between TS LOW and TS HIGH, it is still unclear whether these phenotypes are representative of divergent energy metabolism, such as glycolysis and OXPHOS. Additional respirometry experiments will reveal the contribution of other oxidative or non-oxidative energy pathways to compare the two phenotypes. Here, I discuss our results in light of some recent findings regarding nutritional interventions in cancer.

With the lingering failure of pharmaceutical therapies to provide curative solutions to many haematological malignancies, attention is warranted in nutritional-based approaches to preventing onset and treating these diseases.

Obesity is a leading risk factor for cancer development, including MDS and AML (Ma, 2009; Li, 2017). Epidemiological evidence points to increased risk for developing AML in people with a body mass index (BMI) of over 30 kg/m² compared to 25 kg/m² (Castillo et al., 2012), with similarly findings for MDS in people BMI over 35 kg/m² (Poynter et al., 2016).

Although diet is known to play a significant role in determining cancer risk, identifying precise mechanisms in tumourigenesis is complicated by the large number of effects of obesity. High levels of circulating saturated fatty acids in the serum, such as palmitate, induce inflammation, which is a key factor in cancer development (Balkwill et al., 2005).

Marrow adipose tissue (MAT) is similar in cellular morphology to white adipose tissue, but with a distinct gene expression profile (Zinngrebe et al., 2020). MAT comprises the majority of cells in the bone marrow, accounting up to 70% of the bone marrow volume in adults (Hindorf et al., 2010). Further, the proportion of MAT increases with age (Ambrosi et al., 2017) and obesity (Zinngrebe et al., 2020). Increased fat content can decrease the usable space for other cells to grow, which along with age-related decreased cellularity, contributes to reduced support structures for normal haematopoiesis (Reinisch et al., 2015).

Though blood malignancies are broadly associated with dysfunctional HSC in the bone marrow, excess adipose tissue may increase the risk of haematologic disease, as well as protect cancer cells from drug therapies (Behan et al., 2009). MAT has been shown to be

| Discussion

a negative regulator of normal haematopoiesis (Naveiras et al., 2009), while also providing free fatty acids to proliferating AML cells (Shafat et al., 2017). Protective features most likely come from interactions between adipocytes and LSCs, such that HSCs resident in adipose tissue are protected from the cytotoxic effect of drugs (Ye et al., 2016). Recently, high-fat diet fed to *MLL-AF9* knock-in mice was shown mechanistically to stimulate FLT3 signaling and downstream pathways in HSCs, which, in turn, accelerated leukaemogenesis (Hermetet et al., 2020). Epigenetic-associated mechanisms have been attributed to AML burden in high-fat diet-induced obese mice, whereby aberrant DNA methylation in AML cells was linked to increased FABP4 activity, which is a marker strongly related to fat mass (Yan et al., 2017, 2018).

As we have noted here and others have presented in previous studies (Chapuis et al., 2019), metabolic pathways are a worthy basis for developing therapies as well as devising non-pharmacological strategies for dampening disease risk. As most pharmacological compounds that target fatty acid metabolism remain in preclinical studies (Röhrig & Schulze, 2016), dietary interventions and nutritional supplementation are being considered as a means to reducing risk factors of MDS and AML. Caloric restriction and fasting have been shown to prolong life and increase immune system response (O’Flanagan et al., 2017) and has been promoted as a robust means of reducing cancer risk (Nencioni et al., 2018). However, clinical effects from diet interventions in blood cancers may not follow predicted outcomes, as in other conditions. Paradoxically, MAT has been shown to increase under caloric restriction (Cawthorn et al., 2016), suggesting a distinct metabolism compared to other adipose tissue in the body. Although the effects of such dietary interventions on haematological disease remain largely unexplored, the caloric restriction mimetic drug, temsirolimus, is being studied in the context of AML (O’Flanagan et al., 2017). Bioactive components from nutritional supplements have shown promise as cancer therapies. Curcumin, a component of the Indian spice turmeric, has been shown to have hypomethylating activity and was shown to be effective in down regulating DNMT1 activity in AML cell *in vitro* and *in vivo* (J. Yu et al., 2013). Resveratrol, a polyphenolic compound derived from grapes, has shown promise across a number of cancers for its anti-oxidative effects. Resveratrol has been shown to induce apoptosis and differentiation as well as inhibit growth in AML cells (X. Huang et al., 2019). Overall, the role of dietary lipids deserves further exploration in the context of MDS and AML development.

Conclusions

9. Conclusions

1. We were unable to validate top hits from the shRNA genetic screen, which we propose may have been due to assay design and sub-optimal growth conditions for measuring fatty acid uptake.
2. Sorted sub-populations of SKK-1 cells retained distinct low and high fatty acid uptake phenotypes over time, where other cell lines did not. However, the low OXPHOS capacity of SKK-1 may render these cells unsuitable for studying fatty acid metabolism.
3. U-937 cells expanded over time in SKK-1 parental cells and the sorted TS LOW and TS HIGH cells while growing in culture, most likely due to latent contamination.

Materials and Methods

10. Materials and methods

10.1 Cell lines and cell culture

The human MDS/AML cell lines SKK-1, KG-1, TF-1, HL-60, SKM-1, THP-1, MOLM-13 and F-36P were obtained from the Leibniz-Institute DSMZ - German Collection of Microorganisms and Cell Cultures (Braunschweig, Germany) and in part through collaboration with Prof. Hans Drexler. Following the providers' instructions, cell lines were cultured in RPMI 1640 (ThermoFisher Scientific) supplemented with 10% (SKK-1, KG-1, TF-1, HL-60, THP-1 and MOLM-13) or 20% fetal bovine serum (SKM-1, F-36P), 1% Pen/Strep, and 1% L-glutamine at 37 °C in 5% CO₂. HEK293t cells (ATCC, CRL-3216) were cultured in DMEM supplemented with 10% foetal bovine serum, 1% Pen/Strep, and 1% L-glutamine (Gibco) at 37 °C in 5% CO₂. All cell lines were routinely analysed for the presence of mycoplasma. Details of the cell lines used are shown in Table 5.

Table 5: List of cell lines used

| Cell line | Representative disease | Source | Reference |
|-----------|-----------------------------------------------------------|--------------------------|-----------------------|
| SKK-1 | Progression from MDS to sAML | DSMZ/Hans Drexler | RRID:CVCL_S607 |
| KG-1 | Progression from erythroleukemia to AML | DSMZ | ACC 14 |
| TF-1 | Erythroleukemia | DSMZ | ACC 334 |
| HL-60 | Acute promyelocytic leukemia | DSMZ | ACC 3 |
| SKM-1 | Progression from MDS to acute monoblastic leukemia | DSMZ | ACC 547 |
| THP-1 | acute monocytic leukemia | DSMZ | ACC 16 |
| MOLM-13 | Progression from MDS to AML | DSMZ | ACC 554 |
| F-36P | Progression from MDS to sAML | DSMZ | ACC 543 |

10.2 Fatty acid uptake assay

Fluorescence BODIPY-labelled palmitate (excitation 503 nm/emission 512 nm) and laurate analogues (excitation 558 nm/emission 568 nm) (ThermoFisher Scientific) were solubilised in deionised water to a concentration of 2.4 mM (Figure 47). 1.5 million cells were seeded in 6-well plates in 3 mL RPMI growth media and incubated overnight at 37 °C. The following day the cells were centrifuged and incubated for 60 minutes at 37 °C with 3 mL cell buffer (10% phosphate buffered saline (PBS), 0.5 µM BODIPY-labelled fatty acid and 0.5% bovine serum albumin (BSA)). Based on the initial optimisation assays, 60 minutes and 0.5 µM were chosen as the incubation time and fatty acid concentration, respectively. A stop buffer (10% PBS and 2.5% BSA) was added to the cells to block further uptake of the fluorescent fatty acids, which were centrifuged again and the supernatant was discarded. The cells were then stained with DAPI, incubated in the dark for 15 minutes and brought for acquisition by flow cytometry.

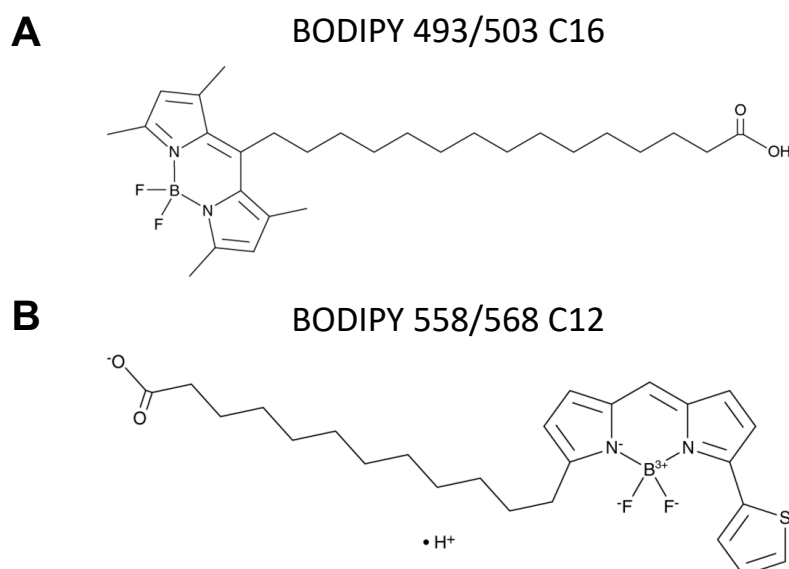


Figure 47: Chemical structures of fluorescence-labelled fatty acid analogues. Both fatty acid analogues are conjugated to BODIPY fluorescence dyes. A) Chemical structure of BODIPY 493/503 C16 (4,4-Difluoro-5,7-Dimethyl-4-Bora-3a,4a-Diaza-s-Indacene-3-Hexadecanoic Acid) showing the 16-carbon chain and BODIPY FL dye with 503 nm excitation and 512 nm emission spectra. B) Chemical structure of BODIPY 558/568 C16 (4,4-Difluoro-5-(2-Thienyl)-4-Bora-3a,4a-Diaza-s-Indacene-3-Dodecanoic Acid) showing the 12-carbon chain and BODIPY FL dye with 558 nm excitation and 568 nm emission spectra.

10.3 Flow cytometry and fluorescence-activated cell sorting (FACS)

For measuring fatty acid uptake, cells were acquired by LSRFortessa flow cytometer (BD Biosciences) at the cytometry facility of the Institut d'Investigació en Ciències de la Salut Germans Trias i Pujol (IGTP). Fluorescence-labelled palmitate was analysed by a 488 nm laser in the green fluorescent protein (GFP) channel and laurate by a 532 nm laser in the phycoerythrin (PE) channel. Non-viable cells were excluded using a DAPI-negative gate. Gating strategy was devised using BD FACSDiva software (BD Biosciences). For sorting, the fatty acid uptake assay was carried out as described above. 20 million cells per cell line were collected in FACS tubes. Cells were sorted on the Aria III cell sorter (BD Biosciences). Based on the Gaussian distribution of palmitate-associated fluorescence, the lowest and highest 10% of the total population were sorted into two separate collection tubes containing RPMI media. The cells were then centrifuged and cultured in fresh media.

10.4 Cell cycle and proliferation

10.4.1 Proliferation assay

PE Mouse anti-Ki67 antibody (BD Pharmingen, USA) and DAPI (4',6-diamidino-2-phenylindole) were used to assess proliferation in SKK-1 cells. Ki-67 is a proliferation marker that is expressed in the cell nucleus during interphase of the cell cycle. As the cells were fixed, DAPI acts as a marker of total DNA content by binding directly to DNA. To detect Ki67 expression, the cells were first fixed by adding cold 70% ethanol dropwise to the cell pellet while vortexing (approximately 0.5×10^6 cells/mL) and incubated at -20°C for at least two hours. Cells were then washed twice with 5 mL PBS with centrifugations of 5 minutes at 1000 rpm between each wash. The cells were then resuspended in PBS to approximately 1×10^6 cells/mL. 100 μL were stained with 10 μL anti-Ki67-PE antibody and incubated at RT for 20-30 minutes in the dark. Cells were then washed twice more with 2 mL PBS with centrifugations of 5 minutes at 1000 rpm between each wash. The supernatant was aspirated and the cells were resuspended in 100 μL PBS containing 1 $\mu\text{g}/\text{mL}$ DAPI. A minimum of 10,000 events were acquired with the LSR Fortessa flow cytometer for each sample were analysed. Analysis was performed using FlowJo software.

10.4.1 Cell cycle analysis

Fixed cells obtained from the Ki-67 proliferation assay were also used for cell cycle analysis with DAPI used as marker of total DNA content. As before, a minimum of 10,000 events for every sample were acquired with the LSR Fortessa flow cytometer. Cell cycle analysis was performed using the Watson univariate model on the FlowJo software, which distinguished the number of cells in sub-G₁ (<G₁), apoptotic cells, G₁, S and G₂/M phases (Watson et al., 1987).

10.4.2 Colony-forming unit (CFU assay)

To study the proliferation and differentiation capacity of SKK-1 cell lines, a clonogenic assay was carried out using MethoCult H4435 Enriched medium (StemCell Technologies). The semi-solid methylcellulose growth media contains a number of cytokines and growth factors: stem cell factor (SCF), interleukin 3 (IL-3), interleukin 6 (IL-6), erythropoietin (EPO), granulocyte colony-stimulating

factor (G-CSF) and granulocyte-macrophage colony-stimulating factor (GM-CSF). These factors facilitate progenitor cells, or colony forming units (CFU), to proliferate and differentiate into distinct colonies of cells where each colony derives from a single CFU. Therefore, the numbers and types of CFUs provides information about the original cell population and their ability to proliferate and differentiate. Three biological replicates and two technical replicates of parental SKK-1, TS LOW and TS HIGH cell lines were tested. First, 1100 cells were added to 1100 μ L MethoCult medium and mixed well. Then, 500 μ L (500 cells) of each replicate were carefully dispensed to wells of a 24-well plate. After 14 days in culture the CFUs were counted using a light microscope.

10.5 Cytogenetics

Cytogenetic studies, karyotype and fluorescent *in situ* hybridization (FISH), were carried out by standard procedures in single cell expanded clones of TS LOW and TS HIGH, at the Cytogenetics Platform, Josep Carreras Leukaemia Research Institute and Institut Català d'Oncologia (ICO).

10.5.1 Karyotyping

20 metaphases were analyzed for each cell line of TS LOW and TS HIGH. Karyotypes analyses were performed as previously described at the Clinical Haematology Department, ICO-Hospital Germans Trias i Pujol (Ruiz-Xivillé et al., 2015). International System for Human Cytogenetic Nomenclature was used to describe the karyotypes (Simons et al., 2013).

10.5.2 Fluorescence *in situ* hybridization

For FISH, conventional G-banding karyotypes were analysed and described following the International System for Human Cytogenetic Nomenclature (ISCN 2016). Cells fixed with Karnoy solution (3 methanol : 1 acetic acid) were hybridized overnight and counterstained with DAPI and analysed under a fluorescent microscope.

Different probes were used to detect several chromosomal abnormalities in single cell expanded clones of TS LOW and TS HIGH. The XL 7q22/7q36 Deletion Probe (MetaSystems, Germany) detects deletions in the long arm of chromosome 7. The IGH/MYC/CEP 8 tri-color dual fusion probe (Abbott, USA) detects the

t(8;14)(q24;q32) reciprocal translocation involving the IGH and MYC gene regions. The BCL2 break apart probe (Abbott, USA) detects chromosomal rearrangements at the BCL2 locus on chromosome 18q21. ETV6/RUNX1 dual color fusion probe (Abbott, USA) detects the t(12;21)(p13;q22) that results in the ETV6/RUNX1 fusion.

10.6 High-resolution respirometry

Oxidative respiration in TS LOW and TS HIGH was measured by Oxygraph-2k high-resolution respirometry (Oroboros Instruments, Austria) using an uncoupler inhibitor protocol. Routine respiration, proton leak and maximal respiratory capacity were measured. 18 hours prior to respirometry cells were seeded at 0.25 million cell per mL in RPMI cell culture medium. The next day, the instrument was calibrated to air (gain for oxygen sensor was set to four) with standard RPMI cell culture medium. The cells were counted and 20 million were resuspended in 100 μ L RPMI media. Cells were added to the stirred chambers (750 rpm) and chambers were sealed to achieve a closed system.

When oxygen consumption reached a plateau, a steady state level was obtained displaying routine respiration. The addition of the oligomycin to a final concentration of 1.25 μ M resulted in leak respiration causing proton leak through the inner mitochondrial membrane. Subsequently, the proton gradient was released by step-wise titration of the uncoupler carbonylcyanide-4-(trifluoromethoxy)phenylhydrazone (FCCP) until maximum respiration was observed. 0.5 μ M rotenone and 5 μ M antimycin A were added to completely block mitochondrial respiration showing residual oxygen consumption which accounts for non-mitochondrial oxygen-consuming processes and was corrected for in the analysis. Analysis of the measurements was performed using Excel DatLabversion5.1.0.20 (Oroboros Instruments, Austria).

10.7 Semi-quantitative analysis of RNA and DNA levels

10.7.1 cDNA synthesis (Reverse Transcriptase)

Total RNA was extracted from cell pellets using the Maxwell RSC simplyRNA Cells Kit (Promega, USA). Briefly, pellets were prepared with 200 μ l homogenisation buffer and then lysed with 200 μ l lysis buffer from the kit. Each sample mix was

vortexed vigorously for 15 seconds and the 400 µl of each lysate was transferred to first well of the cartridge in the Maxwell RSC Instrument. 5 µl of DNase I solution was then added. The remaining steps of the extraction protocol were automated on the Maxwell RSC Instrument. RNA was eluted in 30 µl nuclease-free water. The concentration of extracted RNA and its purity were measured by Nanodrop (Agilent Technologies).

Complementary DNA (cDNA) was synthesized using the SuperScript First-Strand Synthesis System for RT-PCR Invitrogen kit (ThermoFisher Scientific), according to the manufacturer's instructions. Briefly, 2 µg of extracted RNA was mixed with 1 µg of oligo(dT) and nuclease-free water to a volume of 11µl. This was incubated for five minutes at 65 °C in the thermocycler. Then, 4 µl of 5X Reaction buffer, 1 µl of RiboLock RNase Inhibitor, 2 µl of dNTP mix and 2 µl of M-MuLV Reverse Transcriptase were added to the RNA oligo(dT) mix and the entire mixture was incubated for 60 minutes at 37°C followed by a termination heating at 72°C for 5 minutes.

10.7.2 Quantitative reverse transcription PCR (RT-qPCR)

Relative mRNA levels were quantified by quantitative reverse transcription PCR (RT-qPCR) from previously synthesised cDNA. cDNAs were diluted 5- to 20-fold in order to perform RT-qPCR analysis in the QuantStudio 7 Flex system (ThermoFisher Scientific). A mix containing 5 µl SybrGreen (Roche, Switzerland), 0.5 µl of forward and 0.5µl of reverse primer (stock at 10 µM and 2 µl of water was mixed with 2 µl of cDNA in a well of 384-well plate. RT-qPCR conditions are listed in Table 6. For each sample, biological replicates were collected on three separate days and were analysed in as technical triplicates. Relative expression of the gene of interest was obtained by normalizing their concentration to the relative expression the housekeeping gene, GAPDH (primer sequences are listed on Table 15: **List of primers used**). Values were normalized with the expression of the housekeeping gene, GAPDH. Autoclaved double-distilled water (ddH₂O) was used as the non-template control. Primers for qRT-PCR are listed in **Table 15**. Primers were designed in order to span different exons so that by controlling the size of the amplicon genomic DNA contaminations can be avoided. All primers were ordered from either Invitrogen or Integrated DNA technologies in lyophilised form and

were resuspended in nuclease-free water to give a final concentration of 100 μM . For qRT-PCR analysis, primer stocks were at 10 μM and the final concentration in the SybrGreen mix was 0.5 μM . All primers were checked for single product amplification and efficiency doing the standard curve and running the product on 1% agarose gel. The quantification of relative mitochondrial content was carried out as described in Heinonen et al., 2015. The ratio of mitochondrial DNA (MT-CYB gene) and genomic DNA (APP gene) was determined by semiquantitative PCR. The ribosomal RNA-encoded 18S gene was used as housekeeping control.

Table 6: Quantitative reverse transcription PCR (RT-qPCR)

| | | |
|------|---------------|--------------------|
| 95°C | 11 min | X 45 cycles |
| 95°C | 20 sec | |
| 60°C | 3 mins | |
| 60°C | 10 min | |
| 4°C | ∞ | |

10.8 Transcriptomic analysis

For RNA-seq, RNA was sent for library preparation to the Genomic Unit of the Centre for Genomic Regulation Genomics (Barcelona, Spain) where RNA was amplified and enriched for polyA of mRNA. RNA quality control showed RNA integrity number (RIN) was between 9.9 and 10. The sequencing was performed with single read with average read length of 50 bp on an Illumina HiSeq2500 sequencer. Expression transcripts were quantified using Salmon software (Patro et al., 2017). The raw reads were “quasi-aligned” on the human hg19 assembly genome using default option. The statistical analysis was performed using DESeq2 package from Bioconductor (Love et al., 2014). To select statistical differentially expressed genes in each contrast, we applied a cut off of 0.05 on the adjusted p-value and log₂-fold change cut-off of 2. Gene ontology analysis was performed using the online tool PANTHER Classification System, employing Fisher’s exact test with a false discovery rate cut-off of $p = 0.05$ (Mi et al., 2013). The Gene Expression Omnibus (GEO) accession number for the RNA-seq data is GSE152161.

10.9 Differentiation

A 50 mM stock solution of all-trans retinoic acid (ATRA) was made using 10% DMSO. HL-60 cells were seeded in T75 flasks at 0.15×10^6 cells/mL in triplicate and 1 μ M ATRA was added to each flask, along with three replicates of no treatment and DMSO-only controls. 2 mL from each flask was taken for RNA extraction on days 0, 1, 2 and 3 of the three-day treatment. On days 1, 2 and 3, 2 mL samples were taken for flow cytometry analysis using the antibodies CD38-FITC and CD11b-PE to assess differentiation (details of antibodies are listed on **Table 17**). The cells were first washed with 5 mL PBS and centrifuged at 1200 rpm for 5 minutes. The supernatant was discarded and 45 μ L PBS and 5 μ L of each antibody was added to the cell pellet. In addition, to monitor changes in fatty acid uptake capacity as the cells differentiated, fatty acid uptake was measured using fluorescent-labelled palmitate on days 1, 2 and 3 of the treatment, as described above. Finally, RT-qPCR was performed, as described above, to monitor the expression levels of PADI4 over the course of the differentiation period.

10.10 Drug response

10.10.1 PADI4 inhibitors

The PADI4 inhibitors Cl-amidine (cat. no. 506282) and GSK484 (cat. no. SML1658) were purchased from Sigma-Aldrich. 100 mM and 50 mM stock solutions of Cl-amidine and GSK484, respectively, were made up using 10% DMSO. In order to evaluate sub-lethal doses of each compound, serial dilutions were performed in RPMI media: 200, 100, 50, 25, 12.5, 6.25, 3.125, 1.5625, 0.781, 0.39 μ M. Equivalent concentrations were carried out for the DMSO vehicle controls. 1.5×10^6 SKK-1, KG-1 and TF-1 cells were seeded in 6-well plates in 2.5 mL RPMI. 0.5 mL of the relevant concentrations of the compounds and DMSO vehicle controls were added to each well to bring the final cell concentration to 0.5×10^6 cells/mL. The cells were incubated at 37 °C overnight and the next day cell viability was measured using DAPI and MitoTracker, as for Azacitidine. In a separate experiment, fatty acid uptake was measured using fluorescence-labelled palmitate, as described above.

10.10.2 Puromycin selection

To determine the lethal dose of puromycin in non-transfected KG-1 and TF-1 cells, 950 μ L RPMI containing 900,000 cells were seeded in 24-well plates (to simulate the cell concentration during puromycin selection after shRNA transduction). Serial dilutions of puromycin were made such that 50 μ L RPMI containing puromycin could be added to give the following final concentrations: 5, 4, 2.5, 2, 1.25, 1, 0.612, 0.5, 0.306, 0.25 μ M. The cells were then incubated at 37°C for three days. Following this treatment period, cell viability was measured by FACS using DAPI and MitoTracker, as described above.

10.11 Protein expression analysis

10.11.1 Western blot

Triple-sorted SKK-1 cells, TS LOW and TS HIGH, were collected and washed well with PBS by centrifuging at 4°C for 15 minutes at 2000 rpm. They were either processed directly or the cell pellets were stored at -80°C until use. The reagents used for Western blot are listed in **Table 7**. Cell pellets were lysed in 150 μ l lysis buffer (150 mM NaCl₂, 50 mM Tris, 5 mM EDTA, 1% NP₄₀, 1 x cOmplete™ protease inhibitor cocktail tablet, 1 x phosphatase inhibitor tablet) by pipetting up and down and vortexing. The samples were centrifuged at 4°C for 15 minutes at 2000 rpm. The supernatants, containing the mitochondrial and cytoplasmic fractions, were kept. After lysis protein concentration was determined using the BCA Protein Assay Kit (ThermoFisher Scientific) and reading the absorbance using a spectrophotometer. Sample fractions were diluted to same concentration (150 μ g/ μ L) in 4x Laemli SDS buffer (ThermoFisher Scientific). 5% polyacrylamide stacking gels and 10% polyacrylamide running gels were prepared to which equal concentrations of the samples and a standard 10-250 kDa ladder (ThermoFisher Scientific) were added. Samples were run at 110 V for about 2 hours (the time necessary for full migration of the proteins) in the polyacrylamide gels. The migrated proteins were then transferred to nitrocellulose membranes (Whatman, GE Healthcare) at 250 mA per gel for two hours. After the transfer, total protein load was checked by Ponceau staining. The membranes were then blocked using 5% bovine serum albumin in TBS-T for one hour. Membranes were cut with a scalpel at the specific size of each protein of interest. The cut membranes

incubated with primary antibodies overnight in their respective dilutions at 4°C on a roller rack. The antibodies used and their dilutions are listed on **Table 17**. The next day after, the membranes were washed three times with TBS-T to remove excess primary antibody. The membranes were then incubated with either mouse- or rabbit-derived secondary antibodies at room temperature for three hours. The membranes were washed three more times with TBS-T, followed by incubation with Pierce DAB western blotting substrate (ThermoFisher Scientific) reagents in a 1:1 ratio for one minute for chromogenic detection of horse radish peroxidase activity. The dried membranes were overlaid with photographic film (GE Healthcare) and exposed from a few seconds to 60 minutes. After exposure the film was developed with the FujiFilm FPM 100A developer.

Table 7: List and composition of solutions used for Western Blot Analysis

| Buffer | Composition |
|----------------------------|---------------------------------------------|
| Resolving buffer 4x pH 8.8 | 1.5 M Tris |
| | 0.4% SDS |
| Stacking buffer 4x ph 6.8 | 500 nM Tris |
| | 0.4% SDS |
| Running buffer 10x | 250 mM Tris |
| | 2 M Glycine |
| | 10 g/L SDS |
| Transfer buffer 10x | 250 mM Tris |
| | 1.92 M glycine |
| TBS-T wash buffer 10x | 140 mM NaCl |
| | 250 mM Tris |
| | 27 nM KCl |
| Blocking reagent | 5% BSA in TBS-T |
| Laemmli buffer 4x | 250 mM Tris-HCL, pH 6.8 |
| | 50% (v/v) glycerol |
| | 10% SDS |
| | 14.3 M β -mercaptoethanol |
| | 0.05% blue bromphenol |
| Ponceau | 0.05% Ponceau S dissolved in 1% acetic acid |
| 10% NaN ₃ | 10% sodium azide |

10.11.2 Immunophenotypic analysis

Immunophenotypic analysis was performed on the TS LOW and TS HIGH sorted cell lines. Immunostaining and flow cytometry analyses were performed by Sara Vergara of the Clinical Haematology Department at ICO-Hospital Germans Trias i Pujol according to standard procedures with the Navios cytometer (Beckman Coulter). The same antibodies are used as for diagnostic purposes (listed on **Table 17**). Additional cell marker analysis was carried out at the cytometry facility at IGTP.

10.12 shRNA knockdown screen

10.12.1 hEpi9 library

The miR-E-based short hairpin library, hEpi9, expressed on the SGEP vector, was kindly gifted to us by Johannes Zuber (IMP, Austria) (Fellmann et al., 2013). The miR-E backbone, was developed with enhanced processing and knockdown abilities versus previously existing miR30 backbones (Dai et al., 2014). The pooled library contains 7296 short hairpin RNAs targeting 912 human epigenetic-related genes (eight hairpins per gene). Each hairpin is expressed on the GFP-expressing and puromycin-resistant cSGEP plasmid (pRRL) (

Figure 48). In addition to features of the previously developed SGEP vector by Fellmann et al. 2013, cSGEP contains the ubiquitous chromatin opening element (UCOE), as constructed by Jeannine Diesch in our lab. UCOE allows for the stable expression of the SFFV promoter by anti-silencing effects (Müller-Kuller et al., 2015). The cSGEP vector contained luciferase-encoding shRNA as a non-lethal control. The pooled library also included: two positive lethal controls (*Rpl30* and *Psm1*) and one negative non-lethal control (luciferase).

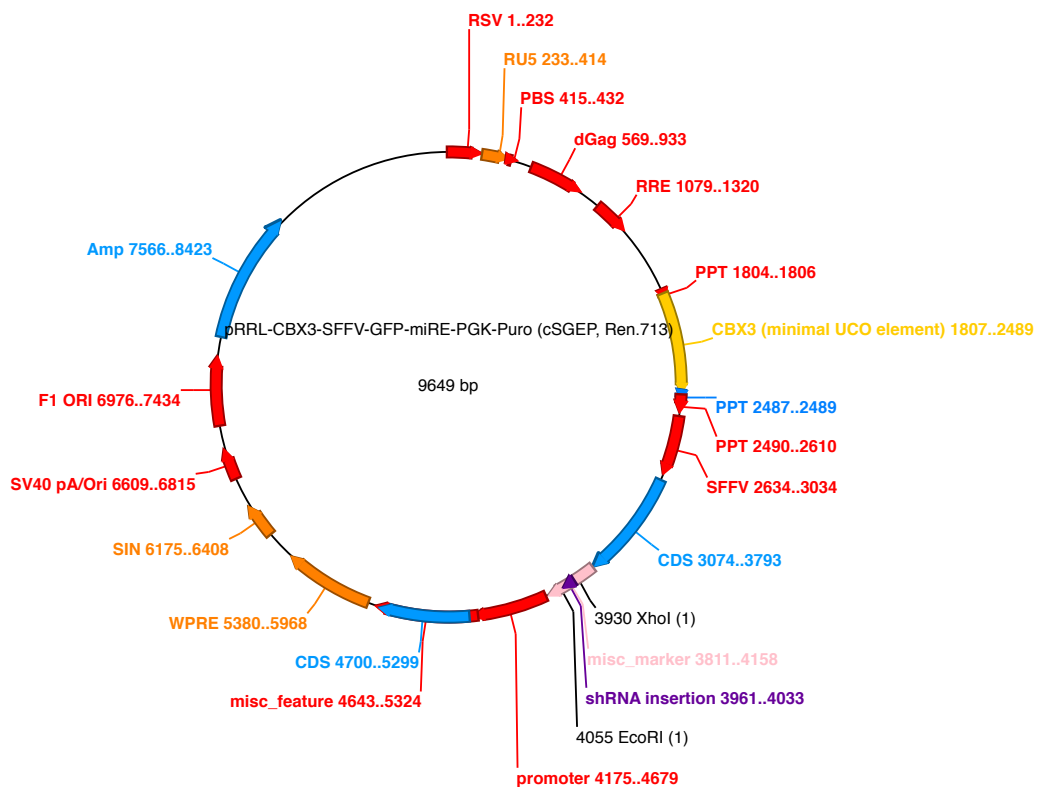


Figure 48: Map of the cSGEP plasmid vector. Each hairpin is expressed on the GFP-expressing and puromycin-resistant cSGEP plasmid (pRRL). cSGEP contains the ubiquitous chromatin opening element (UCOE) that allows for the stable expression of the SFFV promoter, GFP- and puromycin resistance-encoding gene. The cSGEP vector contained luciferase-encoding gene as a non-lethal control.

10.12.2 Transfection

4×10^6 HEK293t cells were seeded in 10 mL DMEM media in five 100 mm culture plates and returned to the incubator overnight so as to allow them to adhere to the culture plate. The next morning a DNA master mix containing the packaging plasmid psPax2 (Addgene #12260) and the envelope-producing plasmid pCMV-VSV-G (Addgene #8454) plasmid and short hairpin library was prepared (listed in shRNA for transfecting five plates of HEK293t cells (Table 8). Together, the three plasmids (packaging, envelope and cSGEP transfer plasmid) comprise the 2nd generation lentiviral system. As the components are split across multiple plasmids, there is increased safety during virus production.

As part of the validation tests, the concentrations for each of the individual shRNA plasmids were calculated.

HEPES-buffered saline (HBS) and calcium chloride (CaCl_2) were thawed at room temperature for 30 minutes before uses. HBS and CaCl_2 are used for the transfer of DNA to target cells. The negatively charged DNA needs to be neutralised in order for it to cross the negatively charged cell membrane. The negative phosphate ions of HBS form a fine precipitate with positive calcium ions of the CaCl_2 . The DNA binds to this precipitate thus allowing uptake into the cell. The master mix was vortexed, 255 μL 2 mM CaCl_2 was added and the mix was vortexed once more. The DNA master mix containing the psPax2 and pCMV-VSV-G plasmids was added drop-wise to 2040 μL HBS while gently vortexing. The mixture was then incubated for 15 minutes at room temperature. For the transfection of the HEK293t cells with the hEPI9 short hairpin library, 700 μL DNA and HBS mix was added drop-wise to each of the five culture plates containing HEK293t cells, ensuring even dispersion. Care was taken so as not to disturb the adhered cells. The cells were returned to the 37°C incubator until the afternoon.

Table 8: Transfection reagents for HEK293t cells

| Reagent | 1 x Sample (µL) | 5.1 x Samples (µL) |
|--------------------------------------------------------------------|-------------------------------------|--------------------|
| dH ₂ O | 232 | 1185 |
| psPAX2 (Addgene #12260) | 10 | 51 |
| pCMV-VSVG (Addgene #8454) | 3 | 15.3 |
| hEpi9 pooled library (cSGEP vector) or individual shRNA plasmid | 5 <i>concentration-dependent</i> | 26 |

Later in the day, the growth media was changed from DMEM of the transfected HEK293t cells to RPMI of the target cells, SKK-1. Extra precautions were taken when handling lentiviral particles: RPMI was aliquoted in a 50 mL Falcon tube and left in the cell culture cabinet for the duration of the transfection protocol so that fresh media was not in contact with virus particles; two layers of nitrile gloves were worn at all times; the UV light was left on in the cell culture cabinet for 30 minutes after each use. All of the DMEM media was aspirated from the five cell culture plates without aspirating the cell monolayer. DMEM media was discarded in 100% bleach so as to avoid contact with virus particles. 8 mL RPMI media was carefully added to each plate and they were returned to the 37°C incubator overnight.

The next day, the transfected HEK293t cells were checked under the microscope for the presence of GFP signal, indicating successful transfection with the pooled hEpi9 library of hairpins. Polybrene was added to five 15 mL Falcon tubes at 8 µg/mL (24 µL). Polybrene assists in efficient transfection of cells with genetic material by changing the charge of the cell membrane and DNA, thereby allowing better absorption of the DNA. Without disturbing the adhered cells, the virus-containing RPMI was carefully removed using a syringe and then transferred to the five Falcon tubes by passing through a 0.45 µm filter to remove debris and avoid mixture of the HEK293t cells with the virus mix. The culture plates were then carefully re-filled with 8 mL fresh RPMI media and returned to the 37°C incubator. The virus supernatants were then stored at -80°C. Filters and syringes were discarded in a bottle containing 100% bleach. The next day the same procedure was repeated where a second lot of viral supernatant was harvested and stored at -80°C.

10.12.3 Infection test

An infection test was carried out as part of the pooled library knockdown to ascertain the volume of viral supernatant required such that one cell receives one virus particle, thereby increasing the chance of single gene knockdowns. For this, SKK-1 cells were first seeded in 6-well plates in 1.4 mL RPMI at 3.1×10^6 cells/mL, as previously determined in our laboratory, and a range of volumes of viral supernatant was added for the first viral hit: 0 (control), 100, 200, 400, 600, 800 μ L. The plates were then centrifuged at 1500 rpm for 30 minutes at 37 °C to increase the contact between the virus particles and target cells. The cells were returned to the 37°C incubator and a second viral hit was carried out the next day using the second viral supernatant collected from the second harvest with the same range of volumes. Later in the day, the media was replaced with 3 mL fresh RPMI and the plates were returned to the incubator. The next day, the cells were checked under the microscope for GFP signal. The percentage GFP expression in the cells was checked by FACS, where a 10-13% was sought for optimal infection efficiency (one shRNA per cell), as previously determined by our laboratory. Briefly, a co-transduction of the target cells using a GFP-expressing cSGEP vector was carried out along with an mCherry-expressing vector. The percentage of infected cells expressing either GFP or mCherry was measured by flow cytometry to determine the volume of viral supernatant to be added for single copy integration of the cSGEP vector.

10.12.4 Transduction

SKK-1 target cells were again seeded in 6-well plates in 1.4 mL RPMI at 3.1×10^6 cells/mL. Three replicates were required for the fatty acid uptake-based cell sorting and so cells were dispensed to 72 wells of the 6-well plates (a total of 233.2 million cells). The number of cells required per sample group – SKK-1 parental, single-sorted low uptake cells (SS LOW), and SS HIGH - for single copy integration of the individual hairpins was calculated as follows

$$\frac{7.3 \times 10^6}{10\% \text{ efficiency}} = 7.3 \times 10^7 \text{ cells per infection}$$

Each replicate: 4 x 6-well plates

3.1 x 10⁶ cells per well

74.4 x 10⁶ cells per 24 wells

3 x replicates: 12 x 6-well plates

223.2 x 10⁶ cells per condition (parental SKK-1, single-sorted LOW, single-sorted HIGH)

For the first viral hit, 400 µL viral supernatant was added to each well and the plates were centrifuged at 1500 rpm for 30 minutes at 37°C. The second viral hit using 400 µL of the second lot of viral supernatant was carried out the next day. Later in the day, the 72 wells were pooled into six 50 mL tubes and then pooled into one tube. The cells were then split into 12 T75 flasks, with four flasks per sample and made up to 35 mL RPMI media. The next day, the percentage GFP expression in the cells was checked by FACS, where again a 10-13% was sought for optimal infection efficiency. After FACS, puromycin antibiotic was added to select for the successfully infected cells. From previous optimisation work in our laboratory, puromycin was added at a concentration of 1.2 µg/mL so that uninfected cells died. Percentage GFP expression was checked again over the next 14 days. Once cells had reached greater than 90% GFP expression, cell numbers were maintained in T75 flasks so that there were sufficient numbers for the fatty acid uptake assay. The uptake assay and subsequent FACS sort was carried out over three days, one replicate per day. 140 million cells were used per replicate, which allowed for the acquisition of between 8 and 10 x 10⁶ cells per SS LOW and SS HIGH populations. Following each sort, the collected populations were snap-frozen and stored at -80°C until the next step.

10.12.5 FACS sorting of low and high uptake SKK-1 populations

SKK-1 cells were separated by FACS into low and high fatty acid uptake populations, as described above. The lowest and highest 10% of the bulk SKK-1 cells

were sorted using red-fluorescence laurate. Three replicates of each populations were sorted. To extract genomic DNA (gDNA), cells of each replicate were pelleted and suspended in 400 μL DNA Extraction Buffer (1 M HCl, pH 8; 5 M NaCl; 0.5 M EDTA) in a 1.5 mL tube and mixed well. 10% SDS was added followed by 4°C L Proteinase K (20 mg/ μL stock) and mixed well. The tubes were incubated overnight at 55°C on a heat block.

10.12.6 PCR and sample preparation for sequencing

All steps were performed in an amplicon- and plasmid-free environment to avoid contamination with other genomic DNA or PCR amplicons.

Three rounds of phenol-based DNA extraction were carried out. The extracted DNA samples were transferred to 1.5 mL PhaseLock tubes and centrifuged at maximum speed for three minutes, after which the aqueous DNA supernatant rises to the top of the tube above the gel phase. The DNA samples were mixed with 400 μL phenol, mixed and transferred to fresh PhaseLock tubes. The tubes were spun at maximum speed for eight minutes at room temperature where the DNA-containing aqueous phase separates from the protein-containing organic phase. The top 350 μL from the water phase was removed and transferred to fresh PhaseLock tubes, leaving the lowest 30-50 μL . 350 μL phenol was added to the DNA mixture, mixed and transferred to fresh PhaseLock tubes. The tubes were spun at maximum speed for eight minutes at room temperature. The top 300 μL from the water phase was removed and transferred to fresh PhaseLock tubes, leaving the lowest 30-50 μL . Finally, 300 μL phenol was added to DNA mixture, mixed and transferred to fresh PhaseLock tubes. The tubes were again spun at maximum speed for eight minutes at room temperature and the top 250 μL from the water phase was removed, leaving the lowest 30-50 μL . For ethanol precipitation of the DNA, 25 μL sodium acetate (NaAc, 3 M, pH 5.2), 750 μL 100% ethanol. The six tubes were then placed at -20°C overnight. The next day the precipitated DNA samples were spun for 30 mins at maximum speed for 30 minutes and 4°C. The supernatant was then aspirated, and the DNA-containing pellet was washed with 200 μL 70% ethanol and spun at 4°C for 5 minutes. The pellet was let dry in the air for five minutes to remove excess ethanol. The pellet was resuspended in 50 μL elution buffer. To facilitate resuspension, the samples were first incubated for one hour at

55°C and then 10 freeze-thaw cycles were performed using dry ice and the heat block. DNA concentration and quality were then measured with the NanoDrop (Agilent, USA) and the final concentration was adjusted to 0.5 µg/µL.

For the amplification of the samples for sequencing, the number of genomes going into the PCR had to match the desired library coverage. For 1000x coverage of the 7300 hairpins:

1000 x 7300 genomes x 6 pg DNA per genome = 43.8 µg gDNA per replicate

Per PCR reaction: 0.5 µg (= 88 reactions per replicate + 1 NTB)

10.12.7 Test PCR and gel

A test PCR was carried out to see if the correct size product was amplified (340 bp). For this, one PCR reaction was performed. Subsequently the amplified products were run on a 1% agarose gel. For amplification of shRNA guide sequences along with the Illumina MiSeq-specific adapters and four nucleotide long barcodes for multiplex sequencing (Table 9), a master mix was prepared using a hot start Taq DNA polymerase, Amplitaq Gold (ThermoFisher, USA), for greater amplification sensitivity (

Table 10). 49 µL of the master mix was removed and added to 1 µL of water as the negative control. 89 µL of purified gDNA of each sample was added to the remaining master mix. 50 µL master mix and template were then dispensed to 88 PCR tubes. The shRNA hairpin guides were then amplified over 31 cycles with pre-defined PCR conditions (Table 11).

Table 9: P7-barcode-loop assignments for sequencing

| Sample | P7-barcode-loop |
|--------------------------|-----------------|
| SKK-1 _{LOW} _1 | ATAG |
| SKK-1 _{HIGH} _1 | ATCC |
| SKK-1 _{LOW} _2 | CTCA |
| SKK-1 _{HIGH} _2 | GAGT |
| SKK-1 _{LOW} _3 | TGTT |
| SKK-1 _{HIGH} _3 | AATG |

Table 10: PCR master mix (shRNA sequencing preparation)

| | x 1 (µL) | x 90 (µL) |
|----------------------------------------------------------------------|--------------|----------------|
| Template DNA (0.5 µg) | 1 | - |
| ddH ₂ O | 31.5 | 2835 |
| 10x PCR Buffer | 5 | 450 |
| MgCl ₂ (25 mM) | 4 | 360 |
| dNTP (2 mM each) | 5 | 450 |
| Rev 4 primer (10 µM) | 1.5 | 135 |
| P7-Barcode-loop new (10 µM; one barcode for each sample) | 1.5 | 135 |
| AmpliTaq Gold | 0.5 | 45 |
| | 50 µL | 4410 µL |

Table 11: PCR conditions (shRNA sequencing preparation)

| | | |
|------|----------------|--------------------|
| 95°C | 10 mins | X 31 cycles |
| 95°C | 30 sec | |
| 52°C | 45 secs | |
| 72°C | 60 secs | |
| 72°C | 7 mins | |
| 4°C | ∞ | |

Following amplification of the shRNA guide sequences and sequencing barcodes, the 88 parallel PCR reactions for each sample were combined into one tube. To avoid cross-contamination of amplicons, the six PCR products were purified in separate locations using QIAquick PCR Purification Kit (QIAGEN, Germany) as per the manufacture's protocol. Half of the PCR volume was purified (2205 µL), with the other half stored at -80°C as backup. The concentrated and purified PCR samples were then run on a 1% agarose gel, each separated by an empty well. The resolved gel was then visualised under ultraviolet light (302 nm) and the correct fragments at 340 bp were carefully excised, thereby excluding off-target bands. DNA was then purified from each of the six gel slices using the QIAquick Gel Extraction Kit (QIAGEN, Germany). The protocol was followed as per the

manufacture, except for some modifications. After addition of 1 volume isopropanol, the samples were incubated for 10 minutes to DNA increase precipitation. A second wash step was carried out with 0.5 mL PE. Finally, the purified DNA was eluted in 30 μ L elution buffer after 15 mins incubation. The final DNA concentration and purity was determined by NanoDrop (Agilent Technologies, USA).

10.12.8 Library preparation for determining shRNA enrichment

Pre-preparation of the samples before sequencing was carried out the Genomics Facility at CRG, Barcelona. Briefly, this included quantification by qPCR and the Bioanalyzer Agilent high-sensitivity DNA kit (Agilent Technologies, USA) to estimate the average size of the library and the average size of the fragments to be sequenced (around 340 bp). Of the library 12 pM was applied to an Illumina flow cell for cluster generation and sequenced on an Illumina HiSeq with 50-base-pair single read using the custom sequencing primer, MiRE_{EcoR1}Seq, following the manufacturers' protocols.

10.12.9 shRNA knockdown screen analysis

FASTA files produced from the sequencing runs were processed using bash commands. The read sequences were trimmed to contain the guide strand and barcode sequences and counted. The reverse complement sequences of the counted reads were then aligned to the hEpi9 shRNA library hairpins. Hairpins with low counts were removed, where counts with at least one read count per million (CPM), which is equivalent to a log-CPM value of 0, in both samples were kept. shRNA hairpin log-CPM values were normalized by the trimmed mean of M-values (TMM) method (Robinson & Oshlack, 2010). The calculated normalization factors were then used as a scaling factor for the library sizes. It was decided to perform a pair-wise comparison between the three replicates of SKK-_{LOW} and SKK-_{HIGH}. The R programme, edgeR, was used to calculate the log-fold change (logFC), counts per million and significance values, p-value and false discovery rate (FDR) (Ritchie, 2014). All shRNA hairpin counts from the six samples were merged into one table, normalised using the `calcNormFactors` function and fitted with a negative binomial generalised linear model using the `glmFIT` function. Hairpin-specific variations were estimated by calculating the square root of coefficient of

variation with `estimateDisp` and visualised on a graph using `plotBCV` to plot biological variability versus average hairpin abundance. Changes in shRNA abundance were calculated with a Fisher's Exact Test (`exactTest`) and the top candidate hairpins were then ranked according to p-value. Hairpins with p-values below 0.05 and log fold change of less than -1 or greater than 1 were chosen for gene-wise differential expression analysis.

Gene set testing was carried out using the `mroast` function, which is part of the bioconductor package *limma* (Wu et al., 2010). The eight hairpins of each of the pre-filtered genes were treated as a unit, whereby a single p-value was assigned to each gene. In this way, it was possible to generate a ranked list of the significantly differentially represented genes, i.e. enriched or depleted hairpins in TS LOW.

10.13 Short hairpin validation

10.13.1 Plasmids

For de novo generation of miRE-based shRNAs, as part of the single gene knockdown validations, 97-mer oligonucleotides (ordered as 4 nmol Ultramers from Integrated DNA Technologies) containing the shRNA fragment were PCR-amplified using primers 5'-miRE-XhoI and 3'-miRE-EcoRI and cloned into the cSGEP (pRLL) plasmid encoded with a lentiviral backbone as before (Fellmann et al., 2013). ShRNA sequences were acquired from the Fellmann et al. study and those used in the present study are listed on **Table 16**. As a negative control, a control cSGEP vector containing a shRNA targeting the renilla luciferase-encoding gene, which the target cells lack, was included.

10.13.2 PCR amplification of shRNA fragments

The Ultramer oligos were dissolved in 120 μ L of ddH₂O to give a stock concentration of 1 μ g/ μ l. (4 nmol of 97mers have a MW of \approx 30 kDa = 120 μ g). For each oligo, a PCR was set up with the forward and reverse primers flanking the gene-specific guide sequences at EcoRI and XhoI restriction digestion sites (**Tables 12 and 13**)

Table 12: PCR master mix for ultramer amplification and colony PCR

| Reagent | Volume (μL) |
|---------------------------------------------------------------|--------------------------|
| Phusion Hot Start II HF PCR master mix (#F-565, ThermoFisher) | 25 |
| Forward primer (5'miRE-XhoI) | 2.5 |
| Reverse primer (3'miRE-EcoRI) | 2.5 |
| Template (Ultramer) | 1 |
| Water | 19 |
| | 50 μL |

Table 13: PCR conditions (shRNA Ultramer amplification)

| | | |
|------|----------|-------------|
| 98°C | 30 sec | |
| 98°C | 10 sec | |
| 66°C | 30 sec | X 35 cycles |
| 72°C | 30 sec | |
| 72°C | 10 mins | |
| 4°C | ∞ | |

Successful amplification of the Ultramer oligos was confirmed by running 2 μL of the PCR product on a 2% (weight/volume) agarose gel, which showed a single band 131 bp in size. 25 μL each of four amplified PCR reactions were pooled for subsequent column purification. The QIAquick PCR Purification Kit (QIAGEN, Germany) was used according to the manufacturer's instructions with the sole modification of eluting the oligos with 30 μL of EB after a 10 minutes on column incubation period. The remaining 25 μL of the PCR reactions were frozen, to be used as backups for those that failed to be cloned.

10.13.3 Digestion and ligation

The purified PCR products were then digested using EcoRI (10 U/ μL) and XhoI (10 U/ μL) restriction enzymes in 2x Tango Buffer (ThermoFisher Scientific, USA). In parallel, digestion of the cSGEP plasmid vector was also carried out. The mixes were incubated for 60 minutes at 37°C to allow the digestion to proceed. After, the digested cSGEP plasmid vector was treated with alkaline phosphatase to avoid self-ligation. The digested samples were then run on a 2% (weight/volume) agarose gel

to confirm the presence of the 110 bp band of the inserts and approximately 8 kb of the digested plasmid. The band was then excised using the QIAquick Gel Extraction Kit (QIAGEN, Germany), according to the manufacturer's instructions, and eluted in 50 µl. DNA concentration was measured by NanoDrop (Agilent Technologies). The purified digested oligos were ligated using T4 DNA Ligase (ThermoFisher Scientific, USA) with the insert (4 ng), cSGEP vector (100 ng) in a molar ratio of approximately 3:1. A vector only control was also included to confirm that there was no re-ligation. The ligation mix was incubated overnight at 16°C.

10.13.4 Cloning

The next day, 5 µl of the ligated reaction was transformed into chemically competent Stbl3 *E. coli* (ThermoFisher Scientific), which is recommended for cloning unstable inserts such as lentiviral DNA containing direct repeats. The ligation reaction and bacteria were kept on ice for 30 minutes. Meanwhile 1 mL/sample of SOC medium (super optimal broth with catabolites repression) was pre-warmed at 37°C. Heat shock was carried out by placing the bacteria mix at 42°C for 45 seconds and returning to ice for two minutes. 300 µl pre-warmed SOC was added to 50 µl of each bacteria sample, which were then placed at 37°C with 300 rpm shaking to allow the bacteria to recover. The bacteria mix was centrifuged for 2 minutes at 2000 rpm. Most of the supernatant was removed, leaving around 50 µl with the pellet. Using aseptic technique, the pellet of the bacteria mix was then plated on LB-ampicillin agar plates and incubated overnight at 37°C. The next day, successful transformations were visualised with the growth of ampicillin-resistant colonies. 10-15 colonies per shRNA pool were picked using a pipette tip and first placed in individual tubes containing 10 µl water, from which 2 µl were placed in a PCR tube. A colony PCR was then performed after which the amplicons were run on a 1% agarose gel to ensure the correct size insert (110 bp) was amplified. The same pipette tip with the remainder of the water was placed in another tube containing 5 mL LB-ampicillin broth. The tubes were placed overnight in an incubator at 37°C with 200 rpm shaking. The next day, plasmids from the tubes with cloudy media (indicating bacteria growth) were extracted using PureLink Quick Plasmid Miniprep Kit (ThermoFisher Scientific), as per manufacturer's instructions. DNA of the isolated plasmids was then quantified using NanoDrop. Samples containing 500 ng DNA mixed with the ZUB-SEQ-SH primer were then

sent to Eurofins Genomics (Germany) for sanger sequencing. Successful clones were confirmed upon detection of the relevant shRNA guide sequences using the freely available software, Serial Cloner.

10.14 Single cell colony expansion

SKK-1, TS LOW and TS HIGH cells were seeded at a density of 0.5 cell per well in 96-well plates in 50 μ L RPMI media supplemented with 20% FBS. The cells were incubated for 14 days at 37°C and visualised by light microscope to identify the wells with colonies. 12 wells were chosen (six with low numbers of cells and six with high numbers of cells) and transferred to 24-well plates in 500 μ L RPMI media. The cells were returned to the 37°C incubator and let grow for 2-3 days. Then, six of the 'low number' wells and six of the 'high number' wells were chosen to be transferred to six-well plates in 3 mL RPMI media. The plates were returned to the 37°C incubator and let to expand until there were sufficient numbers so that they could be transferred to 10 mL culture flasks and later 75 mL flasks. Cells were frozen in FBS and 10% DMSO and also stored as pellets for further characterisation.

10.15 Identifier test

Cells were identified by comparing their short tandem repeat (STR) profiles to their corresponding profiles on the searchable cell line database, Cellosaurus (web.expasy.org/cellosaurus). Genomic DNA was extracted from collected cells using PureLink Genomic DNA Mini Kit (ThermoFisher Scientific). The quantity and purity of the extracted DNA was measured using NanoDrop. Samples were made up to 30 μ L at a concentration of 20 ng/ μ L. The samples were then sent to the Genomics facility at IGTP for the PCR amplification step using the CLA IdentiFiler Plus PCR Amplification kit (ThermoFisher Scientific), which contains dye-tagged primers specific to the 16 human STR loci. Positive and negative controls with the standard ladder were loaded along with 13 samples for PCR amplification of the 16 microsatellite loci with the stated PCR conditions (**Table 14**). Following the PCR, capillary electrophoresis was performed with the amplified microsatellite loci fragments and the allelic ladder, GeneScan 500 LIZ Size Standard, using the Applied Biosystems 3130xl Genetic Analyzer to discriminate alleles that differ by single nucleotides. GeneMapper software (ThermoFisher Scientific) was then used

| Materials and Methods

to call alleles according to size and quality based on the selected allelic ladder. Thus, allelic differences at each locus were identified. Each sample was manually checked to ensure off-ladder (OL) alleles were discounted.

Table 14: PCR conditions (STR profile)

| | | |
|------|----------------|-------------|
| 95°C | 1 min | |
| 94°C | 20 sec | X 28 cycles |
| 59°C | 3 mins | |
| 60°C | 10 min | |
| 4°C | Up to 24 hours | |

10.16 Statistical analysis

Data were analysed with GraphPad Prism 8 using Student's t-test or ANOVA. All graphs show mean values \pm SD. Only significant differences are annotated.

10.17 List of primers

Table 15: List of primers used

| Target | 3' Forward | 5' Reverse |
|-------------------------------------------------------|------------------------------------------------------|--------------------------------------------------------|
| shRNA knockdown screen: sequencing primers | | |
| MiRE _{EcoR1} Seq | TAGCCCCTTGAAG TCCGAGGCAGTAG GCA | |
| Rev4_Long (p5+PGK) | | AATGATACGGCGACCACCGAG ATCTTGATGTGGAATGTGTG CGAGG |
| p7_AGGA_Loop_ new | CAAGCAGAAGACGGCATAACGA AAGCTAGTGAAGCCACAGATG T | |
| p7_ACGT_Loop_ new | CAAGCAGAAGACGGCATAACGA ACGTTAGTGAAGCCACAGATG T | |
| p7_ACTC_Loop_ new | CAAGCAGAAGACGGCATAACGA ACTCTAGTGAAGCCACAGATG T | |
| p7_AGAC_Loop_ new | CAAGCAGAAGACGGCATAACGA AGACTAGTGAAGCCACAGATG T | |
| p7_AGCT_Loop_ new | CAAGCAGAAGACGGCATAACGA AGCTTAGTGAAGCCACAGATG T | |
| p7_AGGA_Loop_ new | CAAGCAGAAGACGGCATAACGA AGGATAGTGAAGCCACAGATG T | |
| 5'-miRE-XhoI | TACAATACTCGAGAAGGTATA TTGCTGTTGACAGTGAGCG | |
| 3'-miRE-EcoRI | TTAGATGAATTCTAGCCCCTT GAAGTCCGAGGCAGTAGGCA | |
| ZUB-SEQ-SH (sequencing primer) | TGTTTGAATGAGGCTTCAGTA C | |
| Housekeeping | | |
| GAPDH | CGACCACTTTGTCAAGCTCA | TCTTACTCCTTGGAGGCCAT |
| shRNA knockdown screen: single gene validation | | |
| SIRT6 | CCCACGGAGTCTGGACCAT | CTCTGCCAGTTTGTCCCTG |
| TET2 | ATACCCTGTATGAAGGGAAGC C | CTTACCCCGAAGTTACGTCTT TC |
| ASXL1 | CGCGCCTGGTATTAGAAAACCT | GCATCCTTCTTGAGCGTGAAA AG |
| PADI4 | CAGGGGACATTGATCCGTGTG | GGGAGGCGTTGATGCTGAA |
| BRCA1 | GAAACCGTGCCAAAAGACTTC | CCAAGGTTAGAGAGTTGGACA C |
| EHMT1 | GCTGTGTGAAAACCGAGCTG | TCCGCTATCCGAGTTAGTGTG |

| Materials and Methods

| | | |
|--------------------------------|---------------------------------|------------------------------|
| BRD3 | TCAAATTGAACCTGCCGGATT | TGCATACATTCGCTTGCACTC |
| BAZ1b | ATCGCCACGAAAACCTTCTAC | CTGGCACGTTACTGATGATCT T |
| SIRT1 | TGTGTCATAGGTTAGGTGGTG A | AGCCAATTCTTTTTGTGTTCG TG |
| CD36 | GGCTGTGACCGGAACTGTG | AGGTCTCCAACCTGGCATTAGA A |
| CPT1a | CATGGAGGCCTCGTATGTG | CCCATTTCGTAGCCTTTGGTA |
| Cell surface antigens | | |
| CD123 | AGACGCCGACTATTCTATGCC | CGGTGTAGTTGGTCACTTCAC A |
| HLA-DRb | CGGGGTTGGTGAGAGCTTC | AACCACCTGACTTCAATGCTG |
| KIT | CACCGAAGGAGGCACTTACAC A | TGCCATTACGAGCCTGTCGT A |
| Fatty acid metabolism | | |
| PPAR | AGCCTGCGAAAGCCTTTTGGT G | GGCTTCACATTCAGCAAACCT GG |
| FABP4 | ACGAGAGGATGATAAACTGGT GG | GCGAACTTCAGTCCAGGTCAA C |
| ACSL1 | ATCAGGCTGCTCATGGATGAC C | AGTCCAAGAGCCATCGCTTCA G |
| LCAD | CTTACAGGGAATAAAAACAAA TGCTAA | CGCAACTACAATCACAACATC AC |
| MCAD | AGAATTGGCTTATGGATGTAC AGG | TTTGTTGATCATTTCAGCAA TAAT |
| CPT2 | GGCACATCTGAAGTACATTCT CTCA | CGGTTCTCACTGGTCAGGTAT G |
| PPARa | CGGTGACTTATCCTGTGGTCC | CCGCAGATTCTACATTCGATG TT |
| FASN | AAGGACCTGTCTAGGTTTGAT GC | TGGCTTCATAGGTGACTTCCA |
| Mitochondrial complexes | | |
| NDUOX | GATCACATTCACCTCCCTGGT | GTGCCAGCAGTTAATGTCAGT G |
| SDHA | ATGTTGGTGCCTGAGAACGA | TCACCTAGTAAACCGTCTGCC |
| UQCRB | CCACTTGCCTGATGCTGAAAC | TGAGTACTGGTTGCTTGCCTA T |
| MT-CO1 | TCTCAGGCTACACCCTAGACC A | ATCGGGGTAGTCCGAGTAACG T |
| MT-CO2 | GCTGTCCCCACATTAGGCTT | ACCGTAGTATAACCCCGGTC |
| MT-CO3 | CAGCCCATGACCCCTAACAG | ACATCGCGCCATCATTGGTA |
| ATP5F1A | GTAAGTGCGGCGTAGACTGA | AGCTGGCATTGTGTTAAGCTT GT |
| Gene fusions | | |
| ETV6-NTRK3 | CATTCTCCACCCTGGAAAC | GGCTCCCTCACCCAGTTCTC |
| MLL10-PICALM | TGAGACCTCCAAACCCCTTT | TCGGCACCATTACCTTCTTC |
| Mitochondrial content | | |
| MT-CYTB | GCCTGCCTGATCCTCCAAAT | AAGGTAGCGGATGATTACGCC |
| APP | TGTGTGCTCTCCAGGTCTA | CAGTTCTGGATGGTCACTGG |

| | | |
|-------------------------------|-----------------------------|-----------------------------|
| 18S (housekeeping) | GTAACCCGTTGAACCCATT | CCATCCAATCGGTAGTAGCG |
| Glucose metabolism | | |
| HK₁ | CACATGGAGTCCGAGGTTTAT G | CGTGAATCCCACAGGTAACCT C |
| HK₂ | GAGCCACCACTCACCTACT | CCAGGCATTTCGGCAATGTG |
| PFKL | GGCTTCGACACCCGTGTAA | CGTCAAACCTCTTGTCATCCA |
| PFKP | GGGACGATCATTGGCAGTG | GAGGTAGGCGTACTTCTGCAC |
| PKM₁ | TGCGAGCCTCAAGTCACTCCA C | TCACGGCACAGGAACAACACG |
| PKM₂ | GCCTGCTGTGTCGGAGAAG | CAGATGCCTTTCGGATGAATG |
| LDHA | TTGACCTACGTGGCTTGGAAG | GGTAACGGAATCGGGCTGAAT |
| LDHB | CCTCAGATCGTCAAGTACAGT CC | ATCACGCGGTGTTTGGGTAAT |
| CS | TAAGGAGCAGGCCAGAATTAA GA | CCACCATACATCATGTCCACA G |
| IDH₁ | ATAATGTTGGCGTCAAATGTG C | CTTGAACTCCTCAACCCTCTT C |
| IDH₂ | CGCCACTATGCCGACAAAAG | ACTGCCAGATAATACGGGTCA |
| OGDH | TTGGCTGGAAAACCCAAAAG | TGTGCTTCTACCAGGGACTGT |
| SDHA | CAAACAGGAACCCGAGGTTTT | CAGCTTGGTAACACATGCTGT AT |

10.18 List of Ultramers for individual shRNA knockdowns**Table 16: List of 97-mer oligos (Ultramers) for single shRNA knockdowns**

| Gene | Hairpin ID | 97-mer guide sequence |
|----------------|------------|-----------------------------------------------------------------------------------------------------------|
| SIRT6 | SIRT6.19 | TGCTGTTGACAGTGAGCGAGCCTCAACAAGGAAAC TTTATAGTGAAGCCACAGATGTATAAAGTTTCCCTTG TTGAGGCCTGCCTACTGCCTCGGA |
| | SIRT6.485 | TGCTGTTGACAGTGAGCGATGCCAAGTGTAAGACGC AGTATAGTGAAGCCACAGATGTATACTGCGTCTTACA CTTGGCACTGCCTACTGCCTCGGA |
| TET2 | TET2.1150 | TGCTGTTGACAGTGAGCGCCAGAACAACAACA ACAATAGTGAAGCCACAGATGTATTGTTGTTGTAGTT GTTCTGGTTGCCTACTGCCTCGGA |
| | TET2.2863 | TGCTGTTGACAGTGAGCGATCACAACAAGCTTCAGTT CTATAGTGAAGCCACAGATGTATAGAAGTGAAGCTT GTTGTGACTGCCTACTGCCTCGGA |
| ASXL1 | ASXL1.485 | TGCTGTTGACAGTGAGCGAGCGCCTGGTATTAGAAA ACTATAGTGAAGCCACAGATGTATAGTTTTCTAATAC CAGGCGCGTGCCTACTGCCTCGGA |
| | ASXL1.508 | TGCTGTTGACAGTGAGCGCCGGATGCTCCAATGACA CCAATAGTGAAGCCACAGATGTATTGGTGTGATTGG AGCATCCGATGCCTACTGCCTCGGA |
| PADI4 | PADI4.1729 | TGCTGTTGACAGTGAGCGACCGCAGCTCTTCAAGCTC AAATAGTGAAGCCACAGATGTATTTGAGCTTGAAGA GCTGCGGGTGCCTACTGCCTCGGA |
| | PADI4.333 | TGCTGTTGACAGTGAGCGAACCAGTCAAAGCTCTACT CTATAGTGAAGCCACAGATGTATAGAGTAGAGCTTT GACTGGTGTGCCTACTGCCTCGGA |
| BRCA1_1 | BRCA1.1106 | TGCTGTTGACAGTGAGCGACAGATAGTTCTACCAGT AAAATAGTGAAGCCACAGATGTATTTTACTGGTAGA ACTATCTGCTGCCTACTGCCTCGGA |
| | BRCA1.1824 | TGCTGTTGACAGTGAGCGACCAGTCTATTAAGAAA GAAATAGTGAAGCCACAGATGTATTTCTTTCTTTAAT AGACTGGGTGCCTACTGCCTCGGA |
| | BRCA1_3356 | TGCTGTTGACAGTGAGCGACCATACAGCTTCATAAA TAATAGTGAAGCCACAGATGTATTATTTATGAAGCTG TATGGTTTGCCTACTGCCTCGGA |
| EHMT1_1 | EHMT1.1495 | TGCTGTTGACAGTGAGCGATCCCTGGATCTCCGAGTC AAATAGTGAAGCCACAGATGTATTTGACTCGGAGAT CCAGGGAGTGCCTACTGCCTCGGA |
| | EHMT1.701 | TGCTGTTGACAGTGAGCGACCAGAGAAGTTCGAGAA GCTATAGTGAAGCCACAGATGTATAGCTTCTCGAACT TCTCTGGGTGCCTACTGCCTCGGA |
| BRD3_1 | BRD3.2654 | TGCTGTTGACAGTGAGCGCCCGTGTGAGATTCGTAC CGAATAGTGAAGCCACAGATGTATTCGGTACGAATC TCACACGGTTGCCTACTGCCTCGGA |
| | BRD3.3234 | TGCTGTTGACAGTGAGCGACCGAGCTTATGTGTATAT AAATAGTGAAGCCACAGATGTATTTATATACATAA GCTCGGGTGCCTACTGCCTCGGA |

| | | |
|----------------|-------------|------------------------------------------------------------------------------------------------------------|
| BAZ1B_1 | BAZ1B.2228* | TGCTGTTGACAGTGAGCGACAGATGCTCAGTATCCTA TTATAGTGAAGCCACAGATGTATAATAGGATACTGA GCATCTGGTGCCTACTGCCTCGGA |
| | BAZ1B.2039 | TGCTGTTGACAGTGAGCGCAAGAACGAAGAGAGAAA GAAATAGTGAAGCCACAGATGTATTTCTTTCTCTCTT CGTTCTTTTGCCTACTGCCTCGGA |
| CD36 | CD36.329 | TGCTGTTGACAGTGAGCGCCAGCAGCAACATTCAAG TTAATAGTGAAGCCACAGATGTATTAACCTGAATGTT GCTGCTGTTGCCTACTGCCTCGGA |
| | CD36.210 | TGCTGTTGACAGTGAGCGCAAGCAAGTTGTCCTCGA AGAATAGTGAAGCCACAGATGTATTCTTCGAGGACA ACTTGCTTTTGCCTACTGCCTCGGA |
| CPT1a | CPT1A.822 | TGCTGTTGACAGTGAGCGCTACAGTGGTATTTGAAGT TAATAGTGAAGCCACAGATGTATTAACCTCAAATACC ACTGTAATGCCTACTGCCTCGGA |
| | CPT1A.292 | TGCTGTTGACAGTGAGCGCAAAGAAGTTCATCAGAT TCAATAGTGAAGCCACAGATGTATTGAATCTGATGA ACTTCTTTTGCCTACTGCCTCGGA |
| SIRT1 | SIRT1.1849 | TGCTGTTGACAGTGAGCGCAAGGTTCAATTTGTATGAT AAATAGTGAAGCCACAGATGTATTTATCATACAAATG AACCTTTTGCCTACTGCCTCGGA |
| | SIRT1_942 | TGCTGTTGACAGTGAGCGAAAGACTCAAGTTCACCA GAAATAGTGAAGCCACAGATGTATTTCTGGTGAACCT GAGTCTTCTGCCTACTGCCTCGGA |
| KIT | KIT.2997 | TGCTGTTGACAGTGAGCGACACGACGATGTCTGAGC AGAATAGTGAAGCCACAGATGTATTCTGCTCAGACA TCGTCGTGCTGCCTACTGCCTCGGA |
| | KIT.2711 | TGCTGTTGACAGTGAGCGATAAGTTCTACAAGATGAT CAATAGTGAAGCCACAGATGTATTGATCATCTTGTAG AACTTAGTGCCTACTGCCTCGGA |

10.19 List of antibodies**Table 17: List of antibodies used.**

| Target | Clone | Fluorophore | Supplier | Cat. No. | Dilution |
|---------------------------------------------------------------|---------------------------|-------------|-----------------|----------|----------|
| Flow cytometry | | | | | |
| CD117 | 104D2D1 (Mouse) | PC7 | Beckman Coulter | B96754 | 1:10 |
| CD123 | SSDCLY107D2 (Mouse) | PE | Beckman Coulter | A32535 | 1:10 |
| HLA-DR | Immu-357 (Mouse) | PB | Beckman Coulter | B36291 | 1:10 |
| CD36 | FA6.152 (Mouse) | APC | Beckman Coulter | A87786 | 1:10 |
| Flow cytometry (differentiation) | | | | | |
| CD38 | T16 (Mouse) | FITC | Beckman Coulter | A07778 | 1:10 |
| CD11b | Bear1 (Mouse) | PE | Beckman Coulter | IM2581U | 1:11 |
| Flow cytometry (Proliferation and cell cycle analysis) | | | | | |
| Ki67 | B56 (Mouse) | PE | BD Pharmingen | 556027 | 1:10 |
| Western blot (Mitochondrial OXPHOS complexes) | | | | | |
| Complex I: NDUFA9 | 20C11B11B11 (Mouse) | - | Abcam | ab14713 | 1:1000 |
| Complex II: SDHA | 2E3GC12FB2AE 2 (Mouse) | - | Abcam | ab14715 | 1:5000 |
| Complex III: UQCRC1 | 16D10AD9AH5 (Mouse) | - | Abcam | ab110252 | 1:2000 |
| Complex IV: MTCO1 | 1D6E1A8 (Mouse) | - | Abcam | ab14705 | 1:1000 |
| Complex V: ATP5A | 15H4C4 (Mouse) | - | Abcam | ab14748 | 1:5000 |

Bibliography

11. Bibliography

- Aadra P. Bhatt, S. R. J., Alex J. Freerman, Liza Makowski, Jeffrey C. Rathmell, Dirk P. Dittmer, and Blossom Damania. (2012). Synthesis and antitumor activity of an inhibitor of fatty acid synthase. *Proceedings of the National Academy of Sciences*.
<https://doi.org/10.1073/pnas.050582897>
- Aagaard, M. M., Siersbæk, R., & Mandrup, S. (2011). Molecular basis for gene-specific transactivation by nuclear receptors. *Biochimica et Biophysica Acta (BBA) - Molecular Basis of Disease*, 1812(8), 824–835. <https://doi.org/10.1016/j.bbadis.2010.12.018>
- Abdel-aleem, S., Li, X., Anstadt, M., Perez-Tamayo, R., & Lowe, J. (1994). Regulation of glucose utilization during the inhibition of fatty acid oxidation in rat myocytes. *Horm Metab Res*, 26(02), 88–91. <https://doi.org/10.1055/s-2007-1000779>
- Abdel-Wahab, O., Adli, M., LaFave, L. M., Gao, J., Hricik, T., Shih, A. H., Pandey, S., Patel, J. P., Chung, Y. R., Koche, R., Perna, F., Zhao, X., Taylor, J. E., Park, C. Y., Carroll, M., Melnick, A., Nimer, S. D., Jaffe, J. D., Aifantis, I., ... Levine, R. L. (2012). ASXL1 Mutations Promote Myeloid Transformation through Loss of PRC2-Mediated Gene Repression. *Cancer Cell*, 22(2), 180–193. <https://doi.org/10.1016/j.ccr.2012.06.032>
- Abu-Elheiga, L., Almarza-Ortega, D. B., Baldini, A., & Wakil, S. J. (1997). Human Acetyl-CoA Carboxylase 2: MOLECULAR CLONING, CHARACTERIZATION, CHROMOSOMAL MAPPING, AND EVIDENCE FOR TWO ISOFORMS. *Journal of Biological Chemistry*, 272(16), 10669–10677. <https://doi.org/10.1074/jbc.272.16.10669>
- Ambrosi, T. H., Scialdone, A., Graja, A., Gohlke, S., Jank, A.-M., Bocian, C., Woelk, L., Fan, H., Logan, D. W., Schürmann, A., Saraiva, L. R., & Schulz, T. J. (2017). Adipocyte Accumulation in the Bone Marrow during Obesity and Aging Impairs Stem Cell-Based Hematopoietic and Bone Regeneration. *Cell Stem Cell*, 20(6).
<https://doi.org/10.1016/j.stem.2017.02.009>
- Anderson, L. A., Pfeiffer, R. M., Landgren, O., Gadalla, S., Berndt, S. I., & Engels, E. A. (2009). Risks of myeloid malignancies in patients with autoimmune conditions. *British Journal of Cancer*, 100(5), 822–828. <https://doi.org/10.1038/sj.bjc.6604935>
- Arber, D. A., Orazi, A., Hasserjian, R., Thiele, J., Borowitz, M. J., Le Beau, M. M., Bloomfield, C. D., Cazzola, M., & Vardiman, J. W. (2016). The 2016 revision to the World Health Organization classification of myeloid neoplasms and acute leukemia. *Blood*, 127(20), 2391–2405. <https://doi.org/10.1182/blood-2016-03-643544>
- Aregger, M., Lawson, K., Billmann, M., Costanzo, M., Tong, A., Chan, K., Rahman, M., Brown, K., Ross, C., Usaj, M., Nedyalkova, L., Sizova, O., Habsid, A., Pawling, J., Lin, Z.-Y., Abdouni, H., Weiss, A., Mero, P., Dennis, J., ... Moffat, J. (2019). Systematic mapping of genetic interactions for de novo fatty acid synthesis. *BioRxiv*, 834721–834721.
<https://doi.org/10.1101/834721>
- Asangani, I. A., Dommeti, V. L., Wang, X., Malik, R., Cieslik, M., Yang, R., Escara-Wilke, J., Wilder-Romans, K., Dhanireddy, S., Engelke, C., Iyer, M. K., Jing, X., Wu, Y. M., Cao, X., Qin, Z. S., Wang, S., Feng, F. Y., & Chinnaiyan, A. M. (2014). Therapeutic targeting of BET bromodomain proteins in castration-resistant prostate cancer. *Nature*, 510(7504), 278–282. <https://doi.org/10.1038/nature13229>
- Bain, B. J. (2001). Bone marrow trephine biopsy. *Journal of Clinical Pathology*, 54(10), 737–742.
<https://doi.org/10.1136/jcp.54.10.737>

| Bibliography

- Bakshi, S. R., Brahmbhatt, M. M., Trivedi, P. J., Dalal, E. N., Patel, D. M., Purani, S. S., Shukla, S. N., Shah, P. M., & Patel, P. S. (2012). Trisomy 8 in leukemia: A GCRI experience. *Indian Journal of Human Genetics*, 18(1), 106–108. <https://doi.org/10.4103/0971-6866.96673>
- Balkwill, F., Charles, K. A., & Mantovani, A. (2005). Smoldering and polarized inflammation in the initiation and promotion of malignant disease. *Cancer Cell*, 7(3). <https://doi.org/10.1016/j.ccr.2005.02.013>
- Ball, B. J., Famulare, C. A., Stein, E. M., Tallman, M. S., Derkach, A., Roshal, M., Gill, S. I., Manning, B. M., Koprivnikar, J., McCloskey, J., Testi, R., Prebet, T., Al Ali, N. H., Padron, E., Sallman, D. A., Komrokji, R. S., & Goldberg, A. D. (2020). Venetoclax and hypomethylating agents (HMAs) induce high response rates in MDS, including patients after HMA therapy failure. *Blood Advances*, 4(13), 2866–2870. <https://doi.org/10.1182/bloodadvances.2020001482>
- Bannister, A. J., & Kouzarides, T. (2011). Regulation of chromatin by histone modifications. *Cell Research*, 21(3). <https://doi.org/10.1038/cr.2011.22>
- Barski, A., Cuddapah, S., Cui, K., Roh, T.-Y., Schones, D. E., Wang, Z., Wei, G., Chepelev, I., & Zhao, K. (2007). High-Resolution Profiling of Histone Methylations in the Human Genome. *Cell*, 129(4), 823–837. <https://doi.org/10.1016/j.cell.2007.05.009>
- Bastie, C. C., Nahlé, Z., McLoughlin, T., Esser, K., Zhang, W., Unterman, T., & Abumrad, N. A. (2005). FoxO1 Stimulates Fatty Acid Uptake and Oxidation in Muscle Cells through CD36-dependent and -independent Mechanisms. *Journal of Biological Chemistry*, 280(14), 14222–14229. <https://doi.org/10.1074/jbc.M413625200>
- Baum, C. M., Weissman, I. L., Tsukamoto, A. S., Buckle, A. M., & Peault, B. (1992). Isolation of a candidate human hematopoietic stem-cell population. *Proceedings of the National Academy of Sciences*, 89(7), 2804–2808. <https://doi.org/10.1073/pnas.89.7.2804>
- Becker, A. J., McCulloch, E. A., & Till, J. E. (1963). Cytological Demonstration of the Clonal Nature of Spleen Colonies Derived from Transplanted Mouse Marrow Cells. *Nature*, 197(4866). <https://doi.org/10.1038/197452a0>
- Beckmann, B. M., Horos, R., Fischer, B., Castello, A., Eichelbaum, K., Alleaume, A. M., Schwarzl, T., Curk, T., Foehr, S., Huber, W., Krijgsveld, J., & Hentze, M. W. (2015). The RNA-binding proteomes from yeast to man harbour conserved enigmRBPs. *Nature Communications*, 6. <https://doi.org/10.1038/ncomms10127>
- Beerman, I., Maloney, W. J., Weissmann, I. L., & Rossi, D. J. (2010). Stem cells and the aging hematopoietic system. *Current Opinion in Immunology*, 22(4), 500–506. <https://doi.org/10.1016/j.coi.2010.06.007>
- Behan, J. W., Yun, J. P., Proektor, M. P., Ehsanipour, E. A., Arutyunyan, A., Moses, A. S., Avramis, V. I., Louie, S. G., Butturini, A., Heisterkamp, N., & Mittelman, S. D. (2009). Adipocytes impair leukemia treatment in mice. *Cancer Research*, 69(19), 7867–7874. <https://doi.org/10.1158/0008-5472.CAN-09-0800>
- Bejar, R., Levine, R., & Ebert, B. L. (2011). Unraveling the molecular pathophysiology of myelodysplastic syndromes. *Journal of Clinical Oncology*, 29(5), 504–515. <https://doi.org/10.1200/JCO.2010.31.1175>
- Bejar, R., Lord, A., Stevenson, K., Bar-Natan, M., Pérez-Ladaga, A., Zaneveld, J., Wang, H., Caughey, B., Stojanov, P., Getz, G., Garcia-Manero, G., Kantarjian, H., Chen, R., Stone, R. M., Neuberg, D., Steensma, D. P., & Ebert, B. L. (2014). TET2 mutations predict response to hypomethylating agents in myelodysplastic syndrome patients. *Blood*, 124(17), 2705–2712. <https://doi.org/10.1182/blood-2014-06-582809>
- Bengoechea-Alonso, M. T., & Ericsson, J. (2007). SREBP in signal transduction: Cholesterol metabolism and beyond. *Current Opinion in Cell Biology*, 19(2), 215–222. <https://doi.org/10.1016/j.ceb.2007.02.004>
- Bennett, J. M., Catovsky, D., Daniel, M. T., Flandrin, G., Galton, D. A. G., Gralnick, H. R., & Sultan, C. (1982). Proposals for the classification of the myelodysplastic syndromes. *British Journal of Haematology*, 51(2), 189–199. <https://doi.org/10.1111/j.1365-2141.1982.tb02771.x>

- Bennett, J. M., Catovsky, D., Daniel, M. T., Flandrin, G., Galton, D. A., Gralnick, H. R., & Sultan, C. (1976). Proposals for the classification of the acute leukaemias. French-American-British (FAB) co-operative group. *British Journal of Haematology*, 33(4), 451–458.
- Bento, L. C., Correia, R. P., Pitangueiras Manguiera, C. L., De Souza Barroso, R., Rocha, F. A., Bacal, N. S., & Marti, L. C. (2017). The Use of Flow Cytometry in Myelodysplastic Syndromes: A Review. *Frontiers in Oncology*, 7. <https://doi.org/10.3389/fonc.2017.00270>
- Berger, T., Saunders, M. E., & Mak, T. W. (2017). Beyond the Oncogene Revolution: Four New Ways to Combat Cancer. *Cold Spring Harbor Symposia on Quantitative Biology*, LXXXI, 031161–031161. <https://doi.org/10.1101/sqb.2016.81.031161>
- Bernstein, B. E., Mikkelsen, T. S., Xie, X., Kamal, M., Huebert, D. J., Cuff, J., Fry, B., Meissner, A., Wernig, M., Plath, K., Jaenisch, R., Wagschal, A., Feil, R., Schreiber, S. L., & Lander, E. S. (2006). A Bivalent Chromatin Structure Marks Key Developmental Genes in Embryonic Stem Cells. *Cell*, 125(2), 315–326. <https://doi.org/10.1016/j.cell.2006.02.041>
- Bhuiyan, H., Masquelier, M., Tatidis, L., Gruber, A., Paul, C., & Vitols, S. (2017). Acute Myelogenous Leukemia Cells Secrete Factors that Stimulate Cellular LDL Uptake via Autocrine and Paracrine Mechanisms. *Lipids*, 52(6), 523–534. <https://doi.org/10.1007/s11745-017-4256-z>
- Bian, X., Yang, Z., Feng, H., Sun, H., & Liu, Y. (2017). A Combination of Species Identification and STR Profiling Identifies Cross-contaminated Cells from 482 Human Tumor Cell Lines. *Scientific Reports*, 7(1), 1–10. <https://doi.org/10.1038/s41598-017-09660-w>
- Blum, W., Klisovic, R. B., Hackanson, B., Liu, Z., Liu, S., Devine, H., Vukosavljevic, T., Huynh, L., Lozanski, G., Kefauver, C., Plass, C., Devine, S. M., Heerema, N. A., Murgo, A., Chan, K. K., Grever, M. R., Byrd, J. C., & Marcucci, G. (2007). Phase I Study of Decitabine Alone or in Combination With Valproic Acid in Acute Myeloid Leukemia. *Journal of Clinical Oncology*, 25(25), 3884–3891. <https://doi.org/10.1200/JCO.2006.09.4169>
- Bowen, D. T., & Hellstrom-Lindberg, E. (2001). Best supportive care for the anaemia of myelodysplasia: Inclusion of recombinant erythropoietin therapy? *Leukemia Research*, 25(1), 19–21. [https://doi.org/10.1016/S0145-2126\(00\)00100-4](https://doi.org/10.1016/S0145-2126(00)00100-4)
- Bowman, R. L., Busque, L., & Levine, R. L. (2018). Clonal Hematopoiesis and Evolution to Hematopoietic Malignancies. *Cell Stem Cell*, 22(2), 157–170. <https://doi.org/10.1016/j.stem.2018.01.011>
- Bracken, A. P. (2006). Genome-wide mapping of Polycomb target genes unravels their roles in cell fate transitions. *Genes & Development*, 20(9). <https://doi.org/10.1101/gad.381706>
- Bracken, Adrian P., & Helin, K. (2009). Polycomb group proteins: Navigators of lineage pathways led astray in cancer. *Nature Reviews Cancer*, 9(11), 773–784. <https://doi.org/10.1038/nrc2736>
- Brand, K. G., & Syverton, J. T. (1962). Results of species-specific hemagglutination tests on “transformed,” nontransformed, and primary cell cultures. *Journal of the National Cancer Institute*, 28(1), 147–157. <https://doi.org/10.1093/jnci/28.1.147>
- Bristow, M. (2000). Etomoxir: A new approach to treatment of chronic heart failure. *The Lancet*, 356(9242), 1621–1622. [https://doi.org/10.1016/S0140-6736\(00\)03149-4](https://doi.org/10.1016/S0140-6736(00)03149-4)
- Bröske, A.-M., Vockentanz, L., Kharazi, S., Huska, M. R., Mancini, E., Scheller, M., Kuhl, C., Enns, A., Prinz, M., Jaenisch, R., Nerlov, C., Leutz, A., Andrade-Navarro, M. A., Jacobsen, S. E. W., & Rosenbauer, F. (2009). DNA methylation protects hematopoietic stem cell multipotency from myeloerythroid restriction. *Nature Genetics*, 41(11), 1207–1215. <https://doi.org/10.1038/ng.463>
- Bungard, D., Fuerth, B. J., Zeng, P.-Y., Faubert, B., Maas, N. L., Viollet, B., Carling, D., Thompson, C. B., Jones, R. G., & Berger, S. L. (2010). Signaling Kinase AMPK Activates Stress-Promoted Transcription via Histone H2B Phosphorylation. 329(5996), 1201–1205. <https://doi.org/10.1126/science.1191241>
- Campbell, S. E., Tandon, N. N., Woldegiorgis, G., Luiken, J. J. F. P., Glatz, J. F. C., & Bonen, A. (2004). A novel function for fatty acid translocase (FAT)/CD36: Involvement in long

| Bibliography

- chain fatty acid transfer into the mitochondria. *The Journal of Biological Chemistry*, 279(35), 36235–36241. <https://doi.org/10.1074/jbc.M400566200>
- Cantó, C., & Auwerx, J. (2009). PGC-1 α , SIRT1 and AMPK, an energy sensing network that controls energy expenditure. *Current Opinion in Lipidology*, 20(2), 98–105. <https://doi.org/10.1097/MOL.0b013e328328doa4>
- Capes-Davis, A., Reid, Y. A., Kline, M. C., Storts, D. R., Strauss, E., Dirks, W. G., Drexler, H. G., MacLeod, R. A. F., Sykes, G., Kohara, A., Nakamura, Y., Elmore, E., Nims, R. W., Alston-Roberts, C., Barallon, R., Los, G. V., Nardone, R. M., Price, P. J., Steuer, A., ... Kerrigan, L. (2013). Match criteria for human cell line authentication: Where do we draw the line? *International Journal of Cancer*, 132(11), 2510–2519. <https://doi.org/10.1002/ijc.27931>
- Capes-Davis, A., Theodosopoulos, G., Atkin, I., Drexler, H. G., Kohara, A., MacLeod, R. A. F., Masters, J. R., Nakamura, Y., Reid, Y. A., Reddel, R. R., & Freshney, R. I. (2010). Check your cultures! A list of cross-contaminated or misidentified cell lines. *International Journal of Cancer*, 127(1), 1–8. <https://doi.org/10.1002/ijc.25242>
- Carretta, M., Brouwers-Vos, A. Z., Bosman, M., Horton, S. J., Martens, J. H. A., Vellenga, E., & Schuringa, J. J. (2017). BRD3/4 inhibition and FLT3-ligand deprivation target pathways that are essential for the survival of human MLL-AF9+ leukemic cells. *PLoS ONE*, 12(12), e0189102–e0189102. <https://doi.org/10.1371/journal.pone.0189102>
- Castillo, J. J., Reagan, J. L., Ingham, R. R., Furman, M., Dalia, S., Merhi, B., Nemr, S., Zarrabi, A., & Mitri, J. (2012). Obesity but not overweight increases the incidence and mortality of leukemia in adults: A meta-analysis of prospective cohort studies. *Leukemia Research*, 36(7). <https://doi.org/10.1016/j.leukres.2011.12.020>
- Cawthorn, W. P., Scheller, E. L., Parlee, S. D., Pham, H. A., Learman, B. S., Redshaw, C. M. H., Sulston, R. J., Burr, A. A., Das, A. K., Simon, B. R., Mori, H., Bree, A. J., Schell, B., Krishnan, V., & MacDougald, O. A. (2016). Expansion of Bone Marrow Adipose Tissue During Caloric Restriction Is Associated With Increased Circulating Glucocorticoids and Not With Hypoleptinemia. *Endocrinology*, 157(2). <https://doi.org/10.1210/en.2015-1477>
- Cazzola, M. (2020). Myelodysplastic Syndromes. *New England Journal of Medicine*, 383(14), 1358–1374. <https://doi.org/10.1056/NEJMr1904794>
- Cazzola, M., Della Porta, M. G., & Malcovati, L. (2008). Clinical Relevance of Anemia and Transfusion Iron Overload in Myelodysplastic Syndromes. *Hematology*, 2008(1), 166–175. <https://doi.org/10.1182/asheducation-2008.1.166>
- Cedar, H., & Bergman, Y. (2011). Epigenetics of haematopoietic cell development. *Nature Reviews Immunology*, 11(7), 478–488. <https://doi.org/10.1038/nri2991>
- Chabowski, A., Coort, S. L. M., Calles-Escandon, J., Tandon, N. N., Glatz, J. F. C., Luiken, J. J. F. P., & Bonen, A. (2005). The subcellular compartmentation of fatty acid transporters is regulated differently by insulin and by AICAR. *FEBS Letters*, 579(11), 2428–2432. <https://doi.org/10.1016/j.febslet.2004.11.118>
- Challen, G. A., Sun, D., Jeong, M., Luo, M., Jelinek, J., Berg, J. S., Bock, C., Vasanthakumar, A., Gu, H., Xi, Y., Liang, S., Lu, Y., Darlington, G. J., Meissner, A., Issa, J.-P. J., Godley, L. A., Li, W., & Goodell, M. A. (2012). Dnmt3a is essential for hematopoietic stem cell differentiation. *Nature Genetics*, 44(1). <https://doi.org/10.1038/ng.1009>
- Chambers, K. T., Chen, Z., Lai, L., Leone, T. C., Towle, H. C., Kralli, A., Crawford, P. A., & Finck, B. N. (2013). PGC-1 β and ChREBP partner to cooperatively regulate hepatic lipogenesis in a glucose concentration-dependent manner. *Molecular Metabolism*, 2(3), 194–204. <https://doi.org/10.1016/j.molmet.2013.05.001>
- Chandhok, N. S., & Prebet, T. (2019). Insights into novel emerging epigenetic drugs in myeloid malignancies. *Therapeutic Advances in Hematology*, 10, 204062071986608. <https://doi.org/10.1177/2040620719866081>
- Chang, X., Han, J., Pang, L., Zhao, Y., Yang, Y., & Shen, Z. (2009). Increased PADI4 expression in blood and tissues of patients with malignant tumors. *BMC Cancer*, 9. <https://doi.org/10.1186/1471-2407-9-40>

- Chapuis, N., Poulain, L., Birsén, R., Tamburini, J., & Bouscary, D. (2019). Rationale for Targeting Deregulated Metabolic Pathways as a Therapeutic Strategy in Acute Myeloid Leukemia. *Frontiers in Oncology*, 9, 405–405. <https://doi.org/10.3389/fonc.2019.00405>
- Chen, C.-W., Koche, R. P., Sinha, A. U., Deshpande, A. J., Zhu, N., Eng, R., Doench, J. G., Xu, H., Chu, S. H., Qi, J., Wang, X., Delaney, C., Bernt, K. M., Root, D. E., Hahn, W. C., Bradner, J. E., & Armstrong, S. A. (2015). DOT1L inhibits SIRT1-mediated epigenetic silencing to maintain leukemic gene expression in MLL-rearranged leukemia. *Nature Medicine*, 21(4). <https://doi.org/10.1038/nm.3832>
- Christman, J., Mendelsohn, N., Herzog, D., & Schneiderman, N. (1983). Effect of 5-azacytidine on differentiation and DNA methylation in human promyelocytic leukemia cells (HL-60). *Cancer Research*, 43(2), 763–769.
- Christophorou, M. A., Castelo-Branco, G., Halley-Stott, R. P., Oliveira, C. S., Loos, R., Radziszheuskaya, A., Mowen, K. A., Bertone, P., Silva, J. C. R., Zernicka-Goetz, M., Nielsen, M. L., Gurdon, J. B., & Kouzarides, T. (2014). Citrullination regulates pluripotency and histone H1 binding to chromatin. *Nature*, 507(7490), 104–108. <https://doi.org/10.1038/nature12942>
- Cluzeau, T., Sebert, M., Rahmé, R., Cuzzubbo, S., Walter-petrich, A., Lehmann che, J., Peterlin, P., Beve, B., Attalah, H., Chermat, F., Miekoutima, E., Beyne-Rauzy, O., Recher, C., Stamatoullas, A., Willems, L., Raffoux, E., Berthon, C., Quesnel, B., Carpentier, A., ... Fenaux, P. (2019). APR-246 Combined with Azacitidine (AZA) in TP53 Mutated Myelodysplastic Syndrome (MDS) and Acute Myeloid Leukemia (AML). A Phase 2 Study By the Groupe Francophone Des Myélodysplasies (GFM). *Blood*, 134(Supplement_1), 677–677. <https://doi.org/10.1182/blood-2019-125579>
- Cogle, C. R., Craig, B. M., Rollison, D. E., & List, A. F. (2011). Incidence of the myelodysplastic syndromes using a novel claims-based algorithm: High number of uncaptured cases by cancer registries. *Blood*, 117(26), 7121–7125. <https://doi.org/10.1182/blood-2011-02-337964>
- Cook, K., Daniels, I., Symonds, P., Pitt, T., Gijon, M., Xue, W., Metheringham, R., Durrant, L., & Brentville, V. (2018). Citrullinated α -enolase is an effective target for anti-cancer immunity. *OncImmunity*, 7(2). <https://doi.org/10.1080/2162402X.2017.1390642>
- Coort, S. L. M., Willems, J., Coumans, W. A., Der, G. J. V., Bonen, A., Glatz, J. F. C., & Luiken, J. J. F. P. (2002). Sulfo- N -succinimidyl esters of long chain fatty acids specifically inhibit fatty acid translocase (FAT / CD36) -mediated cellular fatty acid uptake. *Mol Cell Biochem*, 213–219.
- Corbet, C. and F., Olivier. (2017). Emerging roles of lipid metabolism in cancer progression. *Molecular Cancer*, 16(1), 76–76. <https://doi.org/10.1186/s12943-017-0646-3>
- Corces-Zimmerman, M. R., & Majeti, R. (2014). *Pre-leukemic evolution of hematopoietic stem cells: The importance of early mutations in leukemogenesis*. 28. <https://doi.org/10.1038/leu.2014.211>
- Craig, B. M., Rollison, D. E., List, A. F., & Cogle, C. R. (2012). Underreporting of Myeloid Malignancies by United States Cancer Registries. *Cancer Epidemiology Biomarkers & Prevention*, 21(3), 474–481. <https://doi.org/10.1158/1055-9965.EPI-11-1087>
- Craig, W., Kay, R., Cutler, R. L., & Lansdorp, P. M. (1993). Expression of Thy-1 on human hematopoietic progenitor cells. *Journal of Experimental Medicine*, 177(5), 1331–1342. <https://doi.org/10.1084/jem.177.5.1331>
- Cumbo, C., Tota, G., Anelli, L., Zagaria, A., Specchia, G., & Albano, F. (2020). TP53 in Myelodysplastic Syndromes: Recent Biological and Clinical Findings. *International Journal of Molecular Sciences*, 21(10), 3432–3432. <https://doi.org/10.3390/ijms21103432>
- Cuthbert, G. L., Daujat, S., Snowden, A. W., Erdjument-Bromage, H., Hagiwara, T., Yamada, M., Schneider, R., Gregory, P. D., Tempst, P., Bannister, A. J., & Kouzarides, T. (2004). Histone Deimination Antagonizes Arginine Methylation. *Cell*, 118(5), 545–553. <https://doi.org/10.1016/j.cell.2004.08.020>

| Bibliography

- Dai, Z., Sheridan, J. M., Gearing, L. J., Moore, D. L., Su, S., Wormald, S., Wilcox, S., O'Connor, L., Dickins, R. A., Blewitt, M. E., & Ritchie, M. E. (2014a). EdgeR: a versatile tool for the analysis of shRNA-seq and CRISPR-Cas9 genetic screens. *F1000Research*. <https://doi.org/10.12688/f1000research.3928.2>
- Dai, Z., Sheridan, J. M., Gearing, L. J., Moore, D. L., Su, S., Wormald, S., Wilcox, S., O'Connor, L., Dickins, R. A., Blewitt, M. E., & Ritchie, M. E. (2014b). EdgeR: a versatile tool for the analysis of shRNA-seq and CRISPR-Cas9 genetic screens. *F1000Research*, 3, 95–95. <https://doi.org/10.12688/f1000research.3928.2>
- Daneshbod, Y., Kohan, L., Taghadosi, V., Weinberg, O. K., & Arber, D. A. (2019). Prognostic Significance of Complex Karyotypes in Acute Myeloid Leukemia. *Current Treatment Options in Oncology*, 20(2), 15–15. <https://doi.org/10.1007/s11864-019-0612-y>
- Dawlaty, M. M., Ganz, K., Powell, B. E., Hu, Y. C., Markoulaki, S., Cheng, A. W., Gao, Q., Kim, J., Choi, S. W., Page, D. C., & Jaenisch, R. (2011). Tet1 is dispensable for maintaining pluripotency and its loss is compatible with embryonic and postnatal development. *Cell Stem Cell*, 9(2), 166–175. <https://doi.org/10.1016/j.stem.2011.07.010>
- Dawson, M. A., Prinjha, R. K., Dittmann, A., Giotopoulos, G., Bantscheff, M., Chan, W.-I., Robson, S. C., Chung, C., Hopf, C., Savitski, M. M., Huthmacher, C., Gudgin, E., Lugo, D., Beinke, S., Chapman, T. D., Roberts, E. J., Soden, P. E., Auger, K. R., Mirguet, O., ... Kouzarides, T. (2011). Inhibition of BET recruitment to chromatin as an effective treatment for MLL-fusion leukaemia. *Nature*, 478(7370). <https://doi.org/10.1038/nature10509>
- Dentin, R., Benhamed, F., Pégrier, J. P., Fougelle, F., Viollet, B., Vaulont, S., Girard, J., & Postic, C. (2005). Polyunsaturated fatty acids suppress glycolytic and lipogenic genes through the inhibition of ChREBP nuclear protein translocation. *Journal of Clinical Investigation*, 115(10), 2843–2854. <https://doi.org/10.1172/JCI25256>
- Dentin, R., Pégrier, J.-P., Benhamed, F., Fougelle, F., Ferré, P., Fauveau, V., Magnuson, M. A., Girard, J., & Postic, C. (2004). Hepatic Glucokinase Is Required for the Synergistic Action of ChREBP and SREBP-1c on Glycolytic and Lipogenic Gene Expression. *Journal of Biological Chemistry*, 279(19), 20314–20326. <https://doi.org/10.1074/jbc.M312475200>
- Deplus, R., Denis, H., Putmans, P., Calonne, E., Fourrez, M., Yamamoto, K., Suzuki, A., & Fuks, F. (2014). Citrullination of DNMT3A by PADI4 regulates its stability and controls DNA methylation. *Nucleic Acids Research*, 42(13), 8285–8296. <https://doi.org/10.1093/nar/gku522>
- Desvergne, B., & Wahli, W. (1999). Peroxisome Proliferator-Activated Receptors: Nuclear Control of Metabolism*. *Endocrine Reviews*, 20(5), 649–688. <https://doi.org/10.1210/edrv.20.5.0380>
- Dhalluin, C., Carlson, J. E., Zeng, L., He, C., Aggarwal, A. K., Zhou, M.-M., & Zhou, M.-M. (1999). Structure and ligand of a histone acetyltransferase bromodomain. *Nature*, 399(6735). <https://doi.org/10.1038/20974>
- Dias, S., Månsson, R., Gurbuxani, S., Sigvardsson, M., & Kee, B. L. (2008). E2A Proteins Promote Development of Lymphoid-Primed Multipotent Progenitors. *Immunity*, 29(2), 217–227. <https://doi.org/10.1016/j.immuni.2008.05.015>
- DiNardo, C. D., Jabbour, E., Ravandi, F., Takahashi, K., Daver, N., Routbort, M., Patel, K. P., Brandt, M., Pierce, S., Kantarjian, H., & Garcia-Manero, G. (2016). IDH1 and IDH2 mutations in myelodysplastic syndromes and role in disease progression. *Leukemia*, 30(4), 980–984. <https://doi.org/10.1038/leu.2015.211>
- Ding, Y., Gao, H., & Zhang, Q. (2017). The biomarkers of leukemia stem cells in acute myeloid leukemia. *Stem Cell Investigation*, 2017(MAR). <https://doi.org/10.21037/sci.2017.02.10>
- Doudna, J. A., & Charpentier, E. (2014). The new frontier of genome engineering with CRISPR-Cas9. *Science*, 346(6213), 1258096–1258096. <https://doi.org/10.1126/science.1258096>
- Doulatov, S., Notta, F., Laurenti, E., & Dick, J. E. (2012). Hematopoiesis: A human perspective. *Cell Stem Cell*, 10(2), 120–136. <https://doi.org/10.1016/j.stem.2012.01.006>

- Drexler, H G, Dirks, W. G., Matsuo, Y., & MacLeod, R. A. F. (2003). False leukemia-lymphoma cell lines: An update on over 500 cell lines. *Leukemia*, *17*(2), 416–426. <https://doi.org/10.1038/sj.leu.2402799>
- Drexler, Hans G. (2010). *Guide to Cell Lines Authentication of Cell Lines, 2nd edition*.
- Eberharter, A., & Becker, P. B. (2002). Histone acetylation: A switch between repressive and permissive chromatin: Second in review series on chromatin dynamics. *EMBO Reports*, *3*(3), 224–229. <https://doi.org/10.1093/embo-reports/kvf053>
- Efficace, F., Gaidano, G., Breccia, M., Criscuolo, M., Cottone, F., Caocci, G., Bowen, D., Lübbert, M., Angelucci, E., Stauder, R., Selleslag, D., Platzbecker, U., Sanpaolo, G., Jonasova, A., Buccisano, F., Specchia, G., Palumbo, G. A., Niscola, P., Wan, C., ... Mandelli, F. (2015). Prevalence, severity and correlates of fatigue in newly diagnosed patients with myelodysplastic syndromes. *British Journal of Haematology*, *168*(3), 361–370. <https://doi.org/10.1111/bjh.13138>
- Ehrlich, M., & Ehrlich, K. C. (2014). DNA cytosine methylation and hydroxymethylation at the borders. *Epigenomics*, *6*(6), 563–566. <https://doi.org/10.2217/epi.14.48>
- Elbashir, S. M., Harborth, J., Lendeckel, W., Yalcin, A., Weber, K., & Tuschl, T. (2001). Duplexes of 21-nucleotide RNAs mediate RNA interference in cultured mammalian cells. *Nature*, *411*(6836), 494–498. <https://doi.org/10.1038/35078107>
- El-Brolosy, M. A., & Stainier, D. Y. R. (2017). Genetic compensation: A phenomenon in search of mechanisms. *PLoS Genetics*, *13*(7). <https://doi.org/10.1371/journal.pgen.1006780>
- Espenshade, P. J., & Hughes, A. L. (2007). Regulation of Sterol Synthesis in Eukaryotes. *Annual Review of Genetics*, *41*(1), 401–427. <https://doi.org/10.1146/annurev.genet.41.110306.130315>
- Ettou, S., Audureau, E., Humbrecht, C., Benet, B., Jammes, H., Clozel, T., Bardet, V., Lacombe, C., Dreyfus, F., Mayeux, P., Solary, E., & Fontenay, M. (2012). Fas expression at diagnosis as a biomarker of azacitidine activity in high-risk MDS and secondary AML. *Leukemia*, *26*(10), 2297–2299. <https://doi.org/10.1038/leu.2012.152>
- Evers, B., Jastrzebski, K., Heijmans, J. P. M., Grenrum, W., Beijersbergen, R. L., & Bernards, R. (2016). CRISPR knockout screening outperforms shRNA and CRISPRi in identifying essential genes. *Nature Biotechnology*, *34*(6), 631–633. <https://doi.org/10.1038/nbt.3536>
- Farge, T., Saland, E., de Toni, F., Aroua, N., Hosseini, M., Perry, R., Bosc, C., Sugita, M., Stuaní, L., Fraisse, M., Scotland, S., Larrue, C., Boutzen, H., Féliu, V., Nicolau-Travers, M. L., Cassant-Sourdy, S., Broin, N., David, M., Serhan, N., ... Sarry, J. E. (2017). Chemotherapy-resistant human acute myeloid leukemia cells are not enriched for leukemic stem cells but require oxidative metabolism. *Cancer Discovery*, *7*(7), 716–735. <https://doi.org/10.1158/2159-8290.CD-16-0441>
- Farge, T., Saland, E., Toni, F. D., Aroua, N., Hosseini, M., Perry, R., Bosc, C., Sugita, M., Stuaní, L., Fraisse, M., Scotland, S., Larrue, C., Boutzen, H., Féliu, V., Cassant-sourdy, S., Broin, N., David, M., Serhan, N., Sarry, A., ... Vergez, F. (2017). *Chemotherapy-Resistant Human Acute Myeloid Leukemia Cells Are Not Enriched for Leukemic Stem Cells but Require Oxidative Metabolism*. 1–21. <https://doi.org/10.1158/2159-8290.CD-16-0441>
- Fellmann, C., Hoffmann, T., Sridhar, V., Hopfgartner, B., Muhar, M., Roth, M., Lai, D. Y., Barbosa, I. A. M., Kwon, J. S., Guan, Y., Sinha, N., & Zuber, J. (2013). An optimized microRNA backbone for effective single-copy RNAi. *Cell Reports*, *5*(6), 1704–1713. <https://doi.org/10.1016/j.celrep.2013.11.020>
- Fenaux, P., & Ades, L. (2009). Review of azacitidine trials in Intermediate-2-and High-risk myelodysplastic syndromes. *Leukemia Research*, *33*, S7–S11. [https://doi.org/10.1016/S0145-2126\(09\)70227-9](https://doi.org/10.1016/S0145-2126(09)70227-9)
- Fenaux, P., Mufti, G. J., Hellstrom-Lindberg, E., Santini, V., Finelli, C., Giagounidis, A., Schoch, R., Gattermann, N., Sanz, G., List, A., Gore, S. D., Seymour, J. F., Bennett, J. M., Byrd, J., Backstrom, J., Zimmerman, L., McKenzie, D., Beach, C., & Silverman, L. R. (2009). Efficacy of azacitidine compared with that of conventional care regimens in the treatment

| Bibliography

- of higher-risk myelodysplastic syndromes: A randomised, open-label, phase III study. *The Lancet Oncology*, 10(3), 223–232. [https://doi.org/10.1016/S1470-2045\(09\)70003-8](https://doi.org/10.1016/S1470-2045(09)70003-8)
- Feng, Y., Li, X., Cassady, K., Zou, Z., & Zhang, X. (2019). TET2 Function in Hematopoietic Malignancies, Immune Regulation, and DNA Repair. *Frontiers in Oncology*, 9. <https://doi.org/10.3389/fonc.2019.00210>
- Fenouille, N., Bassil, C. F., Ben-Sahra, I., Benajiba, L., Alexe, G., Ramos, A., Pikman, Y., Conway, A. S., Burgess, M. R., Li, Q., Luciano, F., Auberger, P., Galinsky, I., DeAngelo, D. J., Stone, R. M., Zhang, Y., Perkins, A. S., Shannon, K., Hemann, M. T., ... Stegmaier, K. (2017). The creatine kinase pathway is a metabolic vulnerability in EVI1-positive acute myeloid leukemia. *Nature Medicine*, 23(3). <https://doi.org/10.1038/nm.4283>
- Figuroa, M. E., Lugthart, S., Li, Y., Erpelinck-Verschueren, C., Deng, X., Christos, P. J., Schifano, E., Booth, J., van Putten, W., Skrabanek, L., Campagne, F., Mazumdar, M., Grealley, J. M., Valk, P. J. M., Löwenberg, B., Delwel, R., & Melnick, A. (2010). DNA Methylation Signatures Identify Biologically Distinct Subtypes in Acute Myeloid Leukemia. *Cancer Cell*, 17(1), 13–27. <https://doi.org/10.1016/j.ccr.2009.11.020>
- Figuroa, M. E., Skrabanek, L., Li, Y., Jiemjit, A., Fandy, T. E., Paietta, E., Fernandez, H., Tallman, M. S., Grealley, J. M., Carraway, H., Licht, J. D., Gore, S. D., & Melnick, A. (2009). MDS and secondary AML display unique patterns and abundance of aberrant DNA methylation. *Blood*, 114(16), 3448–3458. <https://doi.org/10.1182/blood-2009-01-200519>
- Filippakopoulos, P., Qi, J., Picaud, S., Shen, Y., Smith, W. B., Fedorov, O., Morse, E. M., Keates, T., Hickman, T. T., Felletar, I., Philpott, M., Munro, S., McKeown, M. R., Wang, Y., Christie, A. L., West, N., Cameron, M. J., Schwartz, B., Heightman, T. D., ... Bradner, J. E. (2010). Selective inhibition of BET bromodomains. *Nature*, 468(7327), 1067–1073. <https://doi.org/10.1038/nature09504>
- Fire, A., Xu, S., Montgomery, M. K., Kostas, S. A., Driver, S. E., & Mello, C. C. (1998). Potent and specific genetic interference by double-stranded RNA in *Caenorhabditis elegans*. *Nature*, 391(6669), 806–811. <https://doi.org/10.1038/35888>
- Fliedner, T., Haas, R., Stehle, H., & Adams, A. (1968). Complete labeling of all cell nuclei in newborn rats with H₃-thymidine. A tool for the evaluation of rapidly and slowly proliferating cell systems. *Lab Invest.*, 18(3), 249–259.
- Fliedner, Theodor M. (1998). The Role of Blood Stem Cells in Hematopoietic Cell Renewal. *Stem Cells*, 16(6), 361–374. <https://doi.org/10.1002/stem.160361>
- Fliedner, T.M., Graessle, D., Paulsen, C., & Reimers, K. (2002). Structure and Function of Bone Marrow Hemopoiesis: Mechanisms of Response to Ionizing Radiation Exposure. *Cancer Biotherapy and Radiopharmaceuticals*, 17(4), 405–426. <https://doi.org/10.1089/108497802760363204>
- Forman, B. M., Chen, J., & Evans, R. M. (1997). Hypolipidemic drugs, polyunsaturated fatty acids, and eicosanoids are ligands for peroxisome proliferator-activated receptors and. *Proceedings of the National Academy of Sciences*, 94(9), 4312–4317. <https://doi.org/10.1073/pnas.94.9.4312>
- Foster, B., Zaidi, D., Young, T., Mobley, M., & Kerr, B. (2018). CD117/c-kit in Cancer Stem Cell-Mediated Progression and Therapeutic Resistance. *Biomedicines*, 6(1), 31–31. <https://doi.org/10.3390/biomedicines6010031>
- Foufelle, F., & Ferré, P. (2002). New perspectives in the regulation of hepatic glycolytic and lipogenic genes by insulin and glucose: A role for the transcription factor sterol regulatory element binding protein-1c. *Biochemical Journal*, 366(2), 377–391. <https://doi.org/10.1042/bj20020430>
- Freudenberg, J. M., Ghosh, S., Lackford, B. L., Yellaboina, S., Zheng, X., Li, R., Cuddapah, S., Wade, P. A., Hu, G., & Jothi, R. (2012). Acute depletion of Tet1-dependent 5-hydroxymethylcytosine levels impairs LIF/Stat3 signaling and results in loss of embryonic stem cell identity. *Nucleic Acids Research*, 40(8), 3364–3377. <https://doi.org/10.1093/nar/gkr1253>

- Friedenson, B. (2007). The BRCA1/2 pathway prevents hematologic cancers in addition to breast and ovarian cancers. *BMC Cancer*, 7(1), 1–11. <https://doi.org/10.1186/1471-2407-7-152>
- Fu, Y., Foden, J. A., Khayter, C., Maeder, M. L., Reyon, D., Joung, J. K., & Sander, J. D. (2013). High-frequency off-target mutagenesis induced by CRISPR-Cas nucleases in human cells. *Nature Biotechnology*, 31(9), 822–826. <https://doi.org/10.1038/nbt.2623>
- Galdieri, L., & Vancura, A. (2012). Acetyl-CoA Carboxylase Regulates Global Histone Acetylation. *Journal of Biological Chemistry*, 287(28), 23865–23876. <https://doi.org/10.1074/jbc.M112.380519>
- Gartler, S. (1967). Genetic markers as tracers in cell culture. *Natl Cancer Inst Monogr*, 26, 167–195.
- Gascón, P., Krendyukov, A., Mathieson, N., & Aapro, M. (2019). Epoetin alfa for the treatment of myelodysplastic syndrome-related anemia: A review of clinical data, clinical guidelines, and treatment protocols. *Leukemia Research*, 81, 35–42. <https://doi.org/10.1016/j.leukres.2019.03.006>
- Gautam, P., Recino, A., Foale, R. D., Zhao, J., Gan, S. U., Wallberg, M., Calne, R., & Lever, A. M. L. (2016). Promoter optimisation of lentiviral vectors for efficient insulin gene expression in canine mesenchymal stromal cells: Potential surrogate beta cells: Insulin expression in MSCs. *The Journal of Gene Medicine*, 18(10), 312–321. <https://doi.org/10.1002/jgm.2900>
- Gelsi-Boyer, V., Brecqueville, M., Devillier, R., Murati, A., Mozziconacci, M. J., & Birnbaum, D. (2012). Mutations in ASXL1 are associated with poor prognosis across the spectrum of malignant myeloid diseases. *Journal of Hematology and Oncology*, 5(1), 12–12. <https://doi.org/10.1186/1756-8722-5-12>
- Genovese, G., Kähler, A. K., Handsaker, R. E., Lindberg, J., Rose, S. A., Bakhoum, S. F., Chambert, K., Mick, E., Neale, B. M., Fromer, M., Purcell, S. M., Svantesson, O., Landén, M., Höglund, M., Lehmann, S., Gabriel, S. B., Moran, J. L., Lander, E. S., Sullivan, P. F., ... McCarroll, S. A. (2014). Clonal Hematopoiesis and Blood-Cancer Risk Inferred from Blood DNA Sequence. *New England Journal of Medicine*, 371(26), 2477–2487. <https://doi.org/10.1056/NEJMoa1409405>
- German, N. J., Yoon, H., Yusuf, R. Z., Scadden, D. T., Kaelin, W. G., Haigis Correspondence, M. C., Murphy, J. P., Finley, L. W. S., Laurent, G. L., Haas, W., Satterstrom, F. K., Guarnerio, J., Zaganjor, E., Santos, D., Pandolfi, P. P., Beck, A. H., Gygi, S. P., & Haigis, M. C. (2016). PHD3 Loss in Cancer Enables Metabolic Reliance on Fatty Acid Oxidation via Deactivation of ACC2. *Molecular Cell*, 63. <https://doi.org/10.1016/j.molcel.2016.08.014>
- Germing, U., Aul, C., Niemeyer, C. M., Haas, R., & Bennett, J. M. (2008). Epidemiology, classification and prognosis of adults and children with myelodysplastic syndromes. *Annals of Hematology*, 87(9), 691–699. <https://doi.org/10.1007/s00277-008-0499-3>
- Gey, G. O. (1954). Some aspects of the constitution and behavior of normal and malignant cells maintained in continuous culture. *Harvey Lectures*, 50, 154–229.
- Giagounidis, A., Mufti, G. J., Fenaux, P., Germing, U., List, A., & MacBeth, K. J. (2014). Lenalidomide as a disease-modifying agent in patients with del(5q) myelodysplastic syndromes: Linking mechanism of action to clinical outcomes. *Annals of Hematology*, 93(1), 1–11. <https://doi.org/10.1007/s00277-013-1863-5>
- Goetze, K. (2009). The role of azacitidine in the management of myelodysplastic syndromes (MDS). *Cancer Management and Research*. <https://doi.org/10.2147/CMR.S4721>
- Gore, S. D., Fenaux, P., Santini, V., Bennett, J. M., Silverman, L. R., Seymour, J. F., Hellstrom-Lindberg, E., Swern, A. S., Beach, C. L., & List, A. F. (2013). A multivariate analysis of the relationship between response and survival among patients with higher-risk myelodysplastic syndromes treated within azacitidine or conventional care regimens in the randomized AZA-001 trial. *Haematologica*, 98(7), 1067–1072. <https://doi.org/10.3324/haematol.2012.074831>
- Goto, M., Miwa, H., Suganuma, K., Tsunekawa-Imai, N., Shikami, M., Mizutani, M., Mizuno, S., Hanamura, I., & Nitta, M. (2014). Adaptation of leukemia cells to hypoxic condition

| Bibliography

- through switching the energy metabolism or avoiding the oxidative stress. *BMC Cancer*, 14(1), 76–76. <https://doi.org/10.1186/1471-2407-14-76>
- Greenberg, P., Cox, C., LeBeau, M. M., Fenaux, P., Morel, P., Sanz, G., Sanz, M., Vallespi, T., Hamblin, T., Oscier, D., Ohyashiki, K., Toyama, K., Aul, C., Mufti, G., & Bennett, J. (1997). International scoring system for evaluating prognosis in myelodysplastic syndromes. *Blood*, 89(6), 2079–2088. <https://doi.org/10.1182/blood.v89.6.2079>
- Greenberg, P., Tuechler, H., Schanz, J., Sanz, G., Garcia-Manero, G., Solé, F., Bennett, J. M., Bowen, D., Fenaux, P., Dreyfus, F., Kantarjian, H., Kuendgen, A., Levis, A., Malcovati, L., Cazzola, M., Cermak, J., Fonatsch, C., Le Beau, M. M., Slovak, M. L., ... Haase, D. (2012). Revised international prognostic scoring system for myelodysplastic syndromes. *Blood*, 120(12), 2454–2465. <https://doi.org/10.1182/blood-2012-03-420489>
- Gregory, M. A., D'Alessandro, A., Alvarez-Calderon, F., Kim, J., Nemkov, T., Adane, B., Rozhok, A. I., Kumar, A., Kumar, V., Pollyea, D. A., Wempe, M. F., Jordan, C. T., Serkova, N. J., Tan, A. C., Hansen, K. C., & DeGregori, J. (2016). ATM/G6PD-driven redox metabolism promotes FLT3 inhibitor resistance in acute myeloid leukemia. *Proceedings of the National Academy of Sciences*, 113(43). <https://doi.org/10.1073/pnas.1603876113>
- Gu, S., Jin, L., Zhang, Y., Huang, Y., Zhang, F., Valdmanis, P. N., & Kay, M. A. (2012). The Loop Position of shRNAs and Pre-miRNAs Is Critical for the Accuracy of Dicer Processing In Vivo. *Cell*, 151(4), 900–911. <https://doi.org/10.1016/j.cell.2012.09.042>
- Haase, D., Germing, U., Schanz, J., Pfeilstöcker, M., Nösslinger, T., Hildebrandt, B., Kundgen, A., Lübbert, M., Kunzmann, R., Giagounidis, A. A. N., Aul, C., Trümper, L., Krieger, O., Stauder, R., Müller, T. H., Wimazal, F., Valent, P., Fonatsch, C., & Steidl, C. (2007). New insights into the prognostic impact of the karyotype in MDS and correlation with subtypes: Evidence from a core dataset of 2124 patients. *Blood*, 110(13), 4385–4395. <https://doi.org/10.1182/blood-2007-03-082404>
- Haferlach, T., Nagata, Y., Grossmann, V., Okuno, Y., Bacher, U., Nagae, G., Schnittger, S., Sanada, M., Kon, A., Alpermann, T., Yoshida, K., Roller, A., Nadarajah, N., Shiraishi, Y., Shiozawa, Y., Chiba, K., Tanaka, H., Koeffler, H. P., Klein, H.-U., ... Ogawa, S. (2014). Landscape of genetic lesions in 944 patients with myelodysplastic syndromes. *Leukemia*, 28, 241–247. <https://doi.org/10.1038/leu.2013.336>
- Handschuh, L., Kazmierczak, M., Milewski, M. C., Goralski, M., Luczak, M., Wojtaszewska, M., Uszczyńska-Ratajczak, B., Lewandowski, K., Komarnicki, M., & Figlerowicz, M. (2018). Gene expression profiling of acute myeloid leukemia samples from adult patients with AML-M1 and -M2 through boutique microarrays, real-time PCR and droplet digital PCR. *International Journal of Oncology*, 52(3), 656–678. <https://doi.org/10.3892/ijo.2017.4233>
- Harada, H., Harada, Y., Niimi, H., Kyo, T., Kimura, A., & Inaba, T. (2004). High incidence of somatic mutations in the AML1/RUNX1 gene in myelodysplastic syndrome and low blast percentage myeloid leukemia with myelodysplasia. *Blood*, 103(6), 2316–2324. <https://doi.org/10.1182/blood-2003-09-3074>
- Harrington, A. M., Olteanu, H., & Kroft, S. H. (2012). A Dissection of the CD45/Side Scatter “Blast Gate”. *American Journal of Clinical Pathology*, 137(5), 800–804. <https://doi.org/10.1309/AJCPN4G1ZPABRLH>
- Heiden, M. G. V., Cantley, L. C., & Thompson, C. B. (2009). Understanding the warburg effect: The metabolic requirements of cell proliferation. *Science*, 324(5930), 1029–1033. <https://doi.org/10.1126/science.1160809>
- Heil, C. S., Wehrheim, S. S., Paithankar, K. S., & Grninger, M. (2019). Fatty Acid Biosynthesis: Chain-Length Regulation and Control. *ChemBioChem*, 20(18), 2298–2321. <https://doi.org/10.1002/cbic.201800809>
- Heinonen, S., Buzkova, J., Muniandy, M., Kaksonen, R., Ollikainen, M., Ismail, K., Hakkarainen, A., Lundbom, J., Lundbom, N., Vuolteenaho, K., Moilanen, E., Kaprio, J., Rissanen, A., Suomalainen, A., & Pietiläinen, K. H. (2015). Impaired Mitochondrial Biogenesis in Adipose Tissue in Acquired Obesity. *Diabetes*, 64(9), 3135–3145. <https://doi.org/10.2337/db14-1937>

- Heng, H. H., Bremer, S. W., Stevens, J. B., Horne, S. D., Liu, G., Abdallah, B. Y., Ye, K. J., & Ye, C. J. (2013). Chromosomal instability (CIN): What it is and why it is crucial to cancer evolution. *Cancer and Metastasis Reviews*, *32*(3–4), 325–340. <https://doi.org/10.1007/s10555-013-9427-7>
- Hermetet, F., Mshaik, R., Simonet, J., Callier, P., Delva, L., & Quéré, R. (2020). High-fat diet intensifies MLL-AF9-induced acute myeloid leukemia through activation of the FLT3 signaling in mouse primitive hematopoietic cells. *Scientific Reports*, *10*(1). <https://doi.org/10.1038/s41598-020-73020-4>
- Hervioui, L., Cavalli, G., Cartron, G., Klein, B., & Moreaux, J. (2016). EZH2 in normal hematopoiesis and hematological malignancies. *Oncotarget*, *7*(3), 2284–2296. <https://doi.org/10.18632/oncotarget.6198>
- Hindorf, C., Glatting, G., Chiesa, C., Lindén, O., & Flux, G. (2010). EANM Dosimetry Committee guidelines for bone marrow and whole-body dosimetry. *European Journal of Nuclear Medicine and Molecular Imaging*, *37*(6). <https://doi.org/10.1007/s00259-010-1422-4>
- Hirai, H. (2003). Molecular Mechanisms of Myelodysplastic Syndrome. *Japanese Journal of Clinical Oncology*, *33*(4), 153–160. <https://doi.org/10.1093/jjco/hygo37>
- Hirotsu, Y., Hataya, N., Katsuoka, F., & Yamamoto, M. (2012). NF-E2-Related Factor 1 (Nrf1) Serves as a Novel Regulator of Hepatic Lipid Metabolism through Regulation of the Lipin1 and PGC-1 Genes. *Molecular and Cellular Biology*, *32*(14), 2760–2770. <https://doi.org/10.1128/MCB.06706-11>
- Hirsch, C., & Schildknecht, S. (2019). In vitro research reproducibility: Keeping up high standards. *Frontiers in Pharmacology*, *10*. <https://doi.org/10.3389/fphar.2019.01484>
- Hoile, S. P., Irvine, N. A., Kelsall, C. J., Sibbons, C., Feunteun, A., Collister, A., Torrens, C., Calder, P. C., Hanson, M. A., Lillycrop, K. A., & Burdge, G. C. (2013). Maternal fat intake in rats alters 20:4n-6 and 22:6n-3 status and the epigenetic regulation of Fads2 in offspring liver. *The Journal of Nutritional Biochemistry*, *24*(7), 1213–1220. <https://doi.org/10.1016/J.JNUTBIO.2012.09.005>
- Horbach, S. P. J. M., & Halffman, W. (2017). The ghosts of HeLa: How cell line misidentification contaminates the scientific literature. *PLOS ONE*, *12*(10), e0186281. <https://doi.org/10.1371/journal.pone.0186281>
- Housman, G., Byler, S., Heerboth, S., Lapinska, K., Longacre, M., Snyder, N., & Sarkar, S. (2014). Drug Resistance in Cancer: An Overview. *Cancers*, *6*(3), 1769–1792. <https://doi.org/10.3390/cancers6031769>
- Hu, Z., & Tee, W.-W. (2017). Enhancers and chromatin structures: Regulatory hubs in gene expression and diseases. *Bioscience Reports*, *37*(2). <https://doi.org/10.1042/BSR20160183>
- Huang, G., Zhang, P., Hirai, H., Elf, S., Yan, X., Chen, Z., Koschmieder, S., Okuno, Y., Dayaram, T., Gowney, J. D., Shivdasani, R. A., Gilliland, D. G., Speck, N. A., Nimer, S. D., & Tenen, D. G. (2008). PU.1 is a major downstream target of AML1 (RUNX1) in adult mouse hematopoiesis. *Nature Genetics*, *40*(1), 51–60. <https://doi.org/10.1038/ng.2007.7>
- Huang, T.-C., Ko, B.-S., Tang, J.-L., Hsu, C., Chen, C.-Y., Tsay, W., Huang, S.-Y., Yao, M., Chen, Y.-C., Shen, M.-C., Wang, C.-H., & Tien, H.-F. (2008). Comparison of hypoplastic myelodysplastic syndrome (MDS) with normo-/hypercellular MDS by International Prognostic Scoring System, cytogenetic and genetic studies. *Leukemia*, *22*(3), 544–550. <https://doi.org/10.1038/sj.leu.2405076>
- Huang, X., Li, X., Xie, M., Huang, Z., Huang, Y., Wu, G., Peng, Z., Sun, Y., Ming, Q., Liu, Y., Chen, J., & Xu, S. (2019). Resveratrol: Review on its discovery, anti-leukemia effects and pharmacokinetics. *Chemico-Biological Interactions*, *306*. <https://doi.org/10.1016/j.cbi.2019.04.001>
- Huang, Y., Liu, Y., Zheng, C., & Shen, C. (2017). Investigation of Cross-Contamination and Misidentification of 278 Widely Used Tumor Cell Lines. *PLOS ONE*, *12*(1), e0170384–e0170384. <https://doi.org/10.1371/journal.pone.0170384>

| Bibliography

- Huang, Z., Ruan, H.-B., Xian, L., Chen, W., Jiang, S., Song, A., Wang, Q., Shi, P., Gu, X., & Gao, X. (2014). The stem cell factor/Kit signalling pathway regulates mitochondrial function and energy expenditure. *Nature Communications*. <https://doi.org/10.1038/ncomms5282>
- Hukku, B., Halton, D. M., Mally, M., & Peterson, W. D. (1984). Cell characterization by use of multiple genetic markers. *Advances in Experimental Medicine and Biology*, 172, 13–31. https://doi.org/10.1007/978-1-4615-9376-8_2
- Hyun, K., Jeon, J., Park, K., & Kim, J. (2017). Writing, erasing and reading histone lysine methylations. *Experimental & Molecular Medicine*, 49(4), e324–e324. <https://doi.org/10.1038/emm.2017.11>
- Ishii, S., Izuka, K., Miller, B. C., & Uyeda, K. (2004). Carbohydrate response element binding protein directly promotes lipogenic enzyme gene transcription. *Proceedings of the National Academy of Sciences*, 101(44), 15597–15602. <https://doi.org/10.1073/pnas.0405238101>
- Ishikawa, F., Yasukawa, M., Lyons, B., Yoshida, S., Miyamoto, T., Yoshimoto, G., Watanabe, T., Akashi, K., Shultz, L. D., & Harada, M. (2005). Development of functional human blood and immune systems in NOD/SCID/IL2 receptor γ chainnull mice. *Blood*, 106(5), 1565–1573. <https://doi.org/10.1182/blood-2005-02-0516>
- Ishizawa, R., Masuda, K., Sakata, S., & Nakatani, A. (2015). Effects of Different Fatty Acid Chain Lengths on Fatty Acid Oxidation-Related Protein Expression Levels in Rat Skeletal Muscles. *Journal of Oleo Science*, 64(4), 415–421. <https://doi.org/10.5650/jos.ess14199>
- Issa, J.-P. (2010). Epigenetic Changes in the Myelodysplastic Syndrome. *Hematology/Oncology Clinics of North America*, 24(2). <https://doi.org/10.1016/j.hoc.2010.02.007>
- Issa, J.-P. J. (2013). The myelodysplastic syndrome as a prototypical epigenetic disease. *Blood*, 121(19). <https://doi.org/10.1182/blood-2013-02-451757>
- Ito, S., Shen, L., Dai, Q., Wu, S. C., Collins, L. B., Swenberg, J. A., He, C., & Zhang, Y. (2011). Tet proteins can convert 5-methylcytosine to 5-formylcytosine and 5-carboxylcytosine. *Science*, 333(6047), 1300–1303. <https://doi.org/10.1126/science.1210597>
- Itzykson, R., Kosmider, O., Renneville, A., Morabito, M., Preudhomme, C., Berthon, C., Adès, L., Fenaux, P., Platzbecker, U., Gagey, O., Rameau, P., Meurice, G., Oréar, C., Delhommeau, F., Bernard, O. A., Fontenay, M., Vainchenker, W., Droin, N., & Solary, E. (2013). Clonal architecture of chronic myelomonocytic leukemias. *Blood*, 121(12). <https://doi.org/10.1182/blood-2012-06-440347>
- Jabbour, E., Takahashi, K., Wang, X., Cornelison, A. M., Abruzzo, L., Kadia, T., Borthakur, G., Estrov, Z., O'Brien, S., Mallo, M., Wierda, W., Pierce, S., Wei, Y., Sole, F., Chen, R., Kantarjian, H., & Garcia-Manero, G. (2013). Acquisition of cytogenetic abnormalities in patients with IPSS defined lower-risk myelodysplastic syndrome is associated with poor prognosis and transformation to acute myelogenous leukemia. *American Journal of Hematology*, 88(10), 831–837. <https://doi.org/10.1002/ajh.23513>
- Jacob, B., Osato, M., Yamashita, N., Wang, C. Q., Taniuchi, I., Littman, D. R., Asou, N., & Ito, Y. (2010). Stem cell exhaustion due to Runx1 deficiency is prevented by Evi5 activation in leukemogenesis. *Blood*, 115(8), 1610–1620. <https://doi.org/10.1182/blood-2009-07-232249>
- Jaenisch, R., & Bird, A. (2003). Epigenetic regulation of gene expression: How the genome integrates intrinsic and environmental signals. *Nature Genetics*, 33(S3), 245–254. <https://doi.org/10.1038/ng1089>
- Jager, S., Handschin, C., St.-Pierre, J., & Spiegelman, B. M. (2007). AMP-activated protein kinase (AMPK) action in skeletal muscle via direct phosphorylation of PGC-1. *Proceedings of the National Academy of Sciences*, 104(29), 12017–12022. <https://doi.org/10.1073/pnas.0705070104>
- Jaiswal, S., Fontanillas, P., Flannick, J., Manning, A., Grauman, P. V., Mar, B. G., Lindsley, R. C., Mermel, C. H., Burt, N., Chavez, A., Higgins, J. M., Moltchanov, V., Kuo, F. C., Kluk, M. J., Henderson, B., Kinnunen, L., Koistinen, H. A., Ladenvall, C., Getz, G., ... Ebert, B. L.

- (2014). Age-Related Clonal Hematopoiesis Associated with Adverse Outcomes. *New England Journal of Medicine*, 371(26), 2488–2498. <https://doi.org/10.1056/NEJMoa1408617>
- Jang, B., Jeon, Y. C., Choi, J. K., Park, M., Kim, J. I., Ishigami, A., Maruyama, N., Carp, R. I., Kim, Y. S., & Choi, E. K. (2012). Peptidylarginine deiminase modulates the physiological roles of enolase via citrullination: Links between altered multifunction of enolase and neurodegenerative diseases. *Biochemical Journal*, 445(2), 183–192. <https://doi.org/10.1042/BJ20120025>
- Jaronczyk, K., Carmichael, J. B., & Hobman, T. C. (2005). Exploring the functions of RNA interference pathway proteins: Some functions are more RISCy than others? *Biochemical Journal*, 387(3), 561–571. <https://doi.org/10.1042/BJ20041822>
- Ji, H., Ehrlich, L. I. R., Seita, J., Murakami, P., Doi, A., Lindau, P., Lee, H., Aryee, M. J., Irizarry, R. A., Kim, K., Rossi, D. J., Inlay, M. A., Serwold, T., Karsunky, H., Ho, L., Daley, G. Q., Weissman, I. L., & Feinberg, A. P. (2010). Comprehensive methylome map of lineage commitment from haematopoietic progenitors. *Nature*, 467(7313), 338–342. <https://doi.org/10.1038/nature09367>
- Jiang, X., Ye, X., Guo, W., Lu, H., & Gao, Z. (2014). Inhibition of HDAC3 promotes ligand-independent PPAR activation by protein acetylation. *Journal of Molecular Endocrinology*, 53(2), 191–200. <https://doi.org/10.1530/JME-14-0066>
- Jiang, Y., Dunbar, A., Gondek, L. P., Mohan, S., Rataul, M., O'Keefe, C., Sekeres, M., Sauntharajah, Y., & Maciejewski, J. P. (2009). Aberrant DNA methylation is a dominant mechanism in MDS progression to AML. *Blood*, 113(6). <https://doi.org/10.1182/blood-2008-06-163246>
- Jiang, Z., Cui, Y., Wang, L., Zhao, Y., Yan, S., & Chang, X. (2013). Investigating citrullinated proteins in tumour cell lines. *World Journal of Surgical Oncology*, 11. <https://doi.org/10.1186/1477-7819-11-260>
- Jinek, M., Chylinski, K., Fonfara, I., Hauer, M., Doudna, J. A., & Charpentier, E. (2012). A Programmable Dual-RNA-Guided DNA Endonuclease in Adaptive Bacterial Immunity. *Science*, 337(6096). <https://doi.org/10.1126/science.1225829>
- Jogl, G., & Tong, L. (2003). Crystal structure of carnitine acetyltransferase and implications for the catalytic mechanism and fatty acid transport. *Cell*, 112(1), 113–122. [https://doi.org/10.1016/S0092-8674\(02\)01228-X](https://doi.org/10.1016/S0092-8674(02)01228-X)
- Johnstone, R. W., & Licht, J. D. (2003). Histone deacetylase inhibitors in cancer therapy. *Cancer Cell*, 4(1), 13–18. [https://doi.org/10.1016/S1535-6108\(03\)00165-X](https://doi.org/10.1016/S1535-6108(03)00165-X)
- Jones, C. L., Stevens, B. M., Culp-Hill, R., Dalessandro, A., Krug, A., Goosman, M., Pei, S., Pollyea, D. A., & Jordan, C. T. (2019). Inhibition of Fatty Acid Metabolism Re-Sensitizes Resistant Leukemia Stem Cells to Venetoclax with Azacitidine (Blood, Vol. 134, Issue Supplement_1, pp. 1272–1272). American Society of Hematology. <https://doi.org/10.1182/blood-2019-125773>
- Jones, C. L., Stevens, B. M., D'Alessandro, A., Reisz, J. A., Culp-Hill, R., Nemkov, T., Pei, S., Khan, N., Adane, B., Ye, H., Krug, A., Reinhold, D., Smith, C., DeGregori, J., Pollyea, D. A., & Jordan, C. T. (2018). Inhibition of Amino Acid Metabolism Selectively Targets Human Leukemia Stem Cells. *Cancer Cell*, 34(5), 724–740.e4. <https://doi.org/10.1016/j.ccell.2018.10.005>
- Jones, P. A., & Taylor, S. M. (1980). Cellular differentiation, cytidine analogs and DNA methylation. *Cell*, 20(1), 85–93. [https://doi.org/10.1016/0092-8674\(80\)90237-8](https://doi.org/10.1016/0092-8674(80)90237-8)
- Jose, C., Bellance, N., & Rossignol, R. (2011). Choosing between glycolysis and oxidative phosphorylation: A tumor's dilemma? *Biochimica et Biophysica Acta - Bioenergetics*, 1807(6), 552–561. <https://doi.org/10.1016/j.bbabi.2010.10.012>
- Ju, H. Q., Zhan, G., Huang, A., Sun, Y., Wen, S., Yang, J., Lu, W. H., Xu, R. H., Li, J., Li, Y., Garcia-Manero, G., Huang, P., & Hu, Y. (2017). ITD mutation in FLT3 tyrosine kinase promotes Warburg effect and renders therapeutic sensitivity to glycolytic inhibition. *Leukemia*, 31(10), 2143–2150. <https://doi.org/10.1038/leu.2017.45>

| Bibliography

- Jung, T. W., Lee, Y. J., Lee, M. W., & Kim, S. M. (2009). Full-length adiponectin protects hepatocytes from palmitate-induced apoptosis via inhibition of c-Jun NH₂ terminal kinase. *FEBS Journal*, 276(8), 2278–2284. <https://doi.org/10.1111/j.1742-4658.2009.06955.x>
- Kameoka, M., Kimura, T., Okada, Y., Nakaya, T., Kishi, M., & Ikuta, K. (1995). High susceptibility of U937-derived subclones to infection with human immunodeficiency virus type 1 is correlated with virus-induced cell differentiation and superoxide generation. *Immunopharmacology*, 30(1), 89–101. [https://doi.org/10.1016/0162-3109\(95\)00012-1](https://doi.org/10.1016/0162-3109(95)00012-1)
- Kaminskas, E. (2005). Approval Summary: Azacitidine for Treatment of Myelodysplastic Syndrome Subtypes. *Clinical Cancer Research*, 11(10), 3604–3608. <https://doi.org/10.1158/1078-0432.CCR-04-2135>
- Kato, M. (2013). Functional and cancer genomics of ASXL family members. *British Journal of Cancer*, 109(2), 299–306. <https://doi.org/10.1038/bjc.2013.281>
- Kawaguchi, T., Takenoshita, M., Kabashima, T., & Uyeda, K. (2001). Glucose and cAMP regulate the L-type pyruvate kinase gene by phosphorylation/dephosphorylation of the carbohydrate response element binding protein. *Proceedings of the National Academy of Sciences*, 98(24), 13710–13715. <https://doi.org/10.1073/pnas.231370798>
- Kelly, M. J., So, J., Rogers, A. J., Gregory, G., Li, J., Zethoven, M., Gearhart, M. D., Bardwell, V. J., Johnstone, R. W., Vervoort, S. J., & Kats, L. M. (2019). Bcor loss perturbs myeloid differentiation and promotes leukaemogenesis. *Nature Communications*, 10(1), 1347. <https://doi.org/10.1038/s41467-019-09250-6>
- Kelsall, C. J., Hoile, S. P., Irvine, N. A., Masoodi, M., Torrens, C., Lillycrop, K. A., Calder, P. C., Clough, G. F., Hanson, M. A., & Burdge, G. C. (2012). Vascular Dysfunction Induced in Offspring by Maternal Dietary Fat Involves Altered Arterial Polyunsaturated Fatty Acid Biosynthesis. *PLoS ONE*, 7(4), e34492. <https://doi.org/10.1371/journal.pone.0034492>
- Kim, H. S., Xiao, C., Wang, R. H., Lahusen, T., Xu, X., Vassilopoulos, A., Vazquez-Ortiz, G., Jeong, W. I., Park, O., Ki, S. H., Gao, B., & Deng, C. X. (2010). Hepatic-specific disruption of SIRT6 in mice results in fatty liver formation due to enhanced glycolysis and triglyceride synthesis. *Cell Metabolism*, 12(3), 224–236. <https://doi.org/10.1016/j.cmet.2010.06.009>
- Kim, J. K., Gimeno, R. E., Higashimori, T., Kim, H.-J., Choi, H., Punreddy, S., Mozell, R. L., Tan, G., Stricker-Krongrad, A., Hirsch, D. J., Fillmore, J. J., Liu, Z.-X., Dong, J., Cline, G., Stahl, A., Lodish, H. F., & Shulman, G. I. (2004). Inactivation of fatty acid transport protein 1 prevents fat-induced insulin resistance in skeletal muscle. *Journal of Clinical Investigation*, 113(5), 756–763. <https://doi.org/10.1172/jci18917>
- Kim, K.-H. (1997). Regulation of mammalian acetyl-coenzyme A carboxylase. *Annual Review of Nutrition*, 17(1), 77–99. <https://doi.org/10.1146/annurev.nutr.17.1.77>
- Kim, T., Tyndel, M. S., Kim, H. J., Ahn, J. S., Choi, S. H., Park, H. J., Kim, Y. K., Yang, D. H., Lee, J. J., Jung, S. H., Kim, S. Y., Min, Y. H., Cheong, J. W., Sohn, S. K., Moon, J. H., Choi, M., Lee, M., Zhang, Z., & Kim, D. D. H. (2017). The clonal origins of leukemic progression of myelodysplasia. *Leukemia*, 31(9), 1928–1935. <https://doi.org/10.1038/leu.2017.17>
- Kitaura, Y., Inoue, K., Kato, N., Matsushita, N., & Shimomura, Y. (2015). Enhanced oleate uptake and lipotoxicity associated with laurate. *FEBS Open Bio*, 5(1), 485–491. <https://doi.org/10.1016/j.fob.2015.05.008>
- Kiyoi, H., Towatari, M., Yokota, S., Hamaguchi, M., Ohno, R., Saito, H., & Naoe, T. (1998). Internal tandem duplication of the FLT3 gene is a novel modality of elongation mutation which causes constitutive activation of the product. *Leukemia*, 12(9), 1333–1337. <https://doi.org/10.1038/sj.leu.2401130>
- Kode, A., Mosialou, I., Manavalan, S. J., Rathinam, C. V., Friedman, R. A., Teruya-Feldstein, J., Bhagat, G., Berman, E., & Kousteni, S. (2016). FoxO1-dependent induction of acute myeloid leukemia by osteoblasts in mice. *Leukemia*, 30(1), 1–13. <https://doi.org/10.1038/leu.2015.161>
- Kohli, L., & Passegué, E. (2014). Surviving change: The metabolic journey of hematopoietic stem cells. *Trends in Cell Biology*, 24(8), 479–487. <https://doi.org/10.1016/j.tcb.2014.04.001>

- Kohli, R. M., & Zhang, Y. (2013). TET enzymes, TDG and the dynamics of DNA demethylation. *Nature*, 502(7472), 472–479. <https://doi.org/10.1038/nature12750>
- Kok, C. H., Brown, A. L., Ekert, P. G., & D'Andrea, R. J. (2010). Gene expression analysis reveals HOX gene upregulation in trisomy 8 AML. *Leukemia*, 24(6), 1239–1243. <https://doi.org/10.1038/leu.2010.85>
- Koobotse, M., Holly, J., & Perks, C. (2018). Elucidating the novel BRCA1 function as a non-genomic metabolic restraint in ER-positive breast cancer cell lines. *Oncotarget*, 9(71), 33562–33576. <https://doi.org/10.18632/oncotarget.26093>
- Kuda, O., Pietka, T. A., Demianova, Z., Kudova, E., Cvacka, J., Kopecky, J., & Abumrad, N. A. (2013). Sulfo-N-succinimidyl oleate (SSO) inhibits fatty acid uptake and signaling for intracellular calcium via binding CD36 lysine 164: SSO also inhibits oxidized low density lipoprotein uptake by macrophages. *Journal of Biological Chemistry*, 288(22), 15547–15555. <https://doi.org/10.1074/jbc.M113.473298>
- Kuendgen, A., Müller-Thomas, C., Lauseker, M., Haferlach, T., Urbaniak, P., Schroeder, T., Brings, C., Wulfert, M., Meggendorfer, M., Hildebrandt, B., Betz, B., Royer-Pokora, B., Gattermann, N., Haas, R., Germing, U., & Götze, K. S. (2018). Efficacy of azacitidine is independent of molecular and clinical characteristics—An analysis of 128 patients with myelodysplastic syndromes or acute myeloid leukemia and a review of the literature. *Oncotarget*, 9(45), 27882–27894. <https://doi.org/10.18632/oncotarget.25328>
- Kuendgen, A., Strupp, C., Aivado, M., Hildebrandt, B., Haas, R., Gattermann, N., & Germing, U. (2006). Myelodysplastic Syndromes in Patients Younger Than Age 50. *Journal of Clinical Oncology*, 24(34), 5358–5365. <https://doi.org/10.1200/JCO.2006.07.5598>
- Kugel, S., & Mostoslavsky, R. (2014). Chromatin and beyond: The multitasking roles for SIRT6. *Trends in Biochemical Sciences*, 39(2), 72–81. <https://doi.org/10.1016/j.tibs.2013.12.002>
- Kunau, W. (1995). β -Oxidation of fatty acids in mitochondria, peroxisomes, and bacteria: A century of continued progress. *Progress in Lipid Research*, 34(4), 267–342. [https://doi.org/10.1016/0163-7827\(95\)00011-9](https://doi.org/10.1016/0163-7827(95)00011-9)
- Kupsa, T., Milos Horacek, J., & Jebavy, L. (2012). The role of cytokines in acute myeloid leukemia: A systematic review. *Biomedical Papers*, 156(4). <https://doi.org/10.5507/bp.2012.108>
- Kurimoto, M., Matsuoka, H., Hanaoka, N., Uneda, S., Murayama, T., Sonoki, T., & Nakakuma, H. (2013). Pretreatment of leukemic cells with low-dose decitabine markedly enhances the cytotoxicity of gemtuzumab ozogamicin. *Leukemia*, 27(1), 233–235. <https://doi.org/10.1038/leu.2012.178>
- Lagadinou, E. D., Sach, A., Callahan, K., Rossi, R. M., Neering, S. J., Minhajuddin, M., Ashton, J. M., Pei, S., Grose, V., Dwyer, K. M. O., Liesveld, J. L., Brookes, P. S., Becker, M. W., & Jordan, C. T. (2013). Article BCL-2 Inhibition Targets Oxidative Phosphorylation and Selectively Eradicates Quiescent Human Leukemia Stem Cells. *Stem Cell*, 12(3), 329–341. <https://doi.org/10.1016/j.stem.2012.12.013>
- Lagadinou, E. D., Sach, A., Callahan, K., Rossi, R. M., Neering, S. J., Minhajuddin, M., Ashton, J. M., Pei, S., Grose, V., O'Dwyer, K. M., Liesveld, J. L., Brookes, P. S., Becker, M. W., & Jordan, C. T. (2013). BCL-2 inhibition targets oxidative phosphorylation and selectively eradicates quiescent human leukemia stem cells. *Cell Stem Cell*, 12(3), 329–341. <https://doi.org/10.1016/j.stem.2012.12.013>
- Laker, R. C., Lillard, T. S., Okutsu, M., Zhang, M., Hoehn, K. L., Connelly, J. J., & Yan, Z. (2014). Exercise Prevents Maternal High-Fat Diet-Induced Hypermethylation of the *Pgc-1 α* Gene and Age-Dependent Metabolic Dysfunction in the Offspring. *Diabetes*, 63(5), 1605–1611. <https://doi.org/10.2337/db13-1614>
- Landberg, N., von Palffy, S., Askmyr, M., Lilljebjörn, H., Sandén, C., Rissler, M., Mustjoki, S., Hjorth-Hansen, H., Richter, J., Ågerstam, H., Järås, M., & Fioretos, T. (2018). CD36 defines primitive chronic myeloid leukemia cells less responsive to imatinib but vulnerable to antibody-based therapeutic targeting. *Haematologica*, 103(3), 447–455. <https://doi.org/10.3324/haematol.2017.169946>

| Bibliography

- Lane, S. W., Scadden, D. T., & Gilliland, D. G. (2009). The leukemic stem cell niche: Current concepts and therapeutic opportunities. *Blood*, *114*(6), 1150–1157. <https://doi.org/10.1182/blood-2009-01-202606>
- Langstein, J., Milsom, M. D., & Lipka, D. B. (2018). Impact of DNA methylation programming on normal and pre-leukemic hematopoiesis. *Seminars in Cancer Biology*, *51*, 89–100. <https://doi.org/10.1016/J.SEMCANCER.2017.09.008>
- Lee, J. Y., Lee, C. H., Shim, S. H., Seo, H. K., Kyhm, J. H., Cho, S., & Cho, Y. H. (2002). Molecular cytogenetic analysis of the monoblastic cell line U937: Karyotype clarification by G-banding, whole chromosome painting, microdissection and reverse painting, and comparative genomic hybridization. *Cancer Genetics and Cytogenetics*, *137*(2), 124–132. [https://doi.org/10.1016/S0165-4608\(02\)00565-4](https://doi.org/10.1016/S0165-4608(02)00565-4)
- Lewis, H. D., Liddle, J., Coote, J. E., Atkinson, S. J., Barker, M. D., Bax, B. D., Bicker, K. L., Bingham, R. P., Campbell, M., Chen, Y. H., Chung, C.-W., Craggs, P. D., Davis, R. P., Eberhard, D., Joberty, G., Lind, K. E., Locke, K., Maller, C., Martinod, K., ... Wilson, D. M. (2015). Inhibition of PAD4 activity is sufficient to disrupt mouse and human NET formation. *Nature Chemical Biology*, *11*(3), 189–191. <https://doi.org/10.1038/nchembio.1735>
- Li, L. J., Tao, J. L., Fu, R., Wang, H. Q., Jiang, H. J., Yue, L. Z., Zhang, W., Liu, H., & Shao, Z. H. (2014). Increased CD34⁺CD38[−]CD123⁺ cells in myelodysplastic syndrome displaying malignant features similar to those in AML. *International Journal of Hematology*, *100*(1), 60–69. <https://doi.org/10.1007/s12185-014-1590-2>
- Lichtman, M. A. (2010). Obesity and the risk for a hematological malignancy: Leukemia, lymphoma, or myeloma. *The Oncologist*, *15*(10), 1083–1101. <https://doi.org/10.1634/theoncologist.2010-0206>
- Liggett, L. A., & Sankaran, V. G. (2020). Unraveling Hematopoiesis through the Lens of Genomics. *Cell*, *182*(6), 1384–1400. <https://doi.org/10.1016/j.cell.2020.08.030>
- Lin, D., Wei, H., Wang, Y., Zhou, C. L., Liu, B. C., Liu, K. Q., Gong, B. F., Wei, S. N., Zhang, G. J., Liu, Y. T., Gong, X. Y., Qiu, S. W., Mi, Y. C., & Wang, J. X. (2016). The clinical and prognostic significance of acute myeloid leukemia with FLT3-ITD. *Zhonghua Xue Ye Xue Za Zhi = Zhonghua Xueyexue Zazhi*, *37*(12), 1017–1021. <https://doi.org/10.3760/cma.j.issn.0253-2727.2016.12.001>
- Lindsley, R. C., Mar, B. G., Mazzola, E., Grauman, P. V., Shareef, S., Allen, S. L., Pigneux, A., Wetzler, M., Stuart, R. K., Erba, H. P., Damon, L. E., Powell, B. L., Lindeman, N., Steensma, D. P., Wadleigh, M., DeAngelo, D. J., Neuberg, D., Stone, R. M., & Ebert, B. L. (2015). Acute myeloid leukemia ontogeny is defined by distinct somatic mutations. *Blood*, *125*(9), 1367–1376. <https://doi.org/10.1182/blood-2014-11-610543>
- Lisec, J., Jaeger, C., Rashid, R., Munir, R., & Zaidi, N. (2019). Cancer cell lipid class homeostasis is altered under nutrient-deprivation but stable under hypoxia. *BMC Cancer*, *19*(1), 501–501. <https://doi.org/10.1186/s12885-019-5733-y>
- Lister, R., Pelizzola, M., Downen, R. H., Hawkins, R. D., Hon, G., Tonti-Filippini, J., Nery, J. R., Lee, L., Ye, Z., Ngo, Q.-M., Edsall, L., Antosiewicz-Bourget, J., Stewart, R., Ruotti, V., Millar, A. H., Thomson, J. A., Ren, B., & Ecker, J. R. (2009). Human DNA methylomes at base resolution show widespread epigenomic differences. *Nature*, *462*(7271), 315–322. <https://doi.org/10.1038/nature08514>
- Liu, G. Y., Liao, Y. F., Chang, W. H., Liu, C. C., Hsieh, M. C., Hsu, P. C., Tsay, G. J., & Hung, H. C. (2006). Overexpression of peptidylarginine deiminase IV features in apoptosis of haematopoietic cells. *Apoptosis*, *11*(2), 183–196. <https://doi.org/10.1007/s10495-006-3715-4>
- Loken, M. R., van de Loosdrecht, A., Ogata, K., Orfao, A., & Wells, D. A. (2008). Flow cytometry in myelodysplastic syndromes: Report from a working conference. *Leukemia Research*, *32*(1), 5–17. <https://doi.org/10.1016/j.leukres.2007.04.020>
- López-Moyado, I. F., & Rao, A. (2020). DNMT3A and TET2 mutations reshape hematopoiesis in opposing ways. *Nature Genetics*, *52*(6). <https://doi.org/10.1038/s41588-020-0641-2>

- López-Otín, C., Blasco, M. A., Partridge, L., Serrano, M., & Kroemer, G. (2013). The hallmarks of aging. *Cell*, *153*(6), 1194–1194. <https://doi.org/10.1016/j.cell.2013.05.039>
- Love, M. I., Huber, W., & Anders, S. (2014). Moderated estimation of fold change and dispersion for RNA-seq data with DESeq2. *Genome Biology*, *15*(12), 550–550. <https://doi.org/10.1186/s13059-014-0550-8>
- Lovén, J., Hoke, H. A., Lin, C. Y., Lau, A., Orlando, D. A., Vakoc, C. R., Bradner, J. E., Lee, T. I., & Young, R. A. (2013). Selective Inhibition of Tumor Oncogenes by Disruption of Super-Enhancers. *Cell*, *153*(2). <https://doi.org/10.1016/j.cell.2013.03.036>
- Lu, C., Ward, P. S., Kapoor, G. S., Rohle, D., Turcan, S., Abdel-Wahab, O., Edwards, C. R., Khanin, R., Figueroa, M. E., Melnick, A., Wellen, K. E., O'Rourke, D. M., Berger, S. L., Chan, T. A., Levine, R. L., Mellinghoff, I. K., & Thompson, C. B. (2012). IDH mutation impairs histone demethylation and results in a block to cell differentiation. *Nature*, *483*(7390), 474–478. <https://doi.org/10.1038/nature10860>
- Lübbert, M., Suciú, S., Hagemeijer, A., Rüter, B., Platzbecker, U., Giagounidis, A., Selleslag, D., Labar, B., Germing, U., Salih, H. R., Muus, P., Pflüger, K.-H., Schaefer, H.-E., Bogatyreva, L., Aul, C., de Witte, T., Ganser, A., Becker, H., Huls, G., ... Wijermans, P. W. (2016). Decitabine improves progression-free survival in older high-risk MDS patients with multiple autosomal monosomies: Results of a subgroup analysis of the randomized phase III study 06011 of the EORTC Leukemia Cooperative Group and German MDS Study Group. *Annals of Hematology*, *95*(2). <https://doi.org/10.1007/s00277-015-2547-0>
- Luiken, J. J. F. P., Coort, S. L. M., Willems, J., Coumans, W. A., Bonen, A., van der Vusse, G. J., & Glatz, J. F. C. (2003). Contraction-Induced Fatty Acid Translocase/CD36 Translocation in Rat Cardiac Myocytes Is Mediated Through AMP-Activated Protein Kinase Signaling. *Diabetes*, *52*(7), 1627–1634. <https://doi.org/10.2337/diabetes.52.7.1627>
- MacLeod, R., Dirks, W. G., Reid, Y. A., Hay, R. J., & Drexler, H. G. (1997). Identity of original and late passage Dami megakaryocytes with HEL erythroleukemia cells shown by combined cytogenetics and DNA fingerprinting. *Leukemia*, *11*(12), 2032–2038. <https://doi.org/10.1038/sj.leu.2400868>
- MacPherson, L., Anokye, J., Yeung, M. M., Lam, E. Y. N., Chan, Y.-C., Weng, C.-F., Yeh, P., Knezevic, K., Butler, M. S., Hoegl, A., Chan, K.-L., Burr, M. L., Gearing, L. J., Willson, T., Liu, J., Choi, J., Yang, Y., Bilardi, R. A., Falk, H., ... Dawson, M. A. (2020). HBO1 is required for the maintenance of leukaemia stem cells. *Nature*, *577*(7789). <https://doi.org/10.1038/s41586-019-1835-6>
- Maher, M., Diesch, J., Casquero, R., & Buschbeck, M. (2018). Epigenetic-transcriptional regulation of fatty acid metabolism and its alterations in leukaemia. *Frontiers in Genetics*, *9*(SEP). <https://doi.org/10.3389/fgene.2018.00405>
- Maimaitili, Y., Inase, A., Miyata, Y., Kitao, A., Mizutani, Y., Kakiuchi, S., Shimono, Y., Saito, Y., Sonoki, T., Minami, H., & Matsuoka, H. (2018). An mTORC1/2 kinase inhibitor enhances the cytotoxicity of gemtuzumab ozogamicin by activation of lysosomal function. *Leukemia Research*, *74*, 68–74. <https://doi.org/10.1016/j.leukres.2018.09.017>
- Majeti, R., Park, C. Y., & Weissman, I. L. (2007). Identification of a Hierarchy of Multipotent Hematopoietic Progenitors in Human Cord Blood. *Cell Stem Cell*, *1*(6), 635–645. <https://doi.org/10.1016/j.stem.2007.10.001>
- Makishima, H., Suzuki, H., Przychodzen, B., Nagata, Y., Meggendorfer, M., Sanada, M., Okuno, Y., Hirsch, C., Kuzmanovic, T., Sato, Y., Sato-otsubo, A., Laframboise, T., Hosono, N., Shiraishi, Y., Chiba, K., Haferlach, C., Kern, W., Tanaka, H., Shiozawa, Y., ... Maciejewski, J. P. (2016). *Dynamics of clonal evolution in myelodysplastic syndromes*. <https://doi.org/10.1038/ng.3742>
- Malcovati, L., Hellström-Lindberg, E., Bowen, D., Adès, L., Cermak, J., del Cañizo, C., Della Porta, M. G., Fenaux, P., Gattermann, N., Germing, U., Jansen, J. H., Mittelman, M., Mufti, G., Platzbecker, U., Sanz, G. F., Selleslag, D., Skov-Holm, M., Stauder, R., Symeonidis, A., ... Cazzola, M. (2013). Diagnosis and treatment of primary myelodysplastic syndromes in

| Bibliography

- adults: Recommendations from the European LeukemiaNet. *Blood*, 122(17), 2943–2964. <https://doi.org/10.1182/blood-2013-03-492884>
- Mandard, S., Müller, M., & Kersten, S. (2004). Peroxisome proliferator-activated receptor a target genes. *Cellular and Molecular Life Sciences (CMLS)*, 61(4), 393–416. <https://doi.org/10.1007/s00018-003-3216-3>
- Mardiana, S., & Gill, S. (2020). CAR T Cells for Acute Myeloid Leukemia: State of the Art and Future Directions. *Frontiers in Oncology*, 10. <https://doi.org/10.3389/fonc.2020.00697>
- Marmorstein, R., & Zhou, M.-M. (2014). Writers and Readers of Histone Acetylation: Structure, Mechanism, and Inhibition. *Cold Spring Harbor Perspectives in Biology*, 6(7), a018762–a018762. <https://doi.org/10.1101/cshperspect.a018762>
- Masters, J. R., Thomson, J. A., Daly-Burns, B., Reid, Y. A., Dirks, W. G., Packer, P., Toji, L. H., Ohno, T., Tanabe, H., Arlett, C. F., Kelland, L. R., Harrison, M., Virmani, A., Ward, T. H., Ayres, K. L., & Debenham, P. G. (2001). Short tandem repeat profiling provides an international reference standard for human cell lines. *Proceedings of the National Academy of Sciences of the United States of America*, 98(14), 8012–8017. <https://doi.org/10.1073/pnas.121616198>
- Matsuoka, H., Murayama, T., Koizumi, T., Nishimura, R., Kawaguchi, R., & Nakagawa, T. (2005). Establishment of a human myeloid cell line with trisomy 8 derived from overt leukemia following myelodysplastic syndrome. *Haematologica*, 90(7), 981–982.
- Maximow, A. (1909). Der Lymphozyt als gemeinsame Stammzelle der verschiedenen Blutelemente in der embryonalen Entwicklung und im postfetalen Leben der Säugetiere. *Folia Haematologica*, 8, 125–141.
- McCulloch, E. A., & Till, J. E. (1960). The Radiation Sensitivity of Normal Mouse Bone Marrow Cells, Determined by Quantitative Marrow Transplantation into Irradiated Mice. *Radiation Research*, 13(1). <https://doi.org/10.2307/3570877>
- McDonnell, E., Crown, S. B., Fox, D. B., Kitir, B., Ilkayeva, O. R., Olsen, C. A., Grimsrud, P. A., & Hirschey, M. D. (2016). Lipids Reprogram Metabolism to Become a Major Carbon Source for Histone Acetylation. *Cell Reports*, 17(6), 1463–1472. <https://doi.org/10.1016/j.celrep.2016.10.012>
- McGarry, J. D., Mannaerts, G. P., & Foster, D. W. (1977). A possible role for malonyl-CoA in the regulation of hepatic fatty acid oxidation and ketogenesis. *Journal of Clinical Investigation*, 60(1), 265–270. <https://doi.org/10.1172/JCI108764>
- McGinty, R. K., & Tan, S. (2015). Nucleosome Structure and Function. *Chemical Reviews*, 115(6), 2255–2273. <https://doi.org/10.1021/cr500373h>
- McQuilten, Z. K., Wood, E. M., Polizzotto, M. N., Campbell, L. J., Wall, M., Curtis, D. J., Farrugia, H., McNeil, J. J., & Sundararajan, V. (2014). Underestimation of myelodysplastic syndrome incidence by cancer registries: Results from a population-based data linkage study. *Cancer*, 120(11), 1686–1694. <https://doi.org/10.1002/cncr.28641>
- Medyouf, H. (2017). *The microenvironment in human myeloid malignancies: Emerging concepts and therapeutic implications*. *Affiliations: Contact: Copyright © 2017 American Society of Hematology*. <https://doi.org/10.1182/blood-2016-11-696070>
- Mertens, F., Johansson, M., & Mitelman, F. (1995). The pathogenetic significance of acquired trisomy 8 is not reducible to amplification of a single chromosome band. *Cancer Genetics and Cytogenetics*, 83(2), 176–177. [https://doi.org/10.1016/0165-4608\(95\)00066-X](https://doi.org/10.1016/0165-4608(95)00066-X)
- Mi, H., Muruganujan, A., & Thomas, P. D. (2013). PANTHER in 2013: Modeling the evolution of gene function, and other gene attributes, in the context of phylogenetic trees. *Nucleic Acids Res.*, 41, D377–D386. <https://doi.org/10.1093/nar/gks1118>
- MIWA, H., SHIKAMI, M., GOTO, M., MIZUNO, S., TAKAHASHI, M., TSUNEKAWA-IMAI, N., ISHIKAWA, T., MIZUTANI, M., HORIO, T., GOTOU, M., YAMAMOTO, H., WAKABAYASHI, M., WATARAI, M., HANAMURA, I., IMAMURA, A., MIHARA, H., & NITTA, M. (2013). Leukemia cells demonstrate a different metabolic perturbation

- provoked by 2-deoxyglucose. *Oncology Reports*, 29(5), 2053–2057.
<https://doi.org/10.3892/or.2013.2299>
- Mondal, S., & Thompson, P. R. (2019). Protein Arginine Deiminases (PADs): Biochemistry and Chemical Biology of Protein Citrullination. *Accounts of Chemical Research*, 52(3), 818–832.
<https://doi.org/10.1021/acs.accounts.9b00024>
- Moore, C. B., Guthrie, E. H., Huang, M. T., & Taxman, D. J. (2010). RNA Therapeutics. *Methods*, 629(2), 141–158. <https://doi.org/10.1007/978-1-60761-657-3>
- Moran-Crusio, K., Reavie, L., Shih, A., Abdel-Wahab, O., Ndiaye-Lobry, D., Lobry, C., Figueroa, M. E., Vasanthakumar, A., Patel, J., Zhao, X., Perna, F., Pandey, S., Madzo, J., Song, C., Dai, Q., He, C., Ibrahim, S., Beran, M., Zavadil, J., ... Levine, R. L. (2011). Tetz Loss Leads to Increased Hematopoietic Stem Cell Self-Renewal and Myeloid Transformation. *Cancer Cell*, 20(1). <https://doi.org/10.1016/j.ccr.2011.06.001>
- Moreau, K., Dizin, E., Ray, H., Luquain, C., Lefai, E., Foufelle, F., Billaud, M., Lenoir, G. M., & Dalla Venezia, N. (2006). BRCA1 affects lipid synthesis through its interaction with acetyl-CoA carboxylase. *Journal of Biological Chemistry*, 281(6), 3172–3181.
<https://doi.org/10.1074/jbc.M504652200>
- Moussaieff, A., Rouleau, M., Kitsberg, D., Cohen, M., Levy, G., Barasch, D., Nemirovski, A., Shen-Orr, S., Laevsky, I., Amit, M., Bomze, D., Elena-Herrmann, B., Scherf, T., Nissim-Rafinia, M., Kempa, S., Itskovitz-Eldor, J., Meshorer, E., Aberdam, D., & Nahmias, Y. (2015). Glycolysis-Mediated Changes in Acetyl-CoA and Histone Acetylation Control the Early Differentiation of Embryonic Stem Cells. *Cell Metabolism*, 21(3), 392–402.
<https://doi.org/10.1016/j.cmet.2015.02.002>
- Müller-Kuller, U., Ackermann, M., Kolodziej, S., Brendel, C., Fritsch, J., Lachmann, N., Kunkel, H., Lausen, J., Schambach, A., Moritz, T., & Grez, M. (2015). A minimal ubiquitous chromatin opening element (UCOE) effectively prevents silencing of juxtaposed heterologous promoters by epigenetic remodeling in multipotent and pluripotent stem cells. *Nucleic Acids Research*, 43(3), 1577–1592. <https://doi.org/10.1093/nar/gkvo19>
- Munday, M. R., Carling, D., & Hardie, D. G. (1988). Negative interactions between phosphorylation of acetyl-CoA carboxylase by the cyclic AMP-dependent and AMP-activated protein kinases. *FEBS Letters*, 235(1–2), 144–148. [https://doi.org/10.1016/0014-5793\(88\)81251-1](https://doi.org/10.1016/0014-5793(88)81251-1)
- Musselman, C. A., Lalonde, M.-E., Côté, J., & Kutateladze, T. G. (2012). Perceiving the epigenetic landscape through histone readers. *Nature Structural & Molecular Biology*, 19(12), 1218–1227. <https://doi.org/10.1038/nsmb.2436>
- Nakajima, H., & Kunitomo, H. (2014). *TET2* as an epigenetic master regulator for normal and malignant hematopoiesis. *Cancer Science*, 105(9), 1093–1099.
<https://doi.org/10.1111/cas.12484>
- Naveiras, O., Nardi, V., Wenzel, P. L., Hauschka, P. V., Fahey, F., & Daley, G. Q. (2009). Bone-marrow adipocytes as negative regulators of the haematopoietic microenvironment. *Nature*, 460(7252), 259–263. <https://doi.org/10.1038/nature08099>
- Nelson-Rees, W., & Flandermeyer, R. (1976). HeLa cultures defined. *Science*, 191(4222), 96–98.
<https://doi.org/10.1126/science.1246601>
- Nencioni, A., Caffa, I., Cortellino, S., & Longo, V. D. (2018). Fasting and cancer: Molecular mechanisms and clinical application. *Nature Reviews Cancer*, 18(11).
<https://doi.org/10.1038/s41568-018-0061-0>
- Nicodeme, E., Jeffrey, K. L., Schaefer, U., Beinke, S., Dewell, S., Chung, C., Chandwani, R., Marazzi, I., Wilson, P., Coste, H., White, J., Kirilovsky, J., Rice, C. M., Lora, J. M., Prinjha, R. K., Lee, K., & Tarakhovskiy, A. (2010). Suppression of inflammation by a synthetic histone mimic. *Nature*, 468(7327), 1119–1123. <https://doi.org/10.1038/nature09589>
- Niculescu, M. D., Lupu, D. S., & Craciunescu, C. N. (2013). Perinatal manipulation of α -linolenic acid intake induces epigenetic changes in maternal and offspring livers. *The FASEB Journal*, 27(1), 350–358. <https://doi.org/10.1096/fj.12-210724>

| Bibliography

- Nikoloski, G., Langemeijer, S. M. C., Kuiper, R. P., Knops, R., Massop, M., Tönnissen, E. R. L. T. M., van der Heijden, A., Scheele, T. N., Vandenberghe, P., de Witte, T., van der Reijden, B. A., & Jansen, J. H. (2010). Somatic mutations of the histone methyltransferase gene EZH2 in myelodysplastic syndromes. *Nature Genetics*, *42*(8), 665–667. <https://doi.org/10.1038/ng.620>
- O'Flanagan, C. H., Smith, L. A., McDonnell, S. B., & Hursting, S. D. (2017). When less may be more: Calorie restriction and response to cancer therapy. *BMC Medicine*, *15*(1). <https://doi.org/10.1186/s12916-017-0873-x>
- Ogata, K. (2002). Clinical significance of phenotypic features of blasts in patients with myelodysplastic syndrome. *Blood*, *100*(12), 3887–3896. <https://doi.org/10.1182/blood-2002-01-0222>
- Ogawa, M. (2002). Changing phenotypes of hematopoietic stem cells. *Experimental Hematology*, *30*(1), 3–6. [https://doi.org/10.1016/S0301-472X\(01\)00770-6](https://doi.org/10.1016/S0301-472X(01)00770-6)
- Ogawa, S. (2019). Genetics of MDS. *Blood*, *133*(10), 1049–1059. <https://doi.org/10.1182/blood-2018-10-844621>
- Ohta, M., Furukawa, Y., Ide, C., Akiyama, N., Utakoji, T., Miura, Y., & Saito, M. (1986). Establishment and characterization of four human monocytoid leukemia cell lines (JOSK-I, -S, -M and -K) with capabilities of monocyte-macrophage lineage differentiation and constitutive production of interleukin 1. *Cancer Research*, *46*(6), 3067–3074.
- Okada, S., Nakauchi, H., Nagayoshi, K., Nishikawa, S., Miura, Y., & Suda, T. (1992). In vivo and in vitro stem cell function of c-kit- and Sca-1-positive murine hematopoietic cells. *Blood*, *80*(12), 3044–3050. <https://doi.org/10.1182/blood.V80.12.3044.3044>
- Orkin, S. H., & Zon, L. I. (2008). Hematopoiesis: An Evolving Paradigm for Stem Cell Biology. *Cell*, *132*(4), 631–644. <https://doi.org/10.1016/j.cell.2008.01.025>
- Palau, A., Mallo, M., Palomo, L., Rodríguez-Hernández, I., Diesch, J., Campos, D., Granada, I., Juncà, J., Drexler, H. G., Solé, F., & Buschbeck, M. (2017). Immunophenotypic, cytogenetic, and mutational characterization of cell lines derived from myelodysplastic syndrome patients after progression to acute myeloid leukemia. *Genes Chromosomes and Cancer*, *56*(3), 243–252. <https://doi.org/10.1002/gcc.22430>
- Pan, D., Rampal, R., & Mascarenhas, J. (2020). Clinical developments in epigenetic-directed therapies in acute myeloid leukemia. *Blood Advances*, *4*(5), 970–982. <https://doi.org/10.1182/bloodadvances.2019001245>
- Pang, W. W., Price, E. A., Sahoo, D., Berman, I., Maloney, W. J., Rossi, D. J., Schrier, S. L., & Weissman, I. L. (2011). Human bone marrow hematopoietic stem cells are increased in frequency and myeloid-biased with age. *Proceedings of the National Academy of Sciences*, *108*(50), 20012–20017. <https://doi.org/10.1073/pnas.116110108>
- Papaemmanuil, E. (2014). Somatic Mutations in Myelodysplastic Syndrome. *Blood*, *124*(21), SCI-22. <https://doi.org/10.1182/blood.V124.21.SCI-22.SCI-22>
- Pape, M. E., Lopez-Casillas, F., & Kim, K.-H. (1988). Physiological regulation of acetyl-CoA carboxylase gene expression: Effects of diet, diabetes, and lactation on acetyl-CoA carboxylase mRNA. *Archives of Biochemistry and Biophysics*, *267*(1), 104–109. [https://doi.org/10.1016/0003-9861\(88\)90013-6](https://doi.org/10.1016/0003-9861(88)90013-6)
- Pappenheim, A. (1896). Ueber Entwicklung und Ausbildung der Erythroblasten. *Archiv Für Pathologische Anatomie Und Physiologie Und Für Klinische Medicin*, *145*(3), 587–643. <https://doi.org/10.1007/BF01969901>
- Pappenheim, A. (1905). *Atlas der menschlichen Blutzellen* (1st ed., Vol. 1, p. undefined). Gustav Fischer.
- Parker, J. E., Mufti, G. J., Rasool, F., Mijovic, A., Devereux, S., & Pagliuca, A. (2000). The role of apoptosis, proliferation, and the Bcl-2-related proteins in the myelodysplastic syndromes and acute myeloid leukemia secondary to MDS. *Blood*, *96*(12), 3932–3938. <https://doi.org/10.1182/blood.V96.12.3932>

- Parson, W., Kirchebner, R., Mühlmann, R., Renner, K., Kofler, A., Schmidt, S., & Kofler, R. (2005). Cancer cell line identification by short tandem repeat profiling: Power and limitations. *The FASEB Journal*, *19*(3), 1–18. <https://doi.org/10.1096/fj.04-3062fje>
- Pastore, F., & Levine, R. L. (2016). Epigenetic regulators and their impact on therapy in acute myeloid leukemia. *Haematologica*, *101*(3), 269–278. <https://doi.org/10.3324/haematol.2015.140822>
- Patro, R., Duggal, G., Love, M. I., Irizarry, R. A., & Kingsford, C. (2017). Salmon provides fast and bias-aware quantification of transcript expression. *Nature Methods*, *14*(4), 417–419. <https://doi.org/10.1038/nmeth.4197>
- Paulsson, K., & Johansson, B. (2007). Trisomy 8 as the sole chromosomal aberration in acute myeloid leukemia and myelodysplastic syndromes. *Pathologie Biologie*, *55*(1), 37–48. <https://doi.org/10.1016/j.patbio.2006.04.007>
- Paulus, A., Maenen, M., Drude, N., Nascimento, E. B. M., Van Marken Lichtenbelt, W. D., Mottaghy, F. M., & Bauwens, M. (2017). Synthesis, radiosynthesis and in vitro evaluation of ¹⁸F-Bodipy-C16/triglyceride as a dual modal imaging agent for brown adipose tissue. *PLoS ONE*, *12*(8). <https://doi.org/10.1371/journal.pone.0182297>
- Peleg, S., Feller, C., Ladurner, A. G., & Imhof, A. (2016). The Metabolic Impact on Histone Acetylation and Transcription in Ageing. *Trends in Biochemical Sciences*, *41*(8), 700–711. <https://doi.org/10.1016/j.tibs.2016.05.008>
- Perea, G., Domingo, A., Villamor, N., Palacios, C., Juncà, J., Torres, P., Llorente, A., Fernández, C., Tormo, M., Queipo de Llano, M. P., Bargay, J., Gallart, M., Florensa, L., Vivancos, P., Martí, J. M., Font, L., Berlanga, J., Esteve, J., Bueno, J., ... CETLAM GroupSpain. (2005). Adverse prognostic impact of CD36 and CD2 expression in adult de novo acute myeloid leukemia patients. *Leukemia Research*, *29*(10), 1109–1116. <https://doi.org/10.1016/j.leukres.2005.02.015>
- Pietras, E. M., Reynaud, D., Kang, Y.-A., Carlin, D., Calero-Nieto, F. J., Leavitt, A. D., Stuart, J. M., Göttgens, B., & Passegué, E. (2015). Functionally Distinct Subsets of Lineage-Biased Multipotent Progenitors Control Blood Production in Normal and Regenerative Conditions. *Cell Stem Cell*, *17*(1), 35–46. <https://doi.org/10.1016/j.stem.2015.05.003>
- Pike, L. S., Smift, A. L., Croteau, N. J., Ferrick, D. A., & Wu, M. (2011). *Inhibition of fatty acid oxidation by etomoxir impairs NADPH production and increases reactive oxygen species resulting in ATP depletion and cell death in human glioblastoma cells* ☆. <https://doi.org/10.1016/j.bbabbio.2010.10.022>
- Poirier, S., Samami, S., Mamarbachi, M., Demers, A., Chang, T. Y., Vance, D. E., Hatch, G. M., & Mayer, G. (2014). The epigenetic drug 5-azacytidine interferes with cholesterol and lipid metabolism. *Journal of Biological Chemistry*, *289*(27), 18736–18751. <https://doi.org/10.1074/jbc.M114.563650>
- Pollyea, D. A., Stevens, B. M., Jones, C. L., Winters, A., Pei, S., Minhajuddin, M., D'Alessandro, A., Culp-Hill, R., Riemondy, K. A., Gillen, A. E., Hesselberth, J. R., Abbott, D., Schatz, D., Gutman, J. A., Purev, E., Smith, C., & Jordan, C. T. (2018). Venetoclax with azacitidine disrupts energy metabolism and targets leukemia stem cells in patients with acute myeloid leukemia. *Nature Medicine*, *24*(12), 1859–1866. <https://doi.org/10.1038/s41591-018-0233-1>
- Pomeroy, C., Oken, M., Rydell, R. E., & Filice, G. A. (1991). Infection in the myelodysplastic syndromes. *Am J Med*, *90*(3), 338–344.
- Porwit, A., van de Loosdrecht, A. A., Bettelheim, P., Brodersen, L. E., Burbury, K., Cremers, E., Della Porta, M. G., Ireland, R., Johansson, U., Matarraz, S., Ogata, K., Orfao, A., Preijers, F., Psarra, K., Subirá, D., Valent, P., van der Velden, V. H. J., Wells, D., Westers, T. M., ... Béné, M. C. (2014). Revisiting guidelines for integration of flow cytometry results in the WHO classification of myelodysplastic syndromes—Proposal from the International/European LeukemiaNet Working Group for Flow Cytometry in MDS. *Leukemia*, *28*(9), 1793–1798. <https://doi.org/10.1038/leu.2014.191>

| Bibliography

- Poulsen, L. la C., Siersbæk, M., & Mandrup, S. (2012). PPARs: Fatty acid sensors controlling metabolism. *Seminars in Cell & Developmental Biology*, 23(6), 631–639. <https://doi.org/10.1016/j.semcdb.2012.01.003>
- Poynter, J. N., Richardson, M., Blair, C. K., Roesler, M. A., Hirsch, B. A., Nguyen, P., Cioc, A., Warlick, E., Cerhan, J. R., & Ross, J. A. (2016). Obesity over the life course and risk of acute myeloid leukemia and myelodysplastic syndromes. *Cancer Epidemiology*, 40. <https://doi.org/10.1016/j.canep.2015.12.005>
- Prébet, T., Gore, S. D., Esterni, B., Gardin, C., Itzykson, R., Thepot, S., Dreyfus, F., Rauzy, O. B., Recher, C., Adès, L., Quesnel, B., Beach, C. L., Fenaux, P., & Vey, N. (2011). Outcome of High-Risk Myelodysplastic Syndrome After Azacitidine Treatment Failure. *Journal of Clinical Oncology*, 29(24), 3322–3327. <https://doi.org/10.1200/JCO.2011.35.8135>
- Pronk, E., & Raaijmakers, M. H. G. P. (2019). The mesenchymal niche in MDS. *Blood*, 133(10), 1031–1038. <https://doi.org/10.1182/blood-2018-10-844639>
- Puigserver, P., Rhee, J., Donovan, J., Walkey, C. J., Yoon, J. C., Oriente, F., Kitamura, Y., Altomonte, J., Dong, H., Accili, D., & Spiegelman, B. M. (2003). Insulin-regulated hepatic gluconeogenesis through FOXO1–PGC-1 α interaction. *Nature*, 423(6939), 550–555. <https://doi.org/10.1038/nature01667>
- Qiang, L., Wang, L., Kon, N., Zhao, W., Lee, S., Zhang, Y., Rosenbaum, M., Zhao, Y., Gu, W., Farmer, S. R., & Accili, D. (2012). Brown Remodeling of White Adipose Tissue by SirT1-Dependent Deacetylation of Pparg. *Cell*, 150(3), 620–632. <https://doi.org/10.1016/j.cell.2012.06.027>
- Qin, T., Castoro, R., El Ahdab, S., Jelinek, J., Wang, X., Si, J., Shu, J., He, R., Zhang, N., Chung, W., Kantarjian, H. M., & Issa, J. P. J. (2011). Mechanisms of resistance to decitabine in the myelodysplastic syndrome. *PLoS ONE*, 6(8). <https://doi.org/10.1371/journal.pone.0023372>
- Quintás-Cardama, A., Santos, F. P. S., & Garcia-Manero, G. (2010). Therapy with azanucleosides for myelodysplastic syndromes. *Nature Reviews Clinical Oncology*, 7(8), 433–444. <https://doi.org/10.1038/nrclinonc.2010.87>
- Raj, K., John, A., Ho, A., Chronis, C., Khan, S., Samuel, J., Pomplun, S., Thomas, N. S. B., & Mufti, G. J. (2007). CDKN2B methylation status and isolated chromosome 7 abnormalities predict responses to treatment with 5-azacytidine. *Leukemia*, 21(9), 1937–1944. <https://doi.org/10.1038/sj.leu.2404796>
- Ramalho-Santos, M., & Willenbring, H. (2007). On the Origin of the Term ‘Stem Cell’. *Cell Stem Cell*, 1(1), 35–38. <https://doi.org/10.1016/j.stem.2007.05.013>
- Rao, D. D., Senzer, N., Cleary, M. A., & Nemunaitis, J. (2009). Comparative assessment of siRNA and shRNA off target effects: What is slowing clinical development. *Cancer Gene Therapy*, 16(11), 807–809. <https://doi.org/10.1038/cgt.2009.53>
- Rasmussen, K. D., Jia, G., Johansen, J. V., Pedersen, M. T., Rapin, N., Bagger, F. O., Porse, B. T., Bernard, O. A., Christensen, J., & Helin, K. (2015). Loss of TET2 in hematopoietic cells leads to DNA hypermethylation of active enhancers and induction of leukemogenesis. *Genes & Development*, 29(9). <https://doi.org/10.1101/gad.260174.115>
- Rathert, P., Roth, M., Neumann, T., Muerdter, F., Roe, J.-S., Muhar, M., Deswal, S., Cerny-Reiterer, S., Peter, B., Jude, J., Hoffmann, T., Boryń, Ł. M., Axelsson, E., Schweifer, N., Tontsch-Grunt, U., Dow, L. E., Gianni, D., Pearson, M., Valent, P., ... Zuber, J. (2015). Transcriptional plasticity promotes primary and acquired resistance to BET inhibition. *Nature*, 525(7570). <https://doi.org/10.1038/nature14898>
- Rathmell, J. C., & Newgard, C. B. (2009). A Glucose-to-Gene Link. *Science*, 324(5930), 1021–1022. <https://doi.org/10.1126/science.1174665>
- Reid, Y., Storts, D., Riss, T., & Minor, L. (2013). *Authentication of Human Cell Lines by STR DNA Profiling Analysis*. Eli Lilly & Company and the National Center for Advancing Translational Sciences. <http://www.ncbi.nlm.nih.gov/pubmed/23805434>
- Reilly, B., Tanaka, T. N., Diep, D., Yeerna, H., Tamayo, P., Zhang, K., & Bejar, R. (2019). DNA methylation identifies genetically and prognostically distinct subtypes of myelodysplastic

- syndromes. *Blood Advances*, 3(19), 2845–2858.
<https://doi.org/10.1182/bloodadvances.2019000192>
- Reinisch, A., Etchart, N., Thomas, D., Hofmann, N. A., Fruehwirth, M., Sinha, S., Chan, C. K., Senarath-Yapa, K., Seo, E.-Y., Wearda, T., Hartwig, U. F., Beham-Schmid, C., Trajanoski, S., Lin, Q., Wagner, W., Dullin, C., Alves, F., Andreeff, M., Weissman, I. L., ... Strunk, D. (2015). Epigenetic and in vivo comparison of diverse MSC sources reveals an endochondral signature for human hematopoietic niche formation. *Blood*, 125(2).
<https://doi.org/10.1182/blood-2014-04-572255>
- Reyes-Garau, Ribeiro, & Roué. (2019). Pharmacological Targeting of BET Bromodomain Proteins in Acute Myeloid Leukemia and Malignant Lymphomas: From Molecular Characterization to Clinical Applications. *Cancers*, 11(10), 1483.
<https://doi.org/10.3390/cancers11101483>
- Ribeiro, M. L., Reyes-Garau, D., Armengol, M., Fernández-Serrano, M., & Roué, G. (2019). Recent Advances in the Targeting of Epigenetic Regulators in B-Cell Non-Hodgkin Lymphoma. *Frontiers in Genetics*, 10. <https://doi.org/10.3389/fgene.2019.00986>
- Ricciardi, M. R., Mirabili, S., Allegretti, M., Licchetta, R., Calarco, A., Torrissi, M. R., Fo, R., Nicolai, R., Peluso, G., & Tafuri, A. (2017). Targeting the leukemia cell metabolism by the CPT1a inhibition: Functional preclinical effects in leukemias. *Blood*, 126(16), 1925–1930.
<https://doi.org/10.1182/blood-2014-12-617498>.The
- Ricciardi, M. R., Mirabili, S., Allegretti, M., Licchetta, R., Calarco, A., Torrissi, M. R., Foà, R., Nicolai, R., Peluso, G., & Tafuri, A. (2015). Targeting the leukemia cell metabolism by the CPT1a inhibition: Functional preclinical effects in leukemias. *Blood*, 126(16), 1925–1929.
<https://doi.org/10.1182/blood-2014-12-617498>
- Ritchie, M. (2014). Analysing data from pooled genetic sequencing screens using edgeR. *EdgeR*, 2014(October). <https://doi.org/10.1111/j.1467-8330.1974.tb00606.x>
- Robinson, M. D., & Oshlack, A. (2010). A scaling normalization method for differential expression analysis of RNA-seq data. *Genome Biology*, 11(3), R25–R25. <https://doi.org/10.1186/gb-2010-11-3-r25>
- Rodgers, J. T., Lerin, C., Haas, W., Gygi, S. P., Spiegelman, B. M., & Puigserver, P. (2005). Nutrient control of glucose homeostasis through a complex of PGC-1 α and SIRT1. *Nature*, 434(7029), 113–118. <https://doi.org/10.1038/nature03354>
- Roe, J.-S., & Vakoc, C. R. (2016). The Essential Transcriptional Function of BRD4 in Acute Myeloid Leukemia. *Cold Spring Harbor Symposia on Quantitative Biology*, 81, 61–66.
<https://doi.org/10.1101/sqb.2016.81.031039>
- Röhrig, F., & Schulze, A. (2016). The multifaceted roles of fatty acid synthesis in cancer. *Nature Reviews Cancer*, 16(11), 732–749. <https://doi.org/10.1038/nrc.2016.89>
- Ruderman, N. B., & Dean, D. (1998). Malonyl CoA, Long Chain Fatty Acyl CoA and Insulin Resistance in Skeletal Muscle. *Journal of Basic and Clinical Physiology and Pharmacology*, 9(2–4), 295–308. <https://doi.org/10.1515/JBCPP.1998.9.2-4.295>
- Ruiz-Xivillé, N., Granada, I., Campos, D., Cisneros, A., Grau, J., Xandri, M., Arnan, M., Lloveras, N., Escoda, L., Font, L., Millá, F., & Ribera, J. M. (2015). Clinical usefulness of fluorescence in situ hybridization for detection of MLL rearrangements in acute myeloid leukemia. *Leukemia and Lymphoma*, 56(9), 2706–2708.
<https://doi.org/10.3109/10428194.2014.1003053>
- Russler-Germain, D. A., Spencer, D. H., Young, M. A., Lamprecht, T. L., Miller, C. A., Fulton, R., Meyer, M. R., Erdmann-Gilmore, P., Townsend, R. R., Wilson, R. K., & Ley, T. J. (2014). The R882H DNMT3A Mutation Associated with AML Dominantly Inhibits Wild-Type DNMT3A by Blocking Its Ability to Form Active Tetramers. *Cancer Cell*, 25(4).
<https://doi.org/10.1016/j.ccr.2014.02.010>
- Saber, W., & Horowitz, M. M. (2016). Transplantation for myelodysplastic syndromes: Who, when, and which conditioning regimens. *Hematology*, 2016(1), 478–484.
<https://doi.org/10.1182/asheducation-2016.1.478>

| Bibliography

- Sakai, J., Duncan, E. A., Rawson, R. B., Hua, X., Brown, M. S., & Goldstein, J. L. (1996). Sterol-Regulated Release of SREBP-2 from Cell Membranes Requires Two Sequential Cleavages, One Within a Transmembrane Segment. *Cell*, *85*(7), 1037–1046. [https://doi.org/10.1016/S0092-8674\(00\)81304-5](https://doi.org/10.1016/S0092-8674(00)81304-5)
- Sallman, D. A., DeZern, A. E., Garcia-Manero, G., Steensma, D. P., Roboz, G. J., Sekeres, M. A., Cluzeau, T., Sweet, K. L., McLemore, A. F., McGraw, K., Puskas, J., Zhang, L., Yao, J., Mo, Q., Nardelli, L., Al Ali, N., Padron, E., Korbel, G., Attar, E. C., ... Komrokji, R. S. (2019). Phase 2 Results of APR-246 and Azacitidine (AZA) in Patients with TP53 mutant Myelodysplastic Syndromes (MDS) and Oligoblastic Acute Myeloid Leukemia (AML). *Blood*, *134*(Supplement_1), 676–676. <https://doi.org/10.1182/blood-2019-131055>
- Salti, L. M., & Goodridge, A. G. (1996). Chapter 4—Fatty acid synthesis in eukaryotes. In *New Comprehensive Biochemistry* (Vol. 31, pp. 101–127). Elsevier.
- Samudio, I., Fiegl, M., McQueen, T., Clise-Dwyer, K., & Andreeff, M. (2008). The warburg effect in leukemia-stroma cocultures is mediated by mitochondrial uncoupling associated with uncoupling protein 2 activation. *Cancer Research*, *68*(13), 5198–5205. <https://doi.org/10.1158/0008-5472.CAN-08-0555>
- Samudio, I., Harmancey, R., Fiegl, M., Kantarjian, H., Konopleva, M., Korchin, B., Kaluarachchi, K., Bornmann, W., Duvvuri, S., Taegtmeier, H., & Andreeff, M. (2010). Pharmacologic inhibition of fatty acid oxidation sensitizes human leukemia cells to apoptosis induction. *J Clin Invest.*, *120*(1), 142–156. <https://doi.org/10.1172/JCI38942.promote>
- Sanchez, P. V., Glantz, S. T., Scotland, S., Kasner, M. T., & Carroll, M. (2014). Induced differentiation of acute myeloid leukemia cells by activation of retinoid X and liver X receptors. *Leukemia*, *28*(4), 749–760. <https://doi.org/10.1038/leu.2013.202>
- Santini, V., Prebet, T., Fenaux, P., Gattermann, N., Nilsson, L., Pfeilstöcker, M., Vyas, P., & List, A. F. (2014). Minimizing risk of hypomethylating agent failure in patients with higher-risk MDS and practical management recommendations. *Leukemia Research*, *38*(12), 1381–1391. <https://doi.org/10.1016/j.leukres.2014.09.008>
- Santoro, F., Botrugno, O. A., Dal Zuffo, R., Pallavicini, I., Matthews, G. M., Cluse, L., Barozzi, I., Senese, S., Fornasari, L., Moretti, S., Altucci, L., Pelicci, P. G., Chiocca, S., Johnstone, R. W., & Minucci, S. (2013). A dual role for Hdac1: Oncosuppressor in tumorigenesis, oncogene in tumor maintenance. *Blood*, *121*(17), 3459–3468. <https://doi.org/10.1182/blood-2012-10-461988>
- Sashida, G., Harada, H., Matsui, H., Oshima, M., Yui, M., Harada, Y., Tanaka, S., Mochizuki-Kashio, M., Wang, C., Saraya, A., Muto, T., Hayashi, Y., Suzuki, K., Nakajima, H., Inaba, T., Koseki, H., Huang, G., Kitamura, T., & Iwama, A. (2014). Ezh2 loss promotes development of myelodysplastic syndrome but attenuates its predisposition to leukaemic transformation. *Nature Communications*, *5*(1), 4177. <https://doi.org/10.1038/ncomms5177>
- Sashida, G., & Iwama, A. (2012). Epigenetic regulation of hematopoiesis. *International Journal of Hematology*, *96*(4), 405–412. <https://doi.org/10.1007/s12185-012-1183-x>
- Sashida, G., Oshima, M., & Iwama, A. (2019). Deregulated Polycomb functions in myeloproliferative neoplasms. *International Journal of Hematology*, *110*(2), 170–178. <https://doi.org/10.1007/s12185-019-02600-6>
- Scarpulla, R. C. (1997). Nuclear Control of Respiratory Chain Expression in Mammalian Cells. *Journal of Bioenergetics and Biomembranes*, *29*(2), 109–119. <https://doi.org/10.1023/A:1022681828846>
- Schanz, J., Tüchler, H., Solé, F., Mallo, M., Luño, E., Cervera, J., Granada, I., Hildebrandt, B., Slovak, M. L., Ohyashiki, K., Steidl, C., Fonatsch, C., Pfeilstöcker, M., Nösslinger, T., Valent, P., Giagounidis, A., Aul, C., Lübbert, M., Stauder, R., ... Haase, D. (2012). New Comprehensive Cytogenetic Scoring System for Primary Myelodysplastic Syndromes (MDS) and Oligoblastic Acute Myeloid Leukemia After MDS Derived From an International Database Merge. *Journal of Clinical Oncology*, *30*(8), 820–829. <https://doi.org/10.1200/JCO.2011.35.6394>

- Schlabach, M. R., Luo, J., Solimini, N. L., Hu, G., Xu, Q., Li, M. Z., Zhao, Z., Smogorzewska, A., Sowa, M. E., Ang, X. L., Westbrook, T. F., Liang, A. C., Chang, K., Hackett, J. A., Harper, J. W., Hannon, G. J., & Elledge, S. J. (2008). Cancer Proliferation Gene Discovery Through Functional Genomics. *Science*, *319*(5863), 620–624. <https://doi.org/10.1126/science.1149200>
- Schönfeld, P., & Wojtczak, L. (2016). *Short- and medium-chain fatty acids in energy metabolism: The cellular perspective* (Vol. 57, Issue 6, p. 954). <https://doi.org/10.1194/jlr.R067629>
- Schübeler, D. (2015). Function and information content of DNA methylation. *Nature*, *517*(7534), 321–326. <https://doi.org/10.1038/nature14192>
- Sekeres, M. A. (2011). Epidemiology, Natural History, and Practice Patterns of Patients with Myelodysplastic Syndromes in 2010. *Journal of the National Comprehensive Cancer Network*, *9*(1), 57–63. <https://doi.org/10.6004/jnccn.2011.0006>
- Shafat, M. S., Oellerich, T., Mohr, S., Robinson, S. D., Edwards, D. R., Marlein, C. R., Piddock, R. E., Fenech, M., Zaitseva, L., Abdul-Aziz, A., Turner, J., Watkins, J. A., Lawes, M., Bowles, K. M., & Rushworth, S. A. (2017). Leukemic blasts program bone marrow adipocytes to generate a protumoral microenvironment. *Blood*, *129*(10), 1320–1332. <https://doi.org/10.1182/blood-2016-08-734798>
- Sharma, S., & Rao, A. (2009). RNAi screening: Tips and techniques. *Nature Immunology*, *10*(8), 799–804. <https://doi.org/10.1038/nio809-799>
- Shen, Y., Zhu, Y.-M., Fan, X., Shi, J.-Y., Wang, Q.-R., Yan, X.-J., Gu, Z.-H., Wang, Y.-Y., Chen, B., Jiang, C.-L., Yan, H., Chen, F.-F., Chen, H.-M., Chen, Z., Jin, J., & Chen, S.-J. (2011). Gene mutation patterns and their prognostic impact in a cohort of 1185 patients with acute myeloid leukemia. *Blood*, *118*(20), 5593–5603. <https://doi.org/10.1182/blood-2011-03-343988>
- Shi, Jinlong, Fu, H., Jia, Z., He, K., Fu, L., & Wang, W. (2016a). *High Expression of CPT1A Predicts Adverse Outcomes: A Potential Therapeutic Target for Acute Myeloid Leukemia*. *14*, 55–64.
- Shi, Jinlong, Fu, H., Jia, Z., He, K., Fu, L., & Wang, W. (2016b). High Expression of CPT1A Predicts Adverse Outcomes: A Potential Therapeutic Target for Acute Myeloid Leukemia. *EBioMedicine*, *14*, 55–64. <https://doi.org/10.1016/J.EBIOM.2016.11.025>
- Shi, Junwei, & Vakoc, C. R. (2014). The Mechanisms behind the Therapeutic Activity of BET Bromodomain Inhibition. *Molecular Cell*, *54*(5), 728–736. <https://doi.org/10.1016/j.molcel.2014.05.016>
- Shih, A. H., Abdel-Wahab, O., Patel, J. P., & Levine, R. L. (2012). The role of mutations in epigenetic regulators in myeloid malignancies. *Nature Reviews Cancer*, *12*(9), 599–612. <https://doi.org/10.1038/nrc3343>
- Shlush, L. I., Mitchell, A., Heisler, L., Abelson, S., Ng, S. W. K., Trotman-Grant, A., Medeiros, J. J. F., Rao-Bhatia, A., Jaciw-Zurakowsky, I., Marke, R., Mcleod, J. L., Doedens, M., Bader, G., Voisin, V., Xu, C., Mcpherson, J. D., Hudson, T. J., Wang, J. C. Y., Minden, M. D., & Dick, J. E. (2017). Tracing the origins of relapse in acute myeloid leukaemia to stem cells. *Nature Publishing Group*, *547*. <https://doi.org/10.1038/nature22993>
- Shukron, O., Vainstein, V., Kündgen, A., Germing, U., & Agur, Z. (2012). Analyzing transformation of myelodysplastic syndrome to secondary acute myeloid leukemia using a large patient database. *American Journal of Hematology*, *87*(9), 853–860. <https://doi.org/10.1002/ajh.23257>
- Silverman, L. R., Demakos, E. P., Peterson, B. L., Kornblith, A. B., Holland, J. C., Odchimar-Reissig, R., Stone, R. M., Nelson, D., Powell, B. L., DeCastro, C. M., Ellerton, J., Larson, R. A., Schiffer, C. A., & Holland, J. F. (2002). Randomized Controlled Trial of Azacitidine in Patients With the Myelodysplastic Syndrome: A Study of the Cancer and Leukemia Group B. *Journal of Clinical Oncology*, *20*(10), 2429–2440. <https://doi.org/10.1200/JCO.2002.04.117>
- Siminovitch, L., McCulloch, E. A., & Till, J. E. (1963). The distribution of colony-forming cells among spleen colonies. *Journal of Cellular and Comparative Physiology*, *62*(3), 327–336. <https://doi.org/10.1002/jcp.1030620313>

| Bibliography

- Simmons, G., Pruitt, W., & Pruitt, K. (2015). Diverse Roles of SIRT1 in Cancer Biology and Lipid Metabolism. *International Journal of Molecular Sciences*, *16*(1), 950–965. <https://doi.org/10.3390/ijms16010950>
- Simons, A., Shaffer, L. G., & Hastings, R. J. (2013). Cytogenetic Nomenclature: Changes in the ISCN 2013 Compared to the 2009 Edition. *Cytogenetic and Genome Research*, *141*(1), 1–6. <https://doi.org/10.1159/000353118>
- Singh, K. K., Shukla, P. C., Yanagawa, B., Quan, A., Lovren, F., Pan, Y., Wagg, C. S., Teoh, H., Lopaschuk, G. D., & Verma, S. (2013). Regulating cardiac energy metabolism and bioenergetics by targeting the DNA damage repair protein BRCA1. *The Journal of Thoracic and Cardiovascular Surgery*, *146*(3), 702–709. <https://doi.org/10.1016/J.JTCVS.2012.12.046>
- Singh, S., Narang, A. S., & Mahato, R. I. (2011). Subcellular Fate and Off-Target Effects of siRNA, shRNA, and miRNA. *Pharmaceutical Research*, *28*(12), 2996–3015. <https://doi.org/10.1007/s11095-011-0608-1>
- Škrčić, M., Sriskanthadevan, S., Jhas, B., Gebbia, M., Wang, X., Wang, Z., Hurren, R., Jitkova, Y., Gronda, M., Maclean, N., Lai, C. K., Eberhard, Y., Bartoszkó, J., Spagnuolo, P., Rutledge, A. C., Datti, A., Ketela, T., Moffat, J., Robinson, B. H., ... Schimmer, A. D. (2011). Inhibition of Mitochondrial Translation as a Therapeutic Strategy for Human Acute Myeloid Leukemia. *Cancer Cell*, *20*(5), 674–688. <https://doi.org/10.1016/j.ccr.2011.10.015>
- Smith, I., Greenside, P. G., Natoli, T., Lahr, D. L., Wadden, D., Tirosh, I., Narayan, R., Root, D. E., Golub, T. R., Subramanian, A., & Doench, J. G. (2017). Evaluation of RNAi and CRISPR technologies by large-scale gene expression profiling in the Connectivity Map. *PLOS Biology*, *15*(11). <https://doi.org/10.1371/journal.pbio.2003213>
- Song, G., Shi, L., Guo, Y., Yu, L., Wang, L., Zhang, X., Li, L., Han, Y., Ren, X., Guo, Q., Bi, K., & Jiang, G. (2016). A novel PAD4/SOX4/PU.1 signaling pathway is involved in the committed differentiation of acute promyelocytic leukemia cells into granulocytic cells. *Oncotarget*, *7*(3), 3144–3157. <https://doi.org/10.18632/oncotarget.6551>
- Spencer, J. A., Ferraro, F., Roussakis, E., Klein, A., Wu, J., Runnels, J. M., Zaher, W., Mortensen, L. J., Alt, C., Turcotte, R., Yusuf, R., Côté, D., Vinogradov, S. A., Scadden, D. T., & Lin, C. P. (2014). Direct measurement of local oxygen concentration in the bone marrow of live animals. *Nature*, *508*(7495), 269–273. <https://doi.org/10.1038/nature13034>
- Sperling, A. S., Gibson, C. J., & Ebert, B. L. (2017). The genetics of myelodysplastic syndrome: From clonal haematopoiesis to secondary leukaemia. *Nature Reviews Cancer*, *17*(1), 5–19. <https://doi.org/10.1038/nrc.2016.112>
- Sriskanthadevan, S., Jeyaraju, D. V., Chung, T. E., Prabha, S., Xu, W., Skrtic, M., Jhas, B., Hurren, R., Gronda, M., Wang, X., Jitkova, Y., Sukhai, M. A., Lin, F. H., Maclean, N., Laister, R., Goard, C. A., Mullen, P. J., Xie, S., Penn, L. Z., ... Schimmer, A. D. (2015). AML cells have low spare reserve capacity in their respiratory chain that renders them susceptible to oxidative metabolic stress. *Blood*, *125*(13), 2120–2130. <https://doi.org/10.1182/blood-2014-08-594408>
- Stacey, G. N., Bolton, B. J., Morgan, D., Clark, S. A., & Doyle, A. (1992). Multilocus DNA fingerprint analysis of cellbanks: Stability studies and culture identification in human B-lymphoblastoid and mammalian cell lines. *Cytotechnology*, *8*(1), 13–20. <https://doi.org/10.1007/BF02540025>
- Stachurski, D., Smith, B. R., Pozdnyakova, O., Andersen, M., Xiao, Z., Raza, A., Woda, B. A., & Wang, S. A. (2008). Flow cytometric analysis of myelomonocytic cells by a pattern recognition approach is sensitive and specific in diagnosing myelodysplastic syndrome and related marrow diseases: Emphasis on a global evaluation and recognition of diagnostic pitfalls. *Leukemia Research*, *32*(2), 215–224. <https://doi.org/10.1016/j.leukres.2007.06.012>
- Steensma, D. P. (2018). Clinical consequences of clonal hematopoiesis of indeterminate potential. *Blood Advances*, *2*(22), 3404–3410. <https://doi.org/10.1182/bloodadvances.2018020222>
- Steensma, D. P., Bejar, R., Jaiswal, S., Lindsley, R. C., Sekeres, M. A., Hasserjian, R. P., & Ebert, B. L. (2015). Clonal hematopoiesis of indeterminate potential and its distinction from

- myelodysplastic syndromes. *Blood*, 126(1), 9–16. <https://doi.org/10.1182/blood-2015-03-631747>
- Steensma, D. P., & Bennett, J. M. (2006). *The myelodysplastic syndromes: Diagnosis and treatment*. 81(1), 104–130. <https://doi.org/10.4065/81.1.104>
- Stein, E. M., Fathi, A. T., DiNardo, C. D., Pollyea, D. A., Roboz, G. J., Collins, R., Sekeres, M. A., Stone, R. M., Attar, E. C., Frattini, M. G., Tosolini, A., Xu, Q., See, W. L., MacBeth, K. J., de Botton, S., Tallman, M. S., & Kantarjian, H. M. (2020). Enasidenib in patients with mutant IDH2 myelodysplastic syndromes: A phase 1 subgroup analysis of the multicentre, AG221-C-001 trial. *The Lancet Haematology*, 7(4), e309–e319. [https://doi.org/10.1016/S2352-3026\(19\)30284-4](https://doi.org/10.1016/S2352-3026(19)30284-4)
- Stenderup, K., Justesen, J., Clausen, C., & Kassem, M. (2003). Aging is associated with decreased maximal life span and accelerated senescence of bone marrow stromal cells. *Bone*, 33(6), 919–926.
- Stengel, A., Shahswar, R., Walter, W., Meggendorfer, M., Kern, W., Haferlach, T., & Haferlach, C. (2019). Application of RNA Sequencing Detects a Large Number of Novel Fusion Transcripts in Patients with AML and MDS. *Blood*, 134(Supplement_1), 887–887. <https://doi.org/10.1182/blood-2019-124310>
- Stevens, B. M., Zhang, W., Pollyea, D. A., Winters, A., Gutman, J., Smith, C., Budde, E., Forman, S. J., Jordan, C. T., & Purev, E. (2019). CD123 CAR T cells for the treatment of myelodysplastic syndrome. *Experimental Hematology*, 74, 52–63.e3. <https://doi.org/10.1016/j.exphem.2019.05.002>
- Stremmel, W., Pohl, J., Ring, A., & Herrmann, T. (2001). A new concept of cellular uptake and intracellular trafficking of long-chain fatty acids. *Lipids*, 36(9), 981–989. <https://doi.org/10.1007/s11745-001-0809-2>
- Stresemann, C., & Lyko, F. (2008). Modes of action of the DNA methyltransferase inhibitors azacytidine and decitabine. *International Journal of Cancer*, 123(1), 8–13. <https://doi.org/10.1002/ijc.23607>
- Suganuma, K., Miwa, H., Imai, N., Shikami, M., Gotou, M., Goto, M., Mizuno, S., Takahashi, M., Yamamoto, H., Hiramatsu, A., Wakabayashi, M., Watarai, M., Hanamura, I., Imamura, A., Mihara, H., & Nitta, M. (2010). Energy metabolism of leukemia cells: Glycolysis versus oxidative phosphorylation. *Leukemia & Lymphoma*, 51(11), 2112–2119. <https://doi.org/10.3109/10428194.2010.512966>
- Sugimoto, K., Hirano, N., Toyoshima, H., Chiba, S., Mano, H., Takaku, F., Yazaki, Y., & Hirai, H. (1993). Mutations of the p53 gene in myelodysplastic syndrome (MDS) and MDS-derived leukemia. *Blood*, 81(11), 3022–3026. <https://doi.org/10.1182/blood.V81.11.3022.3022>
- Sumiyoshi, R., Tashiro, H., Matsuo, T., Yamamoto, T., Oka-Miura, Y., Matsumoto, K., Ooi, J., & Shirafuji, N. (2017). FLT3-ITD Mutation in MDS Patients Is Associated with Early Transformation to AML. *Blood*, 130(Supplement 1).
- Suraweera, A., O'Byrne, K. J., & Richard, D. J. (2018). Combination Therapy With Histone Deacetylase Inhibitors (HDACi) for the Treatment of Cancer: Achieving the Full Therapeutic Potential of HDACi. *Frontiers in Oncology*, 8, 92. <https://doi.org/10.3389/fonc.2018.00092>
- Swerdlow, S. H., Campo, E., Harris, N. L., Jaffe, E. S., Pileri, S. A., Stein, H., & Thiele, J. (2017). *WHO Classification of Tumours of Haematopoietic and Lymphoid Tissues* (4th ed., Vol. 2, p. 188). International Agency for Research on Cancer.
- Tabé, Y., Konopleva, M., & Andreeff, M. (2020). Fatty Acid Metabolism, Bone Marrow Adipocytes, and AML. *Frontiers in Oncology*, 10, 155–155. <https://doi.org/10.3389/fonc.2020.00155>
- Tabé, Y., Yamamoto, S., Saitoh, K., Sekihara, K., Monma, N., Ikeo, K., Mogushi, K., Shikami, M., Ruvolo, V., Ishizawa, J., Jr, N. H., Kazuno, S., Igarashi, M., Matsushita, H., Yamanaka, Y., Arai, H., Nagaoka, I., Miida, T., Hayashizaki, Y., ... Andreeff, M. (2017). Bone marrow adipocytes facilitate fatty acid oxidation activating AMPK and a transcriptional network

| Bibliography

- supporting survival of acute monocytic leukemia cells. *Cancer Research*.
<https://doi.org/10.1158/0008-5472.CAN-16-1645>
- Takahashi, H., McCaffery, J. M., Irizarry, R. A., & Boeke, J. D. (2006). Nucleocytoplasmic Acetyl-Coenzyme A Synthetase Is Required for Histone Acetylation and Global Transcription. *Molecular Cell*, 23(2), 207–217. <https://doi.org/10.1016/j.molcel.2006.05.040>
- Thomas, E. D., Lochte, H. L., Lu, W. C., & Ferrebee, J. W. (1957). Intravenous Infusion of Bone Marrow in Patients Receiving Radiation and Chemotherapy. *New England Journal of Medicine*, 257(11), 491–496. <https://doi.org/10.1056/NEJM195709122571102>
- Thumser, A. E., & Storch, J. (2007). Characterization of a BODIPY-labeled fluorescent fatty acid analogue. Binding to fatty acid-binding proteins, intracellular localization, and metabolism. *Molecular and Cellular Biochemistry*, 299(1–2), 67–73. <https://doi.org/10.1007/s11010-005-9041-2>
- Tien, H.-F., Tang, J.-L., Tsay, W., Liu, M.-C., Lee, F.-Y., Wang, C.-H., Chen, Y.-C., & Shen, M.-C. (2001). Methylation of the p15 INK4B gene in myelodysplastic syndrome: It can be detected early at diagnosis or during disease progression and is highly associated with leukaemic transformation. *British Journal of Haematology*, 112(1). <https://doi.org/10.1046/j.1365-2141.2001.02496.x>
- Till, J., & McCulloch, E. (1961). A direct measurement of the radiation sensitivity of normal mouse bone marrow cells. *Radiat Res*, 14, 213–222.
- Trojer, P. (2016). *Histone Methylation Modifiers in Medical Therapeutics* (p. 729). Elsevier. <https://doi.org/10.1016/B978-0-12-803239-8.00037-5>
- Trowbridge, J. J., Snow, J. W., Kim, J., & Orkin, S. H. (2009). DNA Methyltransferase 1 Is Essential for and Uniquely Regulates Hematopoietic Stem and Progenitor Cells. *Cell Stem Cell*, 5(4), 442–449. <https://doi.org/10.1016/j.stem.2009.08.016>
- Trumble, G. E., Smith, M. A., & Winder, W. W. (1995). Purification and Characterization of Rat Skeletal Muscle Acetyl-CoA Carboxylase. *European Journal of Biochemistry*, 231(1), 192–198. <https://doi.org/10.1111/j.1432-1033.1995.tb20686.x>
- Unnikrishnan, A., Papaemmanuil, E., Beck, D., Wong, J. W. H., Campbell, P. J., & Pimanda, J. E. (2017). Integrative Genomics Identifies the Molecular Basis of Resistance to Azacitidine Therapy in Myelodysplastic Syndromes Article Integrative Genomics Identifies the Molecular Basis of Resistance to Azacitidine Therapy in Myelodysplastic Syndromes. *CellReports*, 20(3), 572–585. <https://doi.org/10.1016/j.celrep.2017.06.067>
- Valent, P., Sadovnik, I., Eisenwort, G., Bauer, K., Herrmann, H., Gleixner, K. V., Schulenburg, A., Rabitsch, W., Sperr, W. R., & Wolf, D. (2019). Immunotherapy-based targeting and elimination of leukemic stem cells in AML and CML. *International Journal of Molecular Sciences*, 20(17). <https://doi.org/10.3390/ijms20174233>
- Valerio, D. G., Xu, H., Chen, C. W., Hoshii, T., Eisold, M. E., Delaney, C., Cusan, M., Deshpande, A. J., Huang, C. H., Lujambio, A., Zheng, Y. G., Zuber, J., Pandita, T. K., Lowe, S. W., & Armstrong, S. A. (2017). Histone acetyltransferase activity of MOF is required for MLL-AF9 leukemogenesis. *Cancer Research*, 77(7), 1753–1762. <https://doi.org/10.1158/0008-5472.CAN-16-2374>
- Valk-Lingbeek, M. E., Bruggeman, S. W. M., & van Lohuizen, M. (2004). Stem Cells and Cancer. *Cell*, 118(4), 409–418. <https://doi.org/10.1016/j.cell.2004.08.005>
- van de Loosdrecht, A. A., Ireland, R., Kern, W., Della Porta, M. G., Alhan, C., Balleisen, J. S., Bettelheim, P., Bowen, D. T., Burbury, K., Eidenschink, L., Cazzola, M., Chu, S. S. C., Cullen, M., Cutler, J. A., Dräger, A. M., Feuillard, J., Fenaux, P., Font, P., Germing, U., ... Westers, T. M. (2013). Rationale for the clinical application of flow cytometry in patients with myelodysplastic syndromes: Position paper of an International Consortium and the European LeukemiaNet Working Group. *Leukemia & Lymphoma*, 54(3), 472–475. <https://doi.org/10.3109/10428194.2012.718341>
- VanSaun, M. N. (2013). Molecular pathways: Adiponectin and leptin signaling in cancer. *Clinical Cancer Research*, 19(8), 1926–1932. <https://doi.org/10.1158/1078-0432.CCR-12-0930>

- Vega, R. B., Huss, J. M., & Kelly, D. P. (2000). The Coactivator PGC-1 Cooperates with Peroxisome Proliferator-Activated Receptor α in Transcriptional Control of Nuclear Genes Encoding Mitochondrial Fatty Acid Oxidation Enzymes. *Molecular and Cellular Biology*, 20(5), 1868–1876. <https://doi.org/10.1128/MCB.20.5.1868-1876.2000>
- Vose, J. M., Bierman, P. J., Lynch, J. C., Atkinson, K., Juttner, C., Hanania, E., Bociek, G., & Armitage, J. O. (2001). Transplantation of highly purified CD34+Thy-1+ hematopoietic stem cells in patients with recurrent indolent non-Hodgkin's lymphoma. *Biology of Blood and Marrow Transplantation*, 7(12), 680–687. <https://doi.org/10.1053/bbmt.2001.v7.pm11787531>
- Voso, M. T., Lo-Coco, F., & Fianchi, L. (2015). Epigenetic therapy of myelodysplastic syndromes and acute myeloid leukemia. *Current Opinion in Oncology*, 27(6), 532–539. <https://doi.org/10.1097/CCO.0000000000000231>
- Wan, L., Xu, K., Wei, Y., Zhang, J., Han, T., Fry, C., Zhang, Z., Wang, Y. V., Huang, L., Yuan, M., Xia, W., Chang, W.-C., Huang, W.-C., Liu, C.-L., Chang, Y.-C., Liu, J., Wu, Y., Jin, V. X., Dai, X., ... Wei, W. (2018). Phosphorylation of EZH2 by AMPK Suppresses PRC2 Methyltransferase Activity and Oncogenic Function. *Molecular Cell*, 69(2), 279–291.e5. <https://doi.org/10.1016/j.molcel.2017.12.024>
- Wang, J. C. Y., Doedens, M., & Dick, J. E. (1997). Primitive Human Hematopoietic Cells Are Enriched in Cord Blood Compared With Adult Bone Marrow or Mobilized Peripheral Blood as Measured by the Quantitative In Vivo SCID-Repopulating Cell Assay. *Blood*, 89(11), 3919–3924. <https://doi.org/10.1182/blood.V89.11.3919>
- Wang, P., Wang, Z., & Liu, J. (2020). Role of HDACs in normal and malignant hematopoiesis. *Molecular Cancer*, 19(1), 5. <https://doi.org/10.1186/s12943-019-1127-7>
- Wang, Z., Gearhart, M. D., Lee, Y.-W., Kumar, I., Ramazanov, B., Zhang, Y., Hernandez, C., Lu, A. Y., Neuenkirchen, N., Deng, J., Jin, J., Kluger, Y., Neubert, T. A., Bardwell, V. J., & Ivanova, N. B. (2018). A Non-canonical BCOR-PRC1.1 Complex Represses Differentiation Programs in Human ESCs. *Cell Stem Cell*, 22(2). <https://doi.org/10.1016/j.stem.2017.12.002>
- Warburg, O. (1956). On the Origin of Cancer Cells. *Science*, 123(3191), 309–314. <https://doi.org/10.1126/science.123.3191.309>
- Watson, J. V., Chambers, S. H., & Smith, P. J. (1987). A pragmatic approach to the analysis of DNA histograms with a definable G1 peak. *Cytometry*, 8(1), 1–8. <https://doi.org/10.1002/cyto.990080101>
- Weightman Potter, P. G., Vlachaki Walker, J. M., Robb, J. L., Chilton, J. K., Williamson, R., Randall, A. D., Ellacott, K. L. J., & Beall, C. (2019). Basal fatty acid oxidation increases after recurrent low glucose in human primary astrocytes. *Diabetologia*, 62(1), 187–198. <https://doi.org/10.1007/s00125-018-4744-6>
- Weishaupt, H., Sigvardsson, M., & Attema, J. L. (2010). Epigenetic chromatin states uniquely define the developmental plasticity of murine hematopoietic stem cells. *Blood*, 115(2), 247–256. <https://doi.org/10.1182/blood-2009-07-235176>
- Weissmann, S., Alpermann, T., Grossmann, V., Kowarsch, A., Nadarajah, N., Eder, C., Dicker, F., Fasan, A., Haferlach, C., Haferlach, T., Kern, W., Schnittger, S., & Kohlmann, A. (2012). Landscape of TET2 mutations in acute myeloid leukemia. *Leukemia*, 26(5), 934–942. <https://doi.org/10.1038/leu.2011.326>
- Wellen, K. E., & Thompson, C. B. (2012). A two-way street: Reciprocal regulation of metabolism and signalling. *Nature Reviews Molecular Cell Biology*, 13(4), 270–276. <https://doi.org/10.1038/nrm3305>
- Wells, S. J., Bray, R. A., Stempora, L. L., & Farhi, D. C. (1996). CD117/CD34 expression in leukemic blasts. *American Journal of Clinical Pathology*, 106(2), 192–195. <https://doi.org/10.1093/ajcp/106.2.192>
- Wilson, A., & Trumpp, A. (2006). Bone-marrow haematopoietic-stem-cell niches. *Nature Reviews Immunology*, 6(2), 93–106. <https://doi.org/10.1038/nri1779>

| Bibliography

- Winder, W. W., Wilson, H. A., Hardie, D. G., Rasmussen, B. B., Hutber, C. A., Call, G. B., Clayton, R. D., Conley, L. M., Yoon, S., & Zhou, B. (1997). Phosphorylation of rat muscle acetyl-CoA carboxylase by AMP-activated protein kinase and protein kinase A. *Journal of Applied Physiology*, 82(1), 219–225. <https://doi.org/10.1152/jap.1997.82.1.219>
- Winiarska, M., Nowis, D., Firczuk, M., Zagozdzon, A., Gabrysiak, M., Sadowski, R., Barankiewicz, J., Dwojak, M., & Golab, J. (2017). Selection of an optimal promoter for gene transfer in normal B cells. *Molecular Medicine Reports*, 16(3), 3041–3048. <https://doi.org/10.3892/mmr.2017.6974>
- Winters, A. C., & Bernt, K. M. (2017). MLL-Rearranged Leukemias—An Update on Science and Clinical Approaches. *Frontiers in Pediatrics*, 5. <https://doi.org/10.3389/fped.2017.00004>
- Wouters, B. J., & Delwel, R. (2016). Epigenetics and approaches to targeted epigenetic therapy in acute myeloid leukemia. *Blood*, 127(1), 42–52. <https://doi.org/10.1182/blood-2015-07-604512>
- Wroblewski, M., Scheller-Wendorff, M., Udonta, F., Bauer, R., Schlichting, J., Zhao, L., Ben Batalla, I., Gensch, V., Päsler, S., Wu, L., Wanior, M., Taipaleenmäki, H., Bolamperti, S., Najafova, Z., Pantel, K., Bokemeyer, C., Qi, J., Hesse, E., Knapp, S., ... Loges, S. (2018). BET-inhibition by JQ1 promotes proliferation and self-renewal capacity of hematopoietic stem cells. *Haematologica*, 103(6), 939–948. <https://doi.org/10.3324/haematol.2017.181354>
- Wu, D., Lim, E., Vaillant, F., Asselin-Labat, M.-L., Visvader, J. E., & Smyth, G. K. (2010). ROAST: rotation gene set tests for complex microarray experiments. 26(17), 2176–2182. <https://doi.org/10.1093/bioinformatics/btq401>
- Wu, L., Shi, W., Li, X., Chang, C., Xu, F., He, Q., Wu, D., Su, J., Zhou, L., & Song, L. (2016). High expression of the human equilibrative nucleoside transporter 1 gene predicts a good response to decitabine in patients with myelodysplastic syndrome. 1–9. <https://doi.org/10.1186/s12967-016-0817-9>
- Xia, X. G. (2003). An enhanced U6 promoter for synthesis of short hairpin RNA. *Nucleic Acids Research*, 31(17). <https://doi.org/10.1093/nar/gng098>
- Xiao, A., Li, H., Shechter, D., Ahn, S. H., Fabrizio, L. A., Erdjument-Bromage, H., Ishibe-Murakami, S., Wang, B., Tempst, P., Hofmann, K., Patel, D. J., Elledge, S. J., & Allis, C. D. (2009). WSTF regulates the H2A.X DNA damage response via a novel tyrosine kinase activity. *Nature*, 457(7225), 57–62. <https://doi.org/10.1038/nature07668>
- Xu, W., Yang, H., Liu, Y., Yang, Y., Wang, P., Kim, S.-H., Ito, S., Yang, C., Wang, P., Xiao, M.-T., Liu, L., Jiang, W., Liu, J., Zhang, J., Wang, B., Frye, S., Zhang, Y., Xu, Y., Lei, Q., ... Xiong, Y. (2011). Oncometabolite 2-Hydroxyglutarate Is a Competitive Inhibitor of α -Ketoglutarate-Dependent Dioxygenases. *Cancer Cell*, 19(1), 17–30. <https://doi.org/10.1016/j.ccr.2010.12.014>
- Yan, F., Shen, N., Pang, J. X., Zhang, Y. W., Rao, E. Y., Bode, A. M., Al-Kali, A., Zhang, D. E., Litzow, M. R., Li, B., & Liu, S. J. (2017). Fatty acid-binding protein FABP4 mechanistically links obesity with aggressive AML by enhancing aberrant DNA methylation in AML cells. *Leukemia*, 31(6), 1434–1442. <https://doi.org/10.1038/leu.2016.349>
- Yan, F., Shen, N., Pang, J. X., Zhao, N., Zhang, Y. W., Bode, A. M., Al-Kali, A., Litzow, M. R., Li, B., & Liu, S. J. (2018). A vicious loop of fatty acid-binding protein 4 and DNA methyltransferase 1 promotes acute myeloid leukemia and acts as a therapeutic target. *Leukemia*, 32(4), 865–873. <https://doi.org/10.1038/leu.2017.307>
- Yates, L. A., Norbury, C. J., & Gilbert, R. J. C. (2013). The Long and Short of MicroRNA. *Cell*, 153(3), 516–519. <https://doi.org/10.1016/j.cell.2013.04.003>
- Ye, H., Adane, B., Khan, N., Stranahan, A. W., Park, C. Y., Jordan, C. T., Ye, H., Adane, B., Khan, N., Sullivan, T., Minhajuddin, M., Gasparetto, M., Stranahan, A. W., Park, C. Y., & Jordan, C. T. (2016). Leukemic Stem Cells Evade Chemotherapy by Metabolic Adaptation to an Adipose Tissue Niche Article Leukemic Stem Cells Evade Chemotherapy by Metabolic Adaptation to an Adipose Tissue Niche. *Cell Stem Cell*, 23–37.
- Ye, H., Adane, B., Khan, N., Sullivan, T., Minhajuddin, M., Gasparetto, M., Stevens, B., Pei, S., Balys, M., Ashton, J. M., Klemm, D. J., Woolthuis, C. M., Stranahan, A. W., Park, C. Y., &

- Jordan, C. T. (2016). Leukemic Stem Cells Evade Chemotherapy by Metabolic Adaptation to an Adipose Tissue Niche. *Cell Stem Cell*. <https://doi.org/10.1016/j.stem.2016.06.001>
- Yu, J., Peng, Y., Wu, L. C., Xie, Z., Deng, Y., Hughes, T., He, S., Mo, X. K., Chiu, M., Wang, Q. E., He, X., Liu, S., Grever, M. R., Chan, K. K., & Liu, Z. (2013). Curcumin Down-Regulates DNA Methyltransferase 1 and Plays an Anti-Leukemic Role in Acute Myeloid Leukemia. *PLoS ONE*. <https://doi.org/10.1371/journal.pone.0055934>
- Yu, Mamie, Selvaraj, S. K., Liang-Chu, M. M. Y., Aghajani, S., Busse, M., Yuan, J., Lee, G., Peale, F., Klijn, C., Bourgon, R., Kaminker, J. S., & Neve, R. M. (2015). A resource for cell line authentication, annotation and quality control. *Nature*, *520*(7547), 307–311. <https://doi.org/10.1038/nature14397>
- Yu, Ming, Mazor, T., Huang, H., Huang, H.-T., Kathrein, K. L., Woo, A. J., Chouinard, C. R., Labadorf, A., Akie, T. E., Moran, T. B., Xie, H., Zacharek, S., Taniuchi, I., Roeder, R. G., Kim, C. F., Zon, L. I., Fraenkel, E., & Cantor, A. B. (2012). Direct Recruitment of Polycomb Repressive Complex 1 to Chromatin by Core Binding Transcription Factors. *Molecular Cell*, *45*(3), 330–343. <https://doi.org/10.1016/j.molcel.2011.11.032>
- Yun, M., Wu, J., Workman, J. L., & Li, B. (2011). Readers of histone modifications. *Cell Research*, *21*(4), 564–578. <https://doi.org/10.1038/cr.2011.42>
- Zeidan, A. M., Stahl, M., Sekeres, M. A., Steensma, D. P., Komrokji, R. S., & Gore, S. D. (2017). A call for action: Increasing enrollment of untreated patients with higher-risk myelodysplastic syndromes in first-line clinical trials. *Cancer*, *123*(19), 3662–3672. <https://doi.org/10.1002/cncr.30903>
- Zhang, F., Frost, A. R., Blundell, M. P., Bales, O., Antoniou, M. N., & Thrasher, A. J. (2010). A Ubiquitous Chromatin Opening Element (UCOE) Confers Resistance to DNA Methylation-mediated Silencing of Lentiviral Vectors. *Molecular Therapy*, *18*(9), 1640–1649. <https://doi.org/10.1038/mt.2010.132>
- Zhang, J., & Zhong, Q. (2014). Histone deacetylase inhibitors and cell death. *Cellular and Molecular Life Sciences*, *71*(20), 3885–3901. <https://doi.org/10.1007/s00018-014-1656-6>
- Zhou, Y., An, L.-L., Chaerkady, R., Mittereder, N., Clarke, L., Cohen, T. S., Chen, B., Hess, S., Sims, G. P., & Mustelin, T. (2018). Evidence for a direct link between PAD4-mediated citrullination and the oxidative burst in human neutrophils. *Scientific Reports*, *8*(1), 15228–15228. <https://doi.org/10.1038/s41598-018-33385-z>
- Zimmer, A. M., Pan, Y. K., Chandrapalan, T., Kwong, R. W. M., & Perry, S. F. (2019). Loss-of-function approaches in comparative physiology: Is there a future for knockdown experiments in the era of genome editing? *The Journal of Experimental Biology*, *222*(7), jeb175737. <https://doi.org/10.1242/jeb.175737>
- Zinngrebe, J., Debatin, K.-M., & Fischer-Posovszky, P. (2020). Adipocytes in hematopoiesis and acute leukemia: Friends, enemies, or innocent bystanders? *Leukemia*, *34*(9). <https://doi.org/10.1038/s41375-020-0886-x>
- Zuber, J., Shi, J., Wang, E., Rappaport, A. R., Herrmann, H., Sison, E. A., Magoon, D., Qi, J., Blatt, K., Wunderlich, M., Taylor, M. J., Johns, C., Chicas, A., Mulloy, J. C., Kogan, S. C., Brown, P., Valent, P., Bradner, J. E., Lowe, S. W., & Vakoc, C. R. (2011). RNAi screen identifies Brd4 as a therapeutic target in acute myeloid leukaemia. *Nature*, *478*(7370), 524–528. <https://doi.org/10.1038/nature10334>

12. Appendix

12.1 Lists of top ranked genes from shRNA screen

Table 18: List of top ranked enriched genes in TS LOW (associated with lower fatty acid uptake) from the

| Rank | Gene | LogFC 1 | LogFC 2 | LogFC 3 | LogFC 4 | LogFC 5 | LogFC 6 | LogFC 7 | LogFC 8 | p |
|------|---------------|------------|------------|------------|------------|------------|------------|------------|------------|-----|
| 1 | HDGFL1 | -8.4009 | -1.7190 | 0.3472 | -2.7975 | -2.4747 | -0.9820 | -2.9156 | -3.1489 | 0.0 |
| 2 | SIRT6 | -1.5198 | -1.5018 | 1.4338 | -2.8611 | -2.5918 | -2.5217 | -1.1714 | -3.7649 | 0.0 |
| 3 | TRIM24 | 0.9423 | 0.0046 | 4.5643 | -3.0846 | -1.1247 | -3.4985 | -2.8747 | -0.5803 | 0.0 |
| 4 | MLL2 | -1.1252 | -0.5803 | -0.9066 | -1.1866 | 0.5241 | -2.7711 | -4.9250 | -5.1652 | 0.0 |
| 5 | EDF1 | -2.8876 | 0.1815 | -1.8577 | 0.7215 | -3.4423 | -1.8926 | -4.0385 | -0.3200 | 0.0 |
| 6 | JMJD7-PLA2G4B | -0.1909 | -0.0088 | 0.1257 | -3.4022 | -3.7952 | -0.4410 | -1.7444 | -4.9768 | 0.0 |
| 7 | L3MBTL2 | -0.7373 | -0.9521 | -3.3950 | 2.4584 | -3.0497 | -1.4507 | -2.4791 | -3.2313 | 0.0 |
| 8 | PADI4 | -0.5391 | -4.2399 | -1.5078 | -1.6397 | -3.5797 | -4.3119 | -1.6724 | NA | 0.0 |
| 9 | PRDM8 | 1.0545 | -1.9516 | 2.8446 | 0.2770 | -3.1621 | -0.3227 | -2.7801 | -2.8928 | 0.0 |
| 10 | EIF4A2 | -2.5457 | -2.0091 | 3.1418 | -2.6311 | -3.9222 | -1.3506 | -0.3483 | NA | 0.0 |
| 11 | CDY1B | -1.6570 | 0.0244 | 0.4717 | -0.7215 | 0.8550 | -1.6948 | -1.2508 | -0.0981 | 0.0 |
| 12 | SCMH1 | -2.4960 | -1.8308 | -4.3365 | -2.2808 | 1.0954 | -2.1055 | -1.6069 | NA | 0.0 |
| 13 | DDX49 | -3.3537 | -0.8162 | -3.4350 | -1.3945 | 0.8084 | -0.9602 | -4.0915 | -0.5947 | 0.0 |
| 14 | UBR5 | 6.1025 | -1.1350 | -1.3803 | -5.4220 | -5.7435 | 0.0033 | -4.7970 | 0.6754 | 0.0 |
| 15 | CDY2A | -1.6570 | 0.4717 | -0.7215 | 0.8550 | -2.5154 | -0.9257 | -1.2508 | -0.0981 | 0.0 |
| 16 | CDY2B | -1.6570 | 0.4717 | -0.7215 | 0.8550 | -2.5154 | -0.9257 | -1.2508 | -0.0981 | 0.0 |
| 17 | CBX1 | -1.1354 | -1.8003 | -2.2413 | 1.9926 | -0.8897 | -1.7335 | -3.9285 | -0.5891 | 0.0 |
| 18 | TRIM13 | -1.1914 | -6.2543 | -2.1951 | -1.1848 | -0.1848 | -1.1347 | 0.2849 | 9.1954 | 0.0 |

| | | | | | | | | | | |
|----|----------|---------|----------|---------|---------|---------|---------|---------|---------|----|
| 19 | BRIP1 | -0.3414 | -1.4301 | -5.4918 | -7.5871 | -0.5283 | -0.2576 | -4.3414 | -0.3363 | 0. |
| 20 | DZIP3 | -0.8943 | -2.9028 | -1.3024 | -2.1406 | -0.1903 | -0.4670 | -2.3037 | -3.5180 | 0. |
| 21 | TDRD5 | -2.0871 | -1.7616 | -2.1911 | -1.4706 | -0.5743 | 3.6514 | -2.4390 | NA | 0. |
| 22 | PKN1 | -2.3207 | -3.3683 | -4.9632 | -0.2951 | 1.2263 | -4.5174 | 0.3403 | -3.1256 | 0. |
| 23 | PAX9 | -7.2094 | -0.6613 | -1.0366 | -1.0793 | 1.2098 | -1.7349 | -1.5784 | NA | 0. |
| 24 | MIS18BP1 | -0.7107 | -1.6661 | -3.0868 | -0.1266 | -2.1989 | -3.4537 | -3.8977 | NA | 0. |
| 25 | UTY | -4.6121 | -1.7065 | -3.1681 | -5.5735 | -3.0101 | -3.3510 | 1.9324 | 4.3238 | 0. |
| 26 | RFWD2 | -0.3149 | -3.0345 | -4.1658 | -4.2576 | -1.5863 | 3.8092 | -4.1908 | NA | 0. |
| 27 | PRDM6 | -0.5522 | -2.5163 | 0.1727 | -0.8519 | 1.7217 | -3.4243 | -1.7032 | -2.9640 | 0. |
| 28 | ATAD2B | -2.0488 | -1.9849 | -3.0393 | -1.4200 | -4.7468 | -3.3684 | -0.3663 | NA | 0. |
| 29 | GADD45A | -2.3877 | -2.4563 | -3.1693 | -1.2410 | 3.4752 | -0.3520 | -2.9419 | 1.8672 | 0. |
| 30 | ARID1B | 0.9734 | -2.9309 | -4.1421 | -5.8702 | -2.6935 | -1.5928 | -2.1174 | 6.3523 | 0. |
| 31 | HLTF | -0.1287 | -2.3235 | -2.4396 | -1.4288 | 1.9639 | -2.7895 | -2.6302 | 5.5572 | 0. |
| 32 | CLOCK | -0.4622 | -1.2692 | -1.0704 | -1.1568 | -2.9950 | 0.2012 | -0.5686 | -2.1556 | 0. |
| 33 | NBN | -1.5194 | -1.0610 | -2.2853 | 1.1288 | -1.6950 | -0.6580 | -1.2801 | -0.7520 | 0. |
| 34 | GLYR1 | -1.6368 | 1.0036 | -3.0276 | -0.2682 | -1.9878 | -2.8482 | -2.5696 | NA | 0. |
| 35 | CAMKMT | -1.2586 | -0.8000 | -2.6007 | -3.4282 | 1.5956 | 1.4379 | -1.9545 | -6.2350 | 0. |
| 36 | BABAM1 | -6.3837 | 2.2424 | -0.1864 | -3.5837 | -2.9301 | 0.0390 | -2.7164 | NA | 0. |
| 37 | PARP6 | -4.0102 | -2.5654 | -1.6867 | 5.8301 | -2.6358 | -1.7113 | -4.9508 | -0.7985 | 0. |
| 38 | FXR2 | -1.5028 | 0.2393 | -4.5136 | -1.3481 | -0.5592 | -1.3038 | 2.1002 | -0.4710 | 0. |
| 39 | TET2 | -7.2629 | -1.6334 | -1.8842 | -2.3571 | -0.0673 | 0.5708 | -2.8683 | -0.2105 | 0. |
| 40 | SIRT1 | 2.8591 | -2.9099 | -3.7616 | -0.4360 | -1.4519 | -2.3262 | 1.9112 | -3.0284 | 0. |
| 41 | RC3H1 | -3.7150 | -2.8861 | -1.8190 | 0.7352 | -0.4049 | 2.4281 | -2.0639 | -0.7475 | 0. |
| 42 | UIMC1 | 0.5955 | -3.7630 | -1.8091 | 2.3175 | -0.9258 | -3.6038 | 0.0572 | -1.1805 | 0. |
| 43 | DMAP1 | -9.5698 | -11.7429 | -3.2995 | -1.4146 | 0.0167 | -0.2336 | -1.0217 | -0.2184 | 0. |

| | | | | | | | | | | |
|----|---------|---------|---------|---------|---------|---------|---------|---------|---------|----|
| 44 | TADA1 | -1.3340 | -4.7595 | -4.5751 | 0.2700 | -0.8084 | -2.0089 | 1.7649 | 0.5751 | 0. |
| 45 | UHRF1 | -2.7911 | -5.4278 | -4.9183 | 0.3754 | -2.4346 | 0.0840 | -2.7266 | 3.1085 | 0. |
| 46 | SMARCA1 | -4.0599 | -0.8431 | -0.2734 | -0.2373 | -5.1652 | -1.3609 | -1.3064 | 3.1347 | 0. |
| 47 | KDM6A | -2.3224 | 2.6696 | -3.7099 | -1.2749 | 0.1099 | -0.7910 | -1.3575 | -2.9153 | 0. |
| 48 | ZMYM3 | -1.5814 | -0.6614 | -2.4032 | 0.2624 | -4.8461 | -0.7415 | -0.6153 | NA | 0. |
| 49 | ING3 | -1.7138 | -0.2259 | -0.6377 | -2.4466 | -6.2655 | -5.2730 | -2.5314 | 1.2137 | 0. |
| 50 | HFM1 | 0.6654 | -3.7128 | 1.0035 | -3.6779 | -0.7647 | -0.6687 | 1.0383 | -1.2559 | 0. |
| 51 | HDAC2 | 0.3906 | -0.3953 | -1.9439 | -0.6211 | 0.1831 | -1.1369 | -0.0262 | -1.0983 | 0. |
| 52 | DDX60L | 1.9096 | -2.6217 | 0.7180 | 0.0608 | -2.8347 | -5.2353 | -0.0152 | -2.6830 | 0. |
| 53 | TRDMT1 | -1.1508 | -0.2302 | -0.0808 | -1.6046 | -1.9751 | -1.4365 | -2.2297 | 0.3447 | 0. |
| 54 | BRD7 | -2.7862 | 0.2982 | -1.9755 | -8.2723 | -0.4934 | -1.4003 | -0.5493 | -2.9248 | 0. |
| 55 | PKNOX1 | -3.8630 | -1.7284 | -1.7927 | -0.2522 | -0.6940 | -0.5224 | -2.6199 | -4.9251 | 0. |
| 56 | SUV39H2 | -1.0885 | -3.3396 | -1.7210 | -1.3356 | -0.0116 | -0.1832 | -4.7589 | -1.4655 | 0. |
| 57 | UBE2N | -3.0427 | -1.4621 | 0.2751 | 0.5478 | 0.7482 | 0.0376 | -0.4224 | -4.8207 | 0. |
| 58 | DDX52 | -1.1681 | 0.4183 | 0.2666 | -3.9876 | 1.6646 | -0.7108 | -2.0987 | -1.3794 | 0. |
| 59 | NEDD4L | -1.1337 | -1.5526 | -1.9208 | -1.3456 | -1.8425 | 1.8161 | 1.7810 | 1.3581 | 0. |
| 60 | PBRM1 | 6.3971 | -2.9083 | -1.9788 | -2.2076 | -2.4687 | 0.2242 | -5.0233 | -2.9879 | 0. |
| 61 | L3MBTL4 | -1.2457 | -0.4645 | -3.3442 | 0.9540 | -5.7952 | 2.7488 | 3.3787 | -2.0930 | 0. |
| 62 | PADI3 | 0.0061 | -4.4247 | 0.7247 | -0.1658 | -4.2668 | 0.5073 | -6.9001 | NA | 0. |
| 63 | RECQL5 | -1.1934 | -1.8895 | -0.3423 | 1.1703 | -3.0737 | -1.7510 | -1.0628 | NA | 0. |
| 64 | BAHD1 | 1.2194 | 0.0280 | -4.1331 | 0.0168 | -5.6617 | -1.6331 | -5.0868 | -2.1678 | 0. |
| 65 | JAK2 | 1.4143 | -1.7143 | 3.1972 | -3.1245 | -0.5701 | -1.4824 | -3.2593 | NA | 0. |
| 66 | ASH1L | -1.4125 | -0.1521 | -3.0136 | 0.4489 | -3.5258 | -2.3265 | -0.9680 | 0.9803 | 0. |
| 67 | TNRC18 | -6.8755 | 3.1434 | 0.3034 | -2.2502 | -0.2514 | -1.3154 | -6.3293 | NA | 0. |
| 68 | NSUN3 | -2.6926 | -0.1320 | -0.7112 | -2.4217 | -1.0221 | -0.3271 | 1.6244 | -4.4121 | 0. |

| | | | | | | | | | | |
|----|---------|---------|---------|---------|---------|---------|---------|---------|---------|----|
| 69 | NAP1L3 | 0.6971 | -0.8880 | -1.6888 | -0.3547 | -3.4342 | -1.0389 | -3.1629 | -5.8058 | 0. |
| 70 | ZNF740 | -1.1883 | -1.0185 | -1.8024 | -3.7659 | -1.9134 | 1.0417 | -0.7754 | 0.8891 | 0. |
| 71 | PYGO2 | -5.9250 | -0.1735 | -2.4352 | -2.2696 | -3.3163 | -0.8796 | 2.8388 | NA | 0. |
| 72 | SATB1 | 0.7834 | -1.3823 | -6.4489 | -0.9625 | -0.6495 | 0.1439 | 1.2226 | -0.0398 | 0. |
| 73 | DHX30 | -7.0004 | -6.6309 | -1.9955 | -2.9492 | 1.7746 | -5.6738 | -0.7338 | -2.8262 | 0. |
| 74 | ATAD2 | -2.1298 | -0.7589 | 0.3468 | -0.6229 | 1.7723 | -1.5151 | -1.3206 | -1.9102 | 0. |
| 75 | PRDM5 | 0.7510 | 1.3861 | -0.4745 | 0.5667 | -2.9250 | -0.2679 | -2.5357 | -2.5390 | 0. |
| 76 | BCL6 | -5.8198 | -2.2454 | -4.8751 | -3.6039 | -0.6078 | -0.5300 | 0.5177 | NA | 0. |
| 77 | SUPV3L1 | -7.4802 | -0.0715 | -0.0729 | -3.8341 | 0.2271 | -0.0448 | 2.1657 | NA | 0. |
| 78 | BCOR | -1.5016 | -0.6834 | -0.1744 | -1.6327 | -2.1810 | 2.8994 | 0.3590 | NA | 0. |
| 79 | MIER2 | 2.2311 | -0.3598 | 0.6203 | -3.4139 | -2.5072 | -4.7085 | -0.7956 | NA | 0. |
| 80 | DHX15 | -0.4720 | -1.8417 | -7.2566 | 1.1389 | -1.4201 | -0.6415 | -0.4236 | 5.5531 | 0. |
| 81 | ING5 | -1.7950 | -7.5400 | -2.1383 | -0.8734 | -2.7582 | -1.6864 | -2.2786 | 0.4487 | 0. |
| 82 | ZNF451 | -3.5572 | 3.0618 | -1.5815 | -5.7054 | -3.8855 | 0.2644 | -3.4742 | 1.2770 | 0. |
| 83 | CHD4 | 1.6278 | 0.0196 | 0.1749 | -4.0526 | -1.8575 | -2.5907 | -4.9351 | NA | 0. |
| 84 | BTAF1 | 0.7457 | -2.5054 | -0.4437 | -3.9408 | -2.7174 | 0.6418 | 1.7088 | NA | 0. |
| 85 | CBX8 | 1.0113 | 1.8310 | -0.1335 | -1.6213 | -2.0972 | -6.9681 | -1.4183 | -2.9108 | 0. |
| 86 | TRIM66 | 1.8975 | 0.4855 | 0.0770 | -0.1781 | -7.0752 | -3.7998 | 0.2653 | -1.9938 | 0. |
| 87 | PPP4C | -2.9005 | -2.3596 | -2.4040 | 0.3091 | -3.1017 | -0.7046 | 1.6743 | NA | 0. |
| 88 | METTL20 | 0.3428 | -5.0051 | -0.7013 | 0.5290 | -3.5177 | -2.3217 | -3.5194 | 1.3071 | 0. |
| 89 | SOX15 | -1.4243 | -2.5298 | 0.5944 | -3.4654 | -0.1126 | -1.5286 | -0.0029 | NA | 0. |
| 90 | ASXL1 | -1.1883 | 0.5546 | -1.0682 | -1.3541 | -5.8268 | -5.4901 | 0.1822 | -1.7029 | 0. |
| 91 | CSNK2A1 | 0.7377 | -0.2150 | -2.8231 | 2.8966 | -2.1071 | -6.4800 | -8.0244 | NA | 0. |
| 92 | ACTL6B | 1.6240 | -1.1607 | 1.3490 | -2.4000 | -0.8652 | -7.7081 | 0.0384 | -0.1698 | 0. |
| 93 | PRDM13 | -4.0490 | -2.9096 | -0.2317 | -1.0411 | -0.4406 | -2.3782 | 5.1660 | 0.1753 | 0. |

| | | | | | | | | | | |
|------------|---------|---------|---------|---------|---------|---------|---------|---------|---------|-----|
| 94 | MDC1 | -2.6387 | 0.4368 | -2.4216 | -4.3236 | 1.9166 | 0.3933 | -6.4795 | 2.2693 | 0.0 |
| 95 | PHF17 | -3.2887 | -6.3117 | -2.3963 | -0.8053 | 1.9902 | 1.5335 | -0.3721 | NA | 0.0 |
| 96 | KEAP1 | -2.7171 | -1.3123 | 1.0993 | -1.0927 | -2.9652 | -5.2849 | 0.0057 | -1.4240 | 0.0 |
| 97 | HELLS | -3.1189 | -2.3879 | 0.8288 | -1.9252 | -3.9947 | -2.8615 | -3.3513 | 1.3599 | 0.0 |
| 98 | HELQ | -1.2125 | -0.9691 | 0.1334 | -1.8703 | -0.3514 | -1.4303 | -0.6004 | NA | 0.0 |
| 99 | GADD45B | -1.0015 | -3.8764 | -0.2459 | 2.2246 | 0.1689 | -1.8751 | -1.6158 | -0.5942 | 0.0 |
| 100 | COQ5 | -4.3134 | -0.2036 | -2.6612 | -1.2372 | -1.0560 | -4.8678 | -0.8405 | -0.6979 | 0.0 |
| 101 | GTF2H1 | -3.5198 | -2.1720 | -0.3144 | -1.7345 | 0.4532 | -1.7962 | -1.1380 | 2.7482 | 0.0 |
| 102 | CREBBP | -3.7070 | -1.8211 | -2.3773 | -1.3056 | -1.6632 | -0.8484 | 0.3184 | 0.1433 | 0.0 |
| 103 | SETD2 | 2.2395 | 1.9819 | -1.7483 | 0.5038 | -3.2182 | -0.6402 | -0.0684 | -3.1467 | 0.0 |
| 104 | CECR2 | 1.2733 | 0.4162 | 0.1368 | -2.2597 | -0.2531 | -1.2522 | -3.4988 | -4.0201 | 0.0 |

Table 19: List of top ranked depleted genes in TS LOW (associated with higher fatty acid uptake) from th

| Rank | Gene | LogFC 1 | LogFC 2 | LogFC 3 | LogFC 4 | LogFC 5 | LogFC 6 | LogFC 7 | LogFC 8 |
|------|---------|------------|------------|------------|------------|------------|------------|------------|------------|
| 1 | USP51 | 3.3180 | -2.0472 | -1.1702 | 3.8645 | 0.0283 | -0.2642 | 1.6835 | 2.5608 |
| 2 | NCOR1 | 1.0197 | 8.5371 | -0.3479 | 1.6643 | 2.4714 | -0.3022 | 3.9430 | 1.2504 |
| 3 | PRMT7 | 0.8015 | -0.0761 | 2.3166 | 5.3889 | 2.2503 | 1.0164 | -3.0599 | NA |
| 4 | IFIH1 | 1.8380 | 0.3198 | 1.0980 | -1.0667 | 2.6403 | 2.5860 | 3.5087 | 1.9239 |
| 5 | TAF6L | 5.7086 | 0.2185 | 6.0522 | 3.0160 | 2.6597 | 2.5296 | -5.7294 | -1.8515 |
| 6 | ZSCAN20 | 1.5879 | -0.3344 | -1.6660 | -0.1054 | -0.0166 | 1.1939 | 2.2935 | 4.7010 |
| 7 | DAXX | 3.7450 | 2.3316 | -0.0861 | 2.1868 | 0.2659 | -0.4372 | -3.2397 | -2.0296 |
| 8 | ESCO1 | 1.9132 | -1.5434 | 0.0346 | -1.2654 | 0.0983 | 5.6629 | 2.9086 | NA |
| 9 | DDX20 | 0.5554 | 0.9952 | 3.6178 | 6.6439 | 0.0473 | -0.3084 | -1.1585 | 3.4788 |
| 10 | RB1 | 1.4272 | 0.0547 | 3.6525 | 1.1145 | -1.3442 | 1.9301 | -0.4163 | 2.0206 |
| 11 | ASF1B | -0.0138 | 1.6715 | 3.0828 | 0.8670 | 0.7269 | 2.0316 | 2.0622 | -5.6039 |
| 12 | BAP1 | 3.0510 | -0.6403 | 2.0217 | 2.3785 | 0.4797 | 1.0887 | 1.0620 | 1.1132 |
| 13 | RBBP5 | 1.6789 | -2.3317 | -2.0376 | 4.6050 | 0.3526 | 2.7970 | 3.9516 | NA |
| 14 | MAP3K12 | 1.0735 | 2.1102 | 5.6595 | 1.9438 | 3.4853 | 0.0389 | 4.3433 | -3.1537 |
| 15 | PHF21A | 0.2470 | 2.5060 | 0.3686 | 3.4490 | 0.6328 | 1.6393 | 6.1866 | 0.1992 |
| 16 | MEAF6 | 4.1767 | -0.1530 | 4.1305 | -4.0421 | -0.6150 | 2.4221 | -0.3123 | 0.3727 |
| 17 | BAZ1B | 7.8037 | 2.8369 | 0.2633 | -0.2294 | 1.5741 | 3.3423 | 1.7465 | 0.9838 |
| 18 | JMJD4 | 0.4229 | 3.0151 | 3.9764 | -1.5254 | 0.0088 | 3.3150 | 8.4789 | -1.1253 |
| 19 | PHF15 | 1.7750 | 2.3195 | -2.8392 | 2.9829 | 1.9031 | 3.7525 | 0.8331 | NA |
| 20 | RPA3 | -0.8865 | 2.8903 | 3.1316 | 3.7368 | 10.4095 | -0.4626 | -0.3053 | 2.3854 |
| 21 | TDRD6 | 1.3545 | 1.3062 | 3.6818 | 0.1709 | 0.2829 | -0.8240 | -2.3151 | 1.9097 |
| 22 | GATAD2B | 2.3517 | -1.6915 | -0.1830 | 0.7903 | 2.2544 | 1.3719 | 1.8472 | 1.5267 |
| 23 | AFF4 | 1.0280 | -0.5673 | 3.8517 | -1.0770 | 5.0449 | 1.8424 | -1.1469 | 1.8413 |
| 24 | USP17L5 | 1.1897 | 5.3807 | -0.2578 | -0.9130 | 0.8515 | 4.3908 | 3.3694 | 5.7283 |
| 25 | DDX25 | 2.3750 | 0.4780 | 3.7887 | 2.6158 | -0.7063 | -0.9689 | 1.4782 | -3.8794 |

| | | | | | | | | | |
|----|----------|---------|---------|---------|---------|---------|---------|---------|---------|
| 26 | RFXANK | 3.0835 | 4.0668 | -1.3020 | 1.4337 | 0.6867 | 1.0013 | 2.7403 | 0.9914 |
| 27 | SUDS3 | 3.6481 | 2.8524 | -2.9030 | 0.0493 | 0.0487 | 6.1132 | -0.9957 | -5.1052 |
| 28 | TCEA1 | -1.9847 | 1.8730 | 1.6052 | 1.5351 | 0.1805 | 0.4842 | 1.6278 | 0.3788 |
| 29 | METTL11B | 2.4464 | -1.9091 | 2.4246 | 2.0683 | 2.8825 | 0.9582 | 2.7390 | 1.0385 |
| 30 | PARP14 | 0.9021 | 3.1956 | -1.4162 | 0.3225 | -0.4221 | 1.1036 | 0.3432 | 0.8575 |
| 31 | CHD5 | -1.3867 | 3.4316 | 0.6771 | 3.9421 | -0.2675 | 0.2813 | -0.0445 | 2.0431 |
| 32 | TDRD7 | 1.4083 | -0.9222 | -0.1774 | 2.5758 | -0.9696 | 1.5652 | 1.5532 | -1.2605 |
| 33 | RPS6KA3 | 1.9090 | 1.5190 | 0.8047 | 2.9007 | -2.3624 | -3.9947 | 0.1935 | NA |
| 34 | PSD3 | 1.9975 | 2.6223 | -1.0691 | 0.7522 | -0.1613 | -0.2020 | 2.3296 | -1.2428 |
| 35 | IWS1 | 1.3839 | -4.7472 | 0.6241 | 2.6687 | 4.2069 | -0.6526 | 5.3233 | -3.5346 |
| 36 | CALCOCO1 | 0.2999 | 2.4380 | 1.4144 | 7.4555 | 1.9474 | 4.2516 | -1.3282 | NA |
| 37 | BRCA1 | 3.2713 | 2.3370 | 1.2048 | 0.5995 | -2.7708 | 2.7507 | 1.7870 | -1.6785 |
| 38 | ERCC6L2 | -0.0282 | 1.9754 | 2.2978 | 1.3528 | 3.5112 | 2.7417 | -2.8536 | 0.0065 |
| 39 | RUNX1 | 0.4203 | 5.8295 | 1.4165 | -0.1301 | -3.8726 | 3.7781 | 0.0993 | NA |
| 40 | CXXC1 | -2.0784 | 3.5316 | -3.0648 | -0.5215 | 6.9245 | 0.8791 | 2.4858 | NA |
| 41 | ZMYND8 | 0.9078 | 1.3761 | 2.3599 | 2.1460 | 2.8676 | -2.4911 | 3.9623 | -2.8628 |
| 42 | EZH1 | 3.0665 | 0.2944 | 1.6806 | 8.2581 | -1.9463 | -0.0825 | -1.0995 | 2.0800 |
| 43 | BRD3 | -3.3263 | 1.9705 | 4.1095 | 1.1426 | 3.1186 | 2.3502 | 2.7849 | -3.5949 |
| 44 | METTL6 | 0.6167 | -0.1891 | 2.2654 | 0.9515 | -0.0878 | 4.9738 | -0.4012 | 0.4094 |
| 45 | DDX23 | 3.2615 | 12.0778 | -2.4876 | 1.6522 | 5.6186 | -3.2636 | 3.1026 | NA |
| 46 | PAXIP1 | -3.3361 | 3.0290 | 4.7532 | -0.5742 | 1.5480 | 1.2896 | 2.0939 | NA |
| 47 | METTL13 | 3.4725 | -0.3868 | 0.6351 | 0.3543 | 6.1402 | -2.4741 | -1.6232 | 0.5660 |
| 48 | MYPOP | 4.3993 | 1.8577 | 0.5038 | 2.9444 | -1.9651 | 4.9286 | 0.3195 | NA |
| 49 | HMGN3 | -0.7364 | 2.9669 | -0.4514 | -3.0224 | 0.5852 | 1.2076 | -0.1831 | 2.5193 |
| 50 | APBB1 | 0.4574 | 0.9796 | 1.0659 | -0.1514 | -0.8890 | 2.4757 | -2.3284 | 0.2232 |
| 51 | TTF1 | 1.0595 | 2.5301 | -1.3909 | 4.6623 | -2.7212 | 0.6077 | -0.1805 | 4.2812 |
| 52 | NFRKB | 0.3755 | 3.9189 | -3.2779 | -1.9899 | 1.6987 | -1.0783 | 1.8124 | NA |

